Life Cycle Assessment of Ammonia Fuel

by Jannick Schmidt, Freja Konradsen, Karen-Emilie Trier Kreutzfeldt, Simon Vemmelund and Mathilde Nilsson
2.-0 LCA consultants, Aalborg, 20th of March 2025

Preface

This report documents the life cycle assessment of ammonia as shipping fuel and presents the environmental impacts of ammonia in comparison with very low sulphur fuel oil. The study has been carried out January 2023 – February 2025 by 2.-0 LCA.

This study was commissioned as part of a broader project aimed at comprehensively assessing the potential environmental impacts of using ammonia as a shipping fuel. The partners of the project include A.P. Moller - Maersk, Environmental Defense Fund Europe, Nippon Yusen Kabushiki Kaisha, CMA CGM, DFDS A/S, American Bureau of Shipping, MAN Energy Solutions, Svitzer A/S and Havenbedrijf Rotterdam N.V.

The partners have taken part in the project scoping, data collection, and review assumptions. It is important to note that while the partners have contributed to validating the technical aspects, they have not participated in the interpretation of the results. Moreover, the opinions and assumptions presented in this report do not necessarily represent those of each partner. The project has been catalysed, led, and funded by A.P. Moller - Maersk.

When citing the current report, please use the following reference:
Schmidt J, Konradsen F, Kreutzfeldt K-E T, Vemmelund S, Nilsson M (2025). Life Cycle Assessment of Ammonia Fuel, 2.-0 LCA consultants, commissioned by A.P. Moller - Maersk, Denmark.

CONTENTS

External appendixes

Appendix 9: Marginal electricity mixes

Appendix 10: LCIA results

Appendix 11: Final review statement and itemized review report

Abbreviations and terms

Abbreviations

ATR	Autothermal reforming
BOR	Boil-off rate
CCS	Carbon capture and storage
EC	The European Commission
EP	The European Parliament
EULA	Privacy Policy & End User Licence Agreement from ecoinvent
EUR	Euro
EUCO	The Council of the European Union
GHG	Greenhouse gas emissions
GWP	Global warming potential
IEA	International Energy Agency
IMO	International Maritime Organization
LCA	Life cycle assessment
LCI	Life cycle inventory
LCIA	Life cycle impact assessment
LHV	Lower heating value
LNG	Liquefied natural gas
MGO	Marine gas oil
NGFS	The Network for Greening the Financial System
NMVOC	Non-methane volatile organic compound
PV	Photovoltaic
RED II	Revised version of The Renewable Energy Directive
RFNBOs	Renewable fuels of non-biological origin
SCR	Selective catalytic reduction
SMR	Steam methane reforming
TEU	Twenty-foot equivalent unit
VLSFO	Very low sulphur fuel oil
WtW	Well-to-wake

See country abbreviations in **Appendix 1: Country codes in EXIOBASE**.

Commonly used terms

Activity	Part of the technosphere. The doing or making of something. Usually, an activity refers to production activities that aim at selling the resulting products to other activities. In LCA literature, LCA activities are sometimes referred to as processes.
Attributional modelling	"*System modelling approach in which inputs and outputs are attributed to the functional unit of a product system by linking and/or partitioning the unit processes of the system according to a normative rule.*" (Sonnemann & Vigon, 2011). In the current study attributional modelling assumes that the products are produced using existing production capacity (current or historical market average), and multiple-output activities are dealt with by applying allocation factors based on energy content or economic value in accordance with the revised version of The Renewable Energy Directive (RED II) and the supplementing delegated regulation 2023/1185 for renewable fuels of non-biological origin (RFNBOs) (EC, 2023; EP & EUCO, 2018).
By-product	Products which can directly displace a determining product supplied by another activity (i.e., without further processing). The difference between determining products and by-

	products is that a change in demand for by-products does not change the production volume of the supplying activity. By-products are also called dependent products or non-determining products.
Consequential modelling	"*System modelling approach in which activities in a product system are linked so that activities are included in the product system to the extent that they are expected to change as a consequence of a change in demand for the functional unit.*" (Sonnemann & Vigon, 2011). Hence, in consequential modelling it is generally a change in demand of the product under study that is modelled. A cause-effect relationship between a change in demand and the related change in supply is intended to be established. This implies that the product is produced by new capacity (if the market trend is increasing) or from the least competitive existing suppliers/technologies (if the market trend is decreasing at a higher pace than the decrease from regular and planned phase-out of old technologies). It is additionally taken into account that the affected production capacity must not be constrained. Multiple-output activities are dealt with using substitution. The modelling principles are comprehensively described in Weidema et al. (2009) and Weidema (2003).
Determining product	Product output of an activity for which a change in demand will affect the production volume of the activity (also called a reference product).
Exchanges with the environment	Exchanges between the technosphere and the environment. Emissions, resource inputs, land use exchanges (occupation and transformation), and other such as radiation, noise, odour, vibrations, aesthetical effects on landscape etc.
GWP	Global warming potential. Defined in IPCC (2014).
GWP100	Global warming potential calculated using a time horizon of 100 years. This is defined in Myhre et al. (2013).
iLUC	Indirect land-use changes. iLUC are defined as the upstream life cycle consequences of a change in land use, regardless of the purpose of the land use. In other words, iLUC are the indirect consequence of the direct land use change, where the occupation of land somewhere else compensate for the area now occupied by the additional demand (Schmidt et al., 2015).
Marginal	'Marginal' describes the technologies or suppliers which will respond to changes in demand for a product.
Material for treatment	Output flow of a human activity that remains in the technosphere and cannot directly (i.e., without further processing in a treatment activity) displace a reference product.
Process	Part of the technosphere. The doing or making of something. Usually, a process refers to production activities that aim at selling the resulting products to other processes. In LCA literature, LCA processes are sometimes referred to as activities.
Product	Output flow from a human activity with a positive either market or non-market value. Further distinction of the products can be made in terms of reference products and by-products.
Reference product	Product output of an activity for which a change in demand will affect the production volume of the activity (also called a determining product).

Executive summary

Background and objectives

The purpose of this study is to conduct a comparative life cycle assessment (LCA) of two production pathways for ammonia as well as very low sulphur fuel oil (VLSFO) used as fuel in shipping. Ammonia must be ignited by a pilot fuel, which is assumed to be VLSFO, and the study therefore compares 1 MJ of ammonia, where VLSFO accounts for 9.6% of the total fuel energy of 1 MJ ammonia, with 1 MJ of VLSFO. Throughout the report, the share of VLSFO as a pilot fuel needed to ignite ammonia is referred to as '*ammonia with 9.6% e/e VLSFO*'.

The default modelling in this LCA study is a consequential approach, which follows the overall requirements in the ISO 14040 and 14044 and aims to assess the environmental impacts of ammonia and VLSFO production with a change in demand for shipping fuel. Furthermore, an attributional LCA study is performed to determine the carbon footprint of the before-mentioned fuels in accordance with the revised version of the Renewable Energy Directive (RED II) guidelines for renewable fuels of non-biological origin (RFNBOs). The RED II guidelines have determined a minimum reduction target of 70% compared to a fossil fuel comparator of 94 g CO_2-eq/MJ, which the attributional carbon footprint results for ammonia is compared to. The consequential and attributional results should not be compared due to the methodological differences. Moreover, the attributional results should only be compared to other RED II-aligned studies.

This report is commissioned by A.P. Moller - Maersk and internal quality assurance has been ensured by inviting several relevant stakeholders to take part on the project scoping, data collection, and review of methods and assumptions. While the partners have contributed to validating the technical aspects, they have not participated in the interpretation of the results. The project partners include: A.P. Moller - Maersk, Environmental Defense Fund Europe, Nippon Yusen Kabushiki Kaisha, CMA CGM, DFDS A/S, American Bureau of Shipping, MAN Energy Solutions, Svitzer A/S and Havenbedrijf Rotterdam N.V.

Scope and system boundary of the study

The LCA includes all life cycle stages from cradle to grave of ammonia fuel and VLSFO, i.e., production of fuel feedstock, fuel production, distribution and bunkering, as well as storage and combustion on board of the ship. This system boundary is often referred to as 'well-to-wake' (WtW). The report presents the results for global warming potential (GWP100), respiratory inorganics, respiratory organics, nature occupation, eutrophication, acidification and photochemical ozone, vegetation for the before-mentioned fuels using the Stepwise life cycle impact assessment method. Note that the GWP100 results are calculated using a characterisation factor of 12.8 kg CO_2-eq/kg hydrogen (H_2), since H_2 is an important emission within this LCA study.

The ammonia is produced through the Haber-Bosch process, where nitrogen (N_2) and H_2 are combined into NH_3. The main difference between the two ammonia production pathways lies in the H_2 production, as the H_2 can be from natural gas (CH_4) in combination with carbon capture and storage (CCS) or via electrolysis of water (H_2O) with renewable electricity sources. Note that the current production methods for ammonia and VLSFO will not necessarily be reflected in this study, as a change in demand will be met by new capacity, e.g., H_2 from natural gas is assumed to be produced using autothermal reforming (ATR), while VLSFO is assumed to be produced through desulphurisation. These modelling choices are based on discussions with project partners and literature research.

Within the industry, the two pathways are often called 'blue' and 'green' ammonia. However, in this report, the following terms are used:

4 fuel scenarios:	3 production pathways:	2 fuel types:
Ammonia with H_2 from solar-based electrolysis	Electrolysis-based ammonia	Ammonia with 9.6% e/e VLSFO
Ammonia with H_2 from wind-based electrolysis		
Ammonia with H_2 from ATR with CCS	Natural gas-based ammonia	
VLSFO	Desulphurisation	VLSFO

Ammonia is liquefied at the production site and therefore distributed, bunkered, stored, and combusted in its liquefied state. Note that the emissions related to the combustion of ammonia on the vessel are based on assumptions and development targets for the engine, as the engine is still under development.

The LCA study has a global geographical scope, but the results are presented for 17 regions, as groupings of countries and regions are needed for communicating results and for the results to be applicable by different actors. Moreover, a mean value is calculated based on the results for the 17 regions, in order to provide a simple overview and interpretation of the results.

Life cycle inventory

The project partners have provided most of the life cycle inventory (LCI) data for H_2, N_2, and ammonia production as well as combustion emissions for VLSFO and ammonia. The remaining LCI data have been collected from literature, the ecoinvent database, or expert estimates.

It is important to highlight that since the ammonia engine described in this LCA study is still under development, the combustion emissions for ammonia are based on assumptions and development targets for the engine. Thus, it is assumed that N_2O emissions from the combustion of ammonia are similar to those from combusting diesel oil. On the other hand, since engine design and size influence the combustion emissions, the data for combustion of ammonia provided by project partners has been deemed the best available and most consistent data. Moreover, the sensitivity analysis includes a test with other N_2O emission values from combustion of ammonia, thus, showing how the results for the two ammonia pathways may change if the development targets for the engine are not met.

Note that the study aims to have a cut-off criterion of 0% for the applied inventory, however, some inputs are excluded due to lack of data. This is for example the case for service inputs related to the buildings, machinery, and infrastructure needed to combust ammonia fuel. Moreover, it has not been possible to find data for the infrastructure needed to distribute and bunker liquid ammonia, thus, data for the distribution and bunkering infrastructure for VLSFO is used as proxy data.

Function and functional unit

For ammonia to fulfil its function as a shipping fuel, ammonia needs to be ignited by a pilot fuel. It is assumed that VLSFO is the closest match to a pilot fuel in this LCA study. Thus, for the functional unit of 1 MJ shipping fuel, VLSFO accounts for 9.6% of the total fuel energy of 1 MJ ammonia (referred to as '*ammonia with 9.6% e/e VLSFO*').

Furthermore, ammonia with 9.6% e/e VLSFO produced with H_2 from ATR and ammonia with 9.6% e/e VLSFO produced with H_2 from electrolysis are compared with VLSFO, because this is the marginal shipping fuel. VLSFO is the marginal because regulation aimed at reducing SO_2 emissions puts constraints on the current main fuel: heavy fuel oil.

Life cycle impact assessment

The midpoint indicators from the Stepwise 2006 method, version 1.8, are used for the life cycle impact assessment (LCIA) method. The method has been updated with characterisation factors for 100 year global warming potential (GWP100) from IPCC (2021) and also includes a GWP100 factor for H_2 of 12.8 kg CO_2-eq/kg. Thus, the default results include the GWP100 impact of H_2, however, the GWP100 results are also presented without the impact from H_2 in the LCIA chapters in the report.

Results

Based on the consequential model, The GWP100 result range is 15.8-26.1 g CO_2-eq/MJ for ammonia with wind-based electrolysis, 16.8-30.1 g CO_2-eq/MJ for ammonia with solar-based electrolysis, 40.1-49.5 g CO_2-eq/MJ for natural gas-based ammonia, and 99.3-122.0 g CO_2-eq/MJ for VSLFO for the 17 regions.

The three ammonia fuel scenarios have similar impacts on respiratory inorganics and their mean value is approximately 17% lower than the mean value for VLSFO, while VLSFO has the lowest results for acidification and both aquatic and terrestrial eutrophication. For nature occupation, photochemical ozone, vegetation, as well as respiratory organics, the result ranges for the 17 regions overlap, thus, the difference between the four fuel scenarios depends on the regions being compared. The difference in results is largest for GWP100, since the mean value for ammonia with 9.6% e/e VLSFO produced with H_2 from electrolysis has an impact that is five times lower than the mean value for VLSFO.

The contribution analysis for GWP100 for the consequential model showcases that there are three main flows that contribute to the results for electrolysis-based ammonia: the CO_2 emissions from combustion of the pilot fuel share, the fuel oil used as feedstock for VLSFO, and the renewable electricity. For natural gas-based ammonia, there are three main flows that contribute to the GWP100 results: the natural gas used for ATR, the CO_2 emissions from the CCS process, and the CO_2 emissions from combustion of the pilot fuel share.

Note that the attributional results are calculated for WtW with both 9.6% e/e and 0% e/e VLSFO. This is done, because project partners argue that the share of pilot fuel will not be included when the results are used in relation to RFNBOs certifications. Moreover, following the RED II guidelines for RFNBOs means that the carbon intensity of renewable electricity is set to zero, that materials, equipment, and machinery necessary for fuel production and distribution are excluded, and that there no differentiation of timing of CO_2 emissions.

For electrolysis-based ammonia with 9.6% e/e VLSFO, the attributional carbon footprint is seven times lower than the WtW fossil fuel comparator value of 94 g CO_2-eq/MJ, which is applied for VLSFO. The carbon footprint for ammonia with H_2 from ATR with CCS with 9.6% e/e VLSFO is 44% lower than the default value of the fossil fuel comparator. The result ranges are 12.6-14.6 g CO_2-eq/MJ and 46.7-59.2 g CO_2-eq/MJ for electrolysis-based and natural gas-based ammonia with 9.6% e/e VLSFO, respectively.

For electrolysis-based ammonia with 0% e/e VLSFO, the attributional carbon footprint ranges from 4.0-6.4 g CO_2-eq/MJ and the mean value is 18 times lower than the fossil fuel comparator. The GWP100 results for ammonia with H_2 from ATR with CCS with 0% e/e VLSFO range from 41.7-55.6 g CO_2-eq/MJ and the mean value is 48% lower than the fossil fuel comparator.

Thus, the attributional results for electrolysis-based ammonia with both 9.6% and 0% e/e VLSFO are below the 70% reduction target from RED II, as the results are lower than 28.2 g CO_2-eq/MJ.

The contribution analysis for the attributional results shows that the CO_2 emissions from the share of pilot fuel is the largest contributor to the impact from electrolysis-based ammonia with 9.6% e/e VLSFO. Without the share of pilot fuel, the largest contributor to electrolysis-based ammonia is the fuel oil used for cooling during the distribution phase. For natural gas-based ammonia with both 9.6% and 0% e/e VLSFO, the two largest contributors are CO_2 emissions from the CCS process and the natural gas input to ATR.

Sensitivity analysis

Since ammonia fuel is relatively new to the shipping industry, there are some uncertainties related to both the production of ammonia and the emissions from combustion. Therefore, an extensive sensitivity analysis has been conducted in order to determine the most important parameters which influence the environmental impacts of ammonia fuel.

For the consequential model, the following parameters can have a high influence on the GWP100 results:

Both ammonia pathways with 9.6% e/e VLSFO:	Electrolysis-based ammonia with 9.6% e/e VLSFO:	Natural gas-based ammonia with 9.6% e/e VLSFO:
1. The N_2O emissions from combustion of ammonia 2. The energy source and energy requirement for cooling of ammonia in the distribution phase 3. The slip of H_2 throughout the product system.	1. The carbon intensity of the renewable electricity 2. The distribution distance for ammonia in the distribution phase 3. The share of pilot fuel	1. Slip of CO_2 from carbon storage 2. The carbon capture rate 3. The energy input to CCS 4. The slip of methane from natural gas extraction 5. The slip of methane from the ATR process

Especially the N_2O emissions from combustion can have a high influence on the results for ammonia fuel scenarios, since N_2O has a characterisation factor of 273 kg CO_2-eq/kg. Thus, two values were tested in the sensitivity analysis: 0.0083 g N_2O/MJ and 0.117 g N_2O/MJ, showing how the results for the two ammonia pathways may change if the development targets for the engine are not met. The first value is based on an industry expectation, stating that higher N_2O emissions are not likely to be accepted from an ammonia ICE design, while the second is deemed the best available estimate for an upper value for higher N_2O emissions before selective catalytic reduction.

If 0.0083 g N_2O is emitted per MJ of ammonia with 9.6% e/e VLSFO, the GWP100 results for the three ammonia fuel scenarios are increased with around 1 g CO_2-eq/MJ. Thus, even though there is a factor 1.5 difference between the industry expectation (0.0083 g N_2O/MJ) and the design parameter for the ammonia engine (0.0056 g N_2O/MJ), it has an effect on the GWP100 results of 1 g CO_2-eq/MJ for the three ammonia scenarios. However, if 0.117 g N_2O is emitted per MJ of ammonia with 9.6% e/e VLSFO, the GWP100 result can increase with 137% and 155% for ammonia with solar- and wind-based electrolysis, resulting in a mean GWP100 impact of 53 and 50 g CO_2-eq/MJ, respectively. For natural gas-based ammonia, the mean GWP100 result can increase to 74 g CO_2-eq/MJ with 0.117 g N_2O/MJ.

Several of the parameters, which can have a large influence on the results from the consequential model, also influence the results from attributional model, except for the carbon footprint of renewable electricity, since following the RED II guidelines for RFNBOs means that the carbon intensity of renewable electricity is set to zero. Moreover, the share of pilot fuel will not influence the results used for RFNBOs certifications, since project partners argue that the share of pilot fuel will not be included when the results are used in this regard.

Thus, for the following parameters, the attributional results are expected to change in a similar magnitude as the consequential results:

- The N_2O emissions from combustion of ammonia
- The H_2 slip in the product system
- Slip of CO_2 from carbon storage
- The carbon capture rate
- The energy input to CCS
- The slip of methane from natural gas extraction
- The slip of methane from the ATR process
- The energy source and energy requirement for cooling of ammonia in the distribution phase
- The distribution distance for ammonia in the distribution phase

Additionally, the attributional results have been calculated with 9.6% e/e bio-based pilot fuel. This is done through a semi-quantitative analysis where a default value from RED II is applied, since RED II specifies that bio-based fuels must have a reduction of at least 65% compared to the WtW fossil fuel comparator of 94 g CO_2-eq/MJ. Therefore, it is assumed that the bio-based pilot fuel will have a carbon footprint of 32.9 g CO_2-eq/MJ from WtW.

The semi-quantitative analysis shows that a RED II-compliant bio-based pilot fuel can reduce the attributional carbon footprint of electrolysis-based ammonia with 46%, as the mean result goes from 13.5 to 7.6 g CO_2-eq/MJ, when the RED II guidelines are used for the calculation. For natural gas-based ammonia, the mean result is reduced by 11%, as it goes from 53.1 to 47.2 g CO_2-eq/MJ.

Conclusions

The main conclusions for this LCA study are as follows:

- Generally, electrolysis-based ammonia has the lowest GWP100 impact, and – depending on the applied LCA methodology – the GWP100 mean result for this ammonia pathway is 5-18 times lower than the mean GWP100 result for VLSFO.

- Both electrolysis-based and natural gas-based ammonia have a lower impact on respiratory inorganics than VLSFO, with the mean value being approximately 17% lower than the mean value for VLSFO.

- VLSFO has the lowest results for acidification and both aquatic and terrestrial eutrophication.

- The attributional carbon footprint calculated in accordance with RED II guidelines for RFNBOs for electrolysis-based ammonia with both 9.6% and 0% e/e VLSFO are below the 70% reduction target from RED II, as the results are lower than 28.2 g CO_2-eq/MJ.

- A semi-quantitative analysis shows that a RED II-compliant bio-based pilot fuel can reduce the attributional carbon footprint of electrolysis-based ammonia with 9.6% e/e pilot fuel with 43%, as the mean result goes from 13.5 to 7.6 g CO_2-eq/MJ. For natural gas-based ammonia, the attributional mean result can be reduced by 11%, as it goes from 53.1 to 47.2 g CO_2-eq/MJ.

- The contribution analysis for the consequential model showcases that there are three main flows that contribute to the GWP100 results for electrolysis-based ammonia: the CO_2 emissions from combustion of the pilot fuel share, the fuel oil used as feedstock for VLSFO, and the renewable electricity.

- For natural gas-based ammonia in the consequential model, there are three main flows that contribute to the GWP100 results: the natural gas used for ATR, the CO_2 emissions from the CCS process, and the CO_2 emissions from combustion of the pilot fuel share.

- The contribution analysis for the RED II-aligned results for ammonia with 9.6% e/e VLSFO shows that the CO_2 emissions from the share of pilot fuel is the largest contributor to the impact from electrolysis-based ammonia. Without the share of pilot fuel, the largest contributor to electrolysis-based ammonia is the fuel oil used for cooling during the distribution phase.

- For the RED II-aligned results for natural gas-based ammonia with both 9.6% and 0% e/e VLSFO, the two largest contributors are CO_2 emissions from the CCS process and the natural gas input to ATR.

- The GWP100 results for both ammonia pathways can be highly influenced by the following three parameters: The N_2O emissions from combustion of ammonia and the energy source, energy requirement for cooling of ammonia in the distribution phase, and the slip of H_2 throughout the product system.

- The GWP100 results for electrolysis-based ammonia can be highly influenced by the following three parameters: The carbon intensity of the renewable electricity, the distribution distance for ammonia in the distribution phase, and the share of pilot fuel.

- The GWP100 results for natural gas-based ammonia can be highly influenced by the following five parameters: Slip of CO_2 from carbon storage, the carbon capture rate, the energy input to CCS, as well as the slip of methane from natural gas extraction and the ATR process.

It is recommended to improve the data availability and quality for the parameters that can have a high influence on the results for both ammonia pathways in order to increase the accuracy of the results for ammonia fuels.

1 Introduction

The purpose of this study is to conduct a comparative LCA of two production pathways for ammonia, being in turn compared to VLSFO. Since ammonia must be ignited by a pilot fuel (assumed to be VLSFO) the study compares 1 MJ of ammonia, where VLSFO accounts for 9.6% of the total fuel energy of 1 MJ ammonia, with 1 MJ of VLSFO. Throughout the report, the share of VLSFO as a pilot fuel needed to ignite ammonia is referred to as '*ammonia with 9.6% e/e VLSFO*'.

The default modelling in this LCA study is a consequential approach, which aims to assess the environmental impacts of ammonia and VLSFO production as a result of a change in demand for shipping fuel. In this context, the modelling choices are based on discussions with the project partners and their expectations for how the market changes based on the current decarbonization targets and how these targets are expected to affect the long-term marginal supply of ammonia as shipping fuel. Thus, the current production methods for ammonia and VLSFO will not necessarily be reflected in this study, as a change in demand will be met by new capacity.

Furthermore, an attributional LCA study is performed to determine the carbon footprint of the before-mentioned fuels in accordance with the RED II guidelines for RFNBOs, where the carbon footprint of the two ammonia pathways is compared to RED II's fossil fuel comparator of 94 CO_2-eq/MJ, assessing whether the carbon reduction target from RED II of at least 70% lower carbon footprint of RFNBOs is met.

Note that the consequential and attributional results should not be compared due to the methodological differences. Moreover, the attributional results should only be compared to other RED II-aligned studies.

The ammonia is produced through the Haber-Bosch process, where nitrogen (N_2) and hydrogen (H_2) are combined into NH_3. The main difference between the two ammonia production pathways lies in the H_2 production, as the H_2 can be from natural gas (CH_4) in combination with carbon capture and storage (CCS) or via electrolysis of water (H_2O) with renewable energy sources. Ammonia is liquefied at the production site and therefore distributed, bunkered, and combusted in its liquefied state. Note that the combustion emissions for ammonia are based on assumptions and development targets for the engine, as the engine is still under development. The following terms are used to refer to the different fuel scenarios, production pathways, and fuel types:

4 fuel scenarios:	3 production pathways:	2 fuel types:
Ammonia with H_2 from solar-based electrolysis	Electrolysis-based ammonia	Ammonia with 9.6% e/e VLSFO
Ammonia with H_2 from wind-based electrolysis		
Ammonia with H_2 from ATR with CCS	Natural gas-based ammonia	
VLSFO	Desulphurisation	VLSFO

For ammonia to fulfil its function as a shipping fuel, it needs to be ignited by a pilot fuel. It is assumed that VLSFO is the closest match to a pilot fuel in this LCA study. Thus, for the functional unit of 1 MJ shipping fuel, VLSFO accounts for 9.6% of the total fuel energy of 1 MJ ammonia (referred to as '*ammonia with 9.6% e/e VLSFO*').

Furthermore, ammonia with 9.6% e/e VLSFO produced with H_2 from ATR and ammonia with 9.6% e/e VLSFO produced with H_2 from electrolysis are compared with VLSFO, because this is the marginal shipping fuel. VLSFO

is the marginal because regulation aimed at reducing SO_2 emissions puts constraints on the current main fuel: heavy fuel oil.

The aim of the report is to document the environmental impacts related to the production and use of the above-mentioned fuel scenarios for shipping. For the consequential model, this report presents the results for global warming potential, respiratory inorganics, respiratory organics, nature occupation, eutrophication, acidification, and photochemical ozone, vegetation, for the before-mentioned fuels.

The consequential LCA is carried out following the provisions in the ISO standards on LCA: ISO 14040:2006 and ISO 14044:2006. Moreover, the carbon footprint is also assessed according to an attributional model in accordance with RED II and the supplementing delegated regulation 2023/1185 for RFNBOs.

The LCA includes all life cycle stages from cradle to grave of the fuels, i.e., from production of the fuel to combustion on board.

The LCA study is conducted on behalf of A.P. Moller - Maersk and in collaboration with the following project partners: A.P. Moller - Maersk, Environmental Defense Fund Europe, Nippon Yusen Kabushiki Kaisha, CMA CGM, DFDS A/S, American Bureau of Shipping, MAN Energy Solutions, Svitzer A/S and Havenbedrijf Rotterdam N.V.

2 Goal and scope

This chapter describes the goal and scope of the LCA study.

2.1 Purpose of the study

The purpose of the consequential study is to conduct a comparative and cause-effect-based LCA of the use of ammonia produced with H_2 from electrolysis or ATR as fuel in shipping with VLSFO as comparison. Since ammonia must be ignited by a pilot fuel (assumed to be VLSFO) the study compares 1 MJ of ammonia, where VLSFO accounts for 9.6% of the total fuel energy of 1 MJ ammonia, with 1 MJ of VLSFO. Throughout the report, the share of VLSFO as a pilot fuel needed to ignite ammonia is referred to as '*ammonia with 9.6% e/e VLSFO*'.

The aim of the LCA is to document the potential environmental impacts related to the production and use of the before-mentioned fuel scenarios for shipping. This is both regarding greenhouse gas (GHG) and non-GHG related environmental impacts belonging to the fuel's life cycle. The target audience includes the shipping industry and fuel producers as well as the general public.

Additionally, this report also presents the normative carbon footprint for ammonia and VLSFO based on an attributional approach following the RED II guidelines. Note that the European Commission (EC) in 2023 specified the methodology for assessing GHG emissions from renewable liquid and gaseous transport fuels of non-biological origin. The carbon footprint of ammonia is therefore assessed in accordance with the RED II Directive and the delegated regulation 2023/1185 (EC, 2023; EP & EUCO, 2018).

2.2 ISO 14040/44

The consequential LCA model presented in this report is compliant with the ISO standards on LCA: ISO 14040 and ISO 14044 (ISO, 2006a, 2006b). The ISO standards identify four phases of an LCA:

1. Definition of goal and scope
2. Life cycle inventory (LCI)
3. Life cycle impact assessment (LCIA)
4. Life cycle interpretation

Chapter 1 defines the goal and scope of this LCA study, while **chapter 3** and **4** presents the LCI. Moreover, the LCIA is in **chapter 6** and **7**, while life cycle interpretation is in **chapter 11**, respectively.

The attributional carbon footprint is assessed in accordance with the RED II Directive and the delegated regulation 2023/1185 (EC, 2023; EP & EUCO, 2018).

According to ISO 14044, an LCA that aims at disclosing comparative assertions to the public, a third-party critical panel review is required. The review panel shall consist of at least three reviewers of which one is appointed as chair. The review panel consisted of:

- Reviewer 1 (chair): Miguel Brandão
- Reviewer 2: Romain Sacchi
- Reviewer 3: Rob Stevens

The review procedure had the following schedule:

- 11th of July 2024: The first iteration of the LCA report was sent to reviewers.
- 16th of August 2024: The revision of the first iteration was sent to 2.-0 LCA consultants
- 27th of August 2024: The review panel's comments were discussed during an online conference call.
- 13th of September 2024: Answers to the first revision were sent to reviewers
- 20th of November 2024: Second iteration of the LCA report was sent to reviewers
- 2nd of December: The revision of the second iteration was sent to 2.-0 LCA consultants
- 17th of December: Answers to the second revision was sent to reviewers along with the third iteration of the LCA report.
- 19th of December: The review panel delivered the final review statement.

Furthermore, the final review statement and the itemized review report is available in appendix 11 (external).

2.3 Modelling approaches: Consequential and attributional models

Generally, two different approaches to modelling in life cycle inventory exist: consequential and attributional modelling.

According to Sonnemann & Vigon (2011, p 133), **consequential modelling** is defined as a "*system modelling approach in which activities in a product system are linked so that activities are included in the product system to the extent that they are expected to change as a consequence of a change in demand for the functional unit.*" Hence, in consequential modelling it is generally a change in demand of the product under study that is modelled. A cause-effect relationship between a change in demand and the related changes in supply is intended to be established. This implies that the product is produced by new capacity (if the market trend is increasing). Additionally, it is taken into account that the affected production capacity must not be constrained. Multiple-output activities are dealt with using substitution. The modelling principles are comprehensively described in Weidema (2003) and Weidema et al. (2009).

According to Sonnemann & Vigon (2011, p 132), **attributional modelling** is defined as a "*system modelling approach in which inputs and outputs are attributed to the functional unit of a product system by linking and/or partitioning the unit processes of the system according to a normative rule*". An attributional model is therefore based on the assumption that the products are produced using existing production capacity (current or historical market average), and multiple-output activities are dealt with by applying allocation factors based on e.g., economic value (revenue).

As the two modelling approaches answer different questions, the consequential and attributional results should not be compared, and the attributional results should only be compared to other RED II-aligned studies.

The default modelling in this LCA study is a cause-effect based model, which follows the overall requirements in the ISO 14040 and 14044 combined with a consequential modelling approach as described in Weidema et al. (2009). Additionally, this report also presents the normative carbon footprint for ammonia and VLSFO based on an attributional approach following the RED II guidelines. Note that the EC in 2023 specified the methodology for assessing GHG emissions from RFNBOs through the delegated regulation 2023/1185. The carbon footprint of ammonia is therefore assessed in accordance with both directive 2018/2001 and delegated regulation 2023/1185 (EC, 2023; EP & EUCO, 2018). The characteristics of the included approaches/standards are summarised in **Table 2.1**.

Table 2.1: Description of the key elements of the modelling in LCI in the applied modelling approaches/standards for ammonia fuel.

Elements in modelling	Consequential	Attributional (RED II & delegated regulation 2023/1185)
Use of by-products / waste as feedstock for fuels	A change in demand for these flows will not affect the quantity produced. Instead, the use of them will divert them from one use or treatment to another. The impact is modelled as demand for the feedstock minus the counterfactual.	Generally, the use of by-products and wastes are free of burden (cut-off)
Supply of by-products / waste from activities in the fuel pathways	By-products are modelled using substitution. Wastes (materials for treatment) are modelled in a similar way by including the required treatment activities as well as substitutions if the treatment supply this.	By-products are modelled using allocation based on energy (LHV) or economic allocation, if one or more by-products do not have an energy content. Wastes (materials for treatment) are modelled using cut-off if the waste treatment is regarded as recycling (i.e., the treatment supplies by-products), else the waste treatment is modelled as in the consequential approach.
Temporal aspects of CO_2 emissions	The timing of CO_2 emissions/removals is accounted for using the GWP100 made time-dependant (see **section 2.12**).	No differentiation of timing of CO_2 emissions/removals are specified in RED II or delegated regulation 2023/1185.
Electricity grid mix	The marginal electricity mix is applied, which is determined by the electricity technologies which will respond to changes in demand for electricity.	An average grid mix is applied, determined at country level or bidding zones. The carbon footprint of electricity from wind, solar, hydro, and geothermal is equal to zero according to the delegated regulation 2023/1185.

There are pros and cons of both consequential and attributional modelling. In view of the authors, the most important ones are listed in **Table 2.2**. The table is based on Schmidt & de Saxcé (2016) and supported by Weidema (2014), Weidema (2018), Weidema et al. (2018), Weidema & Schmidt (2010), and consequential-lca.org (2023).

Table 2.2: Pros and cons of consequential and attributional modelling.

Consequential modelling	Attributional modelling
Pros	
• Strives towards identifying the consequences of demanding the functional unit. • Follows ISO 14044 allocation hierarchy, i.e., the highest priority to model by-products is followed. • Based on scientific criteria. • Mass balances are maintained. • Relatively simple to apply consistent modelling of by-products through the product system.	• Seemingly easy: Since the approach is normative, ad hoc choices can be made to exclude complex issues. • Most industry specific LCA and GHG guidelines are based on attributional modelling. e.g., RED II.
Cons	
• Uncertainties associated with the identification of affected market mixes, i.e., "marginal" suppliers. • Hard to communicate: Since constrained suppliers are excluded, the directly economically connected product chain is not always followed. Negative impacts may be misunderstood.	• Complicated (or impossible) to consistently apply same allocation approach throughout a product system. • Allocated systems do not exist in reality – experts cannot recognise allocated product systems. • Applied market mixes, i.e., "average" suppliers may not represent the consequences of demanding products from the market – because some suppliers are more likely to respond to changes than others. • Most often, the lowest priority to model by-products with regard to the ISO 14044 hierarchy on allocation is followed. • Mass, substance, energy, and other balances are not maintained when allocating. • May lead to misleading results – because of allocation, market averages and normative models. • Hard to communicate: Since allocated product systems do not exist in reality, the modelled system can be difficult to communicate.

2.4 Functional unit

The study's functional unit is combustion of 1 MJ shipping fuel.

Note that in order for ammonia to function as a shipping fuel, it needs to be ignited by a pilot fuel, since ammonia has a low energy content. It is assumed that VLSFO is the closest match to a pilot fuel in this LCA study. Thus, for the functional unit of 1 MJ shipping fuel, VLSFO accounts for 9.6% of the total fuel energy of 1 MJ ammonia. This is referred to as '*ammonia with 9.6% e/e VLSFO*' throughout the report.

Additionally, the LCIA results are also provided for a functional unit of 1 twenty-foot equivalent unit transported for 1 kilometre (1 TEUkm). This is done, since a ship fuelled by ammonia has less space for cargo, because the energy density of ammonia is 12 GJ/m^3, while the energy density is 38.6 GJ/m^3 for VLSFO.

The LCIA results can be recalculated to 1 TEUkm using a conversion factor of 0.291 MJ/TEUkm for ammonia with 9.6% e/e VLSFO and 0.275 MJ/TEUkm for VLSFO. **Appendix 4: Conversion factor from MJ to TEUkm** describes how the conversion factor has been determined. Note that the conversion factors for TEUkm are estimates and can differ based on both ship design and size as well as engine efficiency.

It is important to highlight that the LCA model will not change if the functional unit is 1 EJ instead of 1 MJ, since the modelling choices are based on discussions with the project partners and their expectations for how the market changes based on the current decarbonization targets and how these targets are expected to affect the

demand for ammonia as shipping fuel. Thus, the applied modelling choices aim to assess the long-term marginal supply for ammonia as a shipping fuel.

2.5 System boundaries

The LCA includes all life cycle stages from cradle to grave of ammonia fuel and VLSFO, i.e., production of fuel feedstock, fuel production, distribution and bunkering, as well as storage and combustion on board of the ship. This system boundary is often referred to as 'well-to-wake' (WtW).

The ammonia is produced through the Haber-Bosch process, where nitrogen (N_2) and H_2 are combined into ammonia. The main difference between the two ammonia production pathways lies in the H_2 production, as the H_2 can be produced from natural gas (CH_4) in combination with carbon capture and storage (CCS) or via electrolysis of water (H_2O) with renewable energy sources. Note that within the industry, the two ammonia pathways are often called 'blue' and 'green' ammonia, respectively. However, in this report, the terms in **Table 2.3** are used. Thus, this report includes four different fuel scenarios based on three production pathways, which result in two overall fuel types.

Table 2.3: Terms used to describe the four fuel scenarios and the three production pathways, resulting in two overall fuel types.

4 fuel scenarios:	3 production pathways:	2 fuel types:
Ammonia with H_2 from solar-based electrolysis	Electrolysis-based ammonia	Ammonia with 9.6% e/e VLSFO
Ammonia with H_2 from wind-based electrolysis		
Ammonia with H_2 from ATR with CCS	Natural gas-based ammonia	
VLSFO	Desulphurisation	VLSFO

2.5.1 System boundaries for the consequential modelling

For the consequential model, **Figure 2.1** presents the system boundary for VLSFO**,** while **Figure 2.2** and **Figure 2.3** illustrate the system boundary for ammonia produced with H_2 from either electrolysis or ATR. Ammonia cannot fulfil its function as a shipping fuel without a pilot fuel for ignition. Therefore, the product system for VLSFO is also displayed on **Figure 2.2** and **Figure 2.3.** Note that production of fuel feedstock and the fuel production is modelled to take place at an 'integrated' facility, meaning that H_2, N_2, and ammonia are produced at the same production facility. For the consequential model, EXIOBASE is the applied background database (see description hereof in **section 2.6.1**).

As the consequential LCA study is assessing how ammonia and VLSFO will be produced with a change in demand, the LCA will model how ammonia and VLSFO is expected to be produced by new capacity. Thus, the current production methods for ammonia and VLSFO will not necessarily be reflected in this study, e.g., H_2 for natural gas-based ammonia is assumed to be produced using ATR, while VLSFO is assumed to be produced through desulphurisation. These modelling choices are based on discussions with project partners and the literature research presented in **section 5.2**.

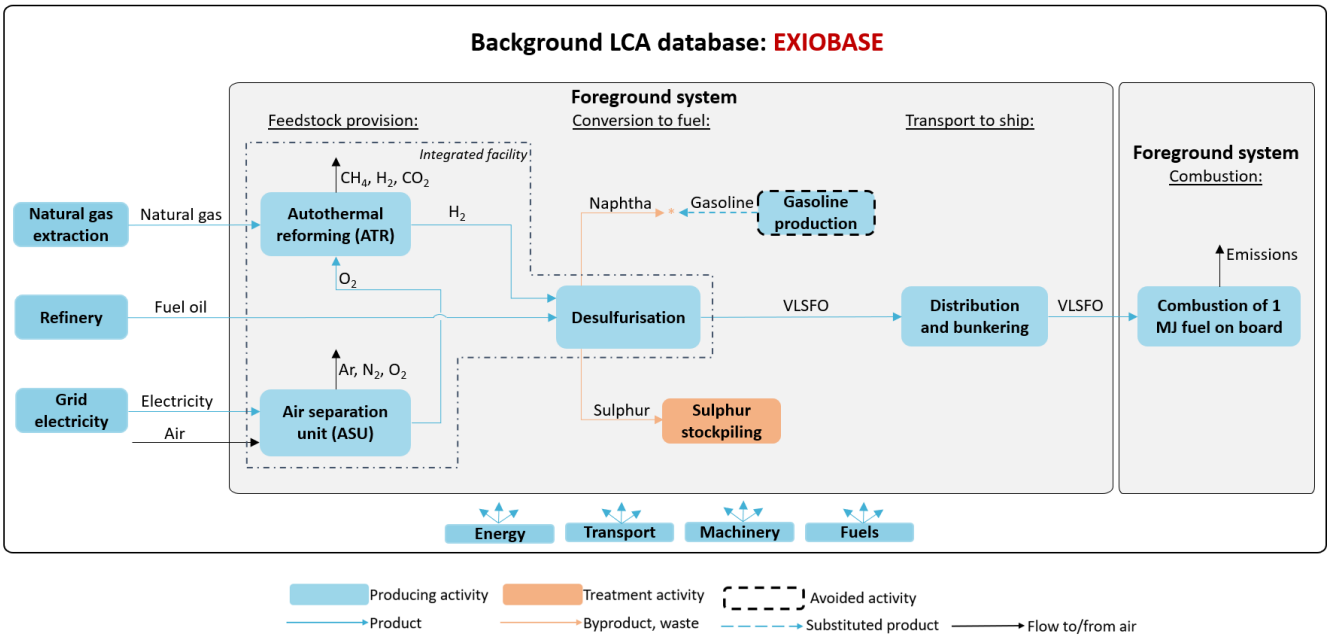

Figure 2.1: System boundary for the consequential modelling of VLSFO with H_2 from autothermal reforming (ATR) used for the desulphurisation process.

As depicted on **Figure 2.1**, VLSFO is produced through desulphurisation of fuel oil. For desulphurisation, the sulphur is removed using H_2 produced from natural gas, because natural gas-based H_2 production is used worldwide (Kim et al., 2021). Moreover, since the demand for H_2 will be met by new production capacity, it is assumed that autothermal reforming (ATR) will be the applied technology. However, the CO_2 emissions are modelled as being emitted to air, since project partners describe that the CO_2 for a typical natural gas-based H_2 facility is either utilised in fertiliser production, by the food and beverage industry, or emitted to air. Thus, even though the CO_2 may be utilised, it will be emitted within a very short period, which would result in a similar impact as if the CO_2 was emitted at the H_2 production facility. Nevertheless, it is tested in the sensitivity analysis, how the results would change if the CO_2 were captured and stored long-term through CCS (see **section 8.14**).

The desulphurisation process has two by-products: naphtha and sulphur. Naphtha is the main combustible component in gasoline (Su-ungkavatin et al., 2023) and is therefore assumed to substitute gasoline production, while sulphur is accumulated and stored through stockpiling, since the amount of sulphur produced as a by-product from refineries is larger than its utilisation in the production of, e.g., sulphuric acid and fertilisers (Apodaca, 2022; Worthington et al., 2017). Thus, sulphur stockpiling is depicted as a treatment process on **Figure 2.1**, since the sulphur is stored until it is demanded for utilisation.

Figure 2.2 shows the electrolysis-based pathway for ammonia production. The electricity for ammonia produced with H_2 from electrolysis is 100% renewable and comes from either solar or wind power. As these electricity sources are highly dependent on weather conditions, H_2 storage is required in order to ensure continuous flow of H_2 to the ammonia synthesis. Note that a project partner highlights that this set-up assumes that the electrolyser is flexible and therefore does not have ramp limitations and there is no impact on ware.

For electrolysis-based ammonia, the input of N_2 stems from avoided venting of N_2, because N_2 is a by-product from air separation, where oxygen (O_2) is the determining product (Aljaghoub et al., 2023). Thus, since the

production of O_2 leads to excess N_2, which is released back into the atmosphere right after the air separation process, the demand for N_2 from the Haber-Bosch process will result in avoided venting of N_2.

Lastly, O_2 is a by-product from the electrolyser, which is possible to utilise. However, since Krishnan et al. (2024) state that O_2 from electrolysers is currently vented to the atmosphere, the O_2 is modelled as emissions to air.

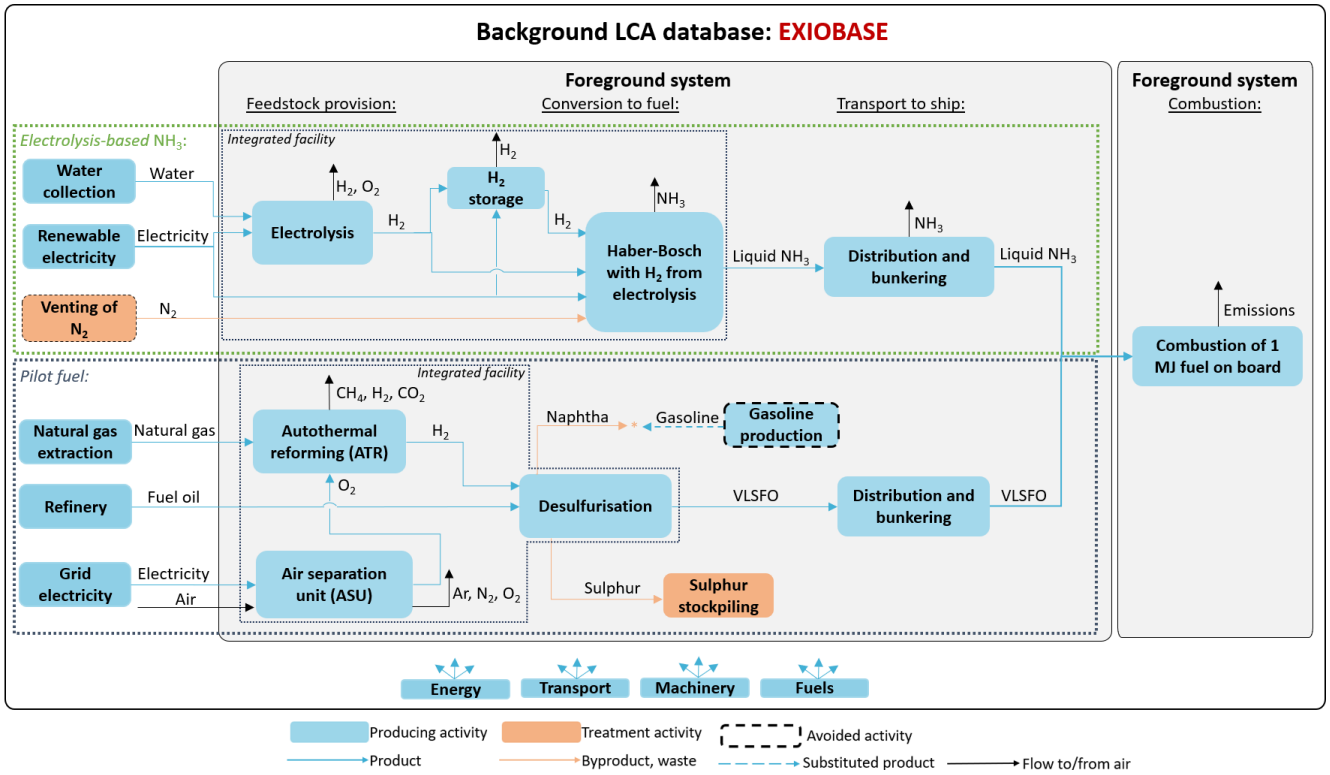

Figure 2.2: System boundary for the **consequential modelling** of ammonia produced with H_2 from electrolysis and with 9.6% e/e VLSFO.

Lastly, **Figure 2.3** shows the natural gas-based pathway for ammonia production, with the primary differences being the use of grid electricity, ATR for H_2 production, CCS of the CO_2 from the ATR process, and the air separation unit (ASU), which is used to produce N_2 for the Haber-Bosch process while it also supplies O_2 to the ATR process.

According to Kim et al. (2021), ATR is a promising technology for H_2 production and based on discussions with project partners, the natural gas-based production pathways for ammonia will be highly influenced by carbon footprint reduction targets, e.g., from RED II and future compliance needs. Thus, if ammonia is based on H_2 produced from natural gas, it is assumed that ATR along with CCS is required.

Note that N_2 is the determining product of the ASU on **Figure 2.3**, which contradicts the modelling of avoided venting of N_2 on **Figure 2.2** since O_2 is the determining product from ASUs according to Aljaghoub et al. (2023). Nevertheless, based on a thorough analysis of the data from project partners (see **section 5.1.1.2**), it has been determined that the demand for N_2 for the Haber-Bosch process is larger than the demand for O_2 for the ATR process. Thus, for natural gas-based ammonia, the excess O_2 from the ASU unit substitutes the primary production of O_2 from another ASU unit. Nevertheless, as there is conflicting information on this topic, a

sensitivity analysis is performed in **section 8.13.2.4** to assess how much the results for natural gas-based ammonia will change, if O_2 is the determining product from the ASU.

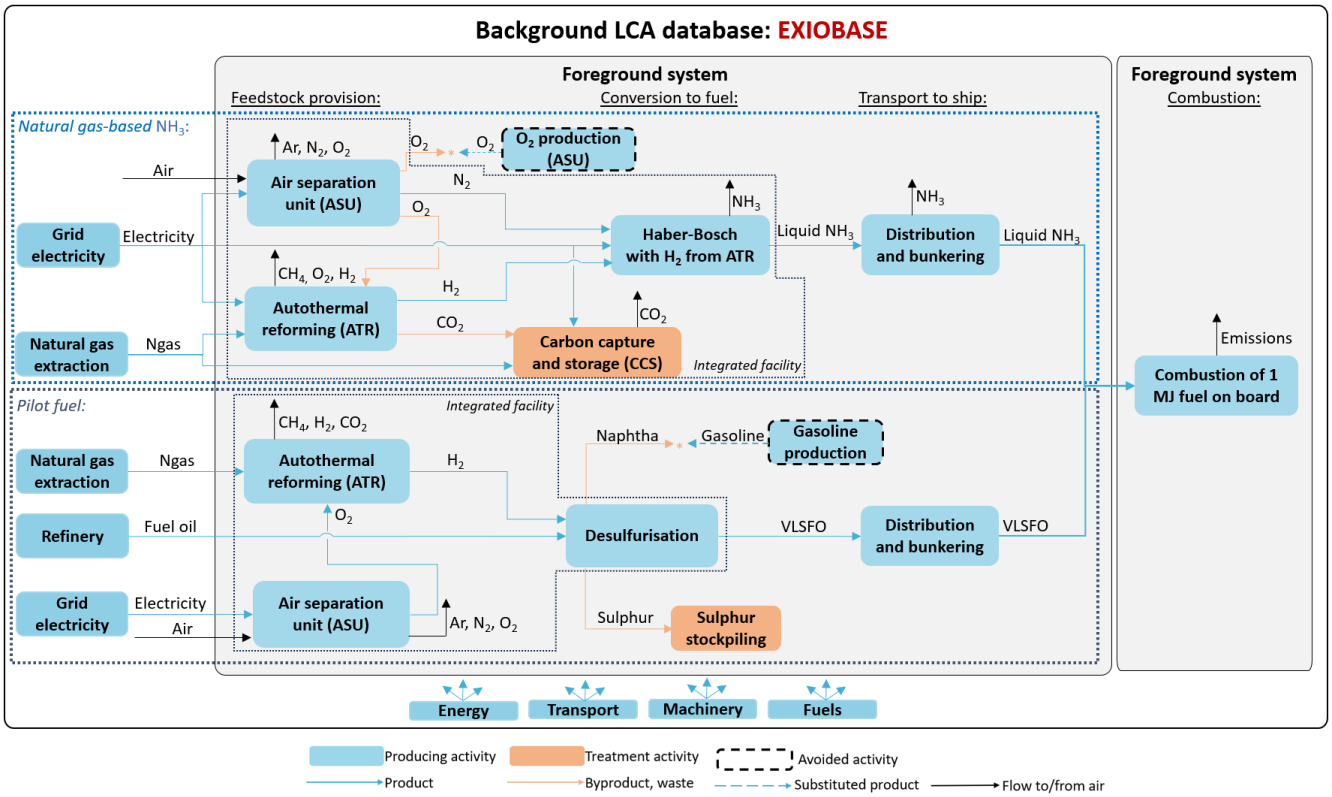

Figure 2.3: System boundary for the **consequential modelling** of ammonia produced with H_2 from autothermal reforming (ATR) and with 9.6% e/e VLSFO.

On both **Figure 2.2** and **Figure 2.3**, ammonia is produced and liquefied at the production facility. Thus, the fuel is transported and stored as a liquid until combustion. This means that energy is used for cooling during distribution and bunkering as well as on board of the ship. For the combustion of ammonia, it is important to highlight that the combustion emissions are based on assumptions and development targets for the engine, as the engine is still under development.

Lastly, it is important to highlight that project partners have discussed the LHV of ammonia throughout the project, since some project partners argue for a LHV of 18.6 MJ/kg instead of 17.2 MJ/kg. The 17.2 MJ/kg corresponds to liquid ammonia, while 18.6 MJ/kg corresponds to gaseous ammonia.

Initially, 17.2 MJ/kg was applied for the study since ammonia is injected to the ammonia engine as a liquid. Moreover, a high LHV of ammonia can result in optimistic ammonia consumption numbers. However, a partner states that some of the energy from the combustion chamber - which is used to evaporate the ammonia fuel - is regained as volume work during the cylinder process. Therefore, the LHV of ammonia is somewhere between the value for liquid ammonia and gaseous ammonia.

Based on these arguments, it is decided to keep the 17.2 MJ/kg in the default scenario, while the 18.6 MJ/kg will be analyzed in the sensitivity analysis (see **section 8.2**).

2.5.2 System boundaries for the attributional model

For the attributional model, **Figure 2.4** and **Figure 2.5** illustrate the system boundary for ammonia produced with H_2 from either electrolysis or ATR along with the input of VLSFO as pilot fuel needed for ignition of ammonia. As shown on **Figure 2.4** and **Figure 2.5**, the production and distribution of VLSFO is not modelled. Instead, standard carbon footprint for the fossil fuel comparator of 94 g CO_2-eq/MJ from RED II for WtW is applied for VLSFO (EC, 2023; EP & EUCO, 2018), since this approach is deemed most in line with the RED II guidelines. For the attributional model, ecoinvent is the applied background database (see description hereof in **section 2.6.2**).

Figure 2.4 shows the electrolysis-based pathway for ammonia production in the attributional model, with the system boundary being similar to the consequential modelling, except for the following: N_2 is produced at an ASU with allocation between the three outputs (N_2, O_2, and argon (Ar)). Additionally, allocation is applied between H_2 and O_2 from the electrolyser process.

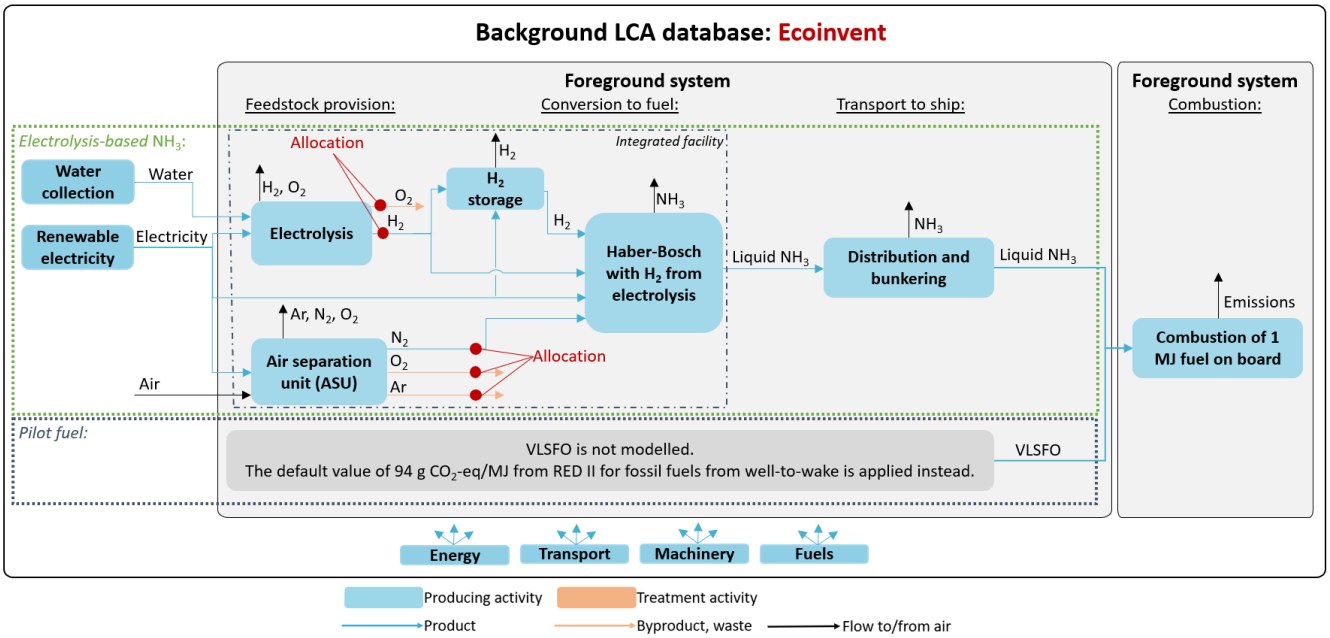

Figure 2.4: System boundary for the **attributional modelling** of ammonia produced with H_2 from electrolysis and with 9.6% e/e VLSFO.

Figure 2.5 shows the natural gas-based pathway for ammonia production in the attributional model, with the system boundary being similar to the consequential modelling, except for the following: Allocation is applied for outputs from the ASU of N_2 and the excess O_2, which is not used for the ATR process.

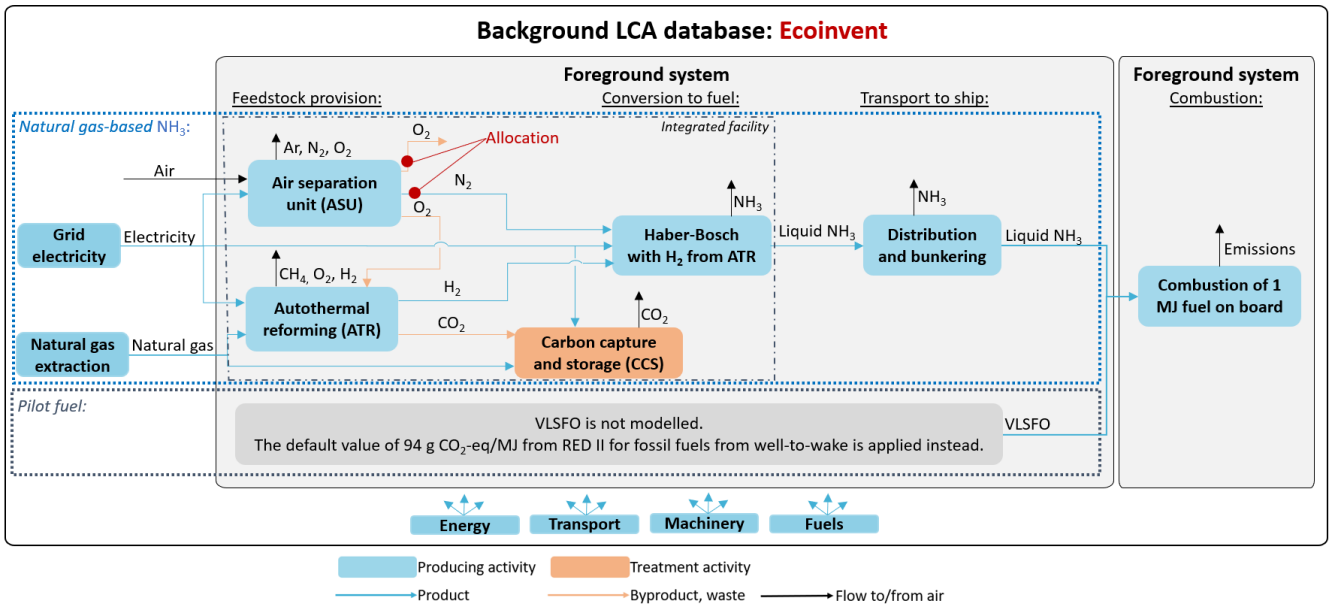

Figure 2.5: System boundary for the **attributional modelling** of ammonia produced with H_2 from autothermal reforming (ATR) and with 9.6% e/e VLSFO.

Just as for the consequential model, both **Figure 2.4** and **Figure 2.5** show that ammonia is liquefied at the production facility and therefore transported and stored as a liquid until combustion. Thus, energy is used for cooling during distribution and bunkering as well as on board of the ship. Moreover, the attributional model applies the same combustion emissions as the consequential model, making it important to highlight that the combustion emissions are based on assumptions and development targets for the engine, as the engine is still under development. Lastly, the attributional model also applies an LHV for ammonia of 17.2 MJ/kg in the default scenario.

2.6 Background databases

2.6.1 EXIOBASE: used in consequential model

In the consequential model, the EXIOBASE 3.3.16 hybrid version is used as the background database.

EXIOBASE is a global hybrid multi-regional environmentally extended input output database. The advantage of using an input output database instead of a process database, such as ecoinvent, is that it operates with a cut-off criterion at 0% and that it has a much more complete geographical scope than any process database. On the other hand, a disadvantage is a lower technological resolution. Moreover, EXIOBASE also includes fewer elementary flows than ecoinvent.

EXIOBASE (version 3.3.16) has the following characteristics:

- Product flows in hybrid units: EUR, kg, MJ.
- 43 countries, 5 Rest-of-the-world regions (see **Figure 2.6**)
- Base year: 2011
- 164 activities/products (this is equivalent to LCA processes in a conventional LCA database)
- 34 emissions, 22 resources, land use, water

Figure 2.6: Geographical coverage of EXIOBASE v3 with 43 countries and 5 rest-of-world regions (WA: rest of Asia; WE: rest of Europe; WF: rest of Africa; WL: rest of America; WM: rest of Middle East)

The used version of EXIOBASE is documented in two core papers: Stadler et al. (2018) and Merciai & Schmidt (2017a). The default version of EXIOBASE has been further refined and adapted to ensure increased completeness, by including indirect land use change, marginal electricity supply and capital goods:

- The applied indirect land use changes (iLUC) method from J. Schmidt et al. (2015) has been integrated in EXIOBASE (Schmidt & De Rosa, 2018a). Read more about land use changes in **Appendix 8: Consequential modelling of land use changes**
- A cause-effect based electricity model is integrated in EXIOBASE: The electricity model methodology is described in Muñoz et al. (2015) and its implementation in EXIOBASE is described in Merciai & Schmidt (2017a)
- Capital goods (investments) are integrated in the core input-output table.

EXIOBASE is used as a background system in the consequential model. Each element of the foreground system is matched with a product category in EXIOBASE. When linking to flows in the background system, average suppliers to the national markets are used, including specified import shares from other countries, and country-specific recycling rates and waste management data. The linking to activities in EXIOBASE can be done in both physical units (mass or energy) and in monetary units.

Note that minor changes have been made to the background database. These are presented in **Appendix 3: Changes made in background database.**

2.6.2 ecoinvent: used in the attributional model

ecoinvent is a process database, meaning that inventory data for each activity is collected bottom-up. Data are collected for one process at a time and can come from various sources. Process databases operate with a certain cut-off criterion, and thus some parts of the product system are excluded. Process databases such as ecoinvent operate at a high level of detail but a lower level of completeness than an input-output database such as EXIOBASE.

ecoinvent 'allocation, cut-off by classification' version 3.8 is applied for the attributional LCA study in this report, meaning economic allocation is applied in the background database and that the database was compiled in November 2021. There is no version of ecoinvent with energy allocation, thus ecoinvent with economic allocation is deemed the nearest match to the RED II approach for processes with multiple products

by partitioning/allocation, which is based on the energy content of the co-products or economic value if one or more products do not have an energy content (EC, 2023; EP & EUCO, 2018).

2.7 Geographical scope

The LCA study has a global geographical scope. Yet, groupings of countries and regions are needed for communicating results and for the results to be applicable by different actors. Grouping is done according to the International Energy Agency's (IEA) groupings of the world regions as well as grouping definitions prescribed by A.P. Moller - Maersk, thus, making 17 regions in total. The IEA groupings are seen below in **Figure 2.7**, and the groupings of regions in terms of EXIOBASE, the background database, are seen in **Table 2.4**.

Figure C.1 ▷ ***World Energy Outlook* main country groupings**

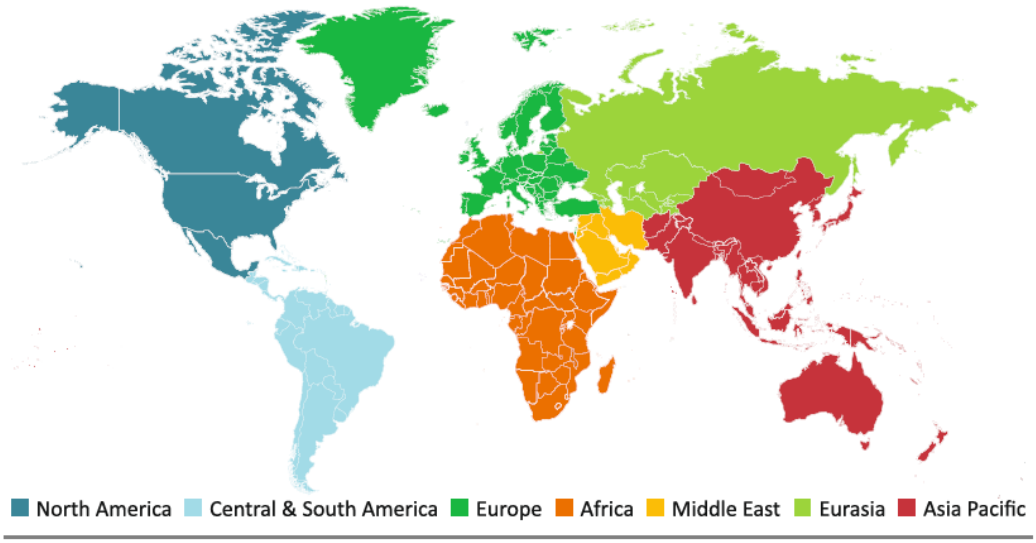

Note: This map is without prejudice to the status of or sovereignty over any territory, to the delimitation of international frontiers and boundaries and to the name of any territory, city or area.

Figure 2.7. Country groupings according to the IEA's World Energy Outlook (2023a).

Table 2.4. List of country groupings for which results are presented. The right column indicates correspondence with countries and regions in EXIOBASE (see appendix 1).

Country groupings	Countries included	EXIOBASE regions
IEA groupings		
North America	Canada, Mexico, US	CA, MX, US
Central and South America	Argentina, Bolivia, Brazil, Chile, Colombia, Costa Rica, Cuba, Curacao, Dominican Republic, Ecuador, El Salvador, Guatemala, Haiti, Honduras, Jamaica, Nicaragua, Panama, Paraguay, Peru, Suriname, Trinidad and Tobago, Uruguay, Venezuela, and other Central and South American countries and territories	BR, WL
Europe	EU regional grouping and Albania, Belarus, Bosnia and Herzegovina, North Macedonia, Gibraltar, Iceland, Israel, Kosovo, Montenegro, Norway, Serbia, Switzerland, Moldova, Turkey, Ukraine, UK	WE, AT, BE, BG, CH, CY, CZ, DE, DK, EE, ES, FI, FR, GB, GR, HR, HU, IE, IT, LT, LU, LV, MT, NL, NO, PL, PT, RO, SE, SI, SK, TR
Africa	North Africa and sub-Saharan Africa regional groupings	WF, ZA
Middle East	Bahrain, Iran, Iraq, Jordan, Kuwait, Lebanon, Oman, Qatar, Saudi Arabia, Syria, UAE, Yemen	WM
Eurasia	Caspian regional grouping (Azerbaijan, Iran, Turkmenistan, Kazakhstan) and Russia	WM, RU
Asia Pacific	Southeast Asia regional grouping and Australia, Bangladesh, China, India, Japan, Korea, Democratic People's Republic of Korea, Mongolia, Nepal, New Zealand, Pakistan, Sri Lanka, Chinese Taipei, and other Asia Pacific countries and territories	AU, CN_TW, ID, IN, JP, KR, WA
Sub-sets		
Brazil	Brazil	BR
China	China	CN_TW
India	India	IN
Indonesia	Indonesia	ID
Japan	Japan	JP
Latin America	Central and South America regional grouping, and Mexico	BR, WL, MX
Russia	Russia	RU
South Africa	South Africa	ZA
Southeast Asia	Brunei Darussalam, Cambodia, Indonesia, Lao, Malaysia, Myanmar, Philippines, Singapore, Thailand, Vietnam	WA, ID
US	US	US

2.8 Temporal scope

The results of the LCA study are aimed for being used for decision support in the choice of and in investments in alternative fuel systems for shipping from current (2024) and the next 5-10 years. It should be noted that choices or investments in fuel systems now have implications for the type of fuels used in shipping several years (decades) after the decision.

The results of the LCA study will be valid and can be used for decision support and for tracking performance over time by changing only the foreground data. The decisive factors for when results are not valid anymore are when the activities surrounding the fuel production change, namely when market responses to changes in supply and demand are different compared to what is modelled in the LCA. Since the future cannot be predicted without uncertainties, it is not possible to state exactly for how long the results are valid. Especially, the determination of marginal electricity mixes, i.e., which electricity technologies will respond to changes in demand for electricity, is associated with uncertainties.

The LCA study is based on foreground data from literature from 2001-2023, the most recent available data from the project partners, and the ecoinvent v.3.8 database, which includes data from approx. 1990-2021. The background database, EXIOBASE 3.3.16 hybrid version, includes data for 2011. Yet, due to the importance of electricity for ammonia production, the LCI data for the marginal electricity mixes in EXIOBASE has been updated with a time-series from 2017-2021 based on data from IEA (2023b), i.e., changes in electricity supply

from different technologies in this timeframe. Moreover, the data for the production of wind and solar electricity has also been updated with LCI data from Bonou et al. (2016) and Frischknecht et al. (2020). This updated LCI data are further described in **section 4.1**.

2.9 Cut-off criteria

2.9.1 Consequential model

The aim for the consequential model is to apply a cut-off at 0% (or at least close to 0%) meaning that no flows in the technosphere are left out. Nevertheless, some inputs for the foreground system, e.g., the services inputs for production facilities, are excluded due to lack of data. For the background database, the cut-off criteria of 0% is ensured for the background database by using the hybrid input-output database EXIOBASE, see **section 2.6**.

2.9.2 Attributional model

The attributional model applies a cut-off at >0% meaning that some flows in the technosphere are excluded, since it is stated in RED II and the delegated regulation 2023/1185 that "*emissions from the manufacture of machinery and equipment shall not be taken into account*" (EC, 2023; EP & EUCO, 2018). Moreover, the cut-off criteria in the applied background database, ecoinvent, is >0% and is not applied consistently. Yet, generally, in ecoinvent a high level of completeness is kept, but most flows of services are not accounted for, e.g., overhead, banking, marketing, consultancy, business travelling, cleaning, etc. Hence, part of the economy is excluded from ecoinvent.

2.10 Data sources and quality

The foreground data are obtained from various sources: The project partners have provided most of the LCI data for H_2, N_2, and ammonia production as well as combustion emissions for VLSFO and ammonia, while the remaining LCI data have been collected from literature, the ecoinvent database, or expert estimates. Further details are provided in the following paragraphs, while detailed data sources are reported in **chapter 5**.

The data from project partners for H_2, N_2, and ammonia production are based on established production facilities and has been provided in ranges for two data sets, 'stand-alone' and 'integrated' production. The 'stand-alone' production applies for scenarios, where H_2, N_2, and ammonia are produced at individual production facilities, while all three products are produced at the same facility for 'integrated' production. Thus, the provided values are average/typical values for these two plant designs estimated by the project partners based on their most recent available data. These data are therefore deemed to be of as high quality as possible given the technology's maturity level.

According to the data from project partners, the inputs to 'stand-alone' facilities are higher than the inputs to 'integrated' production facilities, as the latter are more efficient. Moreover, the data have been provided in ranges, since the project partners underline that the inputs will vary between production facilities, e.g., because of plant design leading to differences in energy efficiency, which can influence the reliability of a plant and how it is operated.

For this LCA study, it is assumed that H_2, N_2, and ammonia are produced at the same facility and the data for 'integrated' production is therefore applied. Yet, it is important to highlight that the data for 'integrated' production is provided in aggregated form. Thus, the data for 'stand-alone' production has been used to estimate the inputs to the H_2, N_2, and ammonia processes with the efficiency of an 'integrated' production.

Moreover, it is important to underline that the combustion emissions for ammonia on board the vessel are based on assumptions and development targets for the engine, as the engine is still under development. Moreover, particulate emissions are estimated based on data from Green Transition Denmark (2021), since this data point was not provided by project partners. Though the data from project partners is deemed to be a good estimate, the project partners have discussed the applied values, especially related to the N_2O emissions, since N_2O has a notable GWP100 impact. Thus, a sensitivity analysis is conducted in order to assess other possible N_2O emission values and how this impacts the LCIA results.

Additionally, a default gas slip of 0.3% is applied for all gases – except for the slip of CO_2 from carbon storage – throughout the product system, however, it is important to recognise that the slip of gases in reality will vary because of differences in, e.g., molecular mass, shape and/or size. Applying a default slip of 0.3% is therefore a limitation to the study. Nevertheless, as more precise data have not been obtained, a default slip of 0.3% is deemed acceptable, while the change in results with a higher slip is tested in the sensitivity analysis.

Other data gaps – e.g., data on distribution and bunkering as well as the necessary buildings, equipment, and machinery for H_2, N_2, and ammonia production – have been estimated based on data from the ecoinvent database due to lack of data from project partners and literature. Other data points, such as LCI data on CCS and H_2 storage has been obtained from scientific literature and has been deemed the best available data, even though it has not been possible to, e.g., specify the dimensions of the H_2 storage facility and align this with the ammonia production capacity. For CCS, a thorough sanity check of the energy requirement has been conducted, and because literature research shows that the energy requirement varies, the parameter is included in the sensitivity analysis.

Lastly, as a last resort, an expert estimate has been applied for the energy requirement for cooling of ammonia in both the distribution and bunkering phase as well as on board the ship before combustion. This parameter is also included in the sensitivity analysis since the applied value is an estimate.

Thus, to summarize, the included data are deemed to be of good quality or the best data available. Moreover, important parameters which may vary are analysed in the sensitivity analysis in order to assess their influence on the LCIA results.

2.11 Life cycle impact assessment method

The method used for LCIA is the Stepwise 2006 method, version 1.8, applying its midpoint indicators, which are explained in **'Appendix 2: Explanation of units in the Stepwise LCIA method**'. The Stepwise 2006 method is described and documented in Annex II in Weidema et al. (2008) and in Weidema (2009) and updates for nature occupation in Schmidt & de Saxcé (2016). Furthermore, the method has been updated with characterisation factors for 100 year global warming potential (GWP100) from IPCC (2021).

The GWP100 of H_2 is not included in IPCC (2021). Yet, according to Muñoz (2023), GWP100 of H_2 could be set to 12.8 kg CO_2-eq/kg. Thus, since H_2 is an important emission within this LCA study, the before-mentioned characterisation factor for H_2 is added to Stepwise 2006.

The characterization module of Stepwise is based on a combination of the Impact 2002+ method (Jolliet et al., 2003) and the EDIP 2003 method (Hauschild & Potting, 2005). Interpretation of results and conclusions are based on characterised results.

Additionally, GWP20 results are presented in **appendix 10** (external appendix) using characterisation factors from IPCC (2021). Note that the attributional GWP20 results are only presented for ammonia with 0% e/e VLSFO, since the WtW fossil fuel comparator of 94 g CO_2-eq/MJ only applies to GWP100. The GWP20 of H_2 is based on Muñoz (2023) as the study states that the GWP20 of H_2 is approximately three times the GWP100 value.

2.11.1 Impact categories

This report presents the environmental impact of the following impact categories:

- GWP100
- Nature occupation
- Acidification
- Eutrophication, aquatic and terrestrial
- Photochemical ozone, vegetation
- Respiratory inorganics
- Respiratory organics

The Stepwise method also includes six other impact categories: aquatic ecotoxicity, terrestrial ecotoxicity, ozone layer depletion, non-renewable energy, as well as carcinogen and non-carcinogen human toxicity. Yet, these impact categories are not included in this report, since EXIOBASE does not include important elementary flows to these six before-mentioned impact categories and their results would therefore be underestimated. Nevertheless, this is a limitation of the study, since ammonia emissions have an effect on non-carcinogen human toxicity as well as aquatic and terrestrial ecotoxicity, as characterisation factors for ammonia are included in these impact categories in the Stepwise LCIA method. However, since ammonia is the only direct emission in the foreground system with an effect on toxicity, it is deemed acceptable to exclude these impact categories, especially since there are considerable uncertainties related to quantification of toxicity in LCA studies (Chen et al., 2021).
Further description of the impact categories is included in **Appendix 2: Explanation of units in the Stepwise LCIA method.**

2.12 Time-dependent emission factors for CO_2 emissions

Since climate change effects are related to a certain threshold beyond which irreversible changes may occur, the timing of GHG emissions matters. The postponement of GHG emissions can for example buy time for technological progress and adaptation and delay or temporarily avoid radiative forcing (Brandão et al., 2013). This allows for a possible increase in the distance between the current GHG concentration in the atmosphere and the aim of limiting temperature rise to 2°C by year 2100 compared to pre-industrial levels, as stated in the Paris Agreement.

The timing of GHG emissions is especially relevant for this LCA study, as it includes CCS (see **section 5.1.1.2.1**). Thus, CO_2 is captured in year 0 and stored for >100 years, though part of the CO_2 is assumed to leak from storage throughout this time-period. Thus, the leakage of 1 kg CO_2 in year 1 has the same GWP100 effect as

emitting 0.9923 kg CO_2-eq in year 0, while the leakage of 1 kg CO_2 in year 99 has a GWP100 effect of 0.0365 kg CO_2-eq. The CO_2 emitted over 100 years are presented as the sum of time aggregated CO_2-eq under '*Carbon dioxide, as CO_2e (GWP aggr timing)*' in the relevant LCI tables.

Further details for the calculation of time-dependent emission factors for CO_2 emissions are described in Schmidt & Brandão (2013).

3 Life cycle inventory model framework

Due to the scope of the current project being wider than just following the ISO 14040/44 standards on LCA (ISO, 2006a, 2006b), this chapter on general life cycle inventory theory is needed. Life cycle results are calculated based on common data inputs, common emission calculation modules, while the linking of the flows is different in the consequential and attributional models. Therefore, the inventory needs to be split into two parts: Common calculations and linking (consequential/attributional model), see **Figure 3.1**.

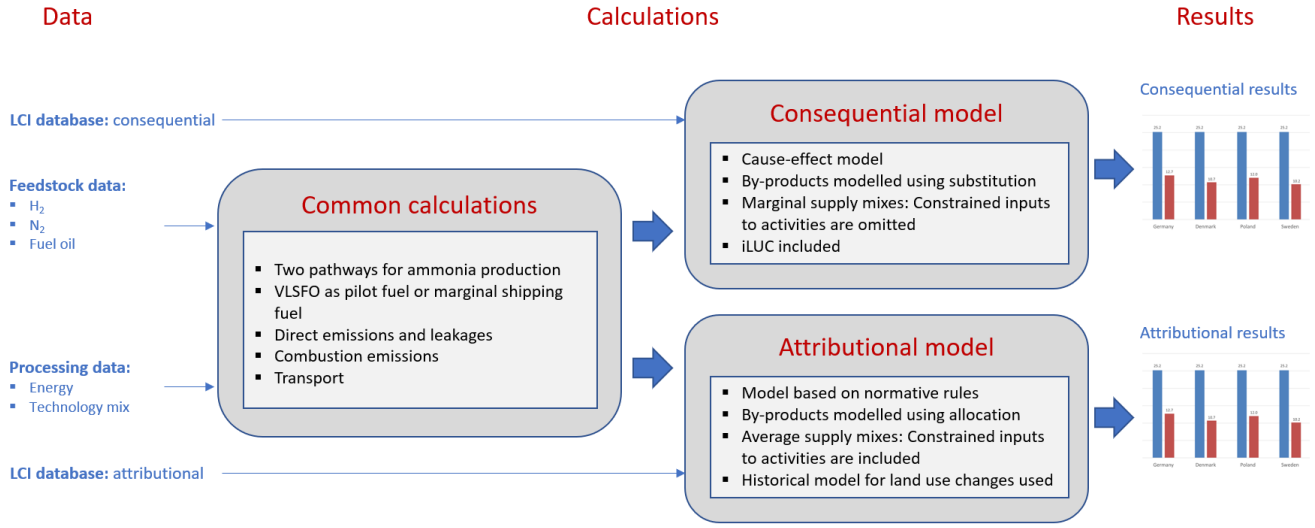

Figure 3.1. Life cycle inventory model with common data inputs and calculations and separate linking (consequential and attributional) to produce consequential and attributional results.

The ISO standards do not provide a framework that enables this, but the report from Schmidt & Dalgaard (2012) does, and is therefore used as a basis for this theoretical chapter on establishing the required life cycle inventory framework.

3.1 Product system, system boundary, and flows

A life cycle inventory consists of several interconnected activities (also known as 'processes'), see **Figure 3.2**. The activities are connected via 'products' and 'materials for treatment'. Here, 'products' includes determining and by-products (dependent co-products). Materials for treatment refers to waste/residual flows that are sent to treatment/recycling. An activity may have exchanges with the environment – i.e., emissions or other exchanges (such as radiation, noise, odour, etc.) *to* the environment, or resource inputs or other exchanges (such as occupation and transformation of land) *from* the environment. Activities are human, and they take place within the technosphere. Product and 'material for treatment' transactions also always take place between activities in the technosphere. When calculating the inventory result, it is the sum of all exchanges with the environment, elementary flows, that are calculated. The inventory result is used for calculating potential environmental impacts.

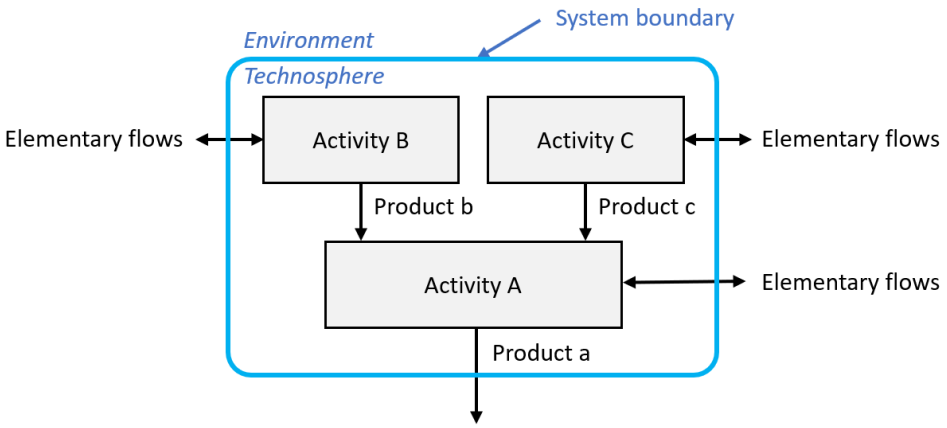

Figure 3.2. Product system with the system boundary between the environment and the technosphere. Within the technosphere are activities which are linked via product and 'material for treatment' flows. The illustrated system has a net output of 'product a'. Exchanges with the environment are flows that cross the system boundary. These are called elementary flows.

3.2 Different types of flows within the technosphere

Flows within the technosphere are differentiated based on the relevant characteristics in an LCI context. The distinction is made between:

- Reference products
- By-products
- Materials for treatment

Reference products are characterized by determining the production volume of an activity. A change in demand for a reference product affects the production volume of the activity. An activity can have one or more reference products, but most often there is only one reference product.

By-products are products which can directly displace a reference product supplied by another activity. The difference between reference products and by-products is that a change in demand for by-products does not change the production volume of the supplying activity.

Materials for treatment are outputs which do not directly displace a reference product supplied by another activity before it has been treated. Treatment activities may turn the material into a by-product, material for (further) treatment, and/or emissions. Like by-products, a change in demand for materials for treatment does not change the production volume of the supplying activity.

3.3 Different types of activities

A distinction is made between three types of activities:

- Transforming activities: Producing activities
- Transforming activities: Treatment activities
- Market activities

A transforming activity is defined as an activity that transforms some inputs to another type of output. There are two types of activities under this category: producing activities and treatment activities. Producing activities are traditional productive processes with a product output as their reference product. A treatment activity is characterised by receiving 'material for treatment'. Unlike the producing activities, a treatment activity has its reference flow as an input, i.e., the production volume of a treatment activity is determined by the amount of

incoming 'material for treatment'. Treatment activities include waste treatment, recycling, reuse, and other processing of material outputs of activities into products that can displace reference products. **Figure 3.3** illustrates an activity A that supplies a reference product *a* and a material for treatment. The material for treatment from activity A needs treatment in the treatment activity before the material can displace another product, here reference product *b* from activity B.

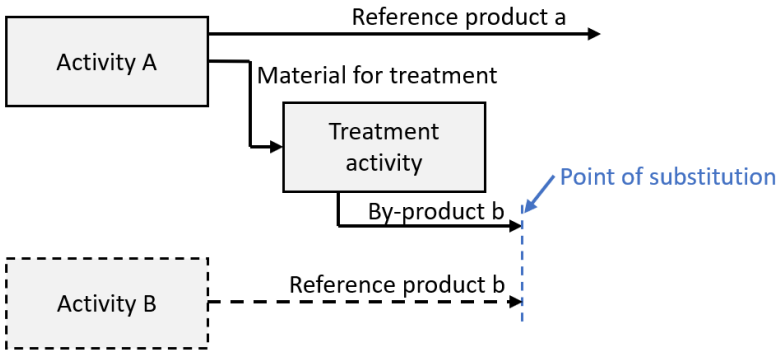

Figure 3.3. Naming conventions of different types of products and activities. The dotted line represents the substitution of product b and activity B.

3.4 Difference between substitution and allocation type I and allocation type II

Multiple-output activities are characterised by having more than one product output. When we demand only one of the co-products, we have a so-called allocation problem. In modelling terms, this problem can be solved either by substitution or by allocation.

In substitution, it is determined which one(s) of the co-products is/are determining, i.e., a change in demand for this/these products affects the production volume of the activity. The remaining co-products are dependant, i.e., the output of these products is not affected by a change in demand. Hence, a change in demand for determining products will also cause a change in the output of the dependent co-products. The general assumption in LCA is that demand determines supply. Thus, a change in output of dependant co-products will cause a reduction in the alternative supply of these products (this is regulated through the markets for substitutable products). The modelling and system boundary for a change in demand for the determining product A is illustrated in **Figure 3.4**. The technicalities and theory behind substitution are described in detail in Weidema et al. (2009).

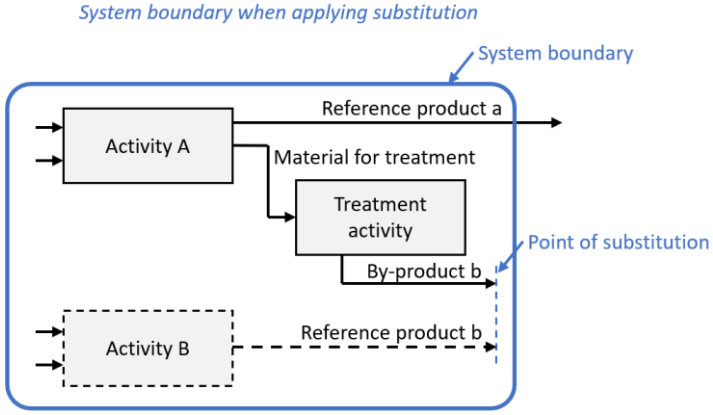

Figure 3.4. Modelling of multiple-output activities: Substitution. The dotted line represents the substitution of product b and activity B.

Figure 3.4 provides an intuitive illustration of how substitution is modelled. In practise the outputs of materials for treatment and by-products of activity A in **Figure 3.4** are moved to the input side and with a negative sign, see **Figure 3.5**.

Figure 3.5. Modelling of multiple-output activities: Substitution – in practise.

When allocation is applied for the modelling of co-products, each of the product outputs is converted to the unit of allocation. This can be monetary flow, mass, carbon, energy etc. The conversion is done on basis of product properties such as prices, dry matter content, carbon content, lower heating value etc. The relative outputs of the co-products measured in the allocation unit determine the portion of the multiple-output system that is ascribed to each co-product. The interactions with other product systems supplying substitutable products to the same market (the avoided activities in substitution) are not considered in allocation.

As illustrated in **Figure 3.6** and **Figure 3.7**, allocation can be carried out in two different ways, or at two different points. In the following, allocation as in **Figure 3.6** and **Figure 3.7** are referred to as type I and type II allocation, respectively.

Type I allocation represents allocation at the point of substitution (after treatment activities).

Type II allocation represents allocation immediately after the multiple output activity before treatment activities and not at point of substitution. Often, type II allocation implies that zero burden is allocated to materials for treatment when these are considered a waste flow.

For the attributional model in this report, type I allocation is applied.

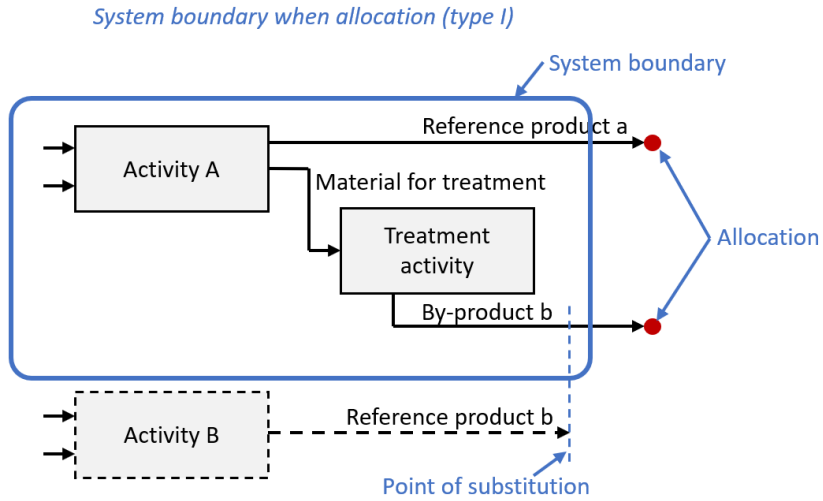

Figure 3.6. Modelling of multiple-output activities: Allocation (type I): allocation is done at point of substitution after the treatment activity.

System boundary when allocation (type II)

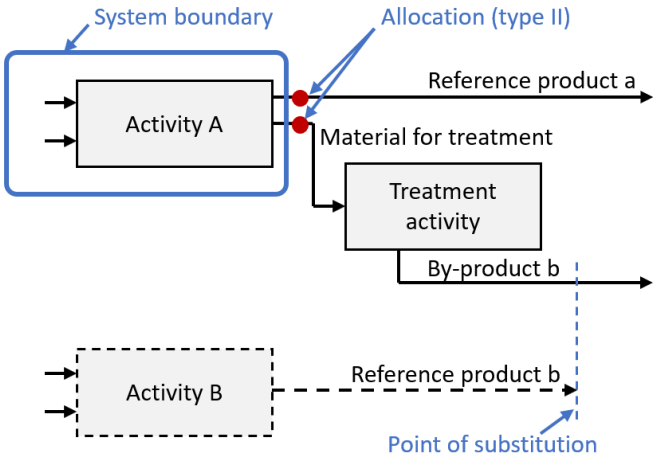

Figure 3.7. Modelling of multiple-output activities: Allocation (type II): allocation is done before treatment activity and not at point of displacement.

4 Life cycle inventory: general activities

For the production of VLSFO and ammonia with H_2 from either electrolysis or ATR, some general activities appear as inputs. These concern energy, transport, water as well as fuels including combustion emissions and are described in the following sections.

4.1 Electricity

For both ammonia production pathways and VLSFO, electricity is an input. Both for the specific Haber-Bosch process but also in the production of H_2 and N_2 as well as H_2 storage, CCS, VLSFO production, and distribution and bunkering.

To produce ammonia with H_2 from ATR with CCS, the electricity inputs are modelled as electricity from grid throughout the life cycle. This is done, since the input of electricity to natural gas-based ammonia production is minor, and since grid electricity is deemed most in line with the definition of 'blue ammonia' used within the industry. However, the LCIA results for ammonia with H_2 from ATR are calculated with renewable electricity in the sensitivity analysis (see **section 8.13.1.2**).

For production of ammonia with H_2 from electrolysis, the electricity inputs to the H_2, N_2, and ammonia production (cradle-to-gate) are modelled as either electricity from solar panels or electricity from wind turbines, while the electricity for distribution and bunkering comes from grid electricity. The input of solar or wind electricity from cradle-to-gate is used, since this is in line with the 'green ammonia' definition used within the industry.

The modelling of the grid electricity, electricity from solar panels or wind turbines is performed for each country included in the defined regions in **section 2.7**. The following sections will describe the modelling of the three electricity sources according to both the consequential and attributional approach.

4.1.1 Consequential modelling of electricity

4.1.1.1 Marginal electricity mix

The marginal electricity mixes are modelled using data from IEA (2023b) for the time-series 2017-2021, as this is the newest available data. The determination of the electricity grid mixes follows the same approach as described in Muñoz and Weidema (2023), which has also been applied in the consequential version of ecoinvent v3.4. This approach takes both technology lifespan, capital replacement rate and production trends. Thus, if the market trend and thereby the demand is increasing, it implies that the electricity is produced by new capacity, while if the market trend and demand is decreasing faster than the decrease from regular and planned phase-out of old technologies, the electricity is supplied by the least competitive existing suppliers/technologies.

All countries' electricity mixes are presented in **appendix 9** (external appendix).

Furthermore, as grid electricity is one of the important inputs for ammonia produced with H_2 from ATR with CCS, a sensitivity analysis is performed in order to assess, how sensitive the results are to the choice of data source, time-series, and time-series intervals for determining the marginal electricity mixes (**section 8.13.1.1**).

4.1.1.2 Electricity from wind power

The expansion in electricity from wind primarily stems from onshore wind turbines (IEA, 2024). Therefore, LCI data for a 3.2 MW onshore wind turbine from Bonou et al. (2016) is used for the modelling of electricity from wind (see **Table 4.1**). The power which the wind turbine can produce is calculated using **Equation 4.1** and the average wind speed for each country obtained from DTU et al. (2024).

Equation 4.1

$$Wind\ Power\ [W] = \frac{1}{2} * \rho * A * v^3$$

Where:

ρ is the density of the air (kg/m^3),
A is the cross-sectional area of the wind turbine's blades (m^2),
v is the average wind speed in each country (m/s)

The amount of wind power from **Equation 4.1** is recalculated to the annual production in kWh by multiplying with number of hours in a year and assuming a life span of 20 years for the wind turbine. Furthermore, the total annual production is calculated using the efficiency of each country's current wind power based on data from Ember (2024) for the countries wind power capacity and wind electricity generation for 2021. Thus, the total annual production is adjusted based on the achievable efficiency in each country.

The efficiency per country and the amount of wind turbine per kWh produced is listed in **Appendix 5: Share of wind turbine and PV plant per kWh electricity from wind and solar.**

Table 4.1: LCI summary for the 3.2 MW onshore wind turbine used to model electricity from wind in the **consequential** model (Bonou et al., 2016)

Flow	Unit	Wind turbine	Link to
Output: reference flow			
3.2 MW wind turbine	t	1,779.6	Reference flow
Inputs			
Cement	t	181.9	EXIOBASE: _69 Manufacture of cement, lime and plaster {region}
Aggregates, for concrete	t	1117.6	EXIOBASE: _32 Quarrying of stone {region}
Steel	t	365.9	EXIOBASE: _72 Manufacture of basic iron and steel and of ferro-alloys and first products thereof {region}
Iron	t	32.1	EXIOBASE: _72 Manufacture of basic iron and steel and of ferro-alloys and first products thereof {region}
Epoxy	t	21.4	EXIOBASE: _63 Chemicals nec {region}
Glass fibre	t	17.9	EXIOBASE: _65 Manufacture of glass and glass products {region}
Plastics	t	14.3	EXIOBASE: _64 Manufacture of rubber and plastic products (25) {region}
Aluminium	t	12.5	EXIOBASE: _76 Aluminium production {region}
Copper	t	12.5	EXIOBASE: _80 Copper production {region}
Wood	t	3.6	EXIOBASE: _50 Manufacture of wood and of products of wood and cork, except furniture; manufacture of articles of straw and plaiting materials (20) {region}

Besides the materials, a service input of 0.013 €/kWh is included, as this covers the operation and maintenance costs for a wind turbine (Steffen et al., 2020). The input is linked to '*114 Construction (45) {region}*' from EXIOBASE.

Lastly, the modelling of wind electricity also includes the land use changes associated with placing the wind turbine onshore. According to U.S. Department of Energy (2015), land transformation from onshore wind turbines vary between 0.0011 and 0.043 km^2/MW. The average hereof is applied for this study, resulting in a

land area of 32,000 m^2 for a 3.2 MW wind turbine. This is link to the elementary flows for '*Occupation, arable*' and '*Occupation, grassland*' for each of the 48 EXIOBASE countries using the share of arable land and grassland for each country determined based on data from FAOSTAT (2024). Note that the share of forest land is disregarded, as it is assumed that only arable land and grassland will be used for wind turbines. Thus, the sum of the arable land and grassland shares equals 100% for all 48 EXIOBASE countries. The indirect land use changes (iLUC) are also accounted for using the NPP0 factor for arable land and grassland for the 48 countries and by linking to the EXIOBASE activities '*Arable land, as ha*year-eq.*' and '*Grassland land, as ha*year-eq.*'. Modelling of land use changes is detailed in **Appendix 8: Consequential modelling of land use changes**.

4.1.1.3 Electricity from solar power

According to data from Philipps et al. (2023), the majority of electricity from photovoltaic (PV) panels are produced using mono-Si PV panels, making mono-Si the marginal technology for electricity from solar. Therefore, electricity from solar is modelled as being produced by a 570 kWp mono-Si solar plant. It is assumed that the plant is placed on the ground.

The bill of material data for the mono-Si solar plant is obtained from Frischknecht et al. (2020), dividing the plant into four main components: PV panels, mounting system, 500kW inverter and electric installation (see **Table 4.2**).

Table 4.2: LCI summary for the 570 kWp mono-Si solar plant used to model electricity from solar in the **consequential** model (Frischknecht et al., 2020).

Flow	Unit	PV plant	Link to
Output: reference flow			
570 kWp mono-Si PV plant	t	121.2	Reference flow
Inputs			
Inverter, 500kW	t	9.8	EXIOBASE: _88 Manufacture of electrical machinery and apparatus n.e.c. (31) {region}
Electric installation	t	1.6	EXIOBASE: _88 Manufacture of electrical machinery and apparatus n.e.c. (31) {region}
Mounting system	t	70.2	
- Aluminium		33.13%	EXIOBASE: _76 Aluminium production {region}
- Cement		0.75%	EXIOBASE: _69 Manufacture of cement, lime and plaster {region}
- Aggregates, for concrete		4.62%	EXIOBASE: _32 Quarrying of stone {region}
- Paper and cardboard		0.36%	EXIOBASE: _54 Paper {region}
- Plastics		0.02%	EXIOBASE: _64 Manufacture of rubber and plastic products (25) {region}
- Iron and steel		61.09%	EXIOBASE: _72 Manufacture of basic iron and steel and of ferro-alloys and first products thereof {region}
- Fabricated metal products		0.02%	EXIOBASE: _85 Manufacture of fabricated metal products, except machinery and equipment (28) {region}
PV panels, mono-Si		39.6	
- Plastics		11.24%	EXIOBASE: _64 Manufacture of rubber and plastic products (25) {region}
- Glass		67.01%	EXIOBASE: _65 Manufacture of glass and glass products {region}
- Aluminium		16.16%	EXIOBASE: _76 Aluminium production {region}
- Electrical machinery and apparatus		5.59%	EXIOBASE: _88 Manufacture of electrical machinery and apparatus n.e.c. (31) {region}

The amount of PV plant per kWh produced is calculated based on the annual production for a 570 kWp crystalline silicone plant with optimised slope and azimuth for each country based on the GIS tool from Joint Research Centre (2022) and a PV plant lifespan of 30 years. The amount of PV plant per kWh produced is listed in **Appendix 5: Share of wind turbine and PV plant per kWh electricity from wind and solar.**

Based on PV resources (2015), a service input of 0.06 €/kWh from the PV plant is included by linking to '*114 Construction (45) {region}*' from EXIOBASE. This is done, since PV resources (2015) states that the operation and maintenance costs range from 0,02 to 0,1 €/kWh.

Lastly, the modelling of solar electricity also includes the land use changes associated with installing the PV plant on the ground. This is done by linking the size of the plant (2,923 m^2 according to Frischknecht et al. (2020)) to the share of arable land and grassland in the 48 EXIOBASE countries to the elementary flows for '*Occupation, arable'* and '*Occupation, grassland*'. The share of arable land and grassland is determined based on data from FAOSTAT (2024). Note that the share of forest land is disregarded, as it is assumed that only arable land and grassland will be used for the PV plant. Thus, the sum of the arable land and grassland shares equals 100% for all 48 EXIOBASE countries. iLUC is also accounted for using the NPP0 factor for arable land and grassland for the 48 countries and linking to the EXIOBASE activities '*Arable land, as ha*year-eq.*' and '*Grassland land, as ha*year-eq.*'. Modelling of land use changes is detailed in **Appendix 8: Consequential modelling of land use changes**.

4.1.2 Attributional modelling of electricity

According to the delegated regulation 2023/1185 for RFNBOs, electricity from wind, solar, hydro, and geothermal has a carbon footprint of zero (EC, 2023). Thus, electricity from wind and solar in this report's attributional LCA study does not have an impact. Nevertheless, in the sensitivity analysis, it is assessed how much the carbon footprint changes if the GHG emissions from solar and wind electricity is accounted for (see **section 9.2**).

For the attributional grid electricity, average grid electricity mixes are obtained from ecoinvent v3.8. However, the average grid mixes have been modified, so there is no impact from wind, solar, hydro, and geothermal, as this is deemed most in line with the delegated regulation 2023/1185 for RFNBOs. This means that the share of electricity produced by wind, solar, hydro, and geothermal in an average grid mix in the attributional model has a carbon footprint of zero.

4.2 Natural gas

Natural gas is an important input to several processes, e.g., ATR and CCS. This section therefore describes how this is modelled in the consequential and attributional model, respectively.

4.2.1 Consequential modelling of natural gas

The input of natural gas is modelled using the EXIOBASE activity '*_22 Extraction of natural gas and services related to natural gas extraction, excluding surveying'* for each of the 48 EXIOBASE countries included in the defined regions in **section 2.7**. The EXIOBASE activity includes the environmental impacts from the extraction of the natural gas as well as the slip of methane from extraction. **Table 4.3** presents the methane slip for the 17 regions in the LCA study.

Table 4.3: Overview of methane slip from natural gas extraction for the 17 regions in the **consequential** LCA model.

Regions in the LCA study	Methane slip from natural gas extraction
Africa	0.58%
Asia Pacific	0.42%
Brazil	0.56%
Central & South America	0.63%
China	0.42%
Eurasia	0.63%
Europe	0.20%
India	0.44%
Indonesia	0.42%
Japan	0.45%
Latin America	0.66%
Middle East	0.57%
North America	0.49%
Russia	0.69%
South Africa	0.62%
Southeast Asia	0.57%
US	0.38%

Note that the EXIOBASE activity is in tonnes, so it is converted to GJ using a lower heating value of 49.5 MJ/kg for natural gas.

4.2.2 Attributional modelling of natural gas

In the attributional model, inputs of natural gas to ATR and CCS are linked to the ecoinvent process '*Natural gas, high pressure {GLO}*'. This means that there are no differences in impact from natural gas between the 17 regions included in the LCA study. The methane slip from the ecoinvent process is approximately 0.6%.

Note that the ecoinvent activity is in m^3 and has a lower heating value of 39 MJ/m^3 (EcoQuery, 2024). The m^3 is converted to GJ using a density of 0.79 kg/m^3 and a lower heating value of 49.5 MJ/kg for natural gas, which corresponds to the applied lower heating value for natural gas in the consequential model.

4.3 Process steam

Process steam is used for the VLSFO production and is assumed to be produced by a fuel mix consisting of biomass, coal, diesel, fuel oil, and natural gas for each country included in the defined regions in **section 2.7** and with a 90% efficiency. The following section describe how the fuel mixes are modelled in the consequential LCA study.

Note that the fuel mixes are not modelled for the attributional LCA study, since the standard carbon footprint for the WtW fossil fuel comparator of 94 g CO_2-eq/MJ from RED II will be applied (EC, 2023; EP & EUCO, 2018), as this approach is deemed most in line with the RED II guidelines.

4.3.1 Consequential modelling of process steam

The fuel mix for each country is based on data from the IEA for 2006-2011, thus determining the marginal supply mix for fuels used to produce steam for the same period as the data implemented in the background database, EXIOBASE. **Appendix 6: Country-specific fuel mixes in consequential LCA** presents the marginal fuel mix for each country as well as a concordance table for the background processes used to model the extraction/production of each fuel.

As the fuel mixes are combusted in order to produce the process steam, the combustion emissions are also included in the modelling of the process steam (see **section 4.4**).

4.4 Emission factors for fuels in the background system

Emission factors, densities, and calorific values are available for all relevant fuels in the product system, as shown in **Table 4.4**. Moreover, **Table 4.5** and **Table 4.6** present the background activities used for the consequential and attributional model, respectively. Note that combustion emissions from ammonia and VLSFO on board the ship are present in **section 5.4**.

Table 4.4. Emission factors, densities, and calorific values for relevant fuels in the product system (Nielsen et al., 2016, 2018; Schmidt & de Saxcé, 2016)

Parameter	Unit	Biomass	Coal	Diesel	Fuel oil	Natural gas
Properties						
Density	kg/m^3					0.8
Calorific value	GJ/t	19	24.3	43.1	42.7	49.5
Emission factors						
Carbon dioxide, fossil	kg/GJ		94.17	74	74	56.95
Methane	kg/GJ	0.015	0.0009	0.003	0.003	0.0017
Non-methane volatile organic compound (NMVOC)	kg/GJ	0.01	0.0012	0.0008	0.0008	0.002
Dinitrogen monoxide	kg/GJ	0.004	0.0014	0.0006	0.0006	0.001
Carbon monoxide	kg/GJ	0.24	0.01	0.015	0.015	0.015
Nitrogen oxides	kg/GJ	0.09	0.03	0.15	0.15	0.055
Sulphur dioxide	kg/GJ	0.025	0.009	0.023	0.023	0.0003
Particulates, <2.5 um	kg/GJ	3.38E-05	3.56E-07	3.33E-07	3.50E-07	6.98E-08

Table 4.5: Background activities used to model production and extraction of fuels in the **consequential** model.

Materials/fuels	LCI
Biomass	_18 Forestry, logging and related service activities {region}
Coal	_20 Mining of coal and lignite; extraction of peat {region}
Diesel	_57 Petroleum Refinery {region}
Fuel oil	_57 Petroleum Refinery {region}
Natural gas	_22 Extraction of natural gas and services related to natural gas extraction, excluding surveying {region}

Table 4.6: Background activities used to model production and extraction of fuels in the **attributional** model.

Materials/fuels	LCI
Biomass	Forestry {region}: *This is modelled based on material inputs to '_18 Forestry, logging and related service activities {region}' linked to ecoinvent processes*
Coal	Hard coal {region}| market for hard coal
Diesel	Petrol, low-sulfur {region}| market for
Fuel oil	Petrol, low-sulfur {region}| market for
Natural gas	Natural gas, high pressure, vehicle grade {region}| market for natural gas, high pressure

4.5 Transport

Ammonia and VLSFO are assumed to be transported from production facilities by ship and pipeline. Moreover, CO_2 is assumed to be transported by pipeline to storage. The following sections describe how sea and pipeline transport are modelled in the consequential and attributional approach.

4.5.1 Modelling of sea transport

4.5.1.1 Consequential modelling of sea transport

Transport by sea is modelled using the EXIOBASE activity '*124 Sea and coastal water transport'* for each of the 48 EXIOBASE countries included in the defined regions in **section 2.7**.

All input data on sea transport to the LCA model are based on transported amounts (t) and distance (km), and the inventory item of transport is given in units of tkm. In the EXIOBASE database, transactions of transport are accounted in monetary units (EUR). Therefore, the reference flow of the transport activities in EXIOBASE are converted from monetary units to tkm. This is done using the inputs of fuel in mass units in the EXIOBASE activities to calculate the fuel use per EUR of transport service (kg diesel/EUR). The amount of fuel used per tkm (kg diesel/tkm) is found in the ecoinvent database activity '*Transport, freight, sea, bulk carrier for dry goods'*. Combining these two data points, the reference flows of the EXIOBASE transport activities can be converted from monetary units to tkm and can be used in modelling.

4.5.1.2 Attributional modelling of sea transport

The sea transport for all 48 countries is linked to the ecoinvent activity *'Transport, freight, sea, bulk carrier for dry goods {GLO}'*. Since the same ecoinvent activity is used for all 48 countries, there is no difference in impact for sea transport between the regions in **section 2.7**.

4.5.2 Modelling of pipe transport

4.5.2.1 Consequential modelling of transport by pipeline

For CO_2 storage as well as distribution and bunkering of ammonia and VLSFO, pipeline is used as means of transport. According to Alfa Laval et al. (2020), ammonia is normally transported by onshore pipelines, while pipeline transport of CO_2 can both be onshore and offshore based on the storage location (Hongfang et al., 2020). In this LCA study, all transportation by pipeline is based on the onshore systems.

The LCI data for the construction of 1 km onshore pipeline is drawn from the ecoinvent activity '*Pipeline, natural gas, long distance, low capacity, onshore {GLO}| construction'.* These data are used since it has not been possible to find more representative data. Thus, it is assumed that both CO_2 and ammonia can be transported by pipelines for natural gas, even though project partners state that transport of CO_2 in natural gas pipelines may result in ductile fractures or dissolvement of non-metal components, while ammonia can be corrosive.

Moreover, the LCI data for onshore pipeline transport is drawn from the ecoinvent activity '*Transport, pipeline, long distance, natural gas {RoW}| processing',* which has an input of the first-mentioned ecoinvent activity. Because of the requirements in the Privacy Policy & End User Licence Agreement (EULA) from ecoinvent, the inputs are aggregated to the ones in **Table 4.7**, thus, the specific modelling is untraceable.

Note that the ecoinvent activity includes a lower slip than the default gas slip of 0.3% in this study, thus, the LCI data are modified to accommodate for this difference. Moreover, the slip of the transported gases is included in the CCS process (see **section 5.1.1.2.1**) and distribution and bunkering phase (see **section 5.3**).

Table 4.7. LCI summary of pipeline construction and transport in the **consequential** model. Data obtained from (ecoinvent, 2021).

Flow	Unit	Construction of pipeline	Pipeline transport	Link to
Output: reference flow				
Pipeline, construction	km	1		Reference flow
Pipeline, transport	tkm		1	Reference flow
Inputs				
Steel	kg	480,000		EXIOBASE: _72 Manufacture of basic iron and steel and of ferro-alloys and first products thereof {region}
Pitch	kg	2,320		EXIOBASE: _63 Chemicals nec {region}
Plastic	kg	4,640		EXIOBASE: _64 Manufacture of rubber and plastic products (25) {region}
Diesel	MJ	3,310,000		See **section 4.4**
Electricity	kWh		0.0989	See **section 4.1, 'Consequential modelling of electricity'**
Pipeline, construction	km		$2.8*10^{-9}$	Construction of pipeline

The input of pipeline, construction, to pipeline transport is very small because 1 km of pipeline can transport a large volume of gas in its lifetime. The $2.8*10^{-9}$ km/tkm corresponds to 363 million t of gas transported by 1 km pipeline during its lifetime.

4.5.2.2 Attributional modelling of transport by pipeline

The inputs to pipeline transport primarily relate to the construction of the pipeline, except for the input of electricity. According to RED II and delegated regulation 2023/1185, "*emissions from the manufacture of machinery and equipment shall not be taken into account*" (EC, 2023; EP & EUCO, 2018), thus, the impact from pipeline transport only stems from the electricity in the attributional model (see **Table 4.8**). Moreover, just as in **section 4.5.1.1**, the electricity input has been adjusted to match the default gas slip of 0.3%.

Table 4.8: LCI summary of pipeline transport in the **attributional** model. Data obtained from (ecoinvent, 2021).

Flow	Unit	Pipeline transport	Link to
Output: reference flow			
Pipeline, transport	tkm	1	Reference flow
Inputs			
Electricity	kWh	0.0989	See **section 4.1, Attributional modelling of electricity**

Note that the LCI data in **Table 4.8** has been modified to the default gas slip of 0.3% applied in this study.

4.6 Water

Water is an important input to several of the processes within the product system, since water is used as a feedstock for H_2 production through electrolysis, and because it is used in ATR to convert carbon monoxide (CO) to carbon dioxide (CO_2).

The LCA study applies surface/ground water as the default scenario. However, as the geographical scope of the study is global, some countries and regions will likely rely on desalination to some extent. Therefore, an additional set of results will be presented with desalinated water in the sensitivity analysis (see **section 8.1**).

4.6.1 Consequential modelling of water

4.6.1.1 Consequential modelling of surface and groundwater

The EXIOBASE activity '*113 Collection, purification and distribution of water*' is used to model water collection for each of the 48 countries in EXIOBASE whereafter the regions are created as described in **section 2.7.**

4.6.1.2 Consequential modelling of desalinated water

Desalinated water may be used if surface or ground water is unavailable. It is assumed that desalination is performed using reverse osmosis as this is the dominant method (Ludwig, 2022).

The electricity input is obtained from Aleisa and Al-Shayji (2018), while the remaining data are obtained from the ecoinvent processes '*Water works, capacity 6.23E10l/year {GLO}| water works construction, capacity 6.23E10l/year, seawater reverse osmosis, conventional pretreatment | Conseq,*' and '*Tap water {GLO}| tap water production, seawater reverse osmosis, conventional pretreatment, baseline module, single stage | Conseq, U*'. Because of the requirements in the EULA from ecoinvent, the inputs are aggregated to the ones in **Table 4.9**, thus, the specific modelling is untraceable.

Table 4.9: LCI summary for desalination in the **consequential** model (Aleisa & Al-Shayji, 2018; ecoinvent, 2021).

Flow	Unit	Desalination	Link to
Output: reference flow			
Water (H_2O), desalinated	t	1	Reference flow
Inputs			
Water (H_2O) - to desalination	t	2.63	Resource: Water, salt, ocean
Electricity	MWh	0.01	See **Section 4.1**
CAPEX			
CAPEX, desalination plant	t	0.00003	See **Section 4.7.1.2.2**
Outputs			
Brine	t	1.59	Emissions to sea*
Evaporated water	t	0.04	Emissions to air*

**Note that the outputs of evaporated water and brine are only showed to ensure mass balance but not modelled, since the input of sea water (including the substances in the brine) has a net effect of zero, since the brine and evaporated water are returned to the environment after the desalination process.*

4.6.2 Attributional modelling of water

4.6.2.1 Attributional modelling of surface and groundwater

The ecoinvent activity '*Tap water {country}| market for*' is used to model the collection of surface and groundwater. However, ecoinvent does not include the same countries/regions as EXIOBASE, therefore, **Table 4.10** presents the concordance between the ecoinvent tap water activities and the 48 countries within the LCA study. The EXIOBASE countries are grouped into regions as described in **section 2.7.**

Table 4.10: Concordance between ecoinvent activities for tap water and EXIOBASE countries/regions

ecoinvent activity and country code	EXIOBASE countries and regions
Tap water {BR}| market for tap water	BR
Tap water {CH}| market for	CH
Tap water {Europe without Switzerland}| market for	WE, AT, BE, BG, CY, CZ, DE, DK, EE, ES, FI, FR, GB, GR, HR, HU, IE, IT, LT, LU, LV, MT, NL, NO, PL, PT, RO, SE, SI, SK, TR
Tap water {IN}| market for tap water	IN
Tap water {RoW}| market for	AU, CA, CN_TW, ID, JP, KR, MX, US, RU, WL, WF, WM, WA,
Tap water {ZA}| market for tap water	ZA

4.6.2.2 Attributional modelling of desalinated water

The LCI data for desalination in the attributional model is similar to the data in **Table 4.9**, except there is no input of CAPEX, since it is stated in RED II and the delegated regulation 2023/1185 that "*emissions from the manufacture of machinery and equipment shall not be taken into account*" (EC, 2023; EP & EUCO, 2018). Moreover, the input of electricity is linked to the attributional electricity modelling described in **'Attributional modelling of electricity'**.

4.7 CAPEX

In the **consequential model**, the term 'CAPEX' is used to describe and include the required machinery, equipment, and infrastructure, which are needed in order to provide the reference flow of the product systems, e.g., 1 MJ of shipping fuel. Therefore, this section describes how the LCA study has estimated the materials needed to construct the ammonia and VLSFO production and distribution facilities, followed by an estimate of the share of these facilities needed to produce or supply 1 t of fuel. As the facilities produce and distribute a vast amount of ammonia and VLSFO in their lifespans, the input of CAPEX per 1 MJ is therefore often quite small.

Since both ammonia and VLSFO are relatively new fuels within the shipping industry, it has been difficult for the project partners to provide data on production facilities and data from the scientific literature has also been limited. Yet, the LCA study includes CAPEX for all processes based on the best available data.

Note that CAPEX does not include inputs related to services, e.g., research, consultancy, banking services, marketing, etc. due to lack of data. Environmental impacts related to services are included in the background database, EXIOBASE, as it has a cut-off criterion at 0%.

CAPEX is not included in the **attributional model**, since it is stated in RED II and the delegated regulation 2023/1185 that "*emissions from the manufacture of machinery and equipment shall not be taken into account*" (EC, 2023; EP & EUCO, 2018).

4.7.1 Consequential modelling of CAPEX

The consequential model includes CAPEX activities for VLSFO production, ammonia production, H_2 storage, desalination, as well as distribution and bunkering for both fuels (see overview in **Table 4.11**).

It is assumed that the CAPEX activity for a VLSFO refinery includes buildings, equipment, and machinery necessary for the ASU and ATR H_2 production since the H_2 and VLSFO is assumed to be produced at the same facility location. The same is the case for N_2, H_2, and ammonia production as well as CCS at ammonia production facilities with H_2 from ATR. This means that there is no difference between the CAPEX for ammonia produced with H_2 from electrolysis and H_2 from ATR due to lack of data.

Individual CAPEX activities are created for H_2 storage and desalination since these facilities are assumed to be 'add-ons' to the existing ammonia production facilities.

Table 4.11: Overview of CAPEX activities and the facilities, which are covered in this LCA study

CAPEX for:	VLSFO production	Ammonia production	H_2 storage	Desalination	Distribution and bunkering
Assumed to include the necessary buildings, equipment, and machinery for:	ASU ATR Desulphurisation See more in **section 4.7.1.1**	There is no difference in CAPEX for the two ammonia pathways due to lack of data. Thus, this CAPEX activity is assumed to cover the necessary buildings, equipment, and machinery for: • N_2 production • H_2 production (electrolysis/ATR) • CCS (if ATR H_2 production) • Liquefaction of ammonia This is described in detail in **section 4.7.1.2**	An 'add-on' to the ammonia production facility with H_2 from electrolysis. See details in **section 4.7.1.2.1**	An 'add-on' to all production facilities when desalinated water is used. See details in **section 4.7.1.2.2.**	Distribution and bunkering infrastructure is assumed to be the same for ammonia and VLSFO. This is further explained in **section 4.7.1.3**

4.7.1.1 CAPEX for VLSFO production

The CAPEX activity for VLSFO production is based on LCI data obtained from the ecoinvent activity *'Petroleum refinery {RER}| construction'* which is presented in aggregated form in **Table 4.12** due to ecoinvent's EULA.

Table 4.12 shows that one VLSFO production facility (1 p) is constructed using a total of 16,323 t materials, with the main inputs being cement as well as metals and steel. The production capacity of the VLSFO facility is described in **section 5.2**.

Table 4.12: LCI summary for CAPEX for VLSFO production in the **consequential** model (ecoinvent, 2021).

	Unit	CAPEX for VLSFO production	Link to
Output: reference flow			
VLSFO production facility	p	1	Reference flow
Inputs:			
Metals and steel	t	4,648	EXIOBASE: _72 Manufacture of basic iron and steel and of ferro-alloys and first products thereof {region}
Concrete	t	1,089	See **section 'Consequential modelling of concrete'**
Cement	t	10,316	EXIOBASE: _69 Manufacture of cement, lime and plaster {region}
Stone wool	t	30	EXIOBASE: _71 Manufacture of other non-metallic mineral products n.e.c. {region}
Plastics	t	48	EXIOBASE: _64 Manufacture of rubber and plastic products (25) {region}
Chemicals	t	192	EXIOBASE: _63 Chemicals nec {region}

4.7.1.2 CAPEX for ammonia production

The CAPEX activity for ammonia production is based on generic data for a chemical production plant due to lack of more specific data. As stated earlier, it is assumed that the CAPEX required for production of H_2 and N_2 is included in the overall ammonia production facility, which is also assumed to be the case for CAPEX for CCS at ammonia production facility with H_2 from ATR. Thus, the CAPEX activity is the same for ammonia production with H_2 from electrolysis and ATR.

The CAPEX for ammonia production is based on chemical production in Germany as this country is one of the largest producers of chemicals (GTAI, 2021). Therefore, the activity *'_63 Chemicals nec {DE}'* in EXIOBASE is selected, with a total production of 17.1 Mt chemicals. The approach is to select the relevant inputs for CAPEX,

e.g., cement, bricks, construction, aluminium etc. The overview of activities selected can be seen in **Appendix 7: CAPEX for German chemical industry**, where the total input of material and machinery for chemical production is 17.8 Mt.

One of the relevant inputs is *'114 Construction (45) {DE}'* with an amount of 385 MEUR2011. To convert this unit into t for '*_63 Chemicals nec {DE}'*, it is necessary to include the activity '*114 Construction (45) {DE}'*, which has a reference flow of 293,499 MEUR2011 in EXIOBASE. The inputs of CAPEX materials in '*114 Construction (45) {DE}'* are 561 Mt. When normalizing these inputs, the total amount is 1,913 t/MEUR2011. Now the total CAPEX for '*_63 Chemicals nec {DE}'* can be calculated by taking the 385 MEUR2011 input of construction and multiply it with 1,913 t/MEUR2011 added with 17.8 Mt of the other CAPEX inputs. By normalizing this, the result is 1.0866 g CAPEX/t product. Thus, it is assumed that 1.0866 g CAPEX/t ammonia is representative for the assets involved in the ammonia production in this study.

The composition of the ammonia production facility is based on LCI data from the ecoinvent activity '*Chemical factory, organics| construction | Conseq, U*'. The ecoinvent activity for an organic chemical factory has been chosen since it is deemed the closest match to an ammonia production facility. Because of the requirements in the EULA from ecoinvent, the LCI data are aggregated and presented in **Table 4.13.**

Table 4.13 shows that a total of 105,514 t materials are needed to construct one ammonia production facility (1 p), with the primary components being concrete, clay bricks, metals and steel, as well as cement. With a CAPEX input of 1.0866 g CAPEX/t ammonia, the total production capacity is assumed to be 97,105 Mt in the facility's lifespan.

Table 4.13: LCI summary for CAPEX for ammonia production in the **consequential** model. The data are from ecoinvent (2021).

	Unit	CAPEX for ammonia production	Link to
Output: reference flow			
Ammonia production facility	p	1	Reference flow
Inputs:			
Metals and steel	t	12,411	EXIOBASE: _72 Manufacture of basic iron and steel and of ferro-alloys and first products thereof {region}
Concrete	t	46,118	See **section 'Consequential modelling of concrete'**
Cement	t	10,316	EXIOBASE: _69 Manufacture of cement, lime and plaster {region}
Electronics	t	515	EXIOBASE: _88 Manufacture of electrical machinery and apparatus n.e.c. (31) {region}
Stone wool	t	443	EXIOBASE: _71 Manufacture of other non-metallic mineral products n.e.c. {region}
Glass	t	534	EXIOBASE: _64 Manufacture of rubber and plastic products (25) {region}
Plastics	t	495	EXIOBASE: _64 Manufacture of rubber and plastic products (25) {region}
Clay bricks	t	29,248	EXIOBASE: _68 Manufacture of bricks, tiles and construction products, in baked clay {region}
Wood	t	4,094	EXIOBASE: _50 Manufacture of wood and of products of wood and cork, except furniture; manufacture of articles of straw and plaiting materials (20) {region}
Copper	t	1,340	EXIOBASE: _80 Copper production {region}

4.7.1.2.1 CAPEX for hydrogen storage

An individual CAPEX activity for H_2 storage is modelled since this facility is assumed to be an 'add-on' to the existing production facility for ammonia produced with H_2 from electrolysis. The LCI for the H_2 storage facility is based on Wulf and Zapp (2018) and is presented in **Table 4.14**.

Table 4.14 shows that a total of 47,885 t materials are needed to construct one H_2 storage facility (1 p) and that the facility mainly consists of concrete. The amount of CAPEX is assumed to be 1.0866 g/t stored H_2 as no data are provided from project partners nor can be found in scientific literature. Thus, the amount of CAPEX per t stored H_2 is the same as per t ammonia, as described in **section 4.7.1.2** and it results in an assumed storage capacity of 44,069 Mt H_2 in the facility's lifespan.

Table 4.14: LCI summary for CAPEX for H_2 storage for the **consequential** model (Wulf & Zapp, 2018)

	Unit	CAPEX for H_2 storage	Link to
Output: reference flow			
Hydrogen (H_2) storage facility	p	1	Reference flow
Inputs:			
Metals and steel	t	1,115	EXIOBASE: _72 Manufacture of basic iron and steel and of ferro-alloys and first products thereof {region}
Concrete	t	46,620	See **Section 'Consequential modelling of concrete'**
Copper	t	150	EXIOBASE: _80 Copper production {region}

4.7.1.2.2 CAPEX for desalination plant

An individual CAPEX activity for desalination plant is modelled since this facility is assumed to be an 'add-on' to the existing production facility for ammonia and VLSFO.

The LCI data for the desalination plant is based on the ecoinvent activity *'Water works, capacity 6.23E10l/year {GLO}| water works construction, capacity 6.23E10l/year, seawater reverse osmosis, conventional pretreatment | Conseq, U'*. According to ecoinvent, the plant has a lifespan of 30 years and produces 170,500 m^3 desalinated water per day, which is used to calculate the amount of CAPEX per t desalinated water. The LCI data are presented in aggregated form in **Table 4.15** due to the requirements in the EULA from ecoinvent.

Table 4.15 shows that a total of 55,297 t materials are needed to construct one desalination facility (1 p). Moreover, the main material input is concrete.

Table 4.15. LCI summary for CAPEX for desalination plant for the **consequential** model (ecoinvent, 2021).

	Unit	CAPEX for desalination	Link to
Output: reference flow			
Desalination facility	p	1	Reference flow
Inputs:			
Metals and steel	t	1087	_72 Manufacture of basic iron and steel and of ferro-alloys and first products thereof {region}
Concrete	t	44,936	See **Section 'Consequential modelling of concrete'**
Plastics	t	273	_64 Manufacture of rubber and plastic products (25) {region}
Charcoal	t	5,690	_63 Chemicals nec {region}
Gravel	t	902	_32 Quarrying of stone {region}
Silica sand	t	2,410	_33 Quarrying of sand and clay {region}

4.7.1.3 CAPEX for distribution and bunkering of ammonia and very low sulphur fuel oil

The CAPEX activities for distribution and bunkering of ammonia and VLSFO is obtained from the ecoinvent activity '*Infrastructure, for regional distribution of oil product {RoW}| construction*' as it has been deemed the most representative data available. The data may be an underestimation for distribution and bunkering of ammonia since the fuel is transported as a liquid and therefore requires cooling. This is therefore a limitation of the study. The applied LCI data are presented in aggregated form in **Table 4.16** due to the requirements in the EULA from ecoinvent.

The distribution and bunkering infrastructure in **Table 4.16** has a total material input of 16,445 t. Moreover, the infrastructure is assumed to have a capacity of approximately 9,615 Mt in its lifespan. Thus, the share of infrastructure needed to transport one t of ammonia or VLSFO is estimated to 1.7 g/t.

Table 4.16: LCI summary for distribution and bunkering CAPEX for ammonia and VLSFO for the **consequential** model (ecoinvent, 2021)

	Unit	CAPEX for VLSFO and ammonia: Distribution and bunkering CAPEX	Link to
Output: reference flow			
Distribution and bunkering infrastructure	p	1	Reference flow
Inputs:			
Metals and steel	t	1,957	_72 Manufacture of basic iron and steel and of ferro-alloys and first products thereof {region}
Concrete	t	11,481	See **Section 'Consequential modelling of concrete'**
Cement	t	772	EXIOBASE: _69 Manufacture of cement, lime and plaster {region}
Stone wool	t	189	_71 Manufacture of other non-metallic mineral products n.e.c. {region}
Glass	t	64	_64 Manufacture of rubber and plastic products (25) {region}
Plastics	t	77	_64 Manufacture of rubber and plastic products (25) {region}
Clay bricks	t	1,530	_68 Manufacture of bricks, tiles and construction products, in baked clay {region}
Gravel	t	300	_32 Quarrying of stone {region}
Pitch	t	75	_63 Chemicals nec {region}

4.7.2 Consequential modelling of concrete

EXIOBASE does not include an activity for concrete production. Therefore, concrete production is modelled using a composition of 86% sand/gravel and 14% cement (Damvad Analytics et al., 2016). The LCI data for concrete is summarized in **Table 4.17**.

Table 4.17. LCI summary for concrete production for the **consequential** model (Damvad Analytics et al., 2016)

Flow	Unit	Amount	Link to
Output: reference flow			
Concrete	t	1	Reference flow
Inputs:			
Sand/gravel	t	0.86	EXIOBASE: _32 Quarrying of stone {region}
Cement	t	0.14	EXIOBASE: _69 Manufacture of cement, lime and plaster {region}

5 Life cycle inventory: specific activities

This chapter presents the LCI data for the specific activities in the foreground of the LCA model, which includes the provision of feedstock, conversion to fuel, distribution and bunkering, as well as the fuel combustion. Note that production of fuel feedstock and the fuel production is modelled to take place at an 'integrated' facility, meaning that H_2, N_2, and ammonia are produced at the same production facility. Moreover, the H_2 for desulphurisation is modelled to take place at the VLSFO production facility.

The LCA study models two production pathways for ammonia (see **section 5.1**), with the main difference being the H_2 production (electrolysis or ATR). The production of the pilot fuel, VLSFO, is described in **section 5.2**, while the distribution and bunkering for the fuels is outlined in **section 5.3**. Lastly, the combustion of ammonia and VLSFO is detailed in **section 5.4**.

Industrial experts and the project partners have provided most of the LCI data for H_2, N_2, and ammonia production as well as combustion emissions for VLSFO and ammonia. The remaining LCI data have been collected from literature, the ecoinvent database, or expert estimates. Note that project partners highlight that values in the LCI tables may give the impression that the energy and material inputs are fixed and do not vary. Project partners underline that the inputs will vary between production facilities, e.g., because of plan design leading to differences in energy efficiency. The partners also stress that the energy efficiency can be influenced by the reliability of a plant and how it is operated. Thus, it is therefore important to note that the values in the LCI tables should only be seen as 'typical' inputs.

Specifically for gas slips, a project partner explains that the slip of gases has not been measured directly yet. However, based on process flow and process safety measurements, the partner expects the gas slips to be very small. On the other hand, other partners have argued that it is unrealistic to have a slip of zero, since all gases are fugitive and hard to contain. Thus, a slip of 0.3% has been assumed for all gases – except for the slip of CO_2 from carbon storage – based on Bertagni et al. (2023) since it is one of the lower values presented in literature.

Note that the 0.3% slip from Bertagni et al. (2023) relates to the slip of natural gas and ammonia. Yet, for this LCA study, it is assumed that the 0.3% is applicable for all gases within the product system, except the CO_2 slip from carbon storage. However, it is important to recognise that the slip of gases in reality will vary because of differences in, e.g., molecular mass, shape and/or size, and applying a default slip of 0.3% is therefore a limitation to the study. Nevertheless, as more precise data have not been obtained, a default slip of 0.3% is deemed acceptable, while the change in results with a higher slip is tested in the sensitivity analysis (see **chapter 8**).

5.1 Ammonia production pathways

The production pathways for ammonia with H_2 from either electrolysis or ATR are illustrated on **Figure 2.2-Figure 2.3** and **Figure 2.4-Figure 2.5** for the consequential and attributional model, respectively. The figures show that the Haber-Bosch process is the same for the two pathways regardless of the modelling approach, except for the source of the electricity. The N_2 input stems from an ASU except for the consequential modelling of electrolysis-based ammonia, where the N_2 input comes from avoided vented of N_2. The ASU also provides the O_2 input to the ATR process, which produces H_2 for natural gas-based ammonia in both modelling approaches. ATR also provides H_2 from the desulphurisation of VLSFO in the consequential model. Lastly, the production and distribution of VLSFO is not modelled in the attributional model, since the standard carbon

footprint for the fossil fuel comparator of 94 g CO_2-eq/MJ from RED II for WtW is applied. This is deemed most in line with the RED II guidelines.
In the following sections, the production of H_2, N_2, and ammonia are detailed for both LCA models. Note that the demand for ammonia as shipping fuel will not affect the production of fertilizer, since none of the inputs to the production are constrained, and since the production of ammonia is expected to be met by new capacity.

5.1.1 Hydrogen production

The H_2 production is the main differentiator between the two ammonia pathways in this LCA study. The H_2 is either produced from water through electrolysis or from natural gas through ATR.

5.1.1.1 Hydrogen from electrolysis

H_2 is produced through electrolysis by using electricity to separate H_2 and O_2 in water molecules. The LCI data are presented in **Table 5.2**. Note that a project partner highlights that this set-up assumes that the electrolyser is flexible and therefore does not have ramp limitations and there is no impact on ware. As for most gases in the product system, a default slip of 0.3% is applied for H_2, with a higher slip being tested in the sensitivity analysis (see **section 8.7**).

According to an industrial expert, the electricity consumption for electrolysis may vary from 50 to 60 MWh/t H_2. Therefore, this parameter is tested in the sensitivity analysis (see **section 8.12**). Yet, according to the data for the project partner, the energy requirement for electrolysis tends to be in the lower end of the range, when the ammonia is produced at an 'integrated' plant, meaning that the H_2, N_2, and ammonia are produced at the same plant. In **Table 5.2**, an energy requirement of 52.24 MWh/kg H_2 is applied, as it is assumed that the H_2, N_2, and ammonia are produced at the same facility in this LCA study. This also corresponds to the assumptions related to CAPEX for the ammonia production facility described in **section 4.7.1.2**.

O_2 is a by-product from the electrolyser, which is possible to utilise, however, since Krishnan et al. (2024) state that O_2 from electrolysers is currently vented to the atmosphere, the O_2 is modelled as emissions to air in the consequential model.

For the attributional model, O_2 is considered a co-product hence allocation is applied. Yet, since O_2 does not have an energy content, economic allocation must be applied using "*the average factory-gate value of the products over the last three years*" (EC, 2023; EP & EUCO, 2018). The average economic value of H_2 and O_2 is obtained from the UN Comtrade Database with 2020-2022 data being the newest available (see **Table 5.1**).

Table 5.1: Economic data for 2022-2020 for H_2 and O_2 (United Nations, 2022)

	Total trade volume 2022-2020	Total trade value 2022-2020	Average price	Allocation factor
Unit	**t**	**US$**	**US$/t**	**%**
Hydrogen (H_2)	337,818	1,315,941,888	3,895	71%
Oxygen (O_2)	7,136,466	1,385,850,235	194	29%

The outputs of H_2 and O_2 are multiplied with the average price per t, resulting in an economic allocation of 71% and 29%, respectively. In **Table 5.2**, the allocation factor for H_2 is applied to the LCI data for the attributional LCA.

Table 5.2: LCI summary for H_2 production from electrolysis from industrial experts and Bertagni et al. **(2023)** for both the **consequential** model and **attributional** model.

Flow	Unit	H_2 production, electrolysis		Link to
Output: reference flow		**Consequential**	**Attributional**	
Hydrogen (H_2)	t	1	1	Reference flow
Inputs:				
Water (H_2O)	t	12.5	12.5*71%	See **section 4.6**
Electricity, solar or wind	MWh	52.4	52.4*71%	See **section 4.1**
Emissions to air				
Hydrogen (H_2) slip	t	0.003	0.003*71%	Emissions to air
Oxygen (O_2) slip	t	0.024	0.024*71%	
Oxygen (O_2)	t	7.98	7.98	**Consequential model**: Emitted to air **Attributional model**: Co-product

The electricity for electrolysis is 100% renewable and comes from either solar or wind. As these electricity sources are highly dependent on weather conditions, battery or H_2 storage is required in order to ensure continuous flow of H_2 to the ammonia synthesis. Based on partner statements, current developments show that battery storage is too expensive and thus not part of the design of ammonia production facilities or stand-alone H_2 plants based on electrolysis. Thus, only H_2 storage is included in the product system of this LCA study as a solution for fluctuating electricity supply from wind and solar.

5.1.1.1.1 Hydrogen storage

H_2 can be stored as either gas or liquid. Liquefaction of H_2 requires a significant amount of energy since the H_2 needs to be cooled to under -252°C (Wulf & Zapp, 2018). Moreover, a project partner highlights that liquefaction is too costly. Thus, only compression of H_2 will be used for H_2 storage in this study.

There are few examples of H_2 storage currently being used, thus, project partners have not been able to provide data on this and they acknowledge that there is no standard pressure for this process. However, an industrial expert explains the chosen storage pressure for H_2 produced at the same facility as the ammonia will often only require storage up to 12 hours, thus, the chosen storage pressure will mostly depend on the costs. H_2 stored for other purposes requires much longer storage times and can also face limitations on space, e.g., when H_2 is stored and transported by truck. Here, the pressure is typically >250 bar.

Andersen and Grönkvist (2019) describe different large-scale H_2 storage options and states that a pressure of 100 bar requires large storage volumes and therefore leads to high operating costs, while 700 bar is often used for truck storage and not stationary storage. Metal containers – both under- and overground – or pipe storage are therefore often the alternative solution, with underground storage having a small advantage when the containers are buried more than a couple of meters below the surface level. Specifically, Andersen and Grönkvist (2019) describe that there is an underground steel cylinder used for hydrogen storage which operates with a pressure of 200 bar in Sweden. Lastly, Andersen and Grönkvist (2019) provide estimates for the electricity input needed for H_2 storage: 1.0, 1.2, and 1.6 kWh/kg H_2 for 100, 200, and 700 bar, respectively. Nevertheless, since the project partners have not been able to specify the specific pressure conditions needed for H_2 storage and since the data from Andersen and Grönkvist (2019) are estimates, the upper value of 1.6 kWh/kg H_2 is applied as a worst case approach (see **Table 5.3**).

Note that due to lack of data, it has not been possible to ensure that the applied data for H_2 storage is applicable for the storage requirement. Moreover, it is not possible to specify the dimensions of the storage facility. This is therefore a limitation of the LCA study. Instead, the amount of CAPEX is assumed to be 1.0866

g/t stored H_2. Thus, the assumed storage capacity is 44,069 Mt H_2 in the facility's lifespan (see details in **section 4.7.1.2.1**).

Table 5.3: LCI summary for H_2 storage (Andersson & Grönkvist, 2019). The LCI data applies for both the consequential model and attributional model. CAPEX is the only input that is not included in the **attributional** model.

	Unit	H_2 storage	Link to
Output: reference flow			
Hydrogen (H_2) from storage	t	1	Reference flow
Inputs:			
Electricity	MWh	1.60	See **section 4.1**
Hydrogen (H_2) from electrolysis	t	1.003	See **Table 5.2**
CAPEX			
Hydrogen (H_2) storage facility	g	1.0866	See **Section 4.7.1.2.1**
Emissions to air			
Hydrogen (H_2)	t	0.003	Emissions to air

5.1.1.2 Hydrogen from autothermal reforming with carbon capture and storage

ATR is a process combined of steam reforming and partial oxidation. The H_2 is obtained from the syngas, which is produced from the reaction between methane (CH_4) from natural gas, O_2, and CO_2 (Kim et al., 2021). According to an industrial expert, the input of O_2 stems both from the steam – produced from the water input to ATR – along with the O_2 captured at the ASU. However, the input of O_2 is confidential since this input is of high importance for the ATR process. Thus, the O_2 needed per t H_2 from ATR has been estimated as follows:

Determining the oxygen input to autothermal reforming

According to Kim et al. (2021), the chemical reactions in the ATR process can be split into the following reactions:

Equation 5.1: Partial oxidation

$$CH_4 + 0.5\,O_2 \rightarrow CO + 2H_2$$

Equation 5.2: steam reforming

$$CH_4 + H_2O \rightarrow CO + 3\,H_2$$

Equation 5.3: Water-gas shift reaction

$$2\,CO + 2\,H_2O \rightarrow 2\,CO_2 + 2\,H_2$$

Thus, based on the stoichiometric reactions, the production of 1 t H_2 from ATR requires a minimum of 2.3 t natural gas, 1.1 t O_2, and 3.9 t H_2O, which also results in the production of 6.3 t CO_2:

Equation 5.1-**Equation 5.3** combined:	2	CH_4	+	0.5	O_2	+	3	H_2O	→	2	CO_2	+	7	H_2
Mass		32			16			54			88			14
Normalised to 1 t H_2		2.3			1.1			3.9			6.3			1.0

In **Table 5.4**, 171 GJ natural gas is used to produce 1 t of H_2 through ATR, which corresponds to 3.45 t natural gas per t H_2. Moreover, there is an input of 11.5 t water per t of H_2. Thus, according to the data for ATR obtained from project partners, the ATR process uses an additional 1.15 t natural gas to produce one t H_2 compared to the stoichiometric reactions. Therefore, the ATR process is estimated to have an efficiency of 66%, based on the ratio between the input of natural gas in the stoichiometric reaction (2.3 t natural gas per t H_2) and the actual input of natural gas in **Table 5.4** (3.45 t natural gas per t H_2).

The ratio between natural gas and water in the stoichiometric reactions and the efficiency of the ATR process is used to estimate, how much of the O_2 in the water input is used for the steam reforming and water-gas shift reaction:

$$3.45\ t\ CH_4 * \frac{3.9\ t\ H_2O}{2.3\ t\ CH_4} * \frac{100\%}{66\%} = 8.80\ t\ H_2O$$

Thus, with an input of 11.5 t water per t of H_2, and 8.80 t water used for the steam reforming and water-gas shift reaction, the residual is 2.7 t water. 2.7 t water contains 2.4 t O_2 which can be utilised for the partial oxidation:

$$3.45\ t\ CH_4 * \frac{1.1\ t\ O_2}{2.3\ t\ CH_4} * \frac{100\%}{66\%} = 2.6\ t\ O_2$$

As the O_2 requirement for partial oxidation (2.6 t O_2) is larger than the O_2 in the excess water (2.4 t O_2), an additional input of 0.2 t O_2/t H_2 must come from the ASU. Yet, as there is an input 0.18 t H_2/t ammonia to the Haber-Bosch process, the ASU only needs to provide 0.04 t O_2/t ammonia. This is met, as the ASU produces 0.25 t O_2 for the input of 0.82 t N_2/t ammonia. Thus, N_2 is still the determining product from the ASU used for natural gas-based ammonia. This contradicts an industrial expert's statement, stressing that the demand for O_2 from the ATR process results in excess N_2. Thus, for the default scenario, N_2 is assumed to be the determining product from the ASU, while the sensitivity analysis will include a scenario with O_2 as the determining product (see **section 8.13.2.4**).

Inventory data for autothermal reforming

According to Kim et al. (2021), ATR is a promising technology for H_2 production. Moreover, project partners argue that steam methane reforming (SMR) cannot currently be considered a realistic option for producing ammonia for shipping. This is because it would be very difficult to produce ammonia with a low enough carbon footprint to meet decarbonization targets and be competitive with, e.g., the 70% reduction requirement against the WtW fossil fuel comparator of 94 g CO_2-eq/MJ determined by RED II. Thus, ATR is assumed to be the most likely technology adapted to produce H_2 from natural gas for utilisation for shipping fuel production. Nevertheless, the adaptation of SMR for H_2 production is tested in the sensitivity analysis (see **section 8.13.2.5**). Note that the input of natural gas to ATR may vary according to the project partner. Thus, this parameter is tested in the sensitivity analysis (see **section 8.13.2.3**).

The LCI data for ATR H_2 production are presented in **Table 5.4**, which has been provided by an industrial expert, except from the gas slips. The slip of H_2, O_2, CO_2, and CH_4 is set to 0.3% based on Bertagni et al. (2023), as described in the beginning of **chapter 5**. Since the default gas slip is an assumption, the influence of methane slip from ATR is analysed in the sensitivity analysis (see **section 8.13.2.2**). Also, the slip of H_2 and CO_2 is tested in **section 8.7** and **section 8.13.2.9**, respectively, in the sensitivity analysis.

Lastly, The CO_2 generated from the ATR process is sent to CCS.

Table 5.4: LCI summary for H_2 produced from autothermal reforming (ATR). The LCI data applies for both the **consequential** model and **attributional** model.

Flow	Unit	H_2 production, ATR	Link to:
Output: reference flow			
Hydrogen (H_2)	t	1	Reference flow
Inputs:			
Natural gas (CH_4)	GJ	171	See **section 4.2**
Water (H_2O)	t	11.5	See **section 4.6**
Oxygen (O_2)	t	0.20	See **section 5.1.2.1**
Electricity	MWh	0.30	See **section 4.1**
Outputs:			
CO_2 in purge sent to CCS	t	9.46	See **Section 5.1.1.2.1**
Emissions to air			
Methane (CH_4) slip	t	0.010	Emissions to air
Oxygen (O_2) slip	t	0.001	
Hydrogen (H_2) slip	t	0.003	
Carbon dioxide (CO_2) slip	t	0.028	

5.1.1.2.1 Carbon capture and storage

The CCS process is assumed to be an amine-based solvent process (amine scrubbing) as it is regarded as one of the most commercially mature technologies (Strojny et al., 2023). The LCI data for the inputs of amines and water are based on Facchino et al. (2022), while the energy inputs are calculated based on estimations from a project partner, stating that adding CCS to ammonia production plants with H_2 from ATR typically increases the energy intensity by 3-7% for a 90-95% capture rate. Yet, a project partner highlights that even though a capture rate of 95% is possible, it will require additional machinery and equipment along with a larger energy input. Thus, a capture rate of 90% is applied for ATR along with an extra energy requirement of 5%. A transport distance of 200 km to storage location is included with data obtained from Volkart et al. (2013), yet, as this transport distance is considered low by some project partners, this parameter is included in the sensitivity analysis (see **section 8.13.2.8**).

The 5% extra energy is calculated based on the total energy input to production of H_2 from ATR in **Table 5.4**, where 171 GJ of energy is used to produce 1 t H_2 and 9.46 t CO_2, which is sent to CCS. With a 90% capture rate, 8.55 GJ are used to capture 8.5 t CO_2, thus, 1 GJ is required per t captured CO_2. This corresponds to 0.9 GJ per t CO_2 in purge sent to CCS. The energy is split between electricity and natural gas based on the total input of energy to the ATR process, thus, 99% of the energy input is assumed to be natural gas, while 1% is assumed to be electricity. See the LCI data for CCS in **Table 5.5**.

It is assumed that the carbon in the used natural gas is included in the purge, where it reacts with O_2 and thereby forms additional CO_2. The additional CO_2 amount is estimated as follows:

$$1\ GJ\ natural\ gas * \frac{1}{\frac{49.5\ GJ}{t\ natural\ gas}} * 0.750 \frac{t\ carbon}{t\ natural\ gas} * \frac{44\ t\ CO_2}{12\ t\ carbon} = 0.056\ t\ CO_2$$

The model includes the additional CO_2 by linking the process to itself, meaning that an input of 1.11 t CO_2 from the ATR process and 0.056 t CO_2 from natural gas input to CCS result in a capture of 1.05 t CO_2 (see **Table 5.5**).

Though 90% of the CO_2 is captured and intended to be stored for at least 100 years, part of the CO_2 is assumed to leak from storage throughout this time-period. A yearly slip of 0.023% is assumed based on an average of

the slip rates of CO_2 from Suh et al. (2023) and Captura (2022). Furthermore, it is assumed that the slip of CO_2 from the transport by pipeline is included in the yearly slip from storage.

As described in **section 2.12**, the leaked CO_2 over 100 years is presented as the sum of time aggregated CO_2-eq under '*Carbon dioxide, as CO_2e (GWP aggr timing)*' for the consequential model. Moreover, the influence of CO_2 slip from storage is analysed in the sensitivity analysis (see **section 8.13.2.9**). Yet, since timing of CO_2 is not included in the attributional model (see **Table 2.1**), the CO_2 leakage has the same GWP characterisation factor as if it was being emitted right after capture in the attributional model.

Table 5.5: LCI summary for carbon capture and storage (CCS) for both the **consequential** and **attributional** model (Facchino et al., 2022; Volkart et al., 2013).

	Unit	Carbon capture and storage	Carbon capture and storage	Link to
Output: reference flow		**Consequential**	**Attributional**	
CO_2, captured	t	1.05	1.05	Reference flow
Inputs:				
CO_2 in purge, total	t	1.166	1.166	
- CO2 from ATR process	t	1.11	1.11	See **Table 5.4**
- CO_2 from natural gas input	t	0.056	0.056	It is assumed that the carbon in the natural gas input is included in the purge, where it reacts with O_2 and thereby forms additional CO_2.
Natural gas	GJ	1.05	1.05	See **section 4.2**
Electricity	MWh	0.0019	0.0019	See **section 4.1**
Water	t	0.032	0.032	See **section 4.6**
Amines (dry matter)	t	0.00093	0.00093	**Consequential model:** EXIOBASE: _63 Chemicals nec {region} **Attributional model:** ecoinvent: Chemical, inorganic {GLO}| market for chemical, inorganic
Transport				
Transport by pipeline	km	200	200	See **section 4.5.2**
Emissions to air				
Carbon dioxide, not captured	t	0.116	0.116	Emissions to air
Carbon dioxide, slip from storage, over 100 years	t	-	0.024	**Attributional model:** Timing of CO_2 emissions not included, see **Table 2.1**
Carbon dioxide, slip from storage, as CO2e (GWP aggr timing)	t	0.013	-	**Consequential model:** Emissions to air, see **section 2.12**

Since commercialised carbon capture technologies are still relatively new, data collection and sanity check of the data have been challenging. Thus, the energy data from a project partner is compared to energy data from Oni et al. (2022) in **Table 5.6**, since Oni et al. (2022) presents data for H_2 from ATR with a carbon capture rate of 91%.

Table 5.6: Comparison of energy data for carbon capture and storage (CCS) from **Table 5.5** with energy data from Oni et al. (2022)

Data source:		Project partner (normalised)	Oni et al. (2022)	
	Unit	Carbon capture and storage	Carbon capture and storage	Comment
Output: reference flow				
CO_2, captured	t	1	1	Reference flow
Inputs:				
CO_2 in purge	t	1.11	1.10	Note, Oni et al. (2022) applied a capture rate of 91%, while a 90% capture rate is applied for the project partner data
Total energy input	GJ	1.00	0.59	

The comparison in **Table 5.6** shows that the energy data from industrial experts is almost twice as high as the electricity input from Oni et al. (2022) per t captured CO_2. Moreover, data from Kähler et al. (2022) show that energy requirement for carbon capture can vary from 0.40 GJ/t CO_2 to 3.46 GJ/t CO_2 depending on the point source of the CO_2. Therefore, the energy requirement for CCS is tested in the sensitivity analysis (see **section 8.13.2.7**). The capture rate is also tested in **section 8.13.2.6.**

5.1.2 Nitrogen production

Since the atmosphere consists of 78% N_2 (Hu et al., 2018), N_2 is obtained through an ASU. The capture of air also results in the capture of two other substances– Ar and O_2 – which are the two other main components of the atmosphere. Yet, it is important to highlight that O_2 is typically the determining product from ASU facilities (Aljaghoub et al., 2023), nevertheless, since the analysis in **section 5.1.1.2** showed that N_2 is the determining product from the ASU used for natural gas-based ammonia, the input of N_2 is modelled differently for electrolysis-based ammonia than for natural gas-based ammonia.

5.1.2.1 Nitrogen production for electrolysis-based ammonia

In the consequential model, the N_2 for electrolysis-based ammonia stems from avoided venting of N_2. This is because N_2 is a by-product from ASUs, where O_2 is the determining product (Aljaghoub et al., 2023). Thus, since the production of O_2 leads to excess N_2, which is released back into the atmosphere right after the air separation process, the demand for N_2 from the Haber-Bosch process for electrolysis-based ammonia will result in avoided venting of N_2 (see LCI in **Table 5.8**).

In the attributional model, which follows RED II and delegated regulation 2023/1185 guidelines, N_2 is produced at an ASU where O_2 and Ar are considered co-products. Thus, allocation must be applied. Yet, since N_2, O_2, and Ar do not have an energy content, economic allocation is applied using "*the average factory-gate value of the products over the last three years*" (EC, 2023; EP & EUCO, 2018). The average economic value of N_2, O_2, and Ar is obtained from the UN Comtrade Database with 2020-2022 data being the newest available (see **Table 5.7**).

Table 5.7: Economic data for 2022-2020 for N_2, O_2 and Ar (United Nations, 2022)

	Total trade volume 2022-2020	Total trade value 2022-2020	Average price	Output	Allocation factor
Unit	**t**	**US$**	**US$/t**	**t**	**%**
Nitrogen (N_2)	9,769,463	1,362,567,834	139	1	67%
Oxygen (O_2)	7,136,466	1,385,850,235	194	0.31	29%
Argon (Ar)	3,999,422	1,615,708,362	404	0.02	4%

The outputs of N_2, O_2, and Ar are multiplied with the average price per t, resulting in an economic allocation of 67%, 29%, and 4%, respectively. In **Table 5.8**, the allocation factor for N_2 is applied to the LCI data for the attributional LCA.

Table 5.8: LCI summary for N_2 production for **electrolysis-based ammonia** for both the **consequential** and **attributional** model. LCI data are obtained from industrial experts and Bertagni et al. (2023).

Flow	Unit	N_2 production		Link to
Output: reference flow		**Consequential**	**Attributional**	
Nitrogen (N_2)	t	1	1	Reference flow
Inputs:				
Air	t		1.33*67%	Resources
- Nitrogen (N_2)	t		1.003*67%	
- Oxygen (O_2)	t		0.31*67%	
- Argon (Ar)	t		0.02*67%	
Electricity	MWh		0.30*67%	See **Section 4.1**
Emissions to air				
Nitrogen (N_2) slip	t		0.003*67%	Emissions to air
Nitrogen (N_2), vented to atmosphere	t	-1		
Oxygen (O_2) slip	t		0.001*67%	
Argon (Ar) slip	t		0.0001*67%	

The slip of Ar, O_2, and N_2 is to 0.3% based on Bertagni et al. (2023) just as for the other gases within the product system. Nevertheless, the slip of Ar, O_2, and N_2 does not have an impact since it has just been captured from the atmosphere. Thus, the slips only result in a slightly increased energy requirement, as more air needs to go into the process in order to capture 1 t of N_2.

5.1.2.2 Nitrogen production for natural gas-based ammonia

The ASU in the product system for natural gas-based ammonia produces both O_2 for the ATR process and N_2 for the Haber-Bosch process. While the input of N_2 to the Haber-Bosch process is obtained from an industrial expert (see **Table 5.10**), the input of O_2 to ATR is confidential. Therefore, the required amount of O_2 to ATR from ASU is estimated to be 0.2 t O_2 per t H_2 in **section 5.1.1.2**. Since the ASU produces 0.25 t O_2 for the input of 0.82 t N_2/t ammonia to the Haber-Bosch process, N_2 is still the determining product from the ASU used for natural gas-based ammonia, because there is produced more O_2 from the ASU per t ammonia than what is required by the ATR process. Nevertheless, in the sensitivity analysis, it is tested how the results change, if O_2 is the determining product (see **section 8.13.2.4**).

In the consequential model, the determining product (either O_2 or N_2) is of high importance: When N_2 is the determining product, the ASU's energy requirement and production will be determined by the amount of N_2 needed for the Haber-Bosch process. Any excess Ar will be vented to the atmosphere, since the marginal effect of changing the demand for N_2 leads to excess Ar, while the excess O_2, which is not used for the ATR process, substitutes the primary production of O_2 from another ASU unit.

In the attributional model, which follows the RED II and delegated regulation 2023/1185 guidelines, excess gases (O_2 and Ar) are considered co-products and allocation must therefore be applied. Yet, since none of the gases have an energy content, economic allocation must be applied using "*the average factory-gate value of the products over the last three years*" (EC, 2023; EP & EUCO, 2018). The average economic value of N_2, O_2, and Ar is obtained from the UN Comtrade Database with 2020-2022 data being the newest available (see **Table 5.7**).

The outputs of N_2, O_2, and Ar are multiplied with the average price per t, resulting in an economic allocation of 67%, 29%, and 4%, respectively. In **Table 5.8**, the allocation factors are applied to the LCI data for the attributional LCA. Note that for the production of 1 t of N_2, there is an input of 0.22 t H_2 from ATR to the Haber-Bosch process, thus, with an additional O_2 demand of 0.2 t O_2/t H_2, 0.045 t O_2 is supplied to the ATR process per t N_2. Thus, as the production of 1 t of N_2 leads to the capture of 0.31 t O_2, 15% of the O_2 by-product is utilised for ATR. The share of utilised O_2 is also part of the allocation in **Table 5.8**.

Table 5.9: LCI summary for N_2 production for **electrolysis-based ammonia** for both the consequential and attributional model. LCI data are obtained from an industrial expert and Bertagni et al. (2023).

Flow	Unit	ASU: N_2 production	ASU: N_2 production	Link to
Output: reference flow		**Consequential**	**Attributional**	
Nitrogen (N_2)	t	1	1	Reference flow
Outputs:				
Oxygen (O_2) to ATR	t	0.045	0.045 (15% of 0.31)	Input to ATR, see **section 5.1.1.2**
Excess oxygen (O_2)	t	0.27	0.27	**Consequential model:** Substitutes primary production of O_2 from another ASU. **Attributional model:** The impact from O_2 is allocated to the next product system using economic allocation.
Argon (Ar)	t	0.02	0.02	**Consequential model:** Emitted to air. **Attributional model:** The impact from Ar is allocated to the next product system using economic allocation.
Inputs:				
Air	t	1.33	1.33*68% + 1.33*29%*15%	Resources
- Nitrogen (N_2)	t	1.003	1.003*68% + 1.003*29%*15%	
- Oxygen (O_2)	t	0.31	0.31*68% + 0.31*29%*15%	
- Argon (Ar)	t	0.02	0.02*68% + 0.02*29%*15%	
Electricity	MWh	0.30	0.30*68% + 0.30*29%*15%	See **Section 4.1**
Emissions to air				
Nitrogen (N_2) slip	t	0.003	0.003*68% + 0.003*29%*15%	Emissions to air
Oxygen (O_2) slip	t	0.001	0.001*68% + 0.001*29%*15%	
Argon (Ar) slip	t	0.0001	0.0001*68% + 0.0001*29%*15%	

The slip of N_2, Ar, and O_2 is set to 0.3% based on Bertagni et al. (2023) similarly to the other gases within the product system. Nevertheless, the slip of N_2, Ar, and O_2 does not have an impact since it has just been captured from the atmosphere. Thus, the slip of N_2, Ar, and O_2 only results in a slightly increased energy requirement, as more air needs to go into the process in order to capture 1 t of N_2.

5.1.3 Haber-Bosch ammonia synthesis

Through the Haber-Bosch process, ammonia is produced from the reaction between N_2 and H_2. The Haber-Bosch process is the same for both ammonia pathways, except for two elements: The source of the H_2 and the source of the electricity, which fuels the Haber-Bosch process. Note that the ammonia is liquefied at the production site and the LCI data presented in **Table 5.10** includes the energy required for the liquefaction.

The ammonia based on H_2 from electrolysis has an input of renewable electricity, and it is assumed that 75% of the H_2 comes directly from the electrolysis process while the remaining 25% of the H_2 comes from H_2 storage, as the renewable electricity sources are highly dependent on weather conditions. The assumption of 25% H_2 from storage has been checked by the project partner, which supplied data for the Haber-Bosch process, and it was deemed acceptable. The ammonia produced with H_2 from ATR obtains electricity from the grid.

The amount of CAPEX per t ammonia – 1.0866 g CAPEX/t ammonia - is determined in **section 4.7.1.2**. This means that both ammonia facilities are assumed to have a capacity of 97,105 Mt ammonia in their lifespan. As previously stated, it is assumed that the CAPEX required for production of H_2 and N_2 is included in the overall ammonia production facility, which is also assumed to be the case for CAPEX for CCS at ammonia production facility with H_2 from ATR. Thus, the CAPEX activity is the same for ammonia production with H_2 from electrolysis and ATR.

According to an industrial expert, the Haber-Bosch process has – until recently – often been designed to run at constant rate, since there historically has been no need to design it to run on varying H_2 or electricity inputs. However, this has changed due to the focus on producing with renewable electricity, especially from off-grid sources.

An industrial expert also state that the design of H_2 and ammonia plants that run partially or fully on intermittent electricity sources is an area of active research and development. The optimum design of a production plant depends on multiple factors. Among others it is the electricity profile, the electricity price, the cost of storage, the operational capabilities of the production plant, the preferences of the operator, the capital expenditures of H_2 storage, the price of ammonia, etc.

The Haber-Bosch process can be ramped up and down and can run at <100% load according to an industrial expert, but it creates several challenges related to heat transfer, stress on materials, and reduced energy efficiency. Industrial experts also state that – in principle – the ramp-up/down rate of the Haber-Bosch unit can be done in a relatively short time, and, as long as the temperature of the H_2 does not significantly change, a 90% reduction in load (i.e. from 100% to 10% load) can be done in one hour. In practice however, the efficiency of the process starts to drastically decline below a 70% load. As energy consumption represents a very large part of the production cost of ammonia, even minor losses of efficiency affect the profitability - unless fully compensated by a significantly lower electricity price. The technical minimum load for current generation Haber-Bosch units is around 30-40%.

Table 5.10: LCI summary for ammonia production with H_2 from electrolysis and ATR for the **consequential** and **attributional** model. LCI data are obtained from an industrial expert and Bertagni et al. (2023). CAPEX is the only input that is not included in the **attributional** model.

	Unit	Ammonia production, H_2 from electrolysis	Ammonia production, H_2 from ATR	Link to
Output: reference flow				
Ammonia (NH_3)	t	1	1	Reference flow
Inputs:				
Hydrogen (H_2) from electrolysis	t	0.181*75%	-	See **Table 5.2**
H_2 from storage	t	0.181*25%	-	See **Table 5.3**
Hydrogen (H_2) from ATR	t	-	0.181	See **Table 5.4**
Nitrogen (N_2)	t	0.822	0.822	See **section 5.1.2**
Electricity	MWh	0.351	0.351	See **Section 4.1**
CAPEX				
CAPEX, ammonia production facility	g	1.0866	1.0866	See **Section 4.7**
Emissions to air				
Ammonia (NH_3) slip	t	0.003	0.003	Emissions to air

As described in the beginning of **chapter 5**, a slip of 0.3% has been assumed for most gases within the product system. Since this is an assumption, the influence of ammonia slips throughout the product system is analysed in the sensitivity analysis (see **section 8.8**).

5.2 Very low sulphur fuel oil production

The demand for VLSFO is increasing due to the sulphur cap from the International Maritime Organization (IMO), which lowered the upper level for the sulphur content to 0.5% in shipping fuels from 2020 (IMO, 2019). As the regulation is newly introduced, there is limited data on how the market for shipping fuel has changed. However, several market forecasts have been conducted, thus, the LCA study will rely on these predictions.

Three market forecasts have been reviewed: Billing and Fitzgibbon (2019), Deloitte (2019) and IEA (2019). All three analyses agree that the lowered sulphur limit will increase the demand for VLSFO. Marine gas oil (MGO) is also considered as a solution, since MGO has a sulphur content below 0.1%. Nevertheless, VLSFO is expected to be mostly used, since it is cheaper than MGO. Furthermore, Deloitte (2019) expect the global desulphurisation capacity to grow, thus resulting in a high supply potential for VLSFO since desulphurisation is one approach to remove sulphur from fuel oil. On the other hand, IEA (2019) expects a lack of desulphurisation capacity, resulting in an increased demand for low-sulphur crude oil. This suggests that even though the desulphurisation capacity may be limited, refineries have other ways to meet the increased demand for VSLFO. Additionally, project partners for this LCA study argue that VLSFO is produced by mixing high sulphur crude oil with low sulphur crude oil or MGO, since H_2 - which is needed for desulphurisation – is too expensive for desulphurisation to be a realistic production pathway for VLSFO sold to the shipping industry.

Based on statements from project partners and the market forecasts, VLSFO can be supplied through several pathways. Nevertheless, in the consequential model - where the environment impacts of a change in demand is analysed - it is assumed that low-sulphur fuels such as MGO and low sulphur crude oil are already utilised for alternative purposes. Thus, if the demand for VLSFO is supplied through the use of MGO or low sulphur crude oil, a counterfactual scenario must be taken into account, meaning that an alternative fuel source must be supplied to the original user of the MGO or low sulphur crude oil. As the low sulphur content of the fuels is most likely an important parameter for the original user, desulphurisation may be the counterfactual scenario. Thus, for this LCA study, desulphurisation is modelled in the consequential LCA as the production pathway for VLSFO.

For the attributional model, the standard carbon footprint for the WtW fossil fuel comparator of 94 g CO_2-eq/MJ from RED II is applied (EC, 2023; EP & EUCO, 2018), as this approach is deemed most in line with the RED II guidelines.

The LCI data for desulphurisation is presented in **Table 5.11** and is obtained from Olindo and Vogtländer (2019). The input of CAPEX per t VLSFO is assumed to be the same as for ammonia (1.0866 g CAPEX/t VLSFO), as no other data have been found. As the total weight of the VLSFO production facility is 16,323 t (see **Table 4.12**), this results in a total production capacity of 15,022 Mt in this VLSFO facility's lifespan.

The EXIOBASE activity '*_57 Petroleum Refinery*' for each country in EXIOBASE is applied to model the feedstock of fuel oil whereafter the countries are split into the respective regions described in **section 2.7**.

Table 5.11: LCI summary for desulphurisation for the **consequential** model (Olindo & Vogtländer, 2019). For the **attributional** model, the standard carbon footprint for the WtW fossil fuel comparator of 94 g CO2-eq/MJ from RED II is applied, as this approach is deemed most in line with the RED II guidelines.

	Unit	Desulphurisation	Link to
Output: reference flow			
VLSFO	t	1	Reference flow
Inputs			
Fuel oil	t	1.14	EXIOBASE: _57 Petroleum Refinery {region}
Hydrogen (H_2), from ATR	t	0.009	See **section 5.2.1**
Electricity	MWh	6.17	See **section 4.1**
Steam	GJ	0.02	See **section 4.2**
CAPEX			
CAPEX, VLSFO production facility	g	1.0866	See **section 4.7.1.1**
Output - by-products			
Naphtha	t	0.011	Substitution of EXIOBASE: _57 Petroleum Refinery {region}
Output – waste			
Sulphur dioxide (SO_2)	t	0.04	See **section 5.2.2**

5.2.1 Hydrogen from autothermal reforming without carbon capture and storage

The H_2 for desulphurisation is modelled as being produced from natural gas since natural gas-based H_2 production is used worldwide (Kim et al., 2021). Moreover, since the demand for H_2 will be met by new production capacity, it is assumed that ATR will be the applied technology. However, the CO_2 emissions are modelled as being emitted to air, since project partners explain that the CO_2 for a typical natural gas-based H_2 facility is either utilised in fertiliser production or the food and beverage industry or emitted to air. Thus, even though the CO_2 is utilised, it will be emitted within a very short period, which would result in a similar impact as if the CO_2 was emitted at the H_2 production facility. Nevertheless, it is tested in the sensitivity analysis, how the results would change if the CO2 were captured and stored long-term through CCS (see **section 8.14**). The applied LCI data for H_2 from ATR without CCS is presented in **Table 5.12**.

Table 5.12: LCI summary for H_2 produced from autothermal reforming (ATR) without carbon capture and storage (CCS) for the **consequential** model.

Flow	Unit	H_2 production, ATR	Link to:
Output: reference flow			
Hydrogen (H_2)	t	1	Reference flow
Inputs:			
Natural gas (CH_4)	GJ	171	See **section 4.2**
Water (H_2O)	t	11.5	See **section 4.6**
Oxygen (O_2)	t	0.20	See **section 5.1.2.1**
Electricity	MWh	0.30	See **section 4.1**
Emissions to air			
Methane (CH_4) slip	t	0.010	Emissions to air
Oxygen (O_2) slip	t	0.001	
Hydrogen (H_2) slip	t	0.003	
Carbon dioxide (CO_2)	t	9.49	

As for the other H_2 production processes (see **section 5.1.1.1** and **5.1.1.2**), a gas slip of 0.3% has been assumed based on Bertagni et al. (2023). Since this is an assumption, the influence of methane slip from ATR is analysed in the sensitivity analysis (see **section 8.14**). Also, the slip of H_2 is tested in **section 8.7** in the sensitivity analysis.

5.2.2 Sulphur stockpiling

According to Worthington et al. (2017) and Apodaca (2022), sulphur is accumulated and stored through stockpiling. This is due to the amount of sulphur produced as a by-product from refineries is larger than its utilisation in the production of, e.g., sulphuric acid and fertilisers. Thus, the demand for VLSFO will result in additional stockpiling of sulphur.

However, it has proven difficult to obtain LCI data on sulphur stockpiling. Nevertheless, based on the ecoinvent activity '*Sulfur stockpiling {RoW}| sulfur stockpiling | Conseq, U*', the only inputs to sulphur stockpiling are a few material inputs – e.g., gravel, asphalt, and steel – as well as the area, which is occupied by the stockpiling. Moreover, the ecoinvent activity does not include any emissions to air, water, or soil. However, due to the limited inputs to the ecoinvent activity and ecoinvent's EULA, it is not possible to apply the LCI from the activity for this study. Instead, the EXIOBASE activity '*157 Landfill of waste: Inert/metal/hazardous*' is modified – since this activity is deemed the closest match to sulphur stockpiling. The activity is modified by removing waste management inputs, unrelated material inputs such as forestry, and emissions to air, water, and soil, since none of these are part of the ecoinvent activity. Thereby, the stockpiling activity includes the CAPEX (the required machinery, equipment, infrastructure, etc.) and the services related to landfill of inert waste as well as the material inputs, which are deemed specifically relevant for sulphur stockpiling.

5.3 Distribution, bunkering, and cooling on board

After the fuel production, both ammonia and VLSFO are distributed and bunkered to ships. Moreover, ammonia must also be cooled on board. The LCI data for these processes are described in the following sections. Note that the LCI data for distribution, bunkering, and cooling of ammonia applies for both the consequential model and attributional model, while the LCI data for VLSFO only applies for the consequential model, since the attributional model applies the standard carbon footprint for the fossil fuel comparator of 94 g CO2-eq/MJ for WtW from RED II.

5.3.1 Distribution and bunkering of ammonia

Today, ammonia is primarily used as fertiliser and as a refrigerant. Thus, ammonia is already traded on a global scale and is usually stored in special isothermal tanks or spherical pressure storages and transported by tankers (Alfa Laval et al., 2020). Furthermore, ammonia is liquefied at the production site and is therefore transported as a liquid. The data collection for distribution and bunkering of ammonia has therefore focused on two key parameters: Data on infrastructure and energy for cooling.

However, no reliable data have been found. Instead, the data for distribution and bunkering of VLSFO is applied as proxy data for ammonia as the best available alternative (see **Table 5.13**). Yet, an additional energy input for cooling based on the expert estimate in **section 5.3.3** is included. Thus, 1.9% of the energy in the transported ammonia with 9.6% e/e VLSFO is assumed to be needed for cooling under distribution, corresponding to 0.32 GJ / t ammonia. This energy requirement is linked to fuel oil, as it is assumed that the energy for cooling is primarily consumed on board of the tanker, which transports the ammonia, and because it is assumed that the tanker is fuelled by fossil fuel.

Lastly, slip of ammonia during distribution is also taken into account, as a slip of 0.3% has been assumed just like the previous processes in the product system for ammonia. The slip is included in the sensitivity analysis, (see **section 8.7**).

5.3.2 Distribution and bunkering of very low sulphur fuel oil

The LCI data for distribution and bunkering of VLSFO is obtained from the ecoinvent activities '*Heavy fuel oil {RoW}*' and '*Infrastructure, for regional distribution of oil product {RoW}*'. It is assumed that there is no difference between the distribution and bunkering of fuel oil and VLSFO. The LCI data are presented in **Table 5.13**, but because of the requirements in the EULA from ecoinvent, the inputs are aggregated, thus, the specific modelling is untraceable.

Table 5.13: LCI summary for distribution and bunkering of ammonia and VLSFO (ecoinvent, 2021). The LCI data for ammonia applies for both the **consequential** model and **attributional** model, yet CAPEX is the only input that is not included in the **attributional** model. The LCI data for VLSFO only applies for the **consequential** model, since the **attributional** model applies the standard carbon footprint for the fossil fuel comparator of 94 g CO2-eq/MJ for WtW from RED II.

	Unit	Distribution and bunkering: Ammonia	Distribution and bunkering: VLSFO	Link to
Output: reference flow		**Consequential and attributional**	**Consequential**	
Ammonia (NH_3)	t	1		Reference flow
Very low sulphur fuel oil (VLSFO)	t		1	Reference flow
Inputs:				
Electricity	MWh	0.00672	0.00670	See **section 4.1**
Fuel oil, for cooling of ammonia	GJ	0.32	-	Fuel oil incl. combustion emissions {region}, see **section 4.4**
Ammonia (NH_3)	t	1.003		See **Table 5.10**
Very low sulphur fuel oil (VLSFO)	t	-	1.00	See **section 5.2**
Transport				
Transport by ship	km	707	707	See **Modelling of sea transport**
Transport by pipeline	km	588	588	See **Modelling of pipe transport**
CAPEX				
Infrastructure for distribution and bunkering	g	1.70	1.70	See **Section 4.7**
Emissions				
Ammonia (NH_3) slip	t	0.003	-	Emissions to air

The CAPEX input per t ammonia and VLSFO is determined to be 1.7 g/t in **section 4.7.1.3** based on a capacity of approximately 9,615 Mt in the infrastructure's lifespan.

5.3.3 Cooling of ammonia on board

Since ammonia is injected into the combustion chamber as a liquid, cooling is required on board. Data on the energy requirement stems from an expert estimate, stating that 135 kWh are needed to cool 1,371 kg ammonia (with 0% e/e VLSFO). It is assumed that ammonia with 9.6% e/e VLSFO is used to supply energy for the cooling. The LCI data with 1 t of ammonia with 9.6% e/e VLSFO as the reference flow is presented in **Table 5.14**.

Table 5.14: LCI data for cooling of ammonia on board. The LCI data applies for both the **consequential** model and **attributional** model.

	Unit	Ammonia cooling on board 0% e/e VLSFO	Link to
Output: reference flow			
Ammonia (NH_3), liquid, 9.6% e/e VLSFO	t	1	Reference flow
Inputs:			
Ammonia (NH_3), 9.6% e/e VLSFO, as energy for cooling	GJ	0.32	See **Table 5.13**

0.36 GJ ammonia corresponds to 1.9% of the energy in 1 t ammonia with 9.6% e/e VLSFO.

5.4 Fuel combustion and ship parameters

A project partner has supplied data on the combustion emissions for ammonia and VLSFO per kWh-shaft, except for the particulate emissions, which are obtained from Green Transition Denmark (2021) (see **Table 5.15**). Note that Green Transition Denmark (2021) does not specify the engine type and a project partner therefore stresses that the particulate emissions can vary between engine designs.

It is important to highlight that some of the data points from the project partner are based on assumptions and development targets for the combustion engine, e.g., the ammonia and N_2O emissions, since the engine is still under development. Some project partners argue that the N_2O emissions from combustion of ammonia may be much higher than the N_2O value in **Table 5.15**. Therefore, this parameter is tested in the sensitivity analysis along with the slip of ammonia (see **section 8.8** and **8.10**).

Note that in order for ammonia to fulfil its function as a shipping fuel, a pilot fuel - in this case VLSFO – is needed to ignite the ammonia. VLSFO accounts for 9.6% e/e of 1 MJ ammonia in the primary data delivered by the project partner. Yet, as the share of pilot fuel can influence the results, ammonia with 5% and 15% e/e VLSFO ammonia analysed in the sensitivity analysis (see **section 8.3**).

Table 5.15: Combustion emissions data for VLSFO and ammonia provided by a project partner.

	Unit	VLSFO	Ammonia with 9.6% e/e VLSFO	Comment
Parameter				
Engine load	%	50	50	
Fuel consumption				
Ammonia (NH_3)	g/kWh-shaft	-	378	
VLSFO	g/kWh-shaft	175	16.9	
Efficiency	%	50	50	
Emissions				
Ammonia (NH_3)	g/kWh-shaft	0	0.04	The slip of ammonia is estimated by a project partner based on development targets for the combustion engine, as the engine is still under development.
Carbon dioxide (CO_2)	g/kWh-shaft	551	53	The CO_2 emissions only relate to the combustion of VLSFO since ammonia does not contain any carbon.
Dinitrogen monoxide (N_2O)	g/kWh-shaft	0.02	0.04	VLSFO value: Estimate by a project partner based on combustion of diesel oil from the Third IMO Greenhouse Gas Study 2014. Ammonia value: Development target for the ammonia engine, which recent engine tests support.
Nitrogen oxides (NO_x)	g/kWh-shaft	14.4	14.4	This value is NO_x Tier II compliant for marine engines and is therefore the same for both VLSFO and ammonia.
Sulphur oxides (SO_x)	g/kWh-shaft	1.78	0.17	The SO_x emissions only relate to the combustion of VLSFO since ammonia does not contain any sulphur.
Particulates, < 2.5 µm	g/kWh-shaft	0.612	0.059	LCI data from Green Transition Denmark (2021). All particulates are assumed to be < 2.5 µm due to the low sulphur content of VLSFO.

The combustion emissions in **Table 5.15** are based on the following parameters and assumptions:

- The consumption of VLSFO as a pilot fuel is based on 6G50ME-C-LGIM-EGRBP rated at 7,500 kW and 87 rpm. L1 is 10,320 kWh at 100 rpm. VLSFO has 0.5% (m/m) sulphur, 85.94% (m/m) carbon, and the remaining is hydrogen. The lower calorific value is 41,200 kJ/kg.
- Ammonia is injected into the combustion chamber as a liquid and the LHV is 17.200 MJ/kg.
- 50% engine load (3,750 kW at 69.1 rpm) and 50% engine thermal efficiency.
- Emissions are after Selective Catalytic Reduction (SCR)

Note that project partners have discussed the LHV of ammonia throughout the project, since some project partners argue for a LHV of 18.6 MJ/kg instead of 17.2 MJ/kg. The 17.2 MJ/kg corresponds to liquid ammonia, while 18.6 MJ/kg corresponds to gaseous ammonia.

Initially, 17.2 MJ/kg was applied for the study since ammonia is injected to the ammonia engine as a liquid. Moreover, a high LHV of ammonia can result in optimistic ammonia consumption numbers. On the other hand, a partner states that some of the energy from the combustion chamber - which is used to evaporate the ammonia fuel - is regained as volume work during the cylinder process. Therefore, the LHV of ammonia is somewhere between the value for liquid ammonia and gaseous ammonia.

Based on these arguments, it has been decided to keep the 17.2 MJ/kg in the default scenario, while the 18.6 MJ/kg will be analyzed in the sensitivity analysis (see **section 8.2**).

The data in **Table 5.15** has been recalculated to fit the functional unit of 1 MJ using the engine efficiency of 50% and the amount of MJ per kWh. Example:

Equation 5.4

$$\frac{551\ \frac{g\ CO_2}{kWh-shaft} * \frac{50\%}{100\%}}{3.6\frac{MJ}{kWh}} = 76.53\frac{g}{MJ}$$

The applied LCI data for combustion of VLSFO and ammonia (with 9.6% e/e VLSFO) is presented in **Table 5.16.**

Table 5.16: LCI summary for combustion of VLSFO and ammonia obtained from a project partner and Green Transition Denmark (2021). The LCI data applies for both the **consequential** model and **attributional** model.

	Unit	VLSFO	Ammonia with 9.6% e/e VLSFO
Parameter			
Engine load	%	50	50
Fuel consumption			
Ammonia (NH_3)	g/MJ	0	52.50
VLSFO	g/MJ	24.31	2.34
Efficiency	%	50	50
Emissions			
Ammonia (NH_3)	g/MJ	-	0.0056
Carbon dioxide (CO_2)	g/MJ	76.53	7.36
Dinitrogen monoxide (N_2O)	g/MJ	0.00278	0.0056
Nitrogen oxides (NO_x)	g/MJ	2.00	2.00
Sulphur oxides (SO_x)	g/MJ	0.247	0.024
Particulates, < 2.5 µm	g/MJ	0.085	0.0082

6 Life cycle impact assessment: consequential model

This chapter presents the LCIA results for the consequential model. Throughout this chapter, the terms in **Table 2.3** are used to refer to the four different fuel scenarios, three production pathways, and two fuel types.

First, the characterised results are presented for each of the four fuel scenarios: ammonia (9.6% e/e VLSFO) with H_2 from electrolysis (based on either solar or wind), ammonia (9.6% e/e VLSFO) with H_2 from ATR with CCS, and VLSFO. The characterised results are presented per MJ and per TEUkm, as described in **section 2.4**. This is followed by a contribution analysis for each fuel for each of the eight impact categories listed in **section 2.10**. Lastly, the regional differences are also presented through graphic visualizations.

In order to provide a simple overview of the LCIA results, the tables in this chapter present a mean of the results for the 17 regions (referred to as 'global mean'), while **appendix 10** (external appendix) includes the characterised results and contribution tables for the individual regions.

6.1 Characterised results

The characterised results for the global mean are presented in **Table 6.1** for the eight impact categories. The results for GWP100 is presented with and without the GWP of H_2, since the GWP for H_2 is not included in IPCC (2021) (see **section 2.11**).

Table 6.1: Characterised global mean results for ammonia (9.6% e/e VLSFO) with H_2 from electrolysis (based on either solar or wind), ammonia (9.6% e/e VLSFO) with H_2 from ATR with CCS, and VLSFO with the functional unit of 1 MJ for the **consequential model**.

Global mean	Production pathway	Haber-Bosch			Desulphurisation
	H_2 production	Electrolysis	Electrolysis	ATR with CCS	ATR
	Electricity source	Solar	Wind	Grid	Grid
	Fuel	Ammonia with 9.6% e/e VLSFO	Ammonia with 9.6% e/e VLSFO	Ammonia with 9.6% e/e VLSFO	VLSFO
Impact categories	**Unit**				
Global warming (GWP100)	g CO_2-eq/MJ	22.3	19.6	44.6	107.1
GWP100 without GWP of H_2	g CO_2-eq/MJ	21.8	19.2	44.2	107.1
Respiratory inorganics	mg $PM_{2.5}$-eq/MJ	323	321	318	387
Respiratory organics	pers*ppm*s/MJ	0.85	0.83	0.86	0.90
Nature occupation	PDF*m²a/MJ	0.00033	0.00024	0.00020	0.00051
Acidification	cm² UES/MJ	242	241	239	195
Eutrophication, aquatic	mg NO_3-eq/MJ	225	222	221	163
Eutrophication, terrestrial	cm² UES/MJ	1,129	1,127	1,129	680
Photochemical ozone, vegetation	cm²*ppm*hours/MJ	33,439	32,920	33,810	34,643

When comparing the results in **Table 6.1**, ammonia (9.6% e/e VLSFO) with H_2 from wind-based electrolysis has the lowest impact for three out of eight impact categories – GWP100, respiratory organics, and photochemical ozone, vegetation – while VLSFO has the lowest impact for acidification and both aquatic and terrestrial eutrophication. Ammonia (9.6% e/e VLSFO) with H_2 from ATR with CCS has the lowest impact for respiratory inorganics and nature occupation. Nevertheless, for nature occupation as well as respiratory organics and inorganics, the differences between the fuels are relatively small. The difference in results is largest for GWP100, since ammonia (9.6% e/e VLSFO) with H_2 from wind-based electrolysis has an impact that is over five times lower than VLSFO, while the difference for the other impact categories is around or under a factor of two.

6.1.1 Conversion of functional unit: From MJ to TEUkm

The characterised results are also provided for a functional unit of 1 twenty-foot equivalent unit transported for 1 kilometre (1 TEUkm). This is done, since a ship fuelled by ammonia has less space for cargo, because the energy density of ammonia (0% e/e VLSFO) is 12 GJ/m^3, while the energy density is 38.6 GJ/m^3 for VLSFO. The results are recalculated to 1 TEUkm using a conversion factor of 0.291 MJ/TEUkm for ammonia with 9.6% e/e VLSFO and 0.275 MJ/TEUkm for VLSFO. **Appendix 4: Conversion factor from MJ to TEUkm** describes how the conversion factor has been determined. Note that the conversion factors for TEUkm are estimates and can differ based on both ship design and size as well as engine efficiency.

Table 6.2 presents the characterised results for the global mean per TEUkm. Also here, the results for GWP100 is presented with and without the GWP of H_2, since the GWP for H_2 is not included in IPCC (2021) (see **section 2.11**).

Table 6.2: Characterised global mean results for ammonia (9.6% e/e VLSFO) with H_2 from electrolysis (based on either solar or wind), ammonia (9.6% e/e VLSFO) with H_2 from ATR with CCS, and VLSFO with the functional unit of 1 TEUkm for the **consequential model**.

Global mean	Production pathway	Haber-Bosch			Desulphurisation
	H_2 production	Electrolysis	Electrolysis	ATR with CCS	ATR
	Electricity source	Solar	Wind	Grid	Grid
	Fuel	Ammonia with 9.6% e/e VLSFO	Ammonia with 9.6% e/e VLSFO	Ammonia with 9.6% e/e VLSFO	VLSFO
Impact categories	**Unit**				
Global warming (GWP100)	g CO_2-eq/TEUkm	6.5	5.7	13.0	29.4
GWP100 without GWP of H_2	g CO_2-eq/TEUkm	6.0	5.3	12.1	29.4
Respiratory inorganics	mg $PM_{2.5}$-eq/TEUkm	94	93	92	106
Respiratory organics	pers*ppm*s/TEUkm	0.25	0.24	0.25	0.25
Nature occupation	PDF*m^2a/TEUkm	0.00010	0.00007	0.00006	0.00014
Acidification	cm^2 UES/TEUkm	70	70	69	54
Eutrophication, aquatic	mg NO_3-eq/TEUkm	65	64	64	45
Eutrophication, terrestrial	cm^2 UES/TEUkm	328	327	328	187
Photochemical ozone, vegetation	cm^2*ppm*hours/TEUkm	9,718	9,567	9,826	9,515

When comparing the results in **Table 6.2**, ammonia (9.6% e/e VLSFO) with H_2 from wind-based electrolysis still has the lowest impact on GWP100 and respiratory organics, though VLSFO now has the lowest impact on photochemical ozone, vegetation, as well as acidification and both aquatic and terrestrial eutrophication. For nature occupation and respiratory inorganics, natural gas-based ammonia still has the lowest impact. Nevertheless, differences between the fuels for nature occupation as well as respiratory organics and inorganics are still relatively small.

The difference in results is still largest for GWP100, as ammonia (9.6% e/e VLSFO) with H_2 from wind-based electrolysis has an impact that is over five times lower than VLSFO. Moreover, the difference for the other impact categories is still around or under a factor of two.

6.2 Regional differences for global warming potential

The regional differences for GWP100 for the four fuel scenarios are presented in **Figure 6.1**. The figure shows that the largest geographical differences occur for VLSFO, as the impact varies from 99 to 122 g CO_2-eq/MJ. The span in results for VLSFO is primarily caused by the differences in the carbon intensity of the fuel oil used as feedstock.

For ammonia (9.6% e/e VLSFO) with H_2 from ATR with CCS, there is a difference of 9 g CO_2-eq between the highest and lowest value on **Figure 6.1**. The variation is primarily caused by the carbon intensity of the natural gas and grid electricity. For ammonia (9.6% e/e VLSFO) with H_2 from electrolysis, the difference is 13 and 10 g CO_2-eq with electricity from solar and wind, respectively. The variation is caused by the carbon intensity per kWh of wind and solar electricity in the 17 regions.

For the majority of the 17 regions, the GWP100 results for ammonia (9.6% e/e VLSFO) with H_2 from wind-based electrolysis are 2-5 g CO_2-eq lower than ammonia (9.6% e/e VLSFO) with solar-based electrolysis. Nevertheless, for two regions – Indonesia and India – the GWP100 results for ammonia with solar-based electrolysis are approximately 1 g CO_2-eq lower compared to the results for ammonia with wind-based electrolysis. The biggest difference between ammonia with solar- and wind-based electrolysis is seen for China, as the difference is 9 g CO_2-eq/MJ.

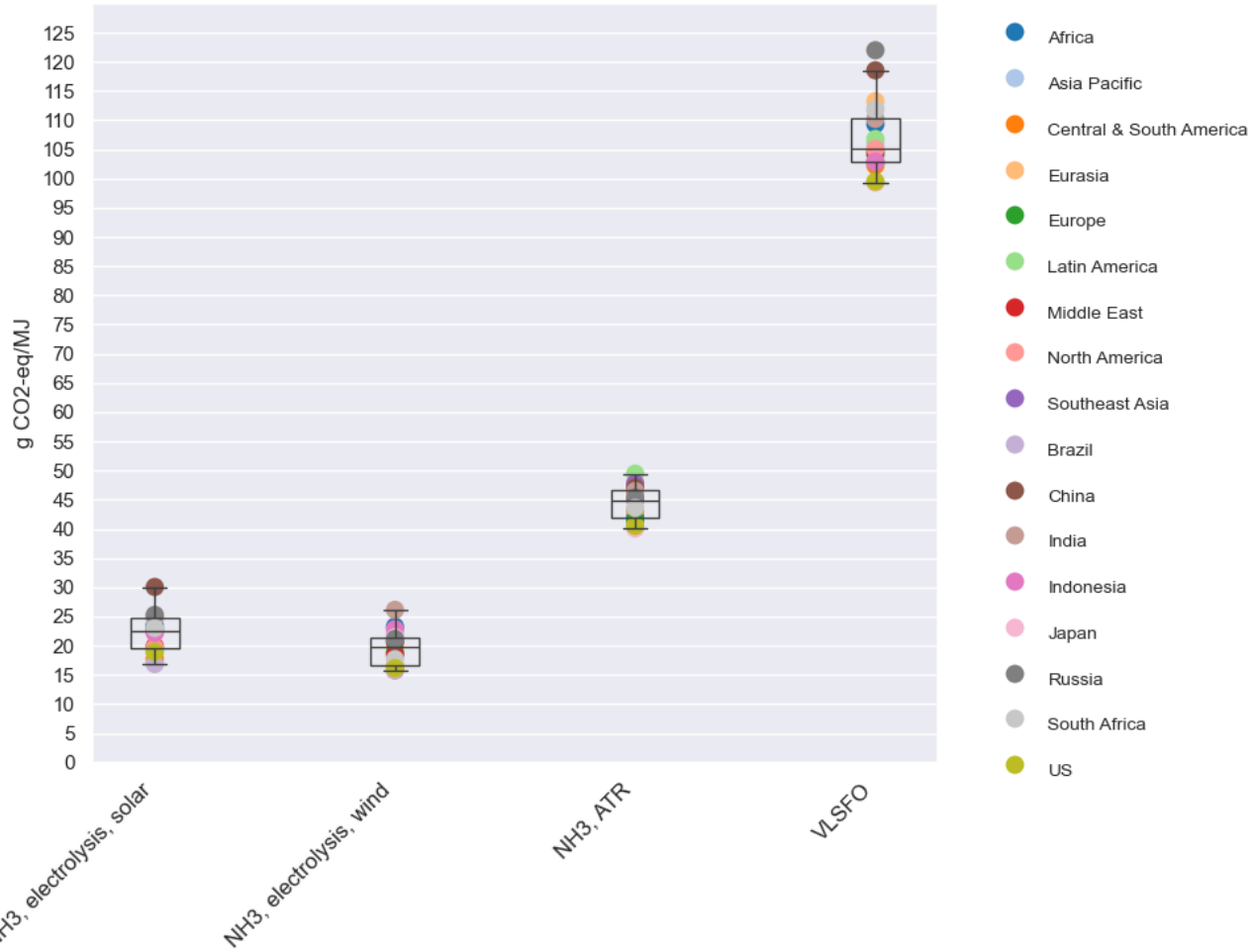

Figure 6.1: Regional differences in the **consequential** GWP100 results for ammonia (9.6% e/e VLSFO) with H_2 from electrolysis (based on either solar or wind), ammonia (9.6% e/e VLSFO) with H_2 from ATR with CCS, and VLSFO with the functional unit of 1 MJ.

6.3 Contribution analysis for global warming potential

A percentual contribution for each process for GWP100 is shown in **Table 6.3**, while a detailed contribution analysis by input is presented in **Table 6.4**.

Table 6.3 displays that there are four processes that are the main contributors to the GWP100 for the electrolysis-based ammonia: fuel combustion, H_2 production, distribution and bunkering of ammonia, and VLSFO production. For ammonia with H_2 from ATR with CCS, the ATR process is the largest contributor followed by CCS and fuel combustion. Lastly, the GWP100 results for VLSFO primarily stem from the combustion.

Table 6.3: GWP100 contribution analysis for each process in percent for global mean ammonia (9.6% e/e VLSFO) with H_2 from electrolysis (based on either solar or wind), ammonia (9.6% e/e VLSFO) with H_2 from ATR with CCS, and VLSFO with the functional unit of 1 MJ for the **consequential model**. The shades of red are used to highlight the highest values.

Global mean	Ammonia (9.6% e/e VLSFO) with H_2 from electrolysis	Ammonia (9.6% e/e VLSFO) with H_2 from electrolysis	Ammonia (9.6% e/e VLSFO) with H_2 from ATR with CCS	VLSFO
Activity	**Solar**	**Wind**		
Total result (g CO_2-eq/MJ)	**22.3**	**19.6**	**44.6**	**107.1**
N_2 production	0%	0%	0.5%	
H_2 production	32%	24%	33%	
H_2 storage	1%	1%		
CCS, ATR, NH_3			29%	
NH_3 production	1%	1%	5%	
VLSFO production	12%	13%	6%	25%
H_2, ATR, to VLSFO	1%	1%	0.5%	2%
O_2, ASU, to ATR for VLSFO	0.002%	0.002%	0.001%	0.004%
Distribution and bunkering, NH_3	12%	14%	6%	
Distribution and bunkering, VLSFO	1%	2%	1%	0.52%
Combustion	40%	45%	20%	72%
Total	100%	100%	100%	100%

Table 6.4 shows that the H_2 electrolysis production is highly influenced by impact from the renewable electricity and the CO_2 emissions from combustion, which stem from the share of pilot fuel. For natural gas-based ammonia, the CCS process has a high impact due to the CO_2 emissions emitted to the atmosphere, since only 90% of the CO_2 emissions and because there is a yearly slip of 0.023% from carbon storage. Moreover, the carbon intensity of the natural gas input to ATR is the largest contributor. Note that input of fuel oil for pilot fuel production accounts for 13% and 15% for ammonia with solar and wind-based electrolysis, respectively, while fuel oil only accounts for 6% for ammonia with H_2 from ATR with CCS.

Table 6.4: Detailed GWP100 contribution analysis for global mean ammonia (9.6% e/e VLSFO) with H_2 from electrolysis (based on either solar or wind), ammonia (9.6% e/e VLSFO) with H_2 from ATR with CCS, and VLSFO with the functional unit of 1 MJ for the **consequential model**. The shades of red are used to highlight the highest values.

Global mean	g CO2-eq/MJ	Ammonia (9.6% e/e VLSFO) with H_2 from electrolysis	Ammonia (9.6% e/e VLSFO) with H_2 from electrolysis	Ammonia (9.6% e/e VLSFO) with H_2 from ATR with CCS	VLSFO
Activity	**Input / Flow**	**Solar**	**Wind**		
N_2 production, for NH_3	Electricity, renewable	0	0		
	Electricity, grid			1.44	
	Excess O_2, substitution			-1.23	
H_2 production, for NH_3	Emissions to air, CO_2			0.02	
	Emissions to air, CH_4			2.98	
	Emissions to air, H_2	0.37	0.37	0.37	
	Water	0.03	0.03	0.03	
	Electricity, renewable	6.75	4.23		
	Electricity, grid			0.32	
	Natural gas, feedstock			11.1	
H_2 storage	Emissions to air, H_2	0.09	0.09		
	Electricity, renewable	0.05	0.03		
	CAPEX, H_2 storage	0.00003	0.00003		
CCS, for ATR H_2, NH_3	Emissions to air, CO_2			10.76	
	Water			0.001	
	Amines			0.30	
	Electricity, grid, carbon capture			0.02	
	Natural gas			0.58	
	Electricity, grid, pipe transport			0.57	
	CAPEX, pipeline			0.54	
NH_3 production	Emissions to air, NH_3				
	Electricity, renewable	0.25	0.16		
	Electricity, grid			2.05	
	CAPEX: ammonia, N_2 & H_2 plant	0.0001	0.0001	0.0001	
VLSFO	Steam	0.004	0.004	0.004	0.04
	Fuel oil, feedstock	2.87	2.87	2.87	29.30
	Electricity, grid	0.005	0.005	0.005	0.05
	Sulphur stockpiling	0.016	0.016	0.016	0.17
	Naphtha, substitution	-0.26	-0.26	-0.26	-2.69
H_2 production, ATR, for VLSFO	Emissions to air, CO_2	0.20	0.20	0.20	2.07
	Emissions to air, CH_4	0.007	0.007	0.007	0.07
	Emissions to air, H_2	0.0008	0.0008	0.0008	0.008
	Water	0.0001	0.0001	0.0001	0.001
	Electricity, grid	0.001	0.001	0.001	0.01
	Natural gas, feedstock	0.025	0.025	0.025	0.25
O_2 production, for H_2 ATR for VLSFO	Electricity, grid	0.0005	0.0005	0.0005	0.005
CAPEX, VLSFO	incl. ATR and ASU	0.002	0.002	0.002	0.02
Distribution and bunkering, NH_3	Emissions, NH_3				
	Sea transport	0.62	0.62	0.62	
	Fuel oil, cooling	1.70	1.70	1.70	
	Electricity, grid, bunkering	0.04	0.04	0.04	
	Electricity, grid, pipe transport	0.18	0.18	0.18	
	CAPEX, pipeline	0.12	0.12	0.12	
Distribution and bunkering, VLSFO	Sea transport	0.03	0.03	0.03	0.28
	Electricity, grid, bunkering	0.002	0.002	0.002	0.02
	Electricity, grid, pipe transport	0.18	0.18	0.18	0.15
	CAPEX, pipeline	0.12	0.12	0.12	0.11
Combustion	CO_2 emissions	7.36	7.36	7.36	76.53
	N_2O emissions	1.52	1.52	1.52	0.76
Total		**22.3**	**19.6**	**44.6**	**107.1**

6.4 Contribution analysis for other impact categories

This section presents the contribution analysis for the remaining eight impact categories. The section includes the contribution for each process in percent, while the contribution analyses by input are in **appendix 10** (external appendix). Moreover, this section also illustrates the geographical differences for the eight impact categories.

6.4.1 Respiratory inorganics

Respiratory inorganics accounts for the impact on human health from particle emissions as well as emissions of NO_x, SO_x, and ammonia. As seen from **Table 6.5**, the largest contributor to respiratory inorganics are the combustion emissions. This is because this life cycle stage emits the most particles, ammonia, and NO_x to the atmosphere.

For the two ammonia pathways, the next largest contributors are the slip of ammonia from the Haber-Bosch process as well as from the distribution and bunkering of ammonia. The contribution from the H_2 production stems from the input of aluminium to the production of solar and wind electricity.

For VLSFO, the feedstock of fuel oil is the largest contributor after fuel combustion, since particles and NO_x are emitted when producing this feedstock.

Table 6.5: Respiratory inorganics contribution analysis for each process in percent for global mean ammonia (9.6% e/e VLSFO) with H_2 from electrolysis (based on either solar or wind), ammonia (9.6% e/e VLSFO) with H_2 from ATR with CCS, and VLSFO with the functional unit of 1 MJ for the **consequential model**. The shades of red are used to highlight the highest values.

Global mean	Ammonia (9.6% e/e VLSFO) with H_2 from electrolysis	Ammonia (9.6% e/e VLSFO) with H_2 from electrolysis	Ammonia (9.6% e/e VLSFO) with H_2 from ATR with CCS	VLSFO
Activity	**Solar**	**Wind**		
Total result (mg $PM_{2.5}$-eq/MJ)	**323**	**321**	**318**	**387**
N_2 production	0%	0%	0.1%	
H_2 production	4%	3%	1%	
H_2 storage	0.03%	0.02%		
CCS, ATR			0.4%	
NH_3 production	6%	6%	7%	
VLSFO production	1%	1%	1%	7%
H_2, ATR, to VLSFO	0.003%	0.003%	0.003%	0.02%
O_2, ASU, to ATR for VLSFO	0%	0%	0%	0%
Distribution and bunkering, NH_3	7%	7%	7%	
Distribution and bunkering, VLSFO	0.1%	0.1%	0.1%	0.2%
Combustion	82%	83%	84%	93%
Total	100%	100%	100%	100%

6.4.1.1 Regional differences for respiratory inorganics

The regional differences for respiratory inorganics are presented in **Figure 6.2** for the four fuel scenarios. The geographical difference for ammonia with H_2 from electrolysis is caused by the renewable electricity, while for ammonia with H_2 from ATR with CCS, the geographical differences are caused by the grid electricity mix and the natural gas input. For VLSFO, the differences are caused by the fuel oil feedstock.

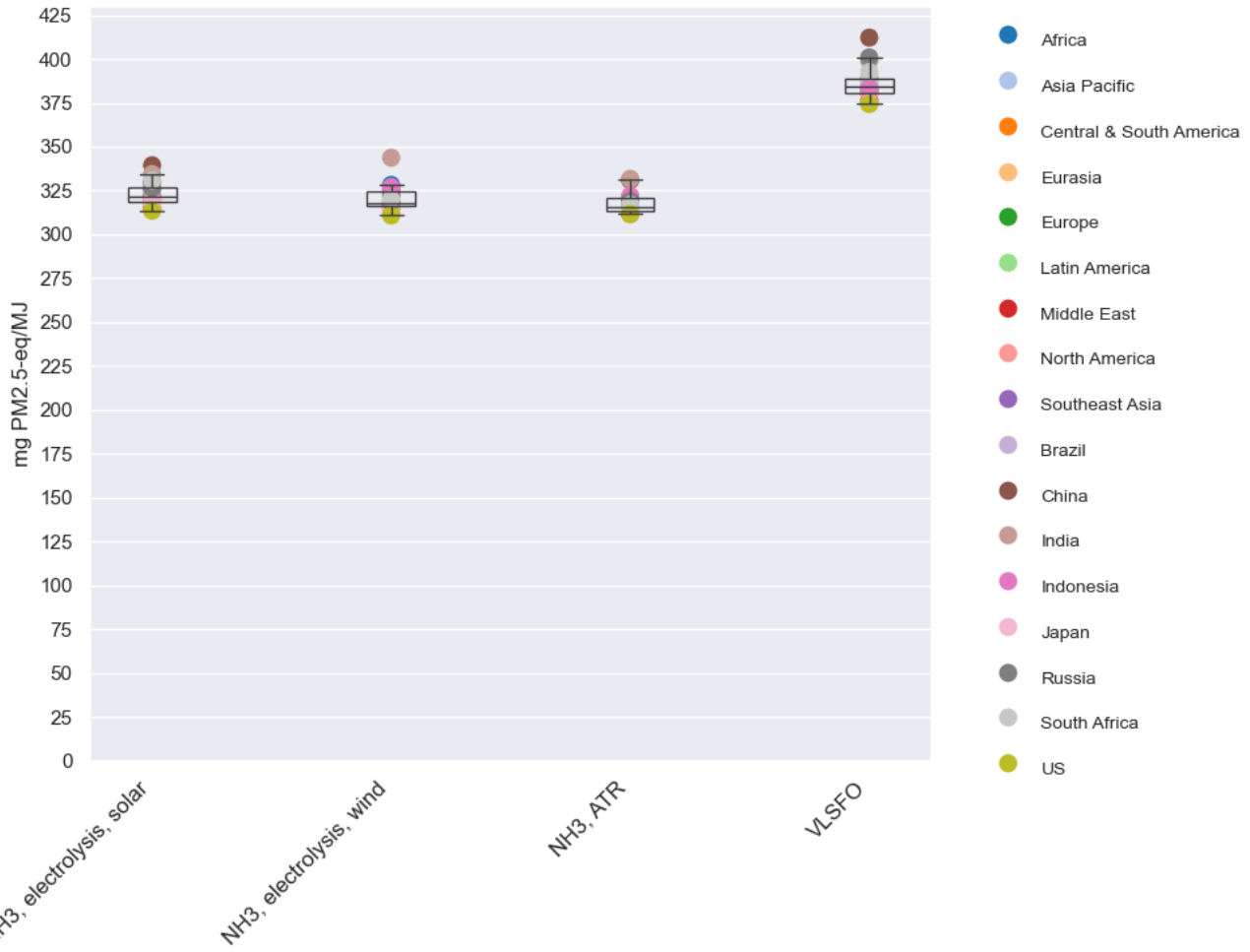

Figure 6.2: Regional differences in the **consequential** respiratory inorganics results for ammonia (9.6% e/e VLSFO) with H_2 from electrolysis (based on either solar or wind), ammonia (9.6% e/e VLSFO) with H_2 from ATR with CCS, and VLSFO with the functional unit of 1 MJ.

Figure 6.2 shows that the respiratory inorganics impact for India is among the higher values for the ammonia fuels, while the opposite is the case for the US. US also has the lowest value for VLSFO, while China has the highest. Note that the impacts from ammonia with H_2 from electrolysis in India on **Figure 6.2** are higher than the upper value for natural gas-based ammonia. The higher impact for India is primarily caused by the emissions from the manufacture of iron and steel used for the wind turbines.

Note that in **section 6.1**, the global mean value for natural gas-based ammonia was lowest for respiratory inorganics, though the differences between the fuels were deemed relatively small. Yet, **Figure 6.2** shows that the result ranges for the ammonia fuel scenarios overlap, thus, it can only be concluded that VLSFO has a higher impact on respiratory inorganics than the ammonia fuel scenarios.

6.4.2 Respiratory organics

Respiratory organics relates to the impact on human health caused by photochemical ozone formation. The main contributor to respiratory organics is the combustion of fuel, regardless of the fuel type and production pathway, as **Table 6.6** shows that the combustion emissions account for 88% or more. This is because of NO_x emitted to the atmosphere.

The next largest contributor to both ammonia pathways is the H_2 production. For electrolysis-based ammonia, the contribution stems from material inputs to the production of renewable electricity. The ATR H_2 production is the next largest contributor for natural gas-based ammonia, since the input of natural gas is associated with methane emissions. For VLSFO, the next largest contributor is VLSFO production, where the production of the fuel oil feedstock results in NO_x, methane, and non-methane volatile organic compounds (NMVOCs) being emitted to the atmosphere.

Table 6.6: Respiratory organics contribution analysis for ammonia (9.6% e/e VLSFO) with H_2 from electrolysis (based on either solar or wind), ammonia (9.6% e/e VLSFO) with H_2 from ATR with CCS, and VLSFO with the functional unit of 1 MJ for the **consequential model**. The shades of red are used to highlight the highest values.

Global mean	Ammonia (9.6% e/e VLSFO) with H_2 from electrolysis	Ammonia (9.6% e/e VLSFO) with H_2 from electrolysis	Ammonia (9.6% e/e VLSFO) with H_2 from ATR with CCS	VLSFO
Activity	**Solar**	**Wind**		
Total result (pers*ppm*s/MJ)	**0.85**	**0.83**	**0.86**	**0.90**
N_2 production	0%	0%	0.03%	
H_2 production	4%	2%	6%	
H_2 storage	0.03%	0.02%		
CCS, ATR			0.4%	
NH_3 production	0.16%	0.07%	0.3%	
VLSFO production	1%	1%	1%	11%
H_2, ATR, to VLSFO	0.01%	0.01%	0.01%	0.1%
O_2, ASU, to ATR for VLSFO	0.0001%	0.0001%	0.0001%	0.0007%
Distribution and bunkering, NH_3	1%	1%	1%	
Distribution and bunkering, VLSFO	0.1%	0.1%	0.1%	0.2%
Combustion	93%	96%	92%	88%
Total	100%	100%	100%	100%

6.4.2.1 Regional differences for respiratory organics

The regional differences for respiratory organics are presented in **Figure 6.3** for the four fuel scenarios. Just as for respiratory inorganics, the geographical difference for ammonia with H_2 from electrolysis is caused by the renewable electricity, while for ammonia with H_2 from ATR with CCS, the geographical differences are caused by the grid electricity mix and the natural gas input. For VLSFO, the differences are caused by the fuel oil feedstock.

Figure 6.3 shows that for all ammonia fuels, the US has the lowest impact, while Japan has the lowest impact from VLSFO. The figure also shows that VLSFO and ammonia with solar-based electrolysis has the largest geographical range, while natural gas-based ammonia has the smallest geographical range.

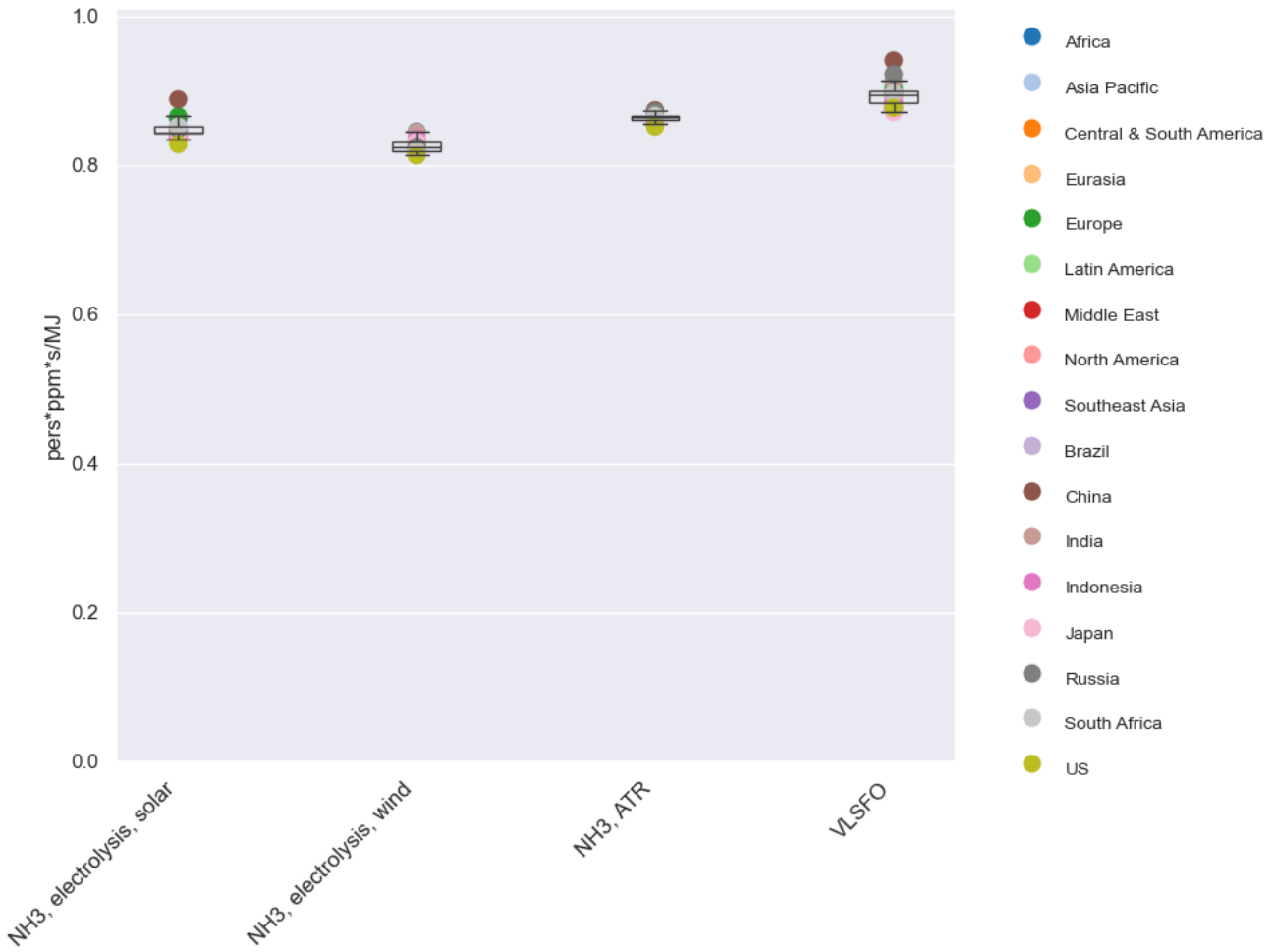

Figure 6.3: Regional differences in the **consequential** respiratory organics results for ammonia (9.6% e/e VLSFO) with H_2 from electrolysis (based on either solar or wind), ammonia (9.6% e/e VLSFO) with H_2 from ATR with CCS, and VLSFO with the functional unit of 1 MJ.

Note that in **section 6.1**, the global mean value for ammonia with wind-based electrolysis was lowest for respiratory organics, though the differences between the fuels were deemed relatively small. Yet, **Figure 6.3** shows that the result ranges for the ammonia fuel scenarios overlap. Moreover, the upper value for ammonia with solar-based electrolysis is close to the median value for VLSFO, while the upper value for natural gas-based ammonia is close to the lowest value for VLSFO. Thus, the difference in results between fuel scenarios are highly dependent on the 17 regions.

6.4.3 Nature occupation

Nature occupation relates to the loss of species in terrestrial ecosystems. The unit PDF*m^2 specifically represents the impact from the occupation of 1 m^2 of land during one year multiplied with a severity score representing the potentially disappeared fraction (PDF) of species in that area during the specified time.

Overall, all four fuel scenarios have a relatively small impact on nature occupation, as the results range from 0.00020-0.00051 PDF*m^{2}a/MJ, meaning that the demand for 1 MJ of each fuel results in the potentially disappeared fraction (PDF) of species from the occupation of 2.0-5.1 cm^2 arable land for one year. There is no occupation of arable land in the foreground system, therefore, the impact on nature occupation stems from the background system.

Table 6.7: Nature occupation contribution analysis for each process in percent for global mean ammonia (9.6% e/e VLSFO) with H_2 from electrolysis (based on either solar or wind), ammonia (9.6% e/e VLSFO) with H_2 from ATR with CCS, and VLSFO with the functional unit of 1 MJ for the **consequential model**. The shades of red are used to highlight the highest values.

Global mean	Ammonia (9.6% e/e VLSFO) with H_2 from electrolysis	Ammonia (9.6% e/e VLSFO) with H_2 from electrolysis	Ammonia (9.6% e/e VLSFO) with H_2 from ATR with CCS	VLSFO
Activity	**Solar**	**Wind**		
Total result (PDF*m^{2}a/MJ)	**0.00033**	**0.00024**	**0.00020**	**0.00051**
N_2 production	0%	0%	1%	
H_2 production	71%	61%	17%	
H_2 storage	0.5%	0.5%		
CCS, ATR			27%	
NH_3 production	3%	2%	11%	
VLSFO production	15%	20%	25%	97%
H_2, ATR, to VLSFO	0.02%	0.03%	0.04%	0.2%
O_2, ASU, to ATR for VLSFO	0.001%	0.002%	0.002%	0.01%
Distribution and bunkering, NH_3	10%	14%	17%	
Distribution and bunkering, VLSFO	1%	2%	2%	3%
Combustion	0%	0%	0%	0%
Total	100%	100%	100%	100%

As seen from **Table 6.7**, the largest contributors to nature occupation for electrolysis-based ammonia are the VLSFO production and electrolysis H_2 production. This is because there is an input of crops or forestry to the production of materials used to produce the solar panels and wind turbines or to the production of the fuel oil feedstock. Thus, since land occupation is linked to agriculture and forestry, this causes the impact on nature occupation. For natural gas-based ammonia, the contribution from the CCS process stems from the input of amines since chemicals are often produced from vegetable oils.

6.4.3.1 Regional differences for nature occupation

Figure 6.4 presents the regional differences for nature occupation results for the four fuel scenarios. Just as for respiratory inorganics and organics, the geographical difference for ammonia with H_2 from electrolysis is caused by the renewable electricity, while for ammonia with H_2 from ATR with CCS, the geographical differences are caused by the grid electricity mix and the natural gas input. For VLSFO, the differences are caused by the fuel oil feedstock. Sea transport in the distribution and bunkering phase also contributes to the impact on nature occupation for all four fuel scenarios.

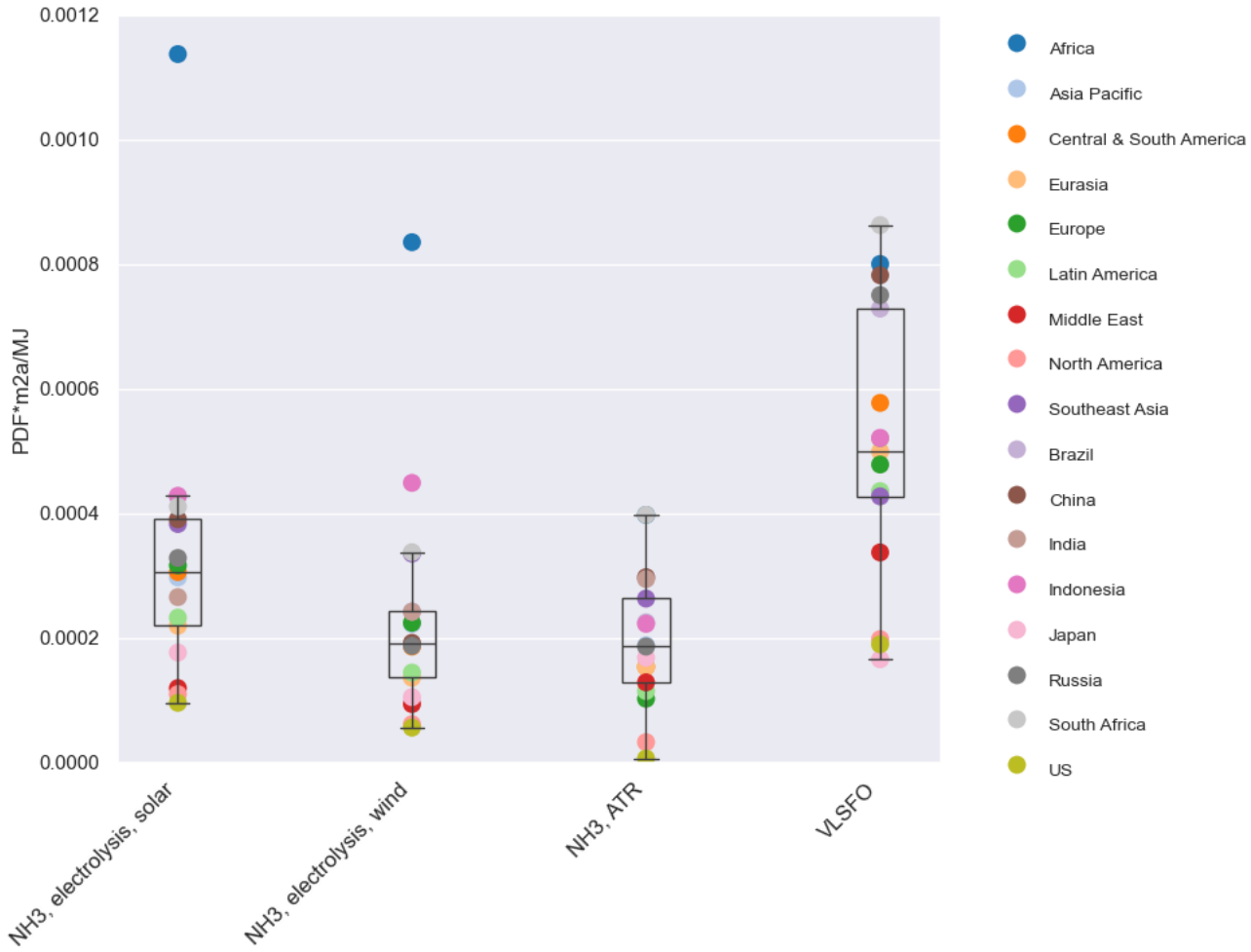

Figure 6.4: Regional differences in the **consequential** nature occupation results for ammonia (9.6% e/e VLSFO) with H_2 from electrolysis (based on either solar or wind), ammonia (9.6% e/e VLSFO) with H_2 from ATR with CCS, and VLSFO with the functional unit of 1 MJ.

The largest nature occupation results on **Figure 6.4** are seen for electrolysis-based ammonia in Africa. The larger impact for this region is caused by the input of wood for the manufacture of plastic and glass, which is used to produce solar panels and wind turbines. Thus, since forestry is linked to land occupation, this causes the impact on nature occupation.

Note that in **section 6.1**, the global mean value for natural gas-based ammonia was lowest for nature occupation, though the differences between the fuels were deemed relatively small. Yet, **Figure 6.2** shows that the result ranges for all four fuel scenarios overlap, thus, the difference in results between fuel scenarios are highly dependent on the 17 regions.

6.4.4 Eutrophication, aquatic and terrestrial

Aquatic eutrophication as an impact category expresses the potential for oxygen reduction in water environments due to nutrient pollution of nitrogen and phosphorous, while terrestrial eutrophication expresses the area of unprotected ecosystems which is brought to exceed the critical load of eutrophication because of emissions. Thus, for this LCA study, the emissions of nitrogen-containing compounds in the foreground system are important contributors to these two impact categories. Aquatic eutrophication is expressed in mg NO_3-eq, while terrestrial eutrophication is expressed in cm^2 area of unprotected ecosystem (cm^2 UES).

Based on **Table 6.8** and **Table 6.9**, there are three processes that are the main contributors to aquatic and terrestrial eutrophication for both ammonia pathways: fuel combustion, ammonia production, and distribution and bunkering of ammonia. This is because ammonia is emitted from all three processes while NO_x is also emitted to the atmosphere from the combustion. For VLSFO, nitrogen-containing compounds are released to the atmosphere from the fuel combustion as well as from the production of the fuel oil used as feedstock.

Table 6.8: Eutrophication, aquatic, contribution analysis for each process in percent for global mean ammonia (9.6% e/e VLSFO) with H_2 from electrolysis (based on either solar or wind), ammonia (9.6% e/e VLSFO) with H_2 from ATR with CCS, and VLSFO with the functional unit of 1 MJ for the **consequential model**. The shades of red are used to highlight the highest values.

Global mean	Ammonia (9.6% e/e VLSFO) with H_2 from electrolysis	Ammonia (9.6% e/e VLSFO) with H_2 from electrolysis	Ammonia (9.6% e/e VLSFO) with H_2 from ATR with CCS	VLSFO
Activity	Solar	Wind		
Total result (mg NO3-eq/MJ)	**225.2**	**221.6**	**221.3**	**162.7**
N_2 production	0%	0%	0.04%	
H_2 production	4%	2%	1%	
H_2 storage	0.03%	0.02%		
CCS, ATR			1%	
NH_3 production	16%	16%	16%	
VLSFO production	1%	1%	1%	14%
H_2, ATR, to VLSFO	0.002%	0.002%	0.002%	0.03%
O_2, ASU, to ATR for VLSFO	0.0001%	0.0001%	0.0001%	0.001%
Distribution and bunkering, NH_3	17%	17%	17%	
Distribution and bunkering, VLSFO	0.1%	0.1%	0.1%	0.4%
Combustion	63%	64%	64%	86%
Total	100%	100%	100%	100%

Table 6.9: Eutrophication, terrestrial, contribution analysis for each process in percent for global mean ammonia (9.6% e/e VLSFO) with H_2 from electrolysis (based on either solar or wind), ammonia (9.6% e/e VLSFO) with H_2 from ATR with CCS, and VLSFO with the functional unit of 1 MJ for the **consequential model**. The shades of red are used to highlight the highest values.

Global mean	Ammonia (9.6% e/e VLSFO) with H_2 from electrolysis	Ammonia (9.6% e/e VLSFO) with H_2 from electrolysis	Ammonia (9.6% e/e VLSFO) with H_2 from ATR with CCS	VLSFO
Activity	**Solar**	**Wind**		
Total result (cm2 UES/MJ)	**1,129.2**	**1,126.8**	**1,128.8**	**680.3**
N_2 production	0%	0%	0.01%	
H_2 production	0.5%	0.3%	0.3%	
H_2 storage	0.004%	0.002%		
CCS, ATR			0.1%	
NH_3 production	20%	20%	20%	
VLSFO production	0.2%	0.2%	0.2%	3%
H_2, ATR, to VLSFO	0.001%	0.001%	0.001%	0.01%
O_2, ASU, to ATR for VLSFO	0.00002%	0.00002%	0.00002%	0.0004%
Distribution and bunkering, NH_3	20%	20%	20%	
Distribution and bunkering, VLSFO	0.02%	0.02%	0.02%	0.1%
Combustion	59%	59%	59%	97%
Total	100%	100%	100%	100%

6.4.4.1 Regional differences for eutrophication, aquatic and terrestrial

Figure 6.5 and **Figure 6.6** display the regional differences for aquatic and terrestrial eutrophication results for the four fuel scenarios. Just as for respiratory inorganics and organics, the geographical differences for ammonia with H_2 from electrolysis are caused by the renewable electricity, while for ammonia with H_2 from ATR with CCS, the geographical differences are caused by the grid electricity mix and the natural gas input. For VLSFO, the differences are caused by the fuel oil feedstock.

On **Figure 6.5**, Africa has the largest impact on aquatic eutrophication for electrolysis-based ammonia. This is due to the input of wood for the manufacture of plastic and glass, which is used to produce solar panels and wind turbines. On **Figure 6.5**, the regional differences for terrestrial eutrophication are less pronounced, since the range in results are 9 and 15 cm^2 UES/MJ for ammonia with wind- and solar-based electrolysis, respectively, while the range is 11 and 25 cm^2 UES/MJ for natural gas-based ammonia and VLSFO, respectively.

Note that both figures confirm the conclusion in **section 6.1**, that VLSFO has the lowest impact on aquatic and terrestrial eutrophication, while the figures also show that the result range for the ammonia fuel scenarios overlap, thus, there is no notable difference in result for the ammonia fuel scenarios for these two impact categories.

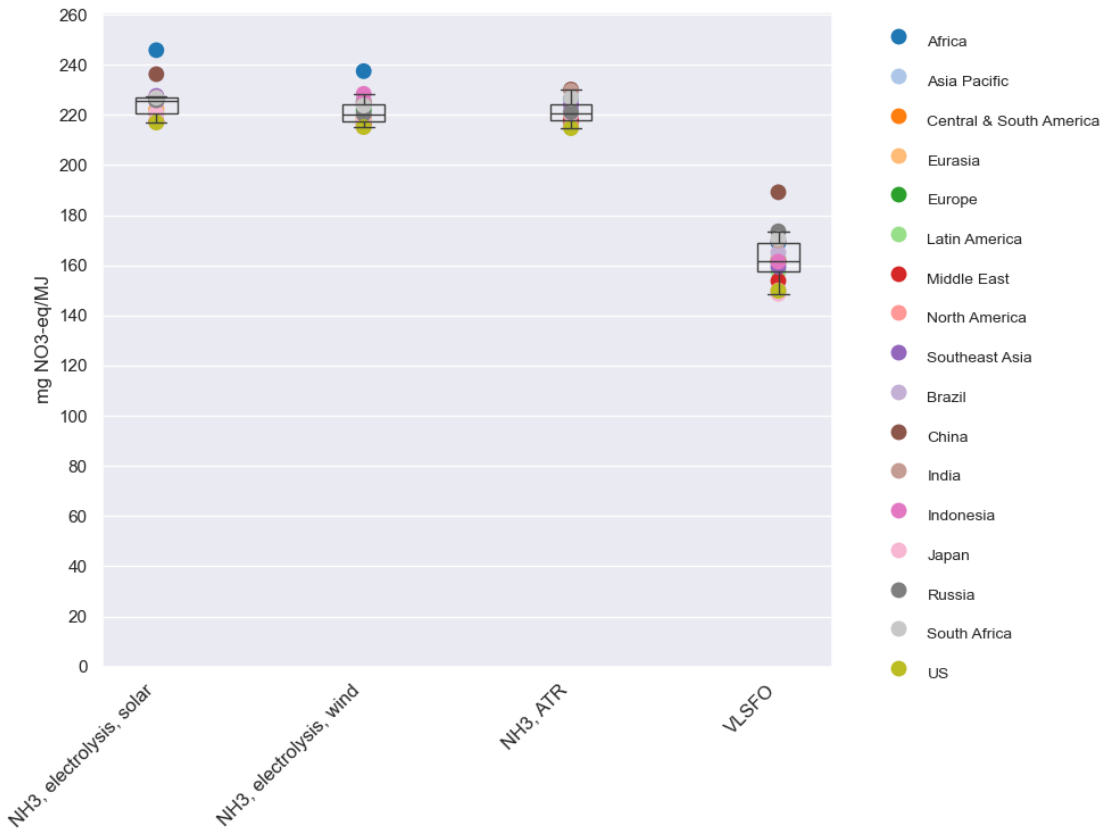

Figure 6.5: Regional differences in the **consequential** aquatic eutrophication results for ammonia (9.6% e/e VLSFO) with H_2 from electrolysis (based on either solar or wind), ammonia (9.6% e/e VLSFO) with H_2 from ATR and VLSFO with the functional unit of 1 MJ.

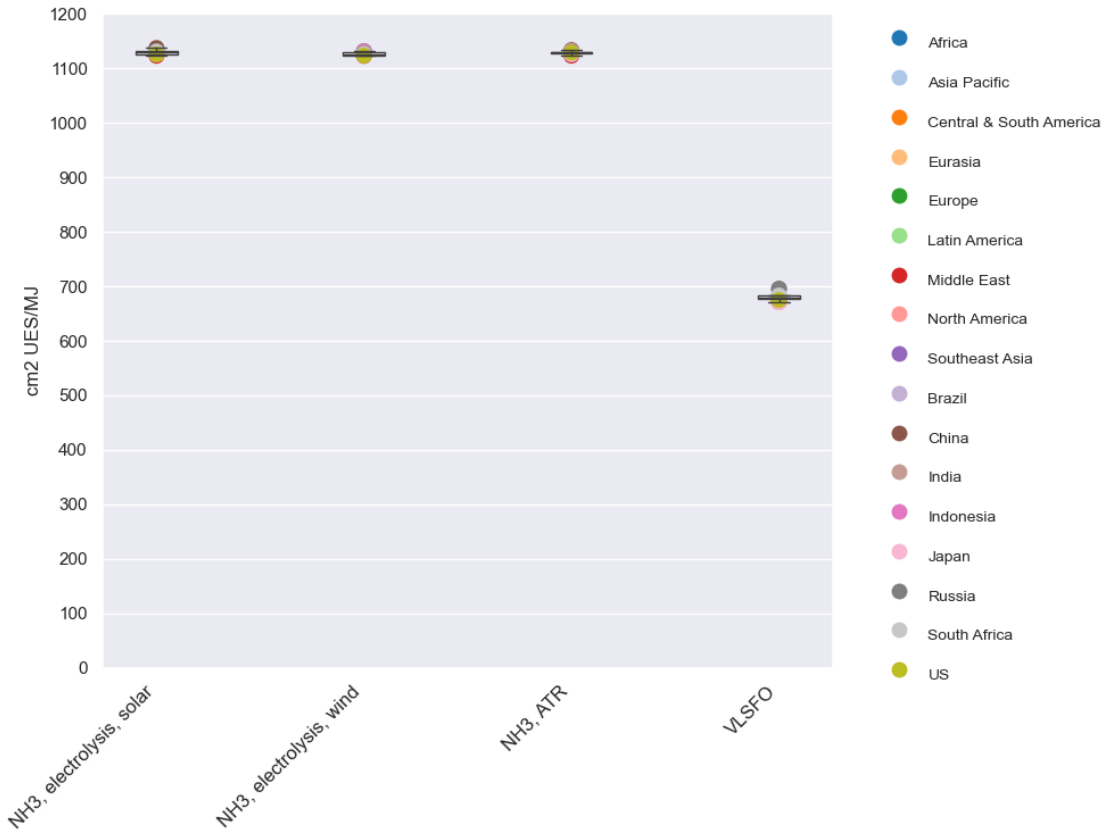

Figure 6.6: Regional differences in the **consequential** terrestrial eutrophication results for ammonia (9.6% e/e VLSFO) with H_2 from electrolysis (based on either solar or wind), ammonia (9.6% e/e VLSFO) with H_2 from ATR and VLSFO with the functional unit of 1 MJ.

6.4.5 Acidification

Acidification is the process of an environment becoming more acidic and this impact category therefore expresses the area of ecosystems, which are brought to exceed the critical load of acidification because of emissions. For example, emissions of ammonia, SO_x, and NO_x have an acidifying effect on the environment. The acidification impact category is expressed in cm^2 area of unprotected ecosystem (cm^2 UES).

As seen from **Table 6.10**, there are three main contributors to acidification for the two ammonia pathways: fuel combustion, distribution and bunkering of ammonia, as well as the ammonia synthesis process. This is because there is a slip of ammonia from each of these processes, while there is also an emission of NO_x from the fuel combustion. For VLSFO, fuel combustion accounts for 90% of the impact because of the NO_x emissions from the combustion, while the VLSFO production process accounts for the remaining 10%, since ammonia, SO_x, and NO_x are released from the production of the fuel oil feedstock.

Table 6.10: Acidification contribution analysis for each process in percent for global mean ammonia (9.6% e/e VLSFO) with H_2 from electrolysis (based on either solar or wind), ammonia (9.6% e/e VLSFO) with H_2 from ATR with CCS, and VLSFO with the functional unit of 1 MJ for the **consequential model**. The shades of red are used to highlight the highest values.

Global mean	Ammonia (9.6% e/e VLSFO) with H_2 from electrolysis	Ammonia (9.6% e/e VLSFO) with H_2 from electrolysis	Ammonia (9.6% e/e VLSFO) with H_2 from ATR with CCS	VLSFO
Activity	**Solar**	**Wind**		
Total result (cm^2 UES/MJ)	**242.2**	**240.9**	**238.8**	**194.8**
N_2 production	0%	0%	0.05%	
H_2 production	3%	2%	1%	
H_2 storage	0.02%	0.02%		
CCS, ATR			0.3%	
NH_3 production	20%	20%	21%	
VLSFO production	1%	1%	1%	10%
H_2, ATR, to VLSFO	0.002%	0.002%	0.002%	0.03%
O_2, ASU, to ATR for VLSFO	0.0001%	0.0001%	0.0001%	0.001%
Distribution and bunkering, NH_3	21%	21%	21%	
Distribution and bunkering, VLSFO	0.1%	0.1%	0.1%	0.3%
Combustion	55%	56%	56%	90%
Total	100%	100%	100%	100%

6.4.5.1 Regional differences for acidification

The regional differences for the acidification results are depicted on **Figure 6.7**. First of all, it is clear that VLSFO has a lower impact on acidification than the two ammonia pathways. Moreover, the figure also shows that the range in results is smallest for natural gas-based ammonia, while VLSFO and ammonia with solar-based electrolysis has the largest range in results.

For ammonia with H_2 from electrolysis, the differences are mainly caused by the renewable electricity, since acidifying emissions are associated with the production of materials used to manufacture solar panels and wind turbines. For ammonia with H_2 from ATR with CCS, the differences are caused by the grid electricity mix and natural gas extraction, which also results in ammonia and NO_x emissions. For VLSFO, the regional differences are mainly caused by the production of fuel oil.

The highest result on **Figure 6.7** is ammonia with solar-based electrolysis in South Africa and the impact stems from the input of electrical machinery and products to the solar panels. This is also the cause of the impact for electrolysis-based ammonia in Africa since South Africa accounts for half of the Africa region (see **Table 2.4**).

The acidification result for ammonia with H_2 from wind-based electrolysis in India is also among the upper values. This is because of emissions from copper and iron production for this country.

Note that **Figure 6.7** confirms that VLSFO has the lowest impact on acidification, which was also concluded in **section 6.1** based on the global mean values. Yet, the figure also shows that the result ranges for the ammonia fuel scenarios overlap and that the median values are fairly close to each other. Thus, the differences between the ammonia fuel scenarios' impact on acidification depend on differences between the 17 regions.

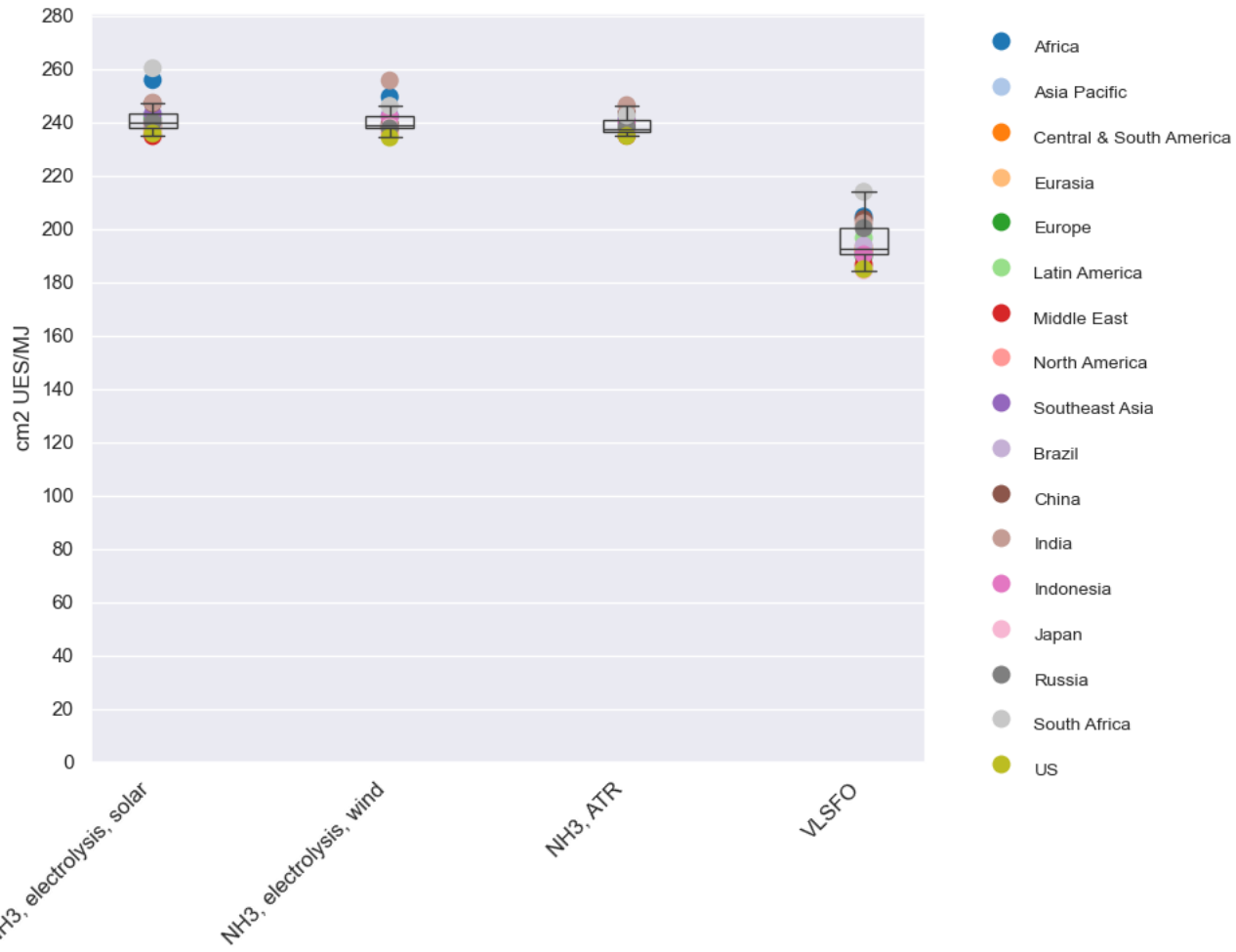

Figure 6.7: Regional differences in the **consequential** acidification results for ammonia (9.6% e/e VLSFO) with H_2 from electrolysis (based on either solar or wind), ammonia (9.6% e/e VLSFO) with H_2 from ATR with CCS, and VLSFO with the functional unit of 1 MJ.

6.4.6 Photochemical ozone, vegetation

The impact category 'photochemical ozone, vegetation' accounts for the formation of ozone, e.g., from oxidation of emissions of methane, NO_x, and NMVOCs and the possible damaging effects, which accumulated exposure of ozone above a certain threshold can have on vegetation, expressed in cm^2*ppm*hours.

Table 6.11 shows that fuel combustion is the main contributor for all four fuel scenarios. This is because all four fuels emit the same amount of NO_x per MJ and because NO_x emissions have an impact of 1,600 m^2*ppm*hours /kg.

Table 6.11: Photochemical ozone, vegetation, contribution analysis for each process in percent for global mean ammonia (9.6% e/e VLSFO) with H_2 from electrolysis (based on either solar or wind), ammonia (9.6% e/e VLSFO) with H_2 from ATR with CCS, and VLSFO with the functional unit of 1 MJ for the **consequential model**. The shades of red are used to highlight the highest values.

Global mean	Ammonia (9.6% e/e VLSFO) with H_2 from electrolysis	Ammonia (9.6% e/e VLSFO) with H_2 from electrolysis	Ammonia (9.6% e/e VLSFO) with H_2 from ATR with CCS	VLSFO
Activity	**Solar**	**Wind**		
Total result (cm^2*ppm*hours/MJ)	**33,439**	**32,920**	**33,810**	**34,643**
N_2 production	0%	0%	0.02%	
H_2 production	3%	1%	3%	
H_2 storage	0.0%	0.0%		
CCS, ATR			0.3%	
NH_3 production	0.1%	0.05%	0.2%	
VLSFO production	1%	1%	1%	7%
H_2, ATR, to VLSFO	0.008%	0.008%	0.008%	0.08%
O_2, ASU, to ATR for VLSFO	0.00005%	0.00005%	0.00005%	0.0005%
Distribution and bunkering, NH_3	1%	1%	1%	
Distribution and bunkering, VLSFO	0.1%	0.1%	0.1%	0.1%
Combustion	96%	97%	95%	92%
Total	100%	100%	100%	100%

6.4.6.1 Regional differences for photochemical ozone, vegetation

The regional differences for photochemical ozone, vegetation, results are presented on **Figure 6.8**. For ammonia with H_2 from electrolysis, the differences are mainly caused by the renewable electricity since production of materials for solar panels and wind turbines are associated with emissions of carbon monoxide and NO_x. For ammonia with H_2 from ATR with CCS, the differences are caused by the grid electricity mix and natural gas extraction, as these processes result in methane, NO_x, and NMVOC emissions. For VLSFO, the regional differences are mainly caused by the production of fuel oil, since this process is also associated with methane, NO_x, and NMVOC emissions.

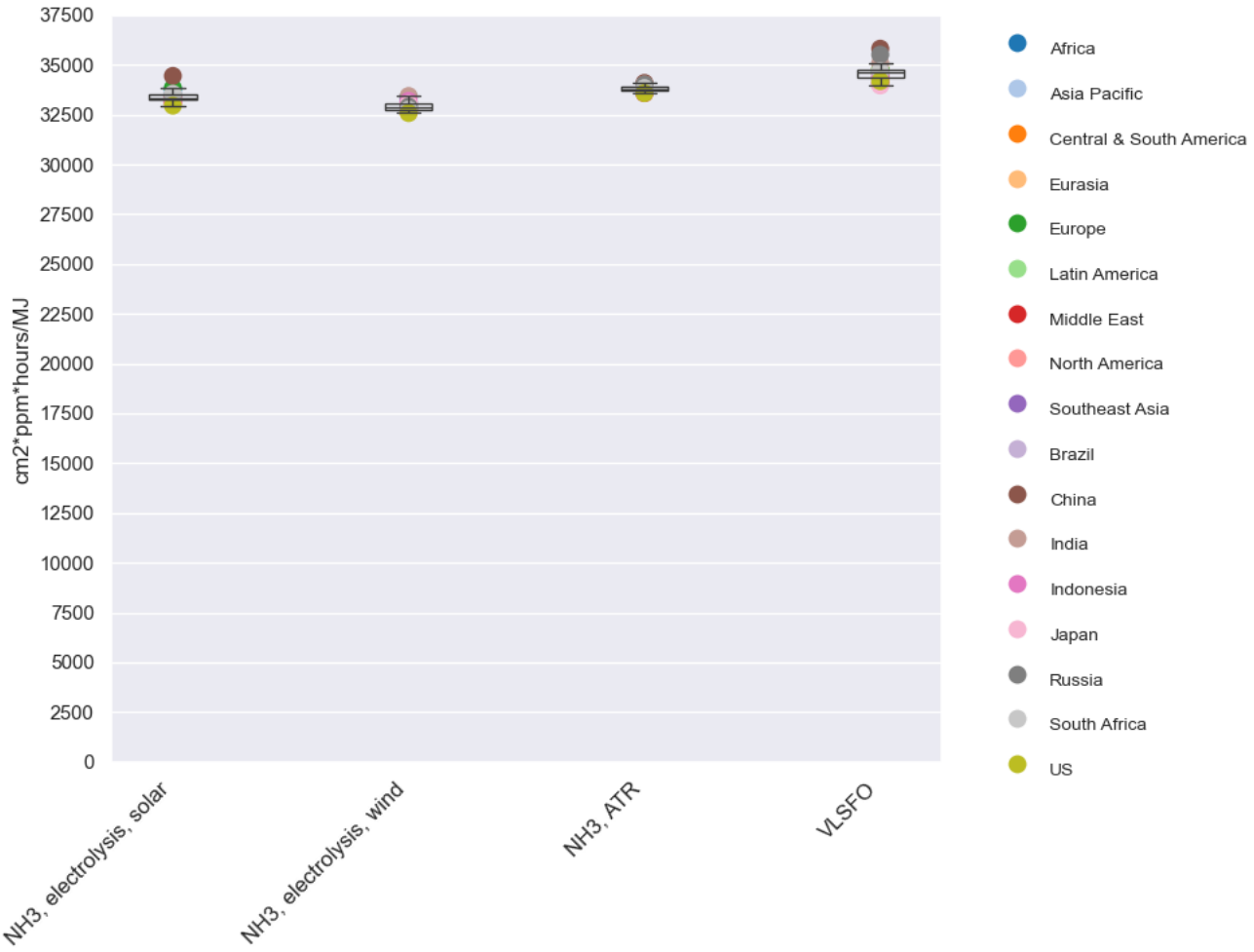

Figure 6.8: Regional differences in the **consequential** photochemical ozone, vegetation, results for ammonia (9.6% e/e VLSFO) with H_2 from electrolysis (based on either solar or wind), ammonia (9.6% e/e VLSFO) with H_2 from ATR and VLSFO with the functional unit of 1 MJ.

Note that in **section 6.1**, the global mean value for ammonia with wind-based electrolysis had the lowest impact on photochemical ozone, vegetation. Nevertheless, as **Figure 6.8** shows that the result ranges for the ammonia fuel scenarios overlap, e.g., the lower values for natural gas-based ammonia is close to the upper values for ammonia with wind-based electrolysis and are approximately the same as the median value for ammonia with solar-based electrolysis. Thus, the difference between the ammonia fuel scenarios depends on the regions being compared.

Figure 6.8 does not shows clearly whether there is a difference between the result range for ammonia with wind-based electrolysis and the result range for VLSFO. Yet, **appendix 10** (external appendix) shows that there is a difference of approximately 500 cm^2*ppm*hours between the lowest value for VLSFO and the maximum value for ammonia with wind-based electrolysis. Nevertheless, the result range for VLSFO does overlap with the upper values for natural gas-based ammonia and ammonia with solar-based electrolysis. Therefore, it can only be concluded that ammonia with wind-based electrolysis has a lower impact on the photochemical ozone, vegetation impact category than VLSFO.

7 Life cycle impact assessment: attributional model

This chapter presents the GWP100 results for the attributional model, since the RED II guidelines focus on carbon footprint of fuels. The characterised results per MJ are presented for each of the four fuel scenarios – ammonia with H_2 from electrolysis (based on either solar or wind), ammonia with H_2 from ATR with CCS, and VLSFO – whereafter the characterised results are presented per TEUkm, as described in **section 2.4**.

Note that the characterised results per MJ and per TEUkm for ammonia are presented with both 9.6% e/e and 0% e/e VLSFO. This is done, because project partners argue that the share of pilot fuel will not be included when the results are used in relation to RFNBOs certifications. The project partners have also discussed whether the results for RFNBOs certifications should be presented with or without combustion emissions (well-to-wake versus well-to tank). However, as the fossil fuel comparator of 94 g CO_2-eq/MJ is including combustion, and since the RED II guidelines only specify that biogenic CO_2 from combustion has a GWP100 effect of zero (EP & EUCO, 2018), the results for ammonia with 0% e/e VLSFO are presented with combustion emissions.

Additionally, in **section 9.3**, a semi-quantitative analysis is presented for ammonia with 9.6% e/e bio-based pilot fuel, assuming a 65% reduction compared to the fossil fuel comparator in accordance with RED II.

The characterised results are followed by the regional differences and a contribution analysis for each fuel. Also here, the results for ammonia are presented with both 9.6% e/e and 0% e/e VLSFO. Just as for **chapter 6**, the terms in **Table 2.3** are used to refer to the different scenarios, production pathways, and fuel types.

In order to provide a simple overview of the LCIA results, the tables in this chapter present a mean of the results for the 17 regions (referred to as 'global mean'), while **appendix 10** (external appendix) includes the characterised results and contribution tables for the individual regions.

7.1 Characterised results

7.1.1 Ammonia with 9.6% e/e VLSFO

The characterised GWP100 results for the global mean are presented in **Table 7.1** for ammonia with 9.6% e/e VLSFO. The results for GWP100 is presented with and without the GWP of H_2, since the GWP for H_2 is not included in IPCC (2021).

Note that the GWP100 results are the same for ammonia with electrolysis based on solar and wind electricity, since the supplementing delegated regulation 2023/1185 for RFNBOs specifies that electricity from solar and wind has a carbon footprint of zero. Moreover, the GWP100 results for ammonia with H_2 from electrolysis are seven times lower than the GWP100 value for VLSFO. The GWP100 result for ammonia with H_2 from ATR with CCS is 44% lower than the default value of 94 g CO_2-eq/MJ of fossil fuel, which is applied for VLSFO.

Table 7.1: GWP100 global mean results for ammonia (9.6% e/e VLSFO) with H_2 from electrolysis (based on either solar or wind), ammonia (9.6% e/e VLSFO) with H_2 from ATR with CCS, and VLSFO with the functional unit of 1 MJ for the **attributional model**.

Global mean	Production pathway	Haber-Bosch			Desulphurisation
	H_2 production	Electrolysis	Electrolysis	ATR with CCS	ATR
	Electricity source	Solar	Wind	Grid	Grid
	Fuel	Ammonia with 9.6% e/e VLSFO	Ammonia with 9.6% e/e VLSFO	Ammonia with 9.6% e/e VLSFO	VLSFO
Impact categories	**Unit**				
Global warming (GWP100)	g CO_2-eq/MJ	13.5	13.5	53.1	94.0
GWP100 without GWP of H_2	g CO_2-eq/MJ	13.2	13.2	52.7	94.0

Based on the results in **Table 7.1**, both ammonia pathways with H_2 from electrolysis is below the 70% reduction target from RED II, as the results are below 28.2 g CO_2-eq/MJ.

7.1.2 Conversion of functional unit for ammonia with 9.6% e/e VLSFO: From MJ to TEUkm

The LCIA results are also provided for a functional unit of 1 TEUkm (1 twenty-foot equivalent unit transported for 1 kilometre). This is done, since a ship fuelled by ammonia has less space for cargo, because the energy density of ammonia (0% e/e VLSFO) is 12 GJ/m^3, while the energy density is 38.6 GJ/m^3 for VLSFO.

It is estimated that 0.291 MJ of ammonia with 9.6% e/e VLSFO as pilot fuel is needed per 1 TEUkm, while 0.275 MJ VLSFO is needed per 1 TEUkm. **Appendix 4: Conversion factor from MJ to TEUkm** describes how the energy requirement per TEUkm has been determined. Note that the conversion factors for TEUkm are estimates and can differ based on both ship design and size as well as engine efficiency.

Table 7.2 presents the characterised results for the global mean per TEUkm. Also here, the results for GWP100 is presented with and without the GWP of H_2, since the GWP for H_2 is not included in IPCC (2021) (see **section 2.11**).

Table 7.2: GWP100 global mean results for ammonia (9.6% e/e VLSFO) with H_2 from electrolysis (based on either solar or wind), ammonia (9.6% e/e VLSFO) with H_2 from ATR with CCS, and VLSFO with the functional unit of 1 TEUkm for the **attributional model**.

Global mean	Production pathway	Haber-Bosch			Desulphurisation
	H_2 production	Electrolysis	Electrolysis	ATR with CCS	ATR
	Electricity source	Solar	Wind	Grid	Grid
	Fuel	Ammonia with 9.6% e/e VLSFO	Ammonia with 9.6% e/e VLSFO	Ammonia with 9.6% e/e VLSFO	VLSFO
Impact categories	**Unit**				
Global warming (GWP100)	g CO_2-eq/TEUkm	3.9	3.9	15.4	25.8
GWP100 without GWP of H_2	g CO_2-eq/TEUkm	3.6	3.6	14.5	28.5

The results in **Table 7.2** show the same tendency as **Table 7.1**: Ammonia with H_2 from electrolysis has the lowest impact and is over six times lower than the GWP100 result for VLSFO per TEUkm. When comparing GWP100 results for natural gas-based ammonia with VLSFO, there is a difference of 40% per TEUkm. Thus, the functional unit of 1 TEUkm does reduce the difference between the GWP100 results for VLSFO and the two ammonia pathways, but the overall tendency stays the same.

7.1.3 Ammonia with 0% e/e VLSFO

The characterised GWP100 results for the global mean are presented in **Table 7.3** for ammonia with 0% e/e VLSFO. Also here, there is no difference between ammonia with solar- or wind-based electrolysis since electricity from solar and wind has a carbon footprint of zero. Moreover, with 0% pilot fuel, the GWP100 results for ammonia with H_2 from electrolysis are 18 times lower than the GWP100 value for VLSFO. For natural gas-based ammonia without pilot fuel, the GWP100 result is 48% lower than the default value of 94 g CO_2-eq/MJ of fossil fuel, which is applied for VLSFO.

Table 7.3: GWP100 global mean results for ammonia (0% e/e VLSFO) with H_2 from electrolysis (based on either solar or wind), ammonia (0% e/e VLSFO) with H_2 from ATR with CCS, and VLSFO with the functional unit of 1 MJ for the **attributional model**.

Global mean	Production pathway	Haber-Bosch			Desulphurisation
	H_2 production	Electrolysis	Electrolysis	ATR with CCS	ATR
	Electricity source	Solar	Wind	Grid	Grid
	Fuel	Ammonia with 0% e/e VLSFO	Ammonia with 0% e/e VLSFO	Ammonia with 0% e/e VLSFO	VLSFO
Impact categories	**Unit**				
Global warming (GWP100)	g CO_2-eq/MJ	5.1	5.1	48.87	94.0
GWP100 without GWP of H_2	g CO_2-eq/MJ	4.7	4.7	48.4	94.0

7.1.4 Conversion of functional unit for ammonia with 0% e/e VLSFO: From MJ to TEUkm

For ammonia with 0% e/e VLSFO, it is estimated that 0.292 MJ is needed per 1 TEUkm, while 0.275 MJ VLSFO is needed per 1 TEUkm. Thus, the energy requirement per 1 TEUkm for ammonia with 0% e/e VLSFO is increased with 0.001 MJ compared to ammonia with 9.6% e/e VLSFO. **Table 7.4** presents the characterised results for the global mean per TEUkm.

Table 7.4: GWP100 global mean results for ammonia (0% e/e VLSFO) with H_2 from electrolysis (based on either solar or wind), ammonia (0% e/e VLSFO) with H_2 from ATR with CCS, and VLSFO with the functional unit of 1 TEUkm for the **attributional model**.

Global mean	Production pathway	Haber-Bosch			Desulphurisation
	H_2 production	Electrolysis	Electrolysis	ATR with CCS	ATR
	Electricity source	Solar	Wind	Grid	Grid
	Fuel	Ammonia with 0% e/e VLSFO	Ammonia with 0% e/e VLSFO	Ammonia with 0% e/e VLSFO	VLSFO
Impact categories	**Unit**				
Global warming (GWP100)	g CO_2-eq/TEUkm	1.5	1.5	14.2	25.8
GWP100 without GWP of H_2	g CO_2-eq/TEUkm	1.3	1.3	13.3	25.8

The results in **Table 7.4** show the same tendency as **Table 7.3**: Electrolysis-based ammonia with 0% e/e VLSFO has the lowest impact and is 17 times lower than the GWP100 result for VLSFO per TEUkm. When comparing GWP100 results for natural gas-based ammonia (0% e/e VLSFO) with VLSFO, there is a difference of 45% per TEUkm. Thus, the functional unit of 1 TEUkm does reduce the difference between the GWP100 results for VLSFO and the two ammonia pathways with 0% e/e VLSFO, but the overall tendency stays the same.

7.2 Regional differences for global warming potential

7.2.1 Ammonia with 9.6% e/e VLSFO

The regional differences for the attributional GWP100 results for ammonia with 9.6% e/e VLSFO are presented in **Figure 7.1**. The figure shows that the ammonia with H_2 from ATR with CCS has the largest geographical variations, as it varies from 47 to 59 g CO_2-eq/MJ. This is mainly due to differences in the carbon footprint of the grid electricity mix for the 17 regions. Note that there is no difference between regions for the natural gas input, since inputs of natural gas to ATR and CCS are linked to the same ecoinvent process, as described in **section 4.2**.

For ammonia with H_2 from electrolysis, the geographical range is only 2 g CO_2-eq/MJ. The variation is caused by the differences in the carbon footprint of the grid electricity mix for the 17 regions, since grid electricity is used for bunkering in the distribution stage. There is no variation in results for VLSFO, since the impact is set to the default value of 94 g CO_2-eq/MJ, because this approach is deemed most in line with the RED II guidelines.

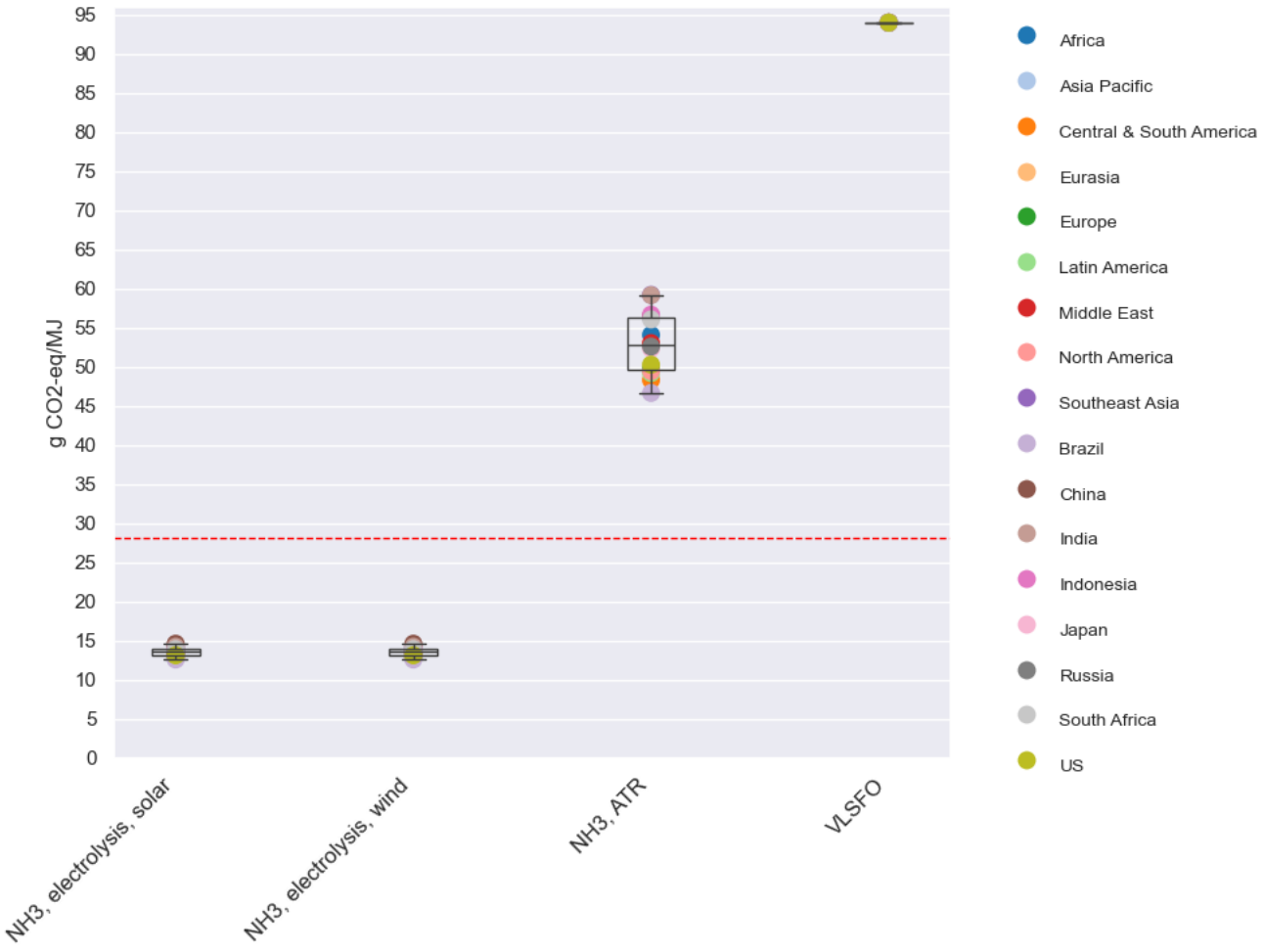

Figure 7.1: Regional differences in the **attributional** GWP100 results for ammonia (9.6% e/e VLSFO) with H_2 from electrolysis (based on either solar or wind), ammonia (9.6% e/e VLSFO) with H_2 from ATR with CCS, and VLSFO with the functional unit of 1 MJ. The dotted, red line indicates the RED II target of 28.2 g CO_2-eq/MJ.

Based on **Figure 7.1**, both ammonia pathways with H_2 from electrolysis are below the 70% reduction target from RED II of 28.2 g CO_2-eq/MJ even with the geographical variations. The lowest GWP100 result for ammonia with H_2 from ATR with CCS of 47 g CO_2-eq/MJ is still almost two times higher than the RED II target.

7.2.2 Ammonia with 0% e/e VLSFO

The regional differences for the attributional GWP100 results for ammonia with 0% e/e VLSFO are presented in **Figure 7.2**. The figure shows that the geographical variations for ammonia with H_2 from ATR with CCS are the largest, as it varies from 42 to 56 g CO_2-eq/MJ. For ammonia with H_2 from electrolysis with 0% e/e VLSFO, the geographical range is approximately 2 g CO_2-eq/MJ.

For both ammonia pathways, the variation is caused by the differences in the carbon footprint of the grid electricity mix for the 17 regions, since grid electricity is used for bunkering in the distribution stage for electrolysis-based ammonia and for the production of natural gas-based ammonia. As stated previously, there is no difference between regions for the natural gas input, since inputs of natural gas to ATR and CCS are linked to the same ecoinvent process (see **section 4.2**).

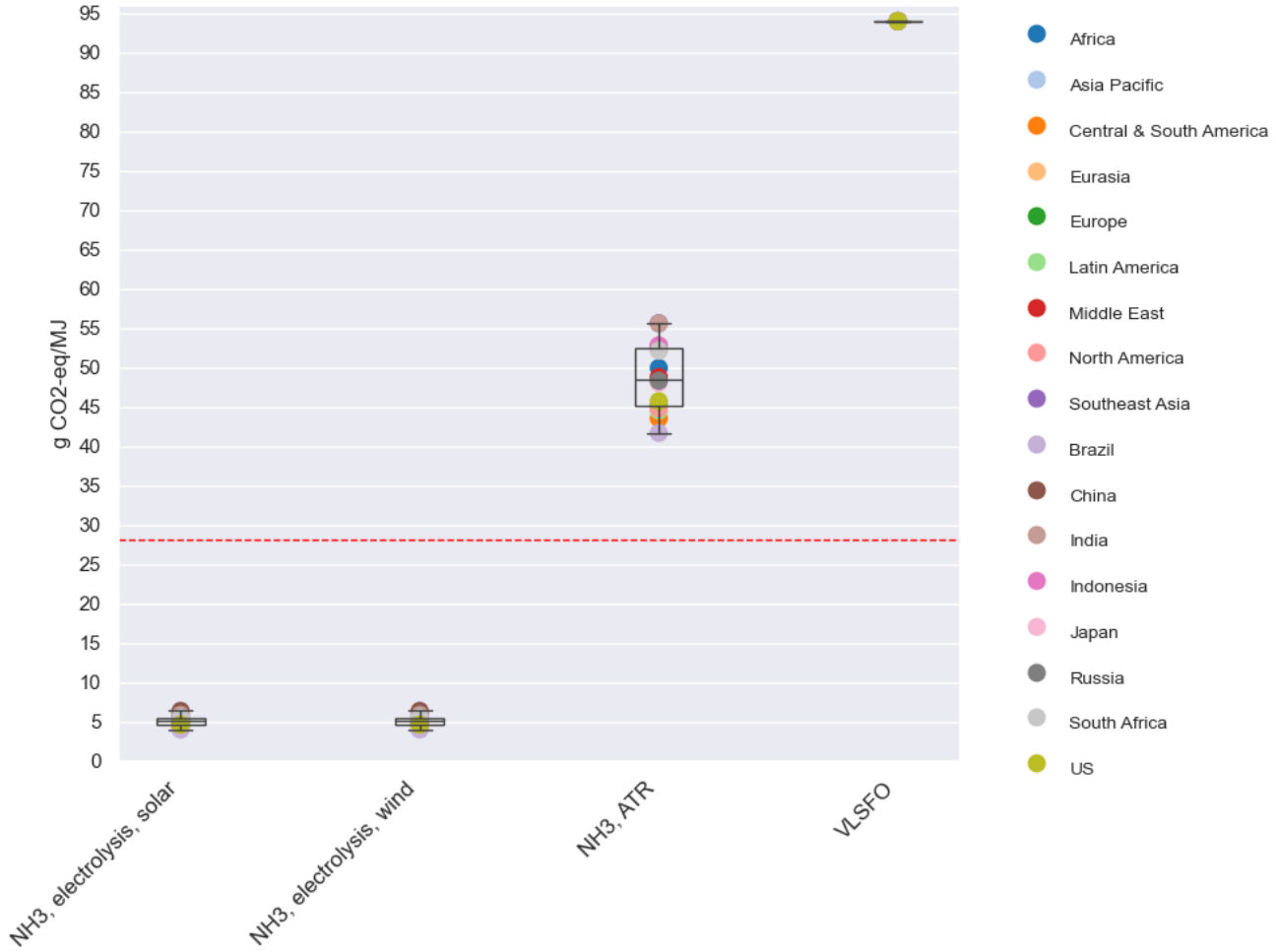

Figure 7.2: Regional differences in the **attributional** GWP100 results for ammonia (0% e/e VLSFO) with H_2 from electrolysis (based on either solar or wind), ammonia (0% e/e VLSFO) with H_2 from ATR with CCS, and VLSFO with the functional unit of 1 MJ. The dotted, red line indicates the RED II target of 28.2 g CO_2-eq/MJ.

Based on **Figure 7.2**, both ammonia pathways with H_2 from electrolysis is below the 70% reduction target from RED II of 28.2 g CO_2-eq/MJ even with the geographical variations. Nevertheless, the lowest GWP100 result for ammonia with H_2 from ATR with CCS of 42 g CO_2-eq/MJ is still 1.5 times higher than the RED II target, even without the share of pilot fuel.

7.3 Contribution analysis for global warming potential

7.3.1 Ammonia with 9.6% e/e VLSFO

Table 7.5 provides an overview of the contribution from each process in percent, while a detailed analysis is presented in **Table 7.6** for ammonia with 9.6% e/e VLSFO. This shows that the majority of the GWP100 impact for ammonia with H_2 from electrolysis (9.6% e/e VLSFO) stem from the combustion emissions.

For ammonia with H_2 from ATR with CCS with 9.6% e/e VLSFO, the main contributors are natural gas used as feedstock for ATR and CO_2 emissions from CCS. It is important to highlight that the impact from CO_2 emissions to air from CCS is higher in the attributional model than in the consequential model, since the RED II guidelines do not include differentiation of timing of CO_2 emissions (see **Table 2.1**). Thus, as described in **section 5.1.1.2.1**, the yearly slip of 0.023% CO_2 has the same GWP100 characterisation factor as if it was being emitted right after capture in the attributional model.

Table 7.5: GWP100 contribution analysis for each process in percent for global mean ammonia (9.6% e/e VLSFO) with H_2 from electrolysis (based on either solar or wind), ammonia (9.6% e/e VLSFO) with H_2 from ATR with CCS, and VLSFO with the functional unit of 1 MJ for the **attributional model**. The shades of red are used to highlight the highest values.

Global mean	Ammonia (9.6% e/e VLSFO) with H_2 from electrolysis	Ammonia (9.6% e/e VLSFO) with H_2 from electrolysis	Ammonia (9.6% e/e VLSFO) with H_2 from ATR with CCS	VLSFO
Activity	**Solar**	**Wind**		
Total result (g CO_2-eq/MJ)	**13.5**	**13.5**	**53.1**	**94.0**
N_2 production	0%	0%	4%	
H_2 production	3%	3%	38%	
H_2 storage	1%	1%		
CCS, ATR			26%	
NH_3 production	0%	0%	7%	
VLSFO production & distribution	12%	12%	3%	18%
Distribution and bunkering, NH_3	19%	19%	5%	
Combustion	66%	66%	17%	82%
Total	100%	100%	100%	100%

Table 7.6: Detailed GWP100 contribution analysis for ammonia (9.6% e/e VLSFO) with H_2 from electrolysis (based on either solar or wind), ammonia (9.6% e/e VLSFO) with H_2 from ATR with CCS, and VLSFO with the functional unit of 1 MJ for the **attributional model**. Thus, the results are in line with the RED II guidelines for RFNBOs. Shades of red are used to highlight the highest values.

Global mean	g CO_2-eq/MJ	Ammonia (9.6% e/e VLSFO) with H_2 from electrolysis	Ammonia (9.6% e/e VLSFO) with H_2 from electrolysis	Ammonia (9.6% e/e VLSFO) with H_2 from ATR with CCS	VLSFO
Activity	**Input / Flow**	**Solar**	**Wind**		
N_2 production, for NH_3	Electricity, renewable	0	0		
	Electricity, grid			1.99	
H_2 production, electrolysis/ATR, for NH_3	Emissions to air, CO_2			0.02	
	Emissions to air, CH_4			2.98	
	Emissions to air, H_2	0.27	0.27	0.37	
	Water	0.09	0.09	0.11	
	Electricity, renewable	0	0		
	Electricity, grid			0.60	
	Natural gas, feedstock			16.00	
H_2 storage	Emissions to air, H_2	0.09	0.09		
	Electricity, renewable	0	0		
CCS, for ATR H_2 production for NH_3	Emissions to air, CO_2			11.61	
	Water			0.003	
	Amines			0.35	
	Electricity, grid, carbon capture			0.03	
	Natural gas, fuel			0.84	
	Electricity, grid, pipe transport			1.16	
NH_3 production	Emissions to air, NH_3				
	Electricity, renewable	0	0		
	Electricity, grid			3.92	
VLSFO production & distribution		1.60	1.60	1.60	16.71
Distribution and bunkering, NH_3	Emissions, NH_3				
	Sea transport	0.25	0.25	0.25	
	Fuel oil, cooling	1.63	1.63	1.63	
	Electricity, grid, bunkering	0.08	0.08	0.08	
	Electricity, grid, pipe transport	0.65	0.65	0.65	
Combustion	CO_2 emissions	7.36	7.36	7.36	76.53
	N_2O emissions	1.52	1.52	1.52	0.76
Total		**13.5**	**13.5**	**53.1**	**94.0**

7.3.2 Ammonia with 0% e/e VLSFO

For ammonia without pilot fuel, an overview of the contribution from each process in percent is presented in **Table 7.7**, while a detailed analysis is presented in **Table 7.8**. This shows that – without the share of pilot fuel – the distribution and bunkering phase is the largest contributor to the carbon footprint of electrolysis-based ammonia. Specifically, **Table 7.8** shows that it is the fuel oil used for cooling which accounts for approximately 49% of the carbon footprint. Moreover, **Table 7.8** also shows that water and H_2 emissions to air are the only input and flow for electrolysis-based ammonia, which has a GWP100 effect until the production gate.

For ammonia with H_2 from ATR with CCS with 0% e/e VLSFO, the main contributors are natural gas used as feedstock for ATR and CO_2 emissions from CCS. Note that compared to **Table 7.5**, the CO_2 emissions from CCS and the natural gas input to ATR has a larger impact in **Table 7.7**, since the share of pilot fuel is now replaced by natural gas-based ammonia.

Again, it is important to highlight that the impact from CO_2 emissions to air from CCS is higher in the attributional model than in the consequential model, since the RED II guidelines do not include differentiation of timing of CO_2 emissions (see **Table 2.1**). Thus, as described in **section 5.1.1.2.1**, the yearly slip of 0.023% CO_2 has the same GWP100 characterisation factor as if it was being emitted right after capture in the attributional model.

Table 7.7: GWP100 contribution analysis for each process in percent for global mean ammonia (0% e/e VLSFO) with H_2 from electrolysis (based on either solar or wind), ammonia (0% e/e VLSFO) with H_2 from ATR with CCS, and VLSFO with the functional unit of 1 MJ for the **attributional model**. The shades of red are used to highlight the highest values.

Global mean	Ammonia (0% e/e VLSFO) with H_2 from electrolysis	Ammonia (0% e/e VLSFO) with H_2 from electrolysis	Ammonia (0% e/e VLSFO) with H_2 from ATR with CCS	VLSFO
Activity	**Solar**	**Wind**		
Total result (g CO_2-eq/MJ)	**5.1**	**5.1**	**48.8**	**94.0**
N_2 production	0%	0%	5%	
H_2 production	8%	8%	46%	
H_2 storage	2%	2%		
CCS, ATR			32%	
NH_3 production	0%	0%	9%	
VLSFO production & distribution				18%
Distribution and bunkering, NH_3	60%	60%	6%	
Combustion	30%	30%	3%	82%
Total	100%	100%	100%	100%

Table 7.8: Detailed GWP100 contribution analysis for ammonia (0% e/e VLSFO) with H_2 from electrolysis (based on either solar or wind), ammonia (0% e/e VLSFO) with H_2 from ATR and VLSFO with the functional unit of 1 MJ for the attributional model. Thus, the results are in line with the RED II guidelines for RFNBOs. Shades of red are used to highlight the highest values.

Global mean	g CO2-eq/MJ	Ammonia (0% e/e VLSFO) with H2 from electrolysis	Ammonia (0% e/e VLSFO) with H2 from electrolysis	Ammonia (0% e/e VLSFO) with H2 from ATR with CCS	VLSFO
Activity	**Input / Flow**	**Solar**	**Wind**		
N_2 production, for NH_3	Electricity, renewable	0	0		
	Electricity, grid			2.20	
H_2 production, electrolysis/ATR, for NH_3	Emissions to air, CO_2			0.02	
	Emissions to air, CH_4			3.31	
	Emissions to air, H_2	0.29	0.29	0.41	
	Water	0.10	0.10	0.12	
	Electricity, renewable	0	0		
	Electricity, grid			0.67	
	Natural gas, feedstock			17.7	
H_2 storage	Emissions to air, H_2	0.10	0.10		
	Electricity, renewable	0	0		
CCS, for ATR H_2 production for NH_3	Emissions to air, CO_2			12.9	
	Water			0.003	
	Amines			0.39	
	Electricity, grid, carbon capture			0.04	
	Natural gas, fuel			0.93	
	Electricity, grid, pipe transport			1.20	
NH_3 production	Emissions to air, NH_3				
	Electricity, renewable	0	0		
	Electricity, grid			4.34	
VLSFO production & distribution					16.71
Distribution and bunkering, NH_3	Emissions, NH_3				
	Sea transport	0.27	0.27	0.27	
	Fuel oil, cooling	2.00	2.00	2.00	
	Electricity, grid, bunkering	0.08	0.08	0.08	
	Electricity, grid, pipe transport	0.72	0.72	0.72	
Combustion	CO_2 emissions				76.53
	N_2O emissions	1.52	1.52	1.52	0.76
Total		**5.1**	**5.1**	**48.8**	**94.0**

7.4 Attributional carbon footprint of ammonia fuel from other studies

This section provides an overview of the attributional carbon footprint for ammonia fuel (so-called 'green' and 'blue' ammonia) from other public studies together with the results from this LCA study (see **Table 7.9** and **Table 7.10**).

Note that there are differences in methodology and the applied characterisation factors between the studies in **Table 7.9** and **Table 7.10**, thus, the studies' results are not comparable. Instead, the overview in the two tables can be used to indicate how the carbon footprint of ammonia can vary depending on the applied data and methodology. It is also important to highlight that the results are without pilot fuel and combustion emissions (well-to-tank), though some studies do not include the distribution phase. This is described in the comment column in the two tables.

Table 7.9: GWP100 results for electrolysis-based ammonia (so-called 'green' ammonia) without pilot fuel and combustion emissions. Note that some studies do not include distribution. The results from the other studies are obtained from Sphera Solutions (2024).

g CO_2-eq/MJ	Electrolysis-based ammonia				
Electricity:	**Carbon footprint when 'green' electricity is 0**	**Solar-based**	**Wind-based**	**Comment**	**Results differ from this study's RED II-aligned results because…**
This LCA study, attributional results, RED II-aligned	3.6 (2.5-4.9)			Distribution is included. The range show the low and high value for geographical differences, while the 'global mean' result is shown before the parentheses.	
Sphera Solutions (2024)		20 (5-41)		Distribution is included with a distance of 20,000 km. The result range represents 'green' ammonia paths with minimum and maximum GHG emissions. The value before the parentheses represents the 'base case'.	• High distribution distance • Carbon footprint of solar and wind electricity is not 0.
IEA (2021)		13	6	Distribution is not included. Cradle-to-gate study.	• Carbon footprint of solar and wind electricity is 26.5 and 11 g CO_2-eq/kWh, respectively.
Liu et al. (2020)	16			Distribution is not included. Cradle-to-gate study. 'Green' electricity is assumed to have a carbon footprint of zero. Energy for ASU and Haber-Bosch process stem from US grid mix from 2019.	• US grid electricity (63% fossil-based) is applied for ASU and Haber-Bosch processes. • Majority of the impact stem from the Haber-Bosch process, which uses 1.2 GJ electricity per t ammonia.
DECHEMA (2022)	48			Distribution is not included. Cradle-to-gate study. Only considers CO_2-emissions. Other GHG emissions are not included. Electricity for electrolysis is assumed to have a carbon footprint of zero. Energy for other processes stem from European average grid mix for 2020.	• European grid electricity (375 g CO_2/kWh) is applied for all processes except electrolysis
Al-Breiki and Bicer (2021)		54	30	Distribution is included with a distance of 18,520 km.	• High distribution distance • Carbon footprint of solar and wind electricity is not 0.

The overview in **Table 7.9** shows that this LCA study's attributional results for electrolysis-based ammonia is lower than all the other studies. This may be because Sphera Solutions (2024), IEA (2021) and Al-Breiki and Bicer (2021) include a carbon footprint of electricity from solar and wind, while this is set to 0 in this study in accordance with RED II guidelines for RFNBOs. The results from Sphera Solutions (2024) and Al-Breiki and Bicer (2021) may also be higher due to the distribution distance of 20,000 km and 18,520 km, respectively.

In the studies by Liu et al. (2020) and DECHEMA (2022), it is only electrolysis, which is run on 'green' electricity with a carbon footprint of zero, while the energy for ASU and Haber-Bosch process stem from grid electricity mix. For DECHEMA (2022), the carbon intensity of the grid electricity mix is 375 g CO_2/kWh, which can explain the higher results. Moreover, the US grid mix applied in the study by Liu et al. (2020) is 63% fossil-based, thus, even though the Haber-Bosch process has an electricity input of 1.2 GJ/t ammonia, which is similar to the LCI in **Table 5.10**, the US grid mix can have a significant global warming impact, as coal and natural gas is used to generate the electricity.

Nevertheless, it is important to highlight that the LCI data for each study can also vary along with the carbon intensity of all inputs, thus, it is expected that the results of other studies will differ from the attributional results presented in this report. Furthermore, it is not possible to dissect the exact reasons for the differences between the before mentioned studies, since the specific LCI data is not presented in the literature and/or because the other studies do not present a detailed contribution analysis.

Table 7.10: GWP100 results for natural gas-based ammonia with CCS (so-called 'blue' ammonia) without pilot fuel and combustion emissions. Note that some studies do not include distribution. The results from the other studies are obtained from Sphera Solutions (2024).

g CO_2-eq/MJ	Natural gas-based ammonia with CCS				
H_2 technology:	**ATR**	**SMR**	**Unspecified**	**Comment**	**Results differ from this study's RED II-aligned results because…**
This LCA study, attributional results, RED II-aligned	47.3 (40.2-54.1)			Distribution is included. The range show the low and high value for geographical differences, while the 'global mean' result is shown before the parentheses.	
Sphera Solutions (2024)	47 (11-109)	46 (12-102)		Distribution is included with a distance of 20,000 km. Carbon capture rate of 95%. The result range represents 'blue' ammonia paths with minimum and maximum GHG emissions. The value before the parentheses represents the 'base case'.	• Large contribution from distribution (8-50% due to transport distance) • Large contribution from ammonia production (49-92% due to energy consumption)
IEA (2021)			27	Distribution is not included. Cradle-to-gate study. H_2 technology not specified. 95% carbon capture rate. 14.4 g CO_2-eq/MJ natural gas (upstream).	• Lower carbon intensity of natural gas input and/or lower natural gas input
DECHEMA (2022)		48		Distribution is not included. Cradle-to-gate study. Only considers CO_2-emissions. Other GHG emissions are not included. Energy for other processes stem from European average grid mix for 2020. Carbon capture rate not specified.	
Lee et al. (2022)		41-62		Distribution is not included. Cradle-to-gate study. Includes two different CCS options: 1) capturing 100% of carbon in process emissions (62 g CO_2-eq/MJ), 2) capturing 100% of carbon in process emissions and 90% from combustion of natural gas (41 g CO_2-eq/MJ).	
Al-Breiki and Bicer (2021)		93		Distribution is included with a distance of 18,520 km. Carbon capture rate of 60%	• Higher distribution distance • Lower carbon capture rate

The overview in **Table 7.10** shows that this LCA study's attributional results for natural gas-based ammonia are higher than the results from IEA (2021). This may be caused by lower GHG emissions from natural gas or a lower input of natural gas since this is an important contributor to the carbon footprint of natural gas-based ammonia.

Al-Breiki and Bicer (2021) presents a result that is higher than the results for the attributional model in this report. This may be caused by a lower carbon capture rate and a higher distribution distance.

This study's RED II-aligned results are within the result range that Sphera Solutions (2024) presents. Yet, the result range from Sphera Solutions (2024) is very broad, as it has a span of 98 g CO_2-eq/MJ for ammonia with H_2

from ATR. In the study from Sphera Solutions (2024), the majority of the impact stem from ammonia production and liquefaction, thus, the difference in results compared to this study may be caused by the GHG emissions from natural gas as well as differences in the LCI data. Moreover, the distribution distance is also varied in the study by Sphera Solutions (2024), resulting in a contribution from the distribution phase of up to 50%, which is notably higher than the contribution from the distribution phase for this study's RED II-aligned results.

Lastly, this study's results are also in line with the results presented by DECHEMA (2022) and Lee et al. (2022).

Nevertheless, as previously stated, it is expected that the results of other studies will differ from the attributional results presented in this report, since the other studies apply different LCI data and other carbon intensity of all inputs, thus influencing the results. Furthermore, it is not possible to dissect the exact reasons for the differences between the before mentioned studies, since the specific LCI data is not presented in the literature and/or because the other studies do not present detailed contribution analyses.

8 Sensitivity analysis: consequential model

The sensitivity analysis is conducted in order to assess different parameter's influence on the LCIA results.

Note that in a 'typical' sensitivity analysis, all parameters are changed with the same magnitude, e.g., with a factor 10. However, for this study, a range is known for most of the parameters, e.g., the LHV of ammonia which is determined to be between 17.2 MJ/kg and 18.6 MJ/kg. Thus, this sensitivity analysis present different scenarios of for the consequential model, thus, investigating how the results for default scenario change based on each parameter's value range. Nevertheless, for some parameters, e.g., transport distances and energy for cooling of ammonia, an arbitrary value is applied, since the range for these parameters are unknown.

An overview of the tested parameters along with the default values are shown in **Table 8.1**, while the justification for each analysis and the chosen values are presented in **section 8.1**-**8.14**.

Table 8.1: Overview of parameters in the sensitivity analysis for the **consequential model** and the default values used to calculate the LCIA results in **chapter 6**.

Parameter:	**Unit**	**Both ammonia pathways with 9.6% e/e VLSFO**	
		Default scenario	**Sensitivity**
Desalination (**section 8.1**)	-	0% desalination 100% ground/surface water	100% desalination 0% ground/surface water
Lower heating value of ammonia (**section 8.2**)	MJ/kg	17.2	18.6
Share of pilot fuel (**section 8.3**)	% VLSFO	9.6%	**High:** 15% **Low:** 5%
Electricity input to Haber-Bosch synthesis (**section 8.4**)	kWh/kg NH_3	0.35	3.5
Transport distance, distribution and bunkering (**section 8.5**)	km	707 km by ship 588 km by pipeline	7,070 km by ship 5,880 km by pipeline
Cooling, distribution and bunkering (**section 8.6**)	%	1.9% of energy in ammonia with 9.6% e/e VLSFO	**Low:** 0.11% of energy in ammonia with 9.6% e/e VLSFO **High:** 19% of energy in ammonia with 9.6% e/e VLSFO
H_2 slip from production (**section 8.7**)	% H_2 slip	0.3%	5%
NH_3 slip from production and distribution (**section 8.7**)	% NH_3 slip	0.3%	5%
NH_3 slip from combustion (**section 8.9**)	g NH_3 / MJ	0.0056	0.1668
N_2O emissions from combustion (**section 8.10**)	g N_2O / MJ	0.0056	**Medium:** 0.0083 **High:** 0.117
Indirect N_2O emissions (**section 8.11**)	-	Not included	1/3 of the emitted N-compounds are assumed to deposit on land and 1% of the deposit N is assumed to converted to N_2O through the microbial processes occurring in soil.

Table 8.1 continued: Overview of parameters in the sensitivity analysis for the **consequential model** and the default values used to calculate the LCIA results in **chapter 6**.

		Ammonia with H_2 from electrolysis and 9.6% e/e VLSFO	
		Default scenario	**Sensitivity**
H_2 from storage to Haber-Bosch synthesis (**section 8.12.1**)	%	25%	100%
Electricity input to electrolysis (**section 8.12.2**)	kWh/kg H_2	52.2	60.0
Carbon intensity of renewable electricity (**section 8.12.3**)	g CO_2-eq / kWh	3-20 for wind, for 5-24 solar (depending on region)	**High:** 100 **Low:** 5
Parameter:	**Unit**	**Ammonia with H_2 from ATR with CCS and 9.6% e/e VLSFO**	
		Default scenario	**Sensitivity**
Choice of marginal electricity grid mix (**section 8.13.1.1**)	g CO_2-eq / kWh	Based on IEA data for 2017-2021	**A:** IEA data for 2019-2021 **B:** IEA data for 2015-2021 **C:** NGFS data for 2020-2025 **D:** NGFS data for 2015-2020 **E:** IEA data for 2015-2020
Carbon intensity of electricity grid mix (**section 8.13.1.2**)	g CO_2-eq / kWh	21-811 (depending on region)	**Medium:** 64.7 (*RFNBO limit*) **Low:** 8 (*corresponds to electricity from wind in Norway*)
Methane slip from natural gas extraction (**section 8.13.2.1**)	g CH_4 / ton natural gas	Varies from country to country (see **section 4.2**)	CH_4 emissions from natural gas extraction is multiplied with a factor 4 for all countries
Methane slip from ATR (**section 8.13.2.2**)	%	0.3%	5%
Natural gas input to ATR (**section 8.13.2.3**)	GJ/t H_2	171	181
Determining product from ASU (**section 8.13.2.4**)	-	N_2	O_2
Natural gas based H_2 production technology (**section 8.13.2.5**)	-	ATR	SMR
Carbon capture rate, ATR (**section 8.13.2.6**)	%	90% -	**High**: 95% **Low:** 50%
Energy to CCS (**section 8.13.2.7**)	kWh/kg captured CO_2	0.28	2.8
Transport distance to carbon storage (**section 8.13.2.8**)	km	200	2,000
CO_2 leakage from storage (**section 8.13.2.9**)	% per year	0.023%	**Medium:** 0.3% **High:** 5%
Parameter:	**Unit**	**VLSFO**	
		Default scenario	**Sensitivity**
Carbon intensity of fuel oil as feedstock (**section 8.14.1**)	kg CO_2-eq / kg	0.75-1.66 (depending on region)	0.68 (*corresponds to RED II value of 94 g CO_2-eq/MJ if 78.16 g CO_2-eq stems from combustion*) 0.43 (*lowest value from EC & COWI (2015)*)
H_2 production from ATR (**section 8.14.2**)	-	No CCS	CCS with 90% capture rate and 0.023% CO_2 leakage from storage
Methane slip from ATR (**section 8.14.3**)	%	0.3%	5%

The relative percentage changes for each sensitivity analysis are presented in **Table 8.2**, **Table 8.3**, **Table 8.4**, and **Table 8.5**. The relative percentage changes are coloured orange, if the change is larger than 10%, while yellow is used to indicate, if the change is -10% or more. Moreover, an empty field indicates a change of 0%. The relative percentage changes can be used to calculate the impact on the eight impact categories by multiplying the percentage with the characterised result in **Table 6.1**.

Table 8.2: The relative percentage changes for the global mean **consequential** LCIA results for ammonia with H_2 from solar-based electrolysis for the sensitivity parameters presented in **Table 8.1**. The orange colour code indicates if a change is ±10%, while yellow indicates a change of -10% or more. An empty field indicates a change of 0%.

Ammonia with H_2 from electrolysis (solar) and 9.6% e/e VLSFO	Water technology	LHV of ammonia	Share of pilot fuel		Electricity to NH_3 synthesis	Distribution distance	Energy for cooling onboard		H_2 slip	NH_3 slip
Original value / parameter	Ground / surface water	17.2 MJ/kg	9.6% e/e VLSFO		0.35 kWh/kg NH_3	707 km by ship 588 km by pipeline	1.9%		0.3%	0.3%
Tested value / parameter	Desalination	18.6 MJ/kg	5% e/e VLSFO	15% e/e VLSFO	3.5 kWh/kg NH_3	7,070 km by ship 5,880 km by pipeline	0.11%	19%	5%	5%
Impact categories										
Global warming (GWP100)	-0.05%	-4%	-19%	23%	10%	48%	-8%	90%	35%	2%
Respiratory inorganics	0.0001%	-1%	-1%	1%	1%	6%	-1%	7%	0.2%	189%
Respiratory organics	0.00%	-0.4%	-0.3%	0.3%	1%	3%	-1%	6%	0.3%	0.2%
Nature occupation	-0.1%	-7%	-3%	3%	24%	77%	-4%	40%	4%	3%
Acidification	-0.001%	-3%	1%	-1%	1%	5%	-1%	10%	0.2%	623%
Eutrophication, aquatic	-0.01%	-3%	1%	-2%	1%	5%	-1%	9%	0.2%	492%
Eutrophication, terrestrial	-0.001%	-3%	2%	-2%	0.2%	1%	-1%	9%	0.03%	624%
Photochemical ozone, vegetation	0.001%	-0.3%	-0.2%	0.2%	0.9%	3%	-0.4%	5%	0.2%	0.1%

Table 8.2 continued: The relative percentage changes for the global mean **consequential** LCIA results for ammonia with H_2 from solar-based electrolysis for the sensitivity parameters presented in **Table 8.1**. The orange colour code indicates if a change is ±10%, while yellow indicates a change of -10% or more. An empty field indicates a change of 0%.

Ammonia with H_2 from electrolysis (solar) and 9.6% e/e VLSFO	NH_3 slip from combustion	g N_2O/MJ from combustion		Indirect N_2O	H_2 from H_2 storage	Electricity input to electrolysis	Carbon intensity of renewable electricity	
Original value / parameter	0.1%	0.0056		Not included	25% H_2 storage	52.2 kWh	3-20 and 5-24 g CO_2-eq/kWh renewable electricity for wind and solar, respectively	
Tested value / parameter	0.3%	0.0083	0.117	Included	100% H_2 storage	60 kWh	5 g CO_2-eq/kWh	100 g CO_2-eq/kWh
Impact categories								
Global warming (GWP100)		3%	137%	6%	2%	4%	-20%	206%
Respiratory inorganics	6%				0.1%	1%		
Respiratory organics					0.1%	1%		
Nature occupation					2%	10%		
Acidification	20%				0.1%	0.4%		
Eutrophication, aquatic	16%				0.1%	1%		
Eutrophication, terrestrial	20%				0.01%	0.1%		
Photochemical ozone, vegetation					0.1%	0.4%		

Table 8.3: The relative percentage changes for the global mean **consequential** LCIA results for ammonia with H_2 from wind-based electrolysis for the sensitivity parameters presented in **Table 8.1**. The orange colour code indicates if a change is ±10%, while yellow indicates a change of -10% or more. An empty field indicates a change of 0%.

Ammonia with H_2 from electrolysis (wind) and 9.6% e/e VLSFO	Water technology	LHV of ammonia	Share of pilot fuel		Electricity to NH_3 synthesis	Distribution distance	Energy for cooling onboard		H_2 slip	NH_3 slip
Original value / parameter	Ground / surface water	17.2 MJ/kg	9.6% e/e VLSFO		0.35 kWh/kg NH_3	707 km by ship 588 km by pipeline	1.9%		0.3%	0.3%
Tested value / parameter	Desalination	18.6 MJ/kg	5% e/e VLSFO	15% e/e VLSFO	3.5 kWh/kg NH_3	7,070 km by ship 5,880 km by pipeline	0.11%	19%	5%	5%
Impact categories										
Global warming (GWP100)	-0.1%	-3%	-23%	26%	7%	55%	-9%	100%	39%	1%
Respiratory inorganics	-0.002%	-1%	-1%	1%	1%	6%	-1%	7%	0.2%	191%
Respiratory organics	-0.003%	-0.2%	-0.4%	0.5%	1%	3%	-0.5%	5%	0.1%	0.1%
Nature occupation	-0.2%	-6%	-6%	7%	20%	108%	-5%	50%	4%	3%
Acidification	-0.002%	-3%	1%	-1%	1%	5%	-1%	10%	0.1%	627%
Eutrophication, aquatic	-0.01%	-3%	1%	-2%	1%	5%	-1%	9%	0.1%	500%
Eutrophication, terrestrial	-0.001%	-3%	2%	-2%	0.1%	1%	-1%	9%	0.02%	625%
Photochemical ozone, vegetation	-0.002%	-0.2%	-0.3%	0.3%	0.4%	3%	-0.4%	4%	0.1%	0.1%

Table 8.3 continued: The relative percentage changes for the global mean **consequential** LCIA results for ammonia with H_2 from wind-based electrolysis for the sensitivity parameters presented in **Table 8.1**. The orange colour code indicates if a change is ±10%, while yellow indicates a change of -10% or more. An empty field indicates a change of 0%.

Ammonia with H_2 from electrolysis (wind) and 9.6% e/e VLSFO	NH_3 slip from combustion	g N_2O/MJ from combustion		Indirect N_2O	H_2 from H_2 storage	Electricity input to electrolysis	Carbon intensity of renewable electricity	
Original value / parameter	0.1%	0.0056		Not included	25% H_2 storage	52.2 kWh	3-20 and 5-24 g CO_2-eq/kWh renewable electricity for wind and solar, respectively	
Tested value / parameter	0.3%	0.0083	0.117	Included	100% H_2 storage	60 kWh	5 g CO_2-eq/kWh	100 g CO_2-eq/kWh
Impact categories								
Global warming (GWP100)		4%	155%	6%	2%	3%	-9%	247%
Respiratory inorganics	6%				0.1%	0.4%		
Respiratory organics					0.05%	0.3%		
Nature occupation					2%	9%		
Acidification	20%				0.1%	0.4%		
Eutrophication, aquatic	16%				0.1%	0.3%		
Eutrophication, terrestrial	20%				0.01%	0.05%		
Photochemical ozone, vegetation					0.03%	0.2%		

Table 8.4: The relative percentage changes for the global mean **consequential** LCIA results for ammonia with H_2 from ATR with CCS for the sensitivity parameters presented in **Table 8.1**. The orange colour code indicates if a change is +10%, while yellow indicates a change of -10% or more. An empty field indicates a change of 0%.

Ammonia with H_2 from ATR with CCS and 9.6% e/e VLSFO	**Water technology**	**LHV of ammonia**	**Share of pilot fuel**		**Electricity to NH_3 synthesis**	**Distribution distance**	**Energy for cooling onboard**		**H_2 slip**	**NH_3 slip**	**NH_3 slip from combustion**	**g N_2O/MJ from combustion**	
Original value / parameter	Ground / surface water	17.2 MJ/kg	9.6% e/e VLSFO		0.35 kWh / kg NH_3	707 km by ship 588 km by pipeline	1.9%		0.3%	0.3%	0.1%	0.0056	
Tested value / parameter	Desalination	18.6 MJ/kg	5% e/e VLSFO	15% e/e VLSFO	3.5 kWh / kg NH_3	7,070 km by ship 5,880 km by pipeline	0.11%	19%	5%	5%	0.3%	0.0083	0.117
Impact categories													
Global warming (GWP100)	0.2%	-6%	-7%	8%	42%	25%	-5%	54%	18%	3%		2%	69%
Respiratory inorganics	0.03%	-1%	-1%	1%	6%	6%	-1%	6%	0.4%	193%	6%		
Respiratory organics	0.01%	-1%	-0.2%	0.2%	3%	3%	-1%	6%	0.4%	0.3%			
Nature occupation	0.3%	-6%	-8%	9.6%	96%	131%	-5%	57%	7%	3%			
Acidification	0.02%	-3%	1%	-1%	4%	5%	-1%	10%	0.3%	632%	20%		
Eutrophication, aquatic	0.01%	-3%	1%	-2%	4%	5%	-1%	9%	0.3%	500%	16%		
Eutrophication, terrestrial	0.004%	-3%	2%	-2%	1%	1%	-1%	9%	0.1%	624%	20%		
Photochemical ozone, vegetation	0.01%	-0.4%	-0.1%	0.1%	2%	3%	-0.4%	5%	0.3%	0.2%			

Table 8.4 continued: The relative percentage changes for the global mean **consequential** LCIA results for ammonia with H2 from ATR with CCS for the sensitivity parameters presented in **Table 8.1**. The orange colour code indicates if a change is ±10%, while yellow indicates a change of -10% or more. An empty field indicates a change of 0%.

Ammonia with H_2 from ATR with CCS and 9.6% e/e VLSFO	**Indirect N_2O**	**Marginal electricity mix**					**Carbon intensity of grid electricity**	
Original value / parameter	Not included	IEA 2017-2021					21-811 g CO_2-eq/kWh (depending on region)	
Tested value / parameter	Included	IEA 2019-2021	IEA 2015-2021	NGFS 2020-2025	NGFS 2015-2020	IEA 2015-2020	64.7 g CO_2-eq/kWh	8 g CO_2-eq/kWh
Impact categories								
Global warming (GWP100)	3%	-0.5%	0.3%	-3%	-0.1%	-0.1%	-3%	-7%
Respiratory inorganics		-0.2%	0.1%	-0.6%	-0.3%	0.1%		
Respiratory organics		-0.02%	0.02%	-0.2%	-0.02%	0.01%		
Nature occupation		2%	0.03%	-3%	-5%	1%		
Acidification		-0.1%	0.03%	-0.4%	-0.1%	0.03%		
Eutrophication, aquatic		0.02%	0.004%	-0.1%	-0.1%	0.01%		
Eutrophication, terrestrial		-0.01%	0.005%	-0.05%	-0.001%	-0.003%		
Photochemical ozone, vegetation		-0.02%	0.01%	-0.1%	-0.01%	0.001%		

Table 8.4 continued: The relative percentage changes for the global mean **consequential** LCIA results for ammonia with H2 from ATR with CCS for the sensitivity parameters presented in **Table 8.1**. The orange colour code indicates if a change is ±10%, while yellow indicates a change of -10% or more. An empty field indicates a change of 0%.

Ammonia with H_2 from ATR with CCS and 9.6% e/e VLSFO	**Methane from natural gas extraction**	**Methane slip from ATR**	**Natural gas to ATR**	**H_2 production technology**	**Determining product from ASU**	**Carbon capture rate**		**Energy input to CCS**	**Transport distance to carbon storage**	**CO_2 leakage from storage**	
Original value / parameter	Varies from country to country	0.3%	171 GJ/H_2	ATR	N_2	90%		0.28 kWh/kg captured CO_2	200 km	0.023%	
Tested value / parameter	4x default slip	5%	181 GJ/H_2	SMR	O_2	50%	95%	2.8 kWh/kg captured CO_2	2,000 km	0.3%	5%
Impact categories											
Global warming (GWP100)	40%	107%	6%	94%	-0.01%	87%	-11%	48%	7%	28%	166%
Respiratory inorganics	0.01%		0.5%	0.5%	-0.002%			1.4%	1%		
Respiratory organics	9%	25%	0.5%	-0.7%	-0.001%			3.9%	0.7%		
Nature occupation	0.4%		9%	21%	-0.02%			40%	17%		
Acidification	0.01%		0.4%	0.4%	-0.001%			1.1%	1%		
Eutrophication, aquatic	0.01%		0.4%	0.9%	-0.001%			1.7%	1%		
Eutrophication, terrestrial	0.001%		0.1%	0.3%	-0.0002%			0.4%	0.2%		
Photochemical ozone, vegetation	5%	14%	0.4%	-0.2%	-0.0005%			2.5%	0.5%		

Table 8.5: The relative percentage changes for the global mean **consequential** LCIA results for VLSFO for the sensitivity parameters presented in **Table 8.1**. The orange colour code indicates if a change is ±10%, while yellow indicates a change of -10% or more. An empty field indicates a change of 0%.

VLSFO	Carbon intensity of fuel oil		H_2 production technology	Methane slip from ATR
Original value / parameter	0.75-1.66 kg CO_2-eq/kg fuel oil (depending on region)		ATR without CCS	0.3%
Tested value / parameter	0.68 kg CO_2-eq/kg fuel oil	0.43 kg CO_2-eq/kg fuel oil	ATR with CCS	5%
Impact categories				
Global warming (GWP100)	-9%	-16%	-2%	1%
Respiratory inorganics			-0.02%	
Respiratory organics			-0.1%	1%
Nature occupation			-0.2%	
Acidification			-0.03%	
Eutrophication, aquatic			-0.03%	
Eutrophication, terrestrial			-0.01%	
Photochemical ozone, vegetation			-0.1%	0.3%

The relative percentage changes in **Table 8.2-Table 8.5** show that the parameters in **Table 8.1** most often impact the GWP100 results. Moreover, in **section 6.1**, GWP100 was the impact category, where the difference between VLSFO and the two ammonia pathways was largest. Therefore, **section 8.1**-**8.14** will primarily focus on global warming. The following sections also describe the sensitivity analyses in more depth and present the changes visually.

8.1 Desalination

The LCA study applies surface/ground water as the default scenario. However, as the geographical scope of the study is global, some countries and regions will likely rely on desalination to some extent. Therefore, the LCIA results for the two ammonia pathways are calculated with desalinated water in the sensitivity analysis.

The relative percentage changes in **Table 8.2** and **Table 8.3** show that the GWP100 results go down with 0.05-0.1% for the electrolysis-based ammonia. This is unexpected since desalination normally requires more energy than surface/groundwater. Yet, this may be caused by the lack of service inputs in the LCI data for desalination (see **section 4.6.1.2**), as there are no inputs related to the costs from operations, maintenance, etc. Nevertheless, service inputs are not expected to have a large influence on the results, thus, the use of desalinated water including service inputs is still expected to have a minor influence.

As seen in **Table 8.4**, the GWP100 results for natural gas-based ammonia goes up with 0.2%, when desalinated water is used instead of ground/surface water. This is because of the higher impact from grid electricity. The results may be underestimated, since service inputs are not included, nevertheless, just as for ammonia with H_2 from electrolysis, the lack of service inputs is expected to have a minor influence.

As the changes in results for both ammonia pathways are minor, a graphic visualisation is not presented for this sensitivity analysis.

8.2 Lower heating value of ammonia

The project partners have discussed whether the LHV of ammonia is 17.2 MJ/kg (corresponding to liquid ammonia) or 18.6 MJ/kg (corresponding to gaseous ammonia). Initially, 17.2 MJ/kg was applied for the study since ammonia is injected to the ammonia engine as a liquid. Moreover, a high LHV of ammonia can result in optimistic ammonia consumption numbers. On the other hand, a partner states that some of the energy from the combustion chamber – which is used to evaporate the ammonia fuel – is regained as volume work during the cylinder process. Therefore, the LHV of ammonia is somewhere between the value for liquid ammonia and gaseous ammonia. As the 17.2 MJ/kg ammonia was kept in the default scenario, this sensitivity analysis applies 18.6 MJ/kg ammonia. The change in GWP100 results is presented on **Figure 8.1**.

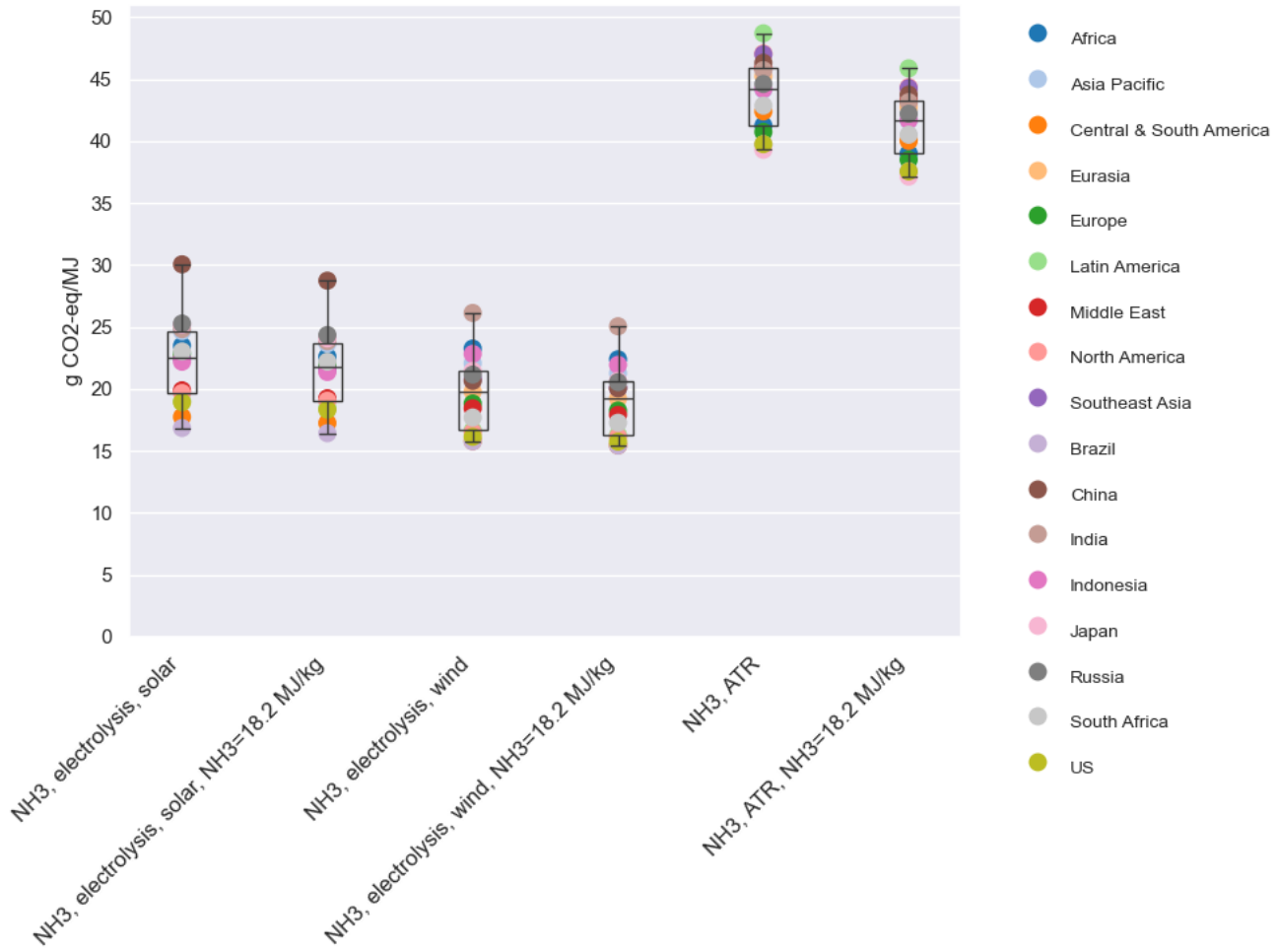

Figure 8.1: Consequential GWP100 results for the two ammonia pathways (9.6% e/e VLSFO) with LHV for ammonia of 18.6 MJ/kg.

Figure 8.1 shows that the results for the two ammonia pathways are decreased, when the LHV of ammonia is increased to 18.6 MJ/kg. This follows the expectations, as a higher LHV value for ammonia results in a lower energy requirement to fulfil the functional unit.

Table 8.2 and **Table 8.3** show that the GWP100 results for electrolysis-based ammonia go down with 3-4%, when the higher LHV for ammonia is applied. For natural gas-based ammonia, **Table 8.4** shows that the GWP100 result goes down by 6%. Thus, compared to other parameters in the sensitivity analysis, the LHV of ammonia is of lower importance than, e.g., the share of pilot fuel and the N_2O emissions from combustion of ammonia (see **section 8.3** and **8.10**).

8.3 Share of pilot fuel

A project partner has supplied data on the combustion emissions for ammonia with 9.6% pilot fuel. Since the share of pilot fuel can influence the results, ammonia with 5% and 15% e/e VLSFO is tested in the sensitivity analysis. Note that the combustion emissions for ammonia with 5% and 15% e/e VLSFO are estimated based on the difference between combustion emissions for VLSFO, ammonia with 0% and 9.6% e/e VLSFO.

The change in share of VLSFO affects the ammonia, CO_2, SO_x, and particulate emissions from the combustion, as ammonia on its own does not contain any carbon or sulphur and since the combustion of VLSFO does not emit any ammonia (see **Table 8.6**). The NO_x emissions are not affected by the share of pilot fuel, as the applied

value is the upper limit for Tier II compliant marine engine emissions. Neither are the N_2O emissions since the project partner assumes that this combustion emission is the same for VLSFO and ammonia regardless of the pilot fuel share. Nevertheless, higher N_2O emissions are tested in **section 8.4**.

Table 8.6: Change in combustion emissions based on change in share of pilot fuel (VLSFO)

Consumption and emissions	Unit	VLSFO	Ammonia with 0% e/e VLSFO	Ammonia with 5% e/e VLSFO	Ammonia with 9.6% e/e VLSFO	Ammonia with 15% e/e VLSFO	Comment
Fuel consumption							
NH_3	g/MJ	0	58.14	55.23	52.50	49.42	
VLSFO	g/MJ	24.31	0	1.21	2.34	3.64	
Emissions							
Ammonia (NH_3)	g/MJ	0	0.0062	0.0058	0.0056	0.0052	The slip of ammonia is estimated by a project partner based on development targets for the combustion engine, as the engine is still under development.
Carbon dioxide (CO_2)	g/MJ	76.53	0	3.83	7.36	11.48	The CO_2 emissions only relates to the combustion of VLSFO since ammonia does not contain any carbon.
Dinitrogen monoxide (N_2O)	g/MJ	0.00278	0.0056	0.0056	0.0056	0.0056	VLSFO value: Estimate by a project partner based on combustion of diesel oil from the Third IMO Greenhouse Gas Study 2014. Ammonia value: Development target for the ammonia engine, which recent engine tests support.
Nitrogen oxides (NO_x)	g/MJ	2.00	2.00	2.00	2.00	2.00	This value is NO_x Tier II compliant for marine engines and is therefore the same for both VLSFO and ammonia.
Sulphur oxides (SO_x)	g/MJ	0.25	0	0.012	0.024	0.037	The SO_x emissions only relate to the combustion of VLSFO since ammonia does not contain any sulphur.
Particulates, < 2.5 um	g/MJ	0.085	0	0.0042	0.0082	0.0127	LCI data from Green Transition Denmark (2021). All particulates are assumed to be < 2.5 µm due to the low sulphur content of VLSFO.

Table 8.2 and **Table 8.3** show that the GWP100 results for electrolysis-based ammonia with 5% e/e VLSFO go down with 19% and 23% for solar- and wind-based electrolysis, respectively, while the results go up with 23% and 26%, when the share of pilot fuel is 15% e/e. For natural gas-based ammonia, **Table 8.4** shows that the GWP100 results change with -7% and +8% for ammonia with 5% and 15% e/e VLSFO, respectively.

The share of pilot fuel also changes the results for the other impact categories, with the largest relative percentage change being 8-9% for nature occupation for natural gas-based ammonia (see **Table 8.2-Table 8.4**). Nevertheless, as the GWP100 results change for both ammonia pathways, this impact category is presented in **Figure 8.2**.

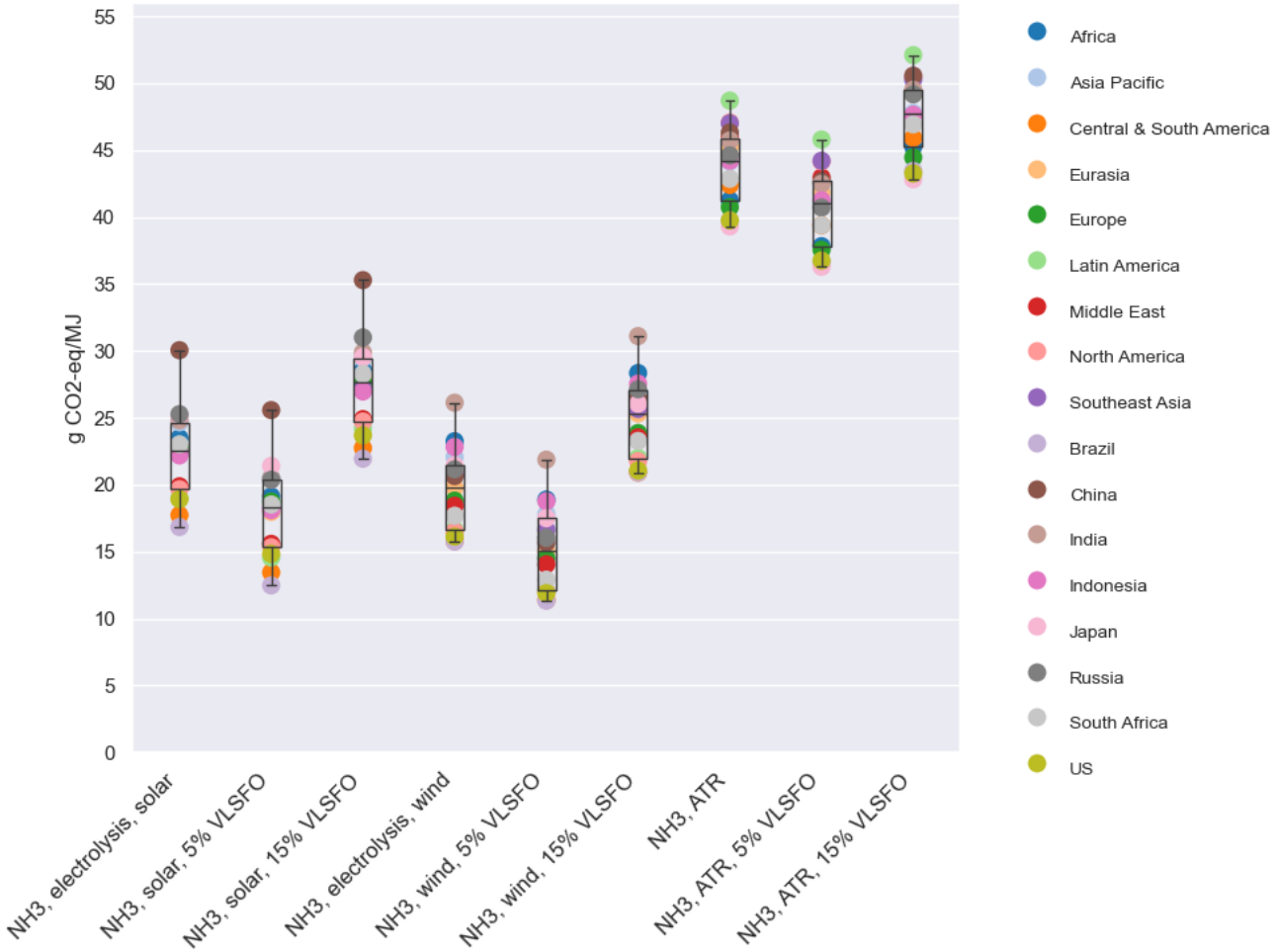

Figure 8.2: Change in **consequential** GWP100 results for the two ammonia pathways with 5% and 15% pilot fuel (VLSFO).

8.4 Electricity input to Haber-Bosch synthesis

The electricity input to the Haber-Bosch process covers both the production of ammonia as well as the liquefaction of ammonia. Yet, compared to data from Dong (2022) - which includes an energy input of 1.16 kWh/kg NH_3 for both Haber-Bosch synthesis and liquefaction - the electricity input of 0.35 kWh/kg NH_3 in **Table 5.10** may be underestimated. Thus, in the sensitivity analysis it is tested how the results change if the energy input is multiplied with a factor 10.

This sensitivity analysis results in a relative percentage change above 10% for both ammonia pathways for nature occupation, while also GWP100 results change more than ±10% for ammonia with H_2 from ATR with CCS and ammonia with solar-based electrolysis (see **Table 8.2-Table 8.4**). These impact categories are affected since material inputs to both renewable and grid electricity are large contributors to nature occupation, while grid electricity also has a notable carbon footprint. Moreover, electricity from solar often has a higher carbon footprint per kWh than electricity from wind, resulting in a higher relative percentage change for GWP100 for ammonia with solar-based electrolysis compared to ammonia with wind-based electrolysis. The changes in GWP100 results are visualised on **Figure 8.3**.

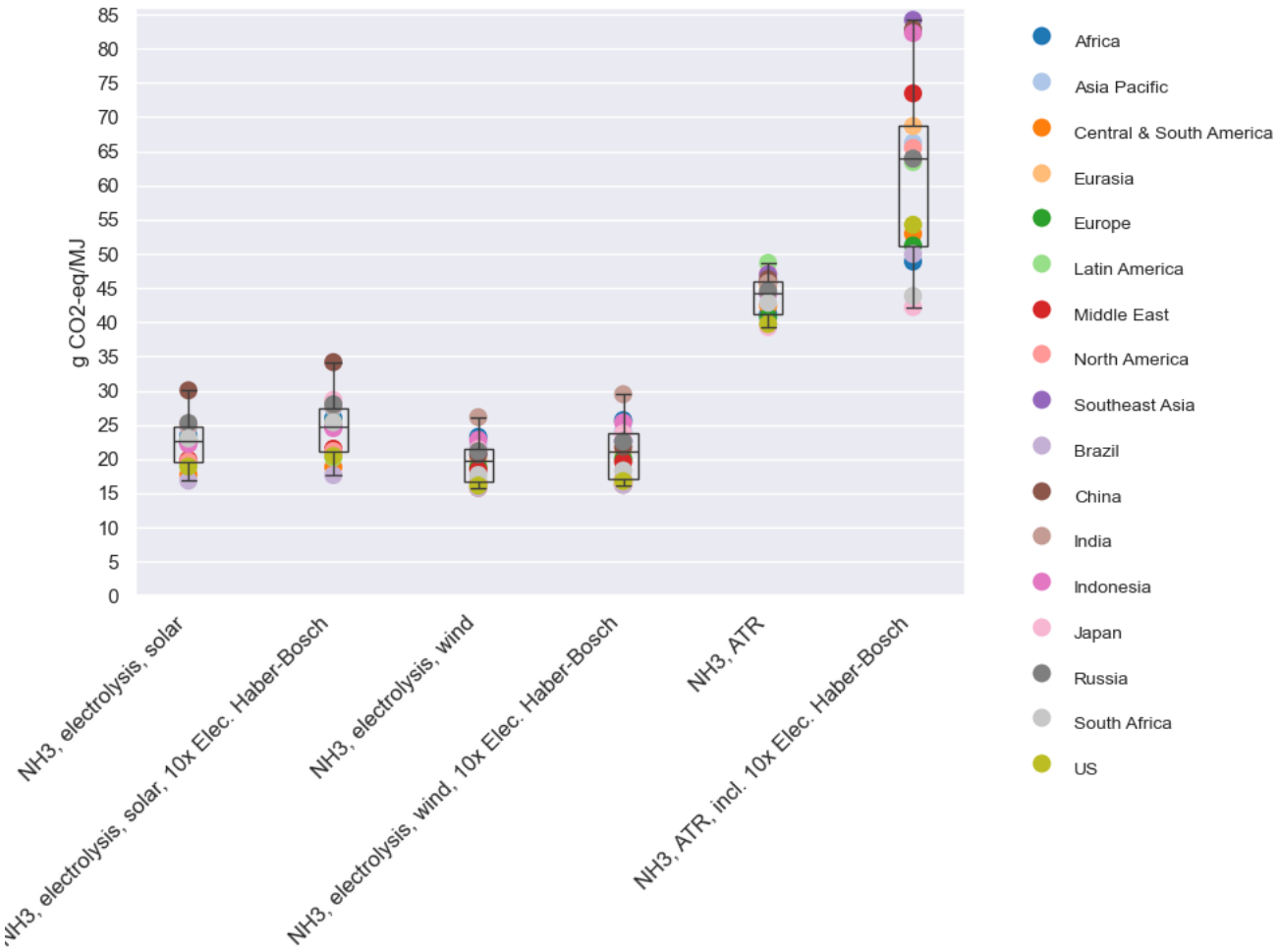

Figure 8.3: Change in **consequential** GWP100 results for the two ammonia pathways (9.6% e/e VLSFO) with a 10 times higher electricity input to the Haber-Bosch process.

8.5 Transport distance, distribution and bunkering phase

The transport distance for the distribution and bunkering phase is set to 707 km by ship and 588 km by pipeline for both ammonia and VLSFO based on data for distribution of heavy fuel oil from the ecoinvent database. However, as these data may not be applicable for ammonia, this sensitivity analysis tests, how much the LCIA results change, if the transport distances are multiplied with a factor 10, since the range for the distribution distance is unknown. However, other ammonia studies such as Al-Breiki and Bicer (2021) and Sphera Solutions (2024) have applied distribution distances of 18-20,000 km, thus, a sum of 12,950 km may not be unrealistic.

Table 8.2-Table 8.4 show that there is a notable change for two out of eight impact categories for both ammonia pathways, when the distribution distance is multiplied with a factor 10. For nature occupation, the change is 131%, 108%, and 77% for natural gas-based ammonia and ammonia with wind-based electrolysis, respectively. The GWP100 results for electrolysis-based ammonia go up by 48% and 55% for solar- and wind-based electrolysis, respectively, while the GWP100 result for natural gas-based ammonia goes up with 25% (see the change in GWP100 results visualised on **Figure 8.4**).

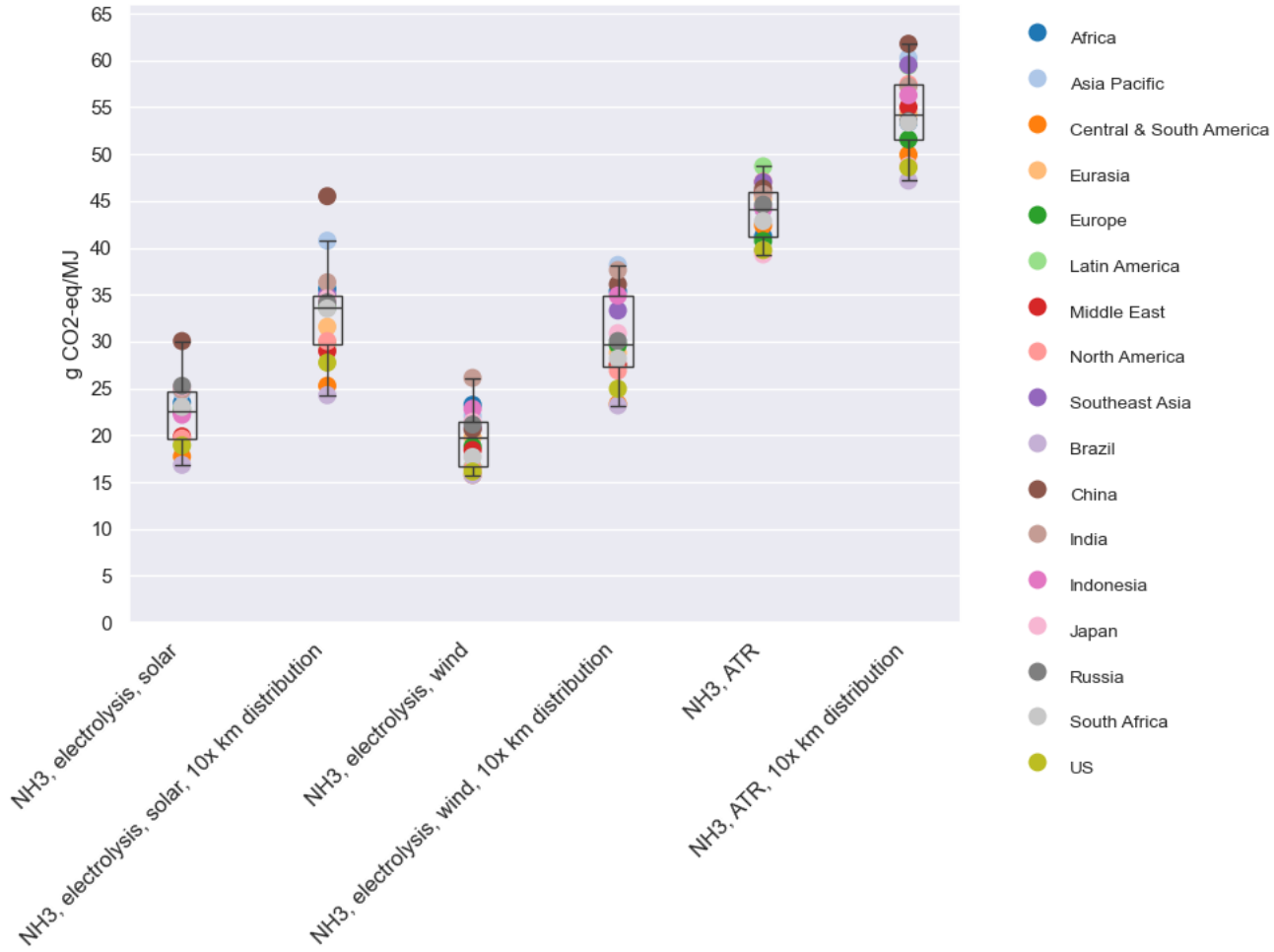

Figure 8.4: Change in **consequential** GWP100 results for the two ammonia pathways (9.6% e/e VLSFO) with 10 times longer transport distance in the distribution phase.

Based on the relative percentage changes and assuming that 12,950 km distribution distance is realistic for ammonia – at least until the production of ammonia as a shipping fuel is well established – the distribution distance is an important parameter for several impact categories. Yet, it is important to note that the larger the influence of the parameter, the lower the default result is. Moreover, the change in GWP100 results is largest for ammonia with wind-based electrolysis, since this fuel scenario has the lowest GWP100 impact.

8.6 Energy for cooling of ammonia

The energy for cooling of ammonia – both in the distribution phase and on board the ship – is based on an expert estimate and is set to 1.9% of the energy in ammonia with 9.6% e/e VLSFO. On board the vessel, it is assumed that ammonia with 9.6% e/e VLSFO is used as fuel for the cooling, while fuel oil is assumed to the used for the distribution phase (see **section 5.3** and **5.4**). As the range for the cooling energy requirement is not known, this sensitivity analysis therefore tests how much the LCIA results change, if the energy requirement for cooling is multiplied with a factor 10.

Additionally, project partners have presented another approach to estimating the energy requirement for cooling of ammonia based on a 3000 m^3 liquefied natural gas (LNG) vessel with a boil-off rate (BOR) of 0.4% per day. The project partners state that the boil-off rate for an ammonia vessel of the same size should be lower than 0.4% per day, since LNG is stored at a lower temperature than liquid ammonia, though this can vary depending on the tank design, shape, etc. Thus, the project partners apply a boil-off rate of 0.4% per day, an

energy requirement of 1,350 MJ for reliquefication of one t of ammonia, and a density of 698 kg/m^3 ammonia to estimate the energy required for cooling of ammonia per hour:

$$\frac{3000\ m^3\ NH_3 * 0.698 \frac{t\ NH_3}{m^3\ NH_3} * 0.4\% \frac{BOR}{day}}{24 \frac{hours}{day}} * 1{,}350 \frac{MJ}{t\ NH_3} = 471.2 \frac{MJ}{hour}$$

Furthermore, the project partners use the 707 km from the distribution phase, an assumed speed for the bunkering vessel of 10 knots (18.52 km/h) and that the bunkering vessel uses two days at the loading port to calculate the energy requirement per t of ammonia:

$$\frac{707\ km}{18.52 \frac{km}{hour}} + 2\ days * 24 \frac{hour}{day} = 86.2\ hours$$

$$\frac{86.2\ hours *\ 471.2 \frac{MJ}{hour}}{3000\ m^3 NH_3 * 0.698 \frac{t\ NH_3}{m^3\ NH_3}} = 19.38 \frac{MJ}{t\ NH_3}$$

Thus, a lower value of 19.38 MJ per t ammonia, corresponding to 0.11% of the energy in one t ammonia with 9.6% e/e VLSFO, is also tested in this sensitivity analysis.

Table 8.2-Table 8.4 show that there is a notable change for three out of eight impact categories for the three ammonia fuel scenarios, when the energy requirement for cooling of ammonia is multiplied with a factor 10. The largest relative percentage change is seen for GWP100 for ammonia with wind-based electrolysis, as the change is 100%. For nature occupation, the change is 40-57% depending on the ammonia fuel scenario, while the change in results for acidification is 10% for all fuel scenarios. When the energy requirement is set to 0.11% of the energy in one t of ammonia, the GWP100 results are reduced with 5-9%. The change in GWP100 results is visualised on **Figure 8.5**.

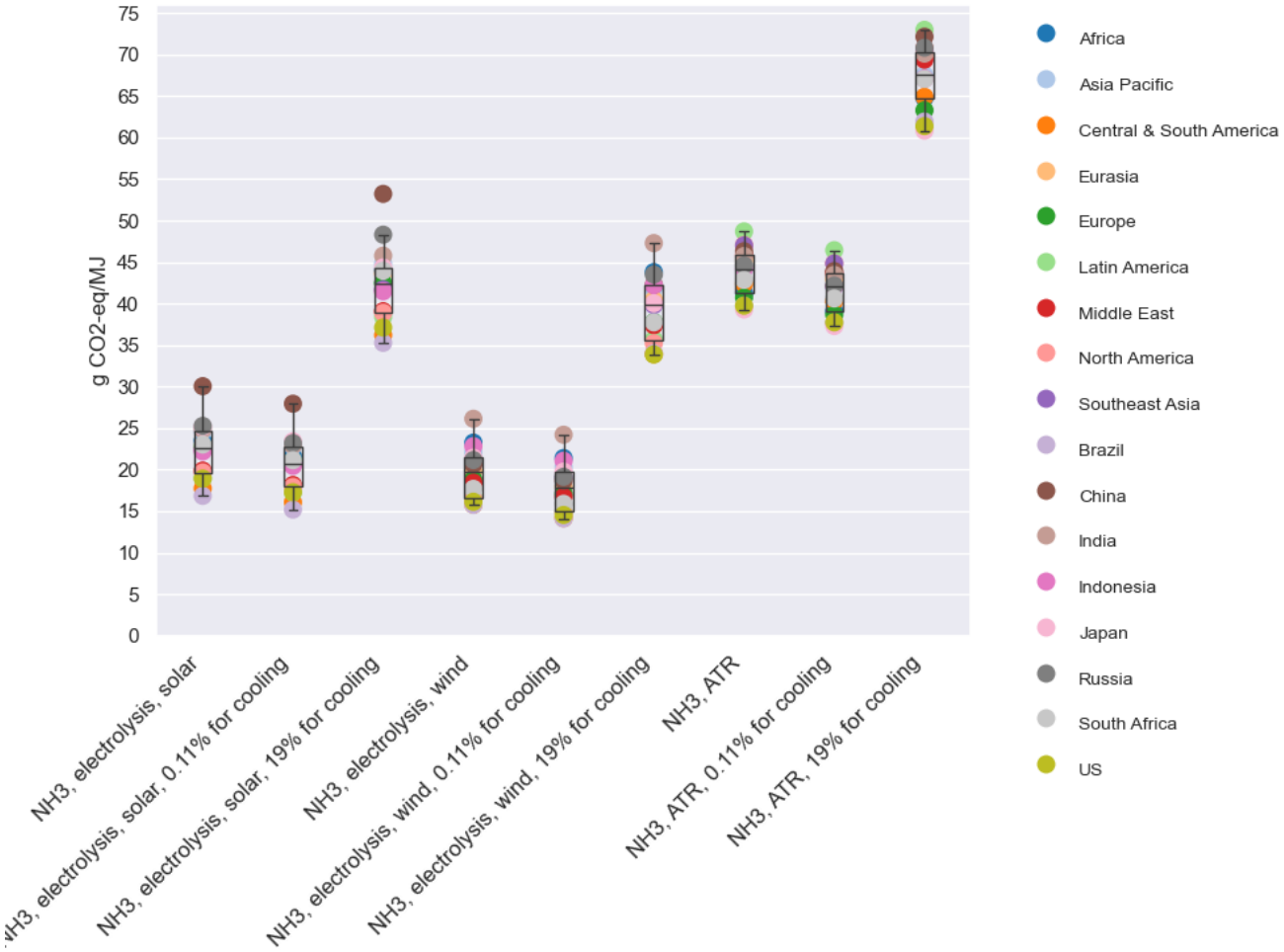

Figure 8.5: Change in **consequential** GWP100 results for the two ammonia pathways (9.6% e/e VLSFO) with a 10 times higher energy requirement for cooling in the distribution phase and on board the vessel.

Based on the relative percentage changes, the energy used for cooling of ammonia is an important parameter for the LCA results. Nevertheless, it is important to highlight that the majority of the change stems from the additional use of fuel oil for cooling in the distribution phase, especially since fuel oil has a larger impact on GWP100 and nature occupation than the ammonia pathways with 9.6% e/e VLSFO. Thus, if an energy source with a lower environmental impact was used in the distribution phase, the relative percentage change could be lower.

8.7 Slip of hydrogen throughout the product system

As for most gases within the product system, a 0.3% slip is assumed. This is also the case for H_2, however, as previously stated, the slip may be up to 5%. Therefore, this upper value is tested in this sensitivity analysis, analysing its influence on the GWP100 results for both ammonia pathways.

As seen in **Table 8.2-Table 8.4**, the slip of H_2 changes the results for GWP100 with 35%, 39%, and 18% for ammonia with solar-based electrolysis, ammonia with wind-based electrolysis, and natural gas-based ammonia, respectively. The change for other impact categories is below 10%. The change in GWP100 results is visualised on **Figure 8.6**.

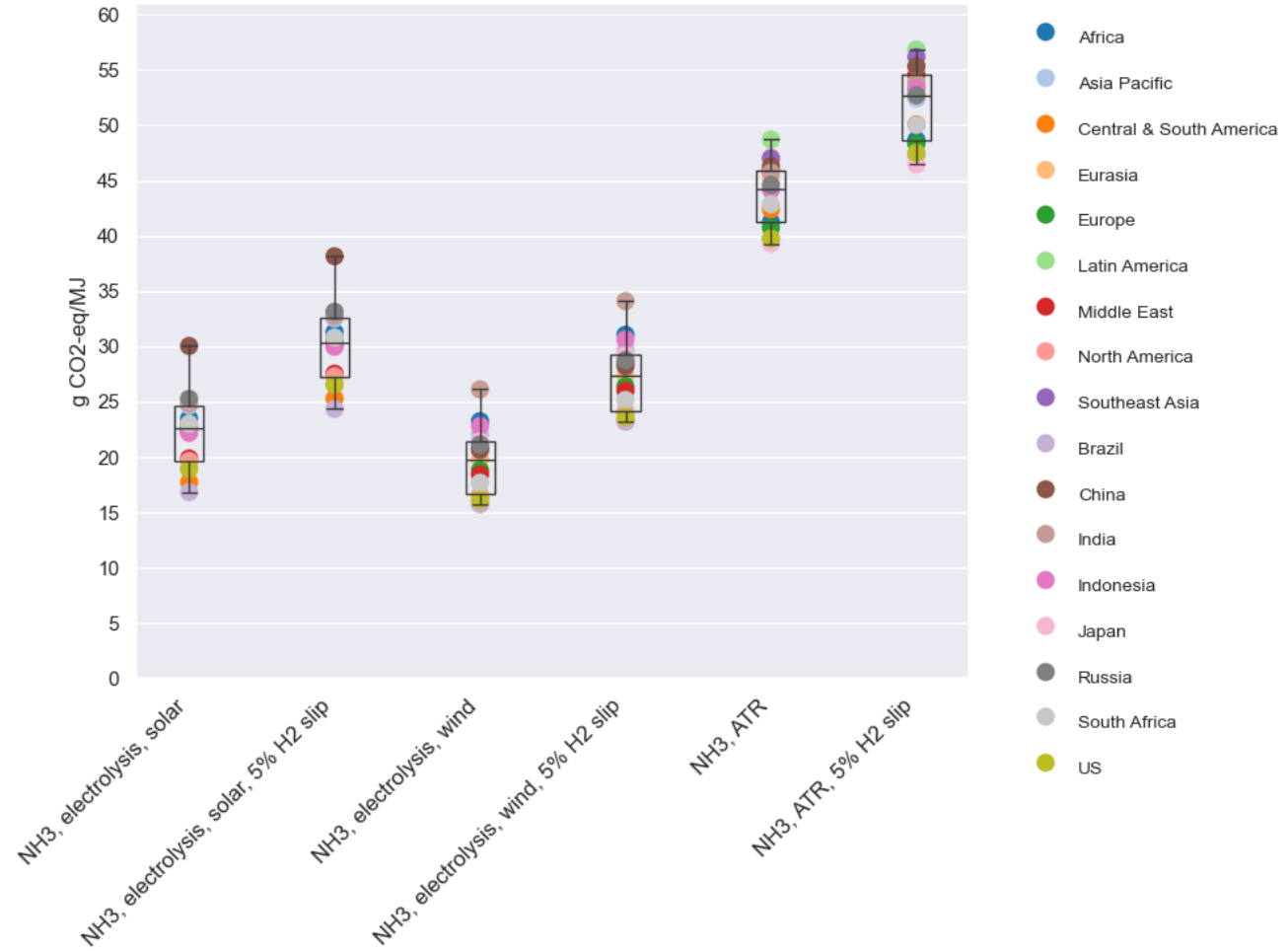

Figure 8.6: Change in **consequential** GWP100 results for the two ammonia pathways (9.6% e/e VLSFO) with a 5% slip of H_2 from H_2 storage and/or H_2 production.

Based on the relative percentage changes, the slip of H_2 is an important parameter. Yet, it is important to note that the influence of the parameter is larger the lower the default GWP100 result is, e.g., the largest relative percentage change of 39% is seen for GWP100 for ammonia with wind-based electrolysis, since this ammonia fuel has the lowest impact on this impact category.

8.8 Slip of ammonia throughout the product system

Throughout the product system, a small amount of ammonia leaks, e.g., from the production of ammonia as well as the distribution and bunkering of ammonia. Yet, according to a project partner, the slip of ammonia (and other gases) has not been measured directly yet. However, based on process flow and process safety measurements, the partner expects the ammonia slip to be very small. Therefore, a slip of 0.3% has been assumed based on Bertagni et al. (2023) since it is one of the lower values presented in literature and relates to the slip of natural gas and ammonia. However, it is important to recognise that the slip of gases in reality will vary because of differences in, e.g., molecular mass, shape and/or size, and applying a default slip of 0.3% is therefore a limitation to the study. Nevertheless, as for other gases within this LCA study, this sensitivity analysis applies an upper value of 5% based on the review of H_2 slip by Muñoz (2023).

As seen in **Table 8.2-Table 8.4**, the slip of ammonia changes the results for acidification and terrestrial eutrophication with more than 600% for the three ammonia fuel scenarios, while the change is close or equal to 500% for aquatic eutrophication. Moreover, the change in results for respiratory inorganics is 189-193%. The

significant changes in results for four out of eight impact categories show that it is important to limit the slip of ammonia in order to minimize the environmental impact of ammonia fuel.

The change in results is visualised on **Figure 8.7** for acidification, as the change for this impact category is among the largest for this sensitivity analysis.

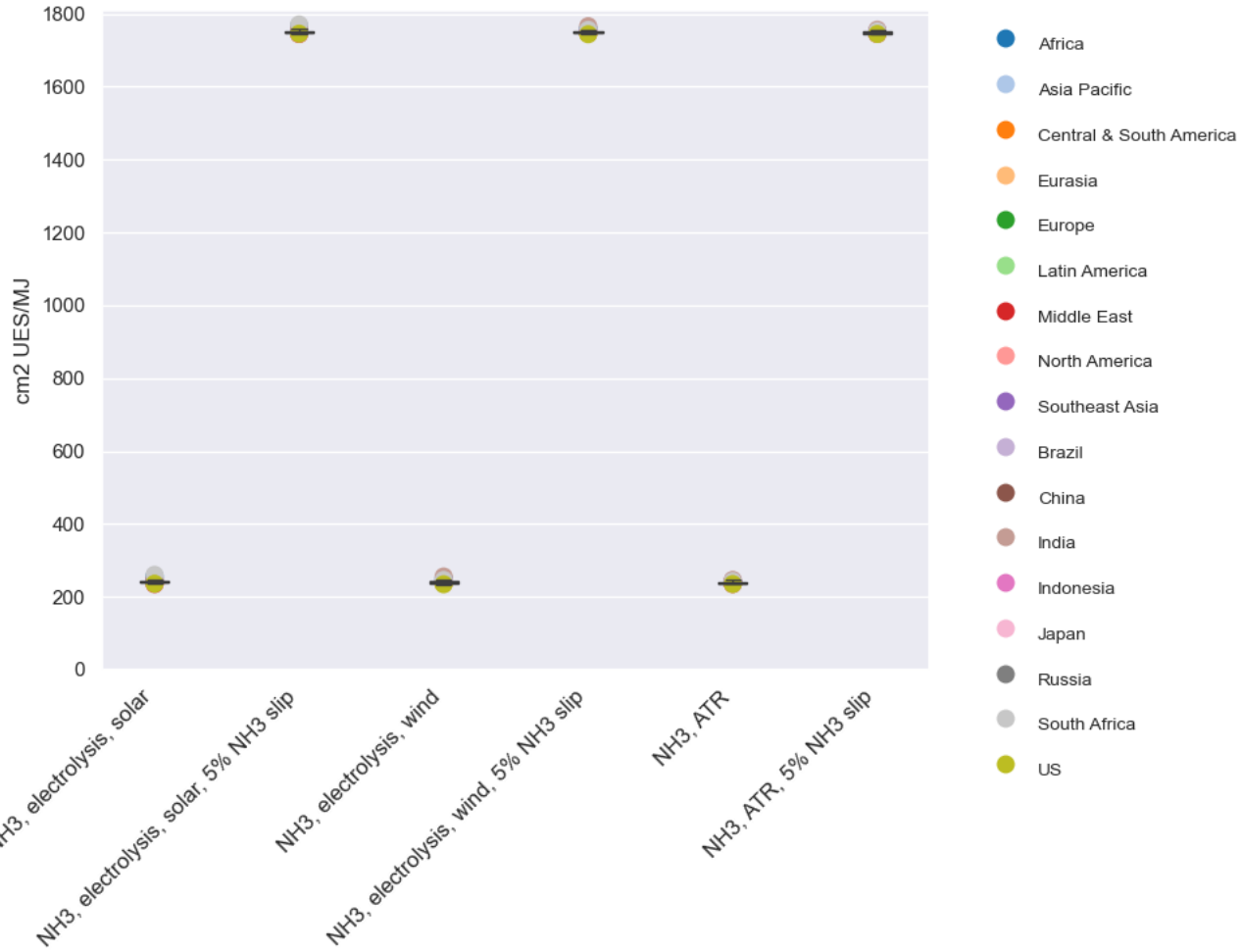

Figure 8.7: Change in **consequential** acidification results for the two ammonia pathways (9.6% e/e VLSFO) with a 5% slip of ammonia from the Haber-Bosch process and the distribution phase.

8.9 NH_3 slip from combustion

The slip of NH_3 emissions from combustion is assumed to be 0.1% in the data provided by project partners. However, as a minimum slip of 0.3% is assumed for other gases within the product system in the default scenario, this sensitivity analysis assesses the change in results if the slip of NH_3 emissions from combustion is set to 0.3%. Note that the increased slip does not influence any other parameters for the combustion, e.g., the larger NH_3 slip does not increase the input of fuel needed to fulfil the functional unit of 1 MJ.

As seen in **Table 8.2-Table 8.4**, an increased slip of NH_3 from combustion results in a relative percentage change of 16-20% for acidification as well as terrestrial and aquatic eutrophication for all three ammonia fuel scenarios. This again shows the importance of limiting gases slip throughout the product systems.

The change in results is visualised on **Figure 8.8** for acidification, as the change for this impact category is among the largest for this sensitivity analysis.

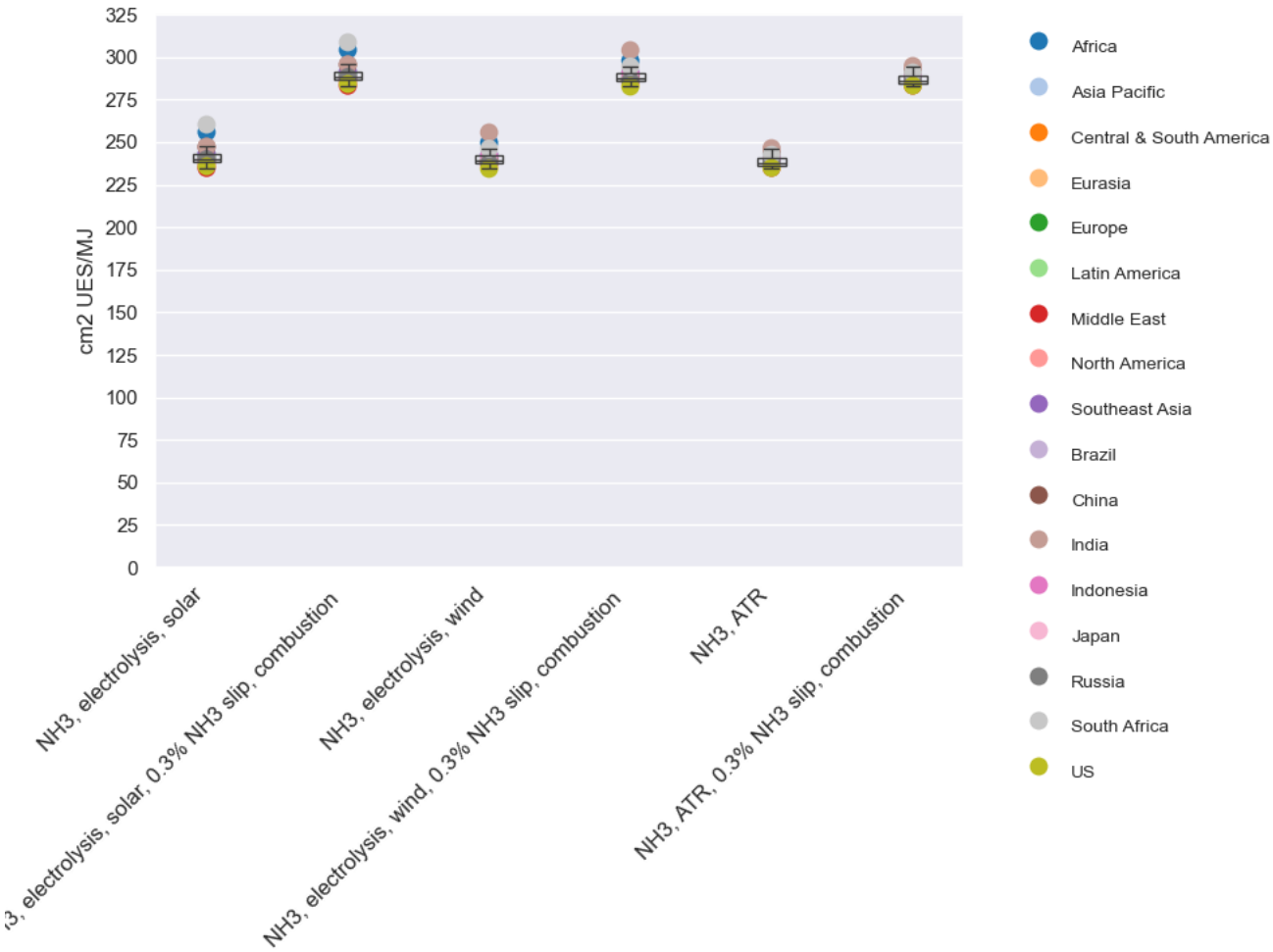

Figure 8.8: Change in **consequential** acidification results for the two ammonia pathways (9.6% e/e VLSFO) with a 0.3% slip of ammonia from the combustion on board the vessel.

8.10 N_2O emissions from combustion

Several project partners argue that the N_2O emissions from combustion of ammonia may be much higher than the N_2O value in **Table 5.15**, since the value is based on the N_2O emissions from diesel oil and is a development target for the ammonia engine. Therefore, additional literature research has been conducted in order to assess if any scientific literature reports measurements of the actual N_2O emissions from the combustion of ammonia.

However, no study reports N_2O emissions after selective catalytic reduction (SCR), which is installed to reduce emissions. Nevertheless, Xu et al. (2023) reports N_2O emissions of 76 ppm before SCR, corresponding to 0.117 g N_2O/MJ. Yet, it is important to highlight that the 0.117 g N_2O/MJ is based on an experimental, dual ammonia engine for ammonia with approximately 24% e/e diesel as pilot fuel. Additionally, a project partner stresses that the N_2O emissions will differ between engine designs, thus, the 0.117 g N_2O/MJ may not be applicable for the engine described in this LCA study. Nevertheless, as the 0.117 g N_2O/MJ is deemed the best available data, the value is included in this sensitivity analysis. Moreover, Mærsk Mc-Kinney Møller Center (2023) expects N_2O emissions to be mostly around 0.06 g N_2O/kWh, corresponding to 0.0083 g N_2O/MJ, since higher values are not likely to be accepted from an ammonia ICE design. Thus, 0.0083 g N_2O/MJ is also tested in the sensitivity analysis. Note that the amount of N_2O emissions resulting in the same GWP100 from combustion of ammonia as for VLSFO, corresponds to 0.253 g N_2O/MJ.

It is clear from **Table 8.2-Table 8.4** that the N_2O emissions from ammonia combustion is of high importance, as the relative percentage change for GWP100 is 3-4% and 137-155% for ammonia with H_2 from electrolysis as well as 2% and 69% for ammonia with H_2 from ATR with CCS with 0.0083 and 0.117 g N_2O/MJ, respectively. The change for GWP100 is visualised on **Figure 8.9**, thus, providing an illustration of the interval that the GWP100 results may vary between, depending on N_2O emissions.

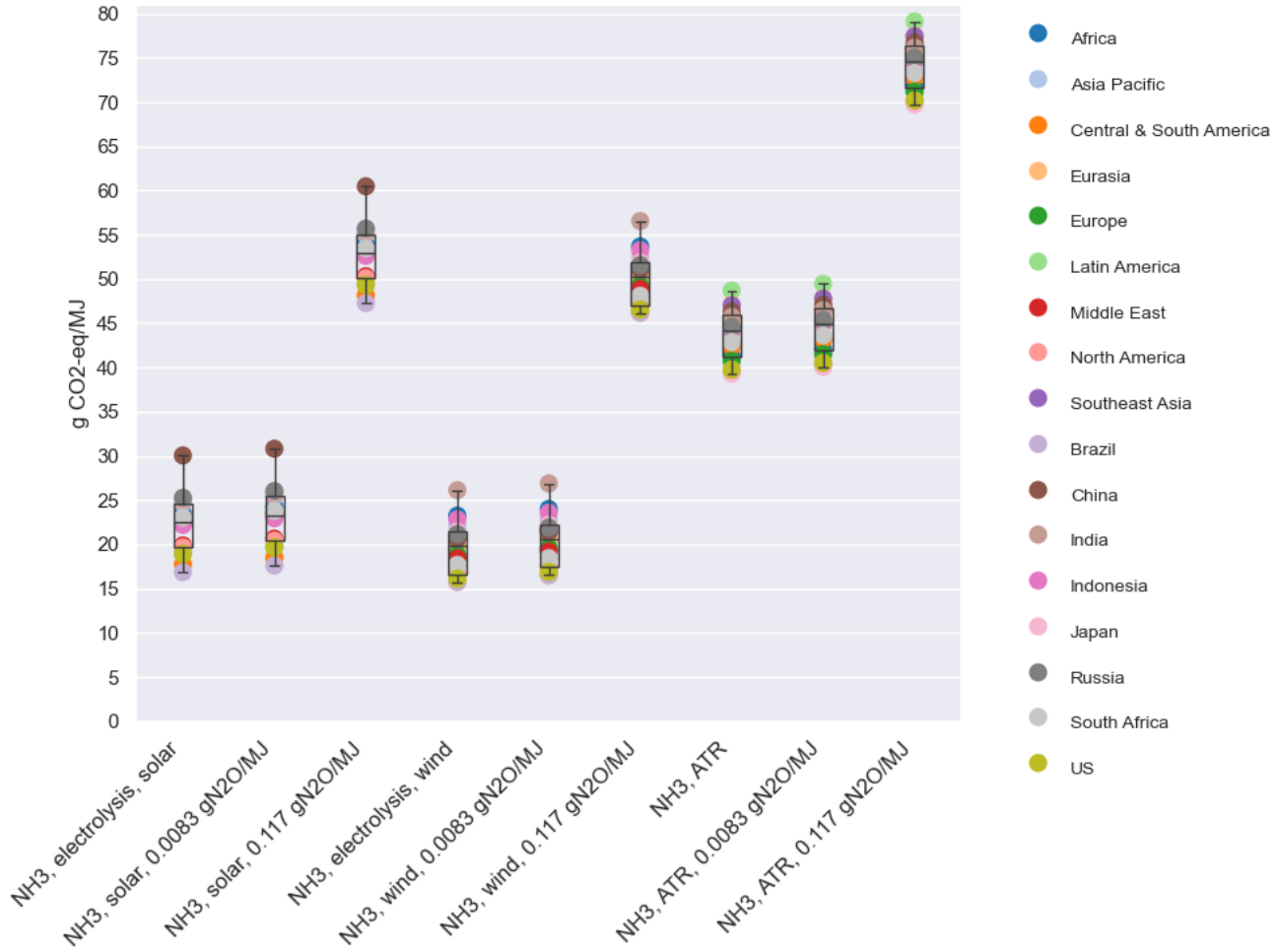

Figure 8.9: Change in **consequential** GWP100 results for the two ammonia pathways (9.6% e/e VLSFO) with 0.0083 and 0.117 g N_2O/MJ from combustion.

Figure 8.9 shows that the GWP100 results for the three ammonia fuel scenarios are increased with around 1 g CO_2-eq/MJ with 0.0083 g N_2O/MJ. Thus, if the design parameter of 0.0056 g N_2O/MJ is not met while the expectations by Mærsk Mc-Kinney Møller Center (2023) are realistic and complied with instead, an increase of 0.0027 g N_2O/MJ will not have a large effect on the GWP100 results.

Nevertheless, the figure also shows that the GWP100 results for ammonia with H_2 from electrolysis and 0.117 g N_2O/MJ are increased to approximately 45-60 g CO_2-eq/MJ. Thus, part of the results is in the same range as the default GWP100 results for natural gas-based ammonia. For ammonia with H_2 from ATR with CCS and 0.117 g N_2O/MJ, the GWP100 results range from around 70 to 79 g CO_2-eq/MJ. This clearly shows that it is important to limit the N_2O from combustion.

8.11 Indirect N_2O emissions

Since ammonia is a nitrogen-based fuel and because nitrogen-containing compounds are released to the atmosphere throughout the product system, this sensitivity analysis includes the potential indirect N_2O emissions from the emitted substances. N_2O emissions are crucial to include in the sensitivity analysis since the characterization factor for N_2O is 273 kg CO_2-eq/kg, thus, the formation of indirect N_2O may have a notable influence on the LCIA results for both ammonia pathways.

The indirect N_2O emissions are estimated based on the emission of NH_3 and NO_x occurring at sea, expecting the emissions to be absorbed by particles and thereby be distributed over long distances (Palmgren et al., 2005). It is assumed that the NH_3 and NO_x emissions deposit evenly over the globe, thus, 1/3 of the emissions are assumed to be deposited on land, as 2/3 of the globe is covered by water (USGS, 2019). Based on IPCC (2019b), it is assumed that 1% of the deposited NH_3 and NO_x emissions are converted to N_2O through the microbial processes occurring in soil. The EF_4 factor from IPCC (2019b) determines the amount of N converted to N_2O through the microbial processes. Thus, the N_2O emissions are calculated using **Equation 8.1**:

Equation 8.1

$$N_2O_{indirect} = \frac{1}{3} * EF_4 \cdot (NH_3 - N + NO_x - N) * \frac{44}{28}$$

Where:

$\frac{1}{3}$ is the share of land on the globe

$EF_4 = 0.01$ and is the N_2O emission factor for deposition of N on soil surfaces, kg N_2O-N (kg NH_3-N + NO_x-N volatilised)$^{-1}$ ((IPCC, 2019b), Table 11.3)

$NH_3 - N = g\ NH_3 * \frac{14}{17}$

$NO_X - N = g\ NOx * \frac{14}{46}$

$\frac{44}{28}$ is the conversion factor from N_2O-N to N_2O

The change in GWP100 results based on the inclusion of indirect N_2O emissions are presented in **Figure 8.10** for both ammonia pathways. Moreover, **Table 8.2-Table 8.4** show that the relative percentage change for GWP100 is 3-6% for the three ammonia fuel scenarios. Thus, the inclusion of indirect N_2O emissions is deemed to be of low importance with a NH_3 slip of 0.3%. Yet, it is important to note that the importance of indirect N_2O emissions increases with the slip of NH_3 from production, distribution, and combustion.

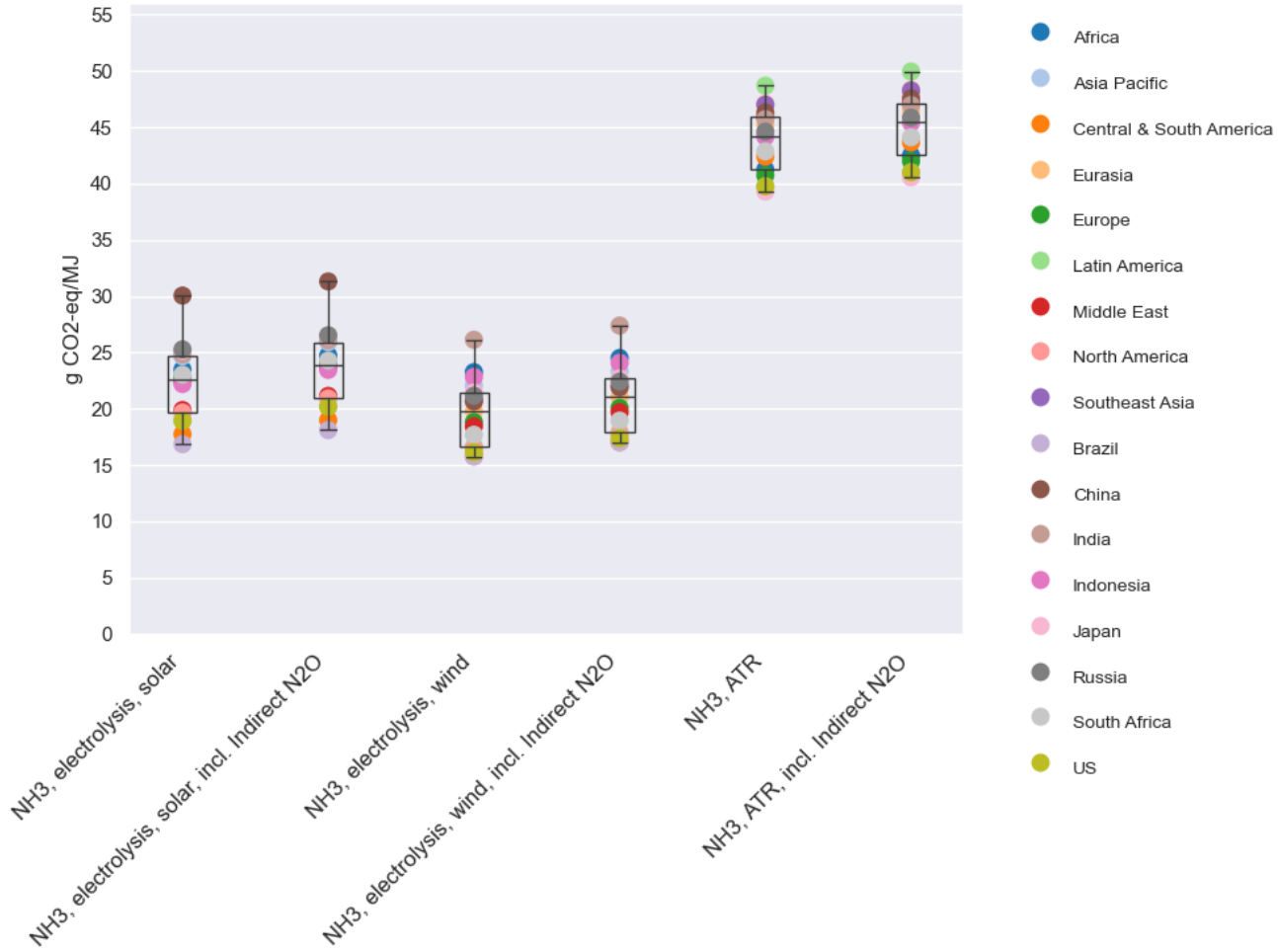

Figure 8.10: Change in **consequential** GWP100 results for the two ammonia pathways (9.6% e/e VLSFO) with indirect N_2O emissions.

8.12 Ammonia with hydrogen from electrolysis

For ammonia with H_2 from electrolysis, three parameters are tested in the sensitivity analysis: The input of H_2 from storage to the Haber-Bosch synthesis, the electricity input to electrolysis, and the carbon intensity of the renewable electricity.

8.12.1 Input of hydrogen from storage to Haber-Bosch synthesis

For the electrolysis H_2 production, the electricity is 100% renewable and comes from either solar or wind. As these electricity sources are highly dependent on weather conditions, part of the H_2 must be compressed and stored in order to ensure continuous flow of H_2 to the ammonia synthesis. For the default scenario, 25% of the H_2 for the ammonia synthesis is assumed to be from H_2 storage. Nevertheless, as this is an estimate, the sensitivity analysis includes 100% from H_2 storage as a 'worst-case' scenario in order to assess this parameter's influence on the LCIA results.

Figure 8.11 illustrates the change in GWP100 results for ammonia with H_2 from electrolysis (both solar- and wind-based). Moreover, **Table 8.2** and **Table 8.3** show that the H_2 storage sensitivity analysis changes the LCIA results with 2% or less for the eight impact categories. Thus, the input of H_2 from storage to the Haber-Bosch process does not have a notable influence on LCIA results.

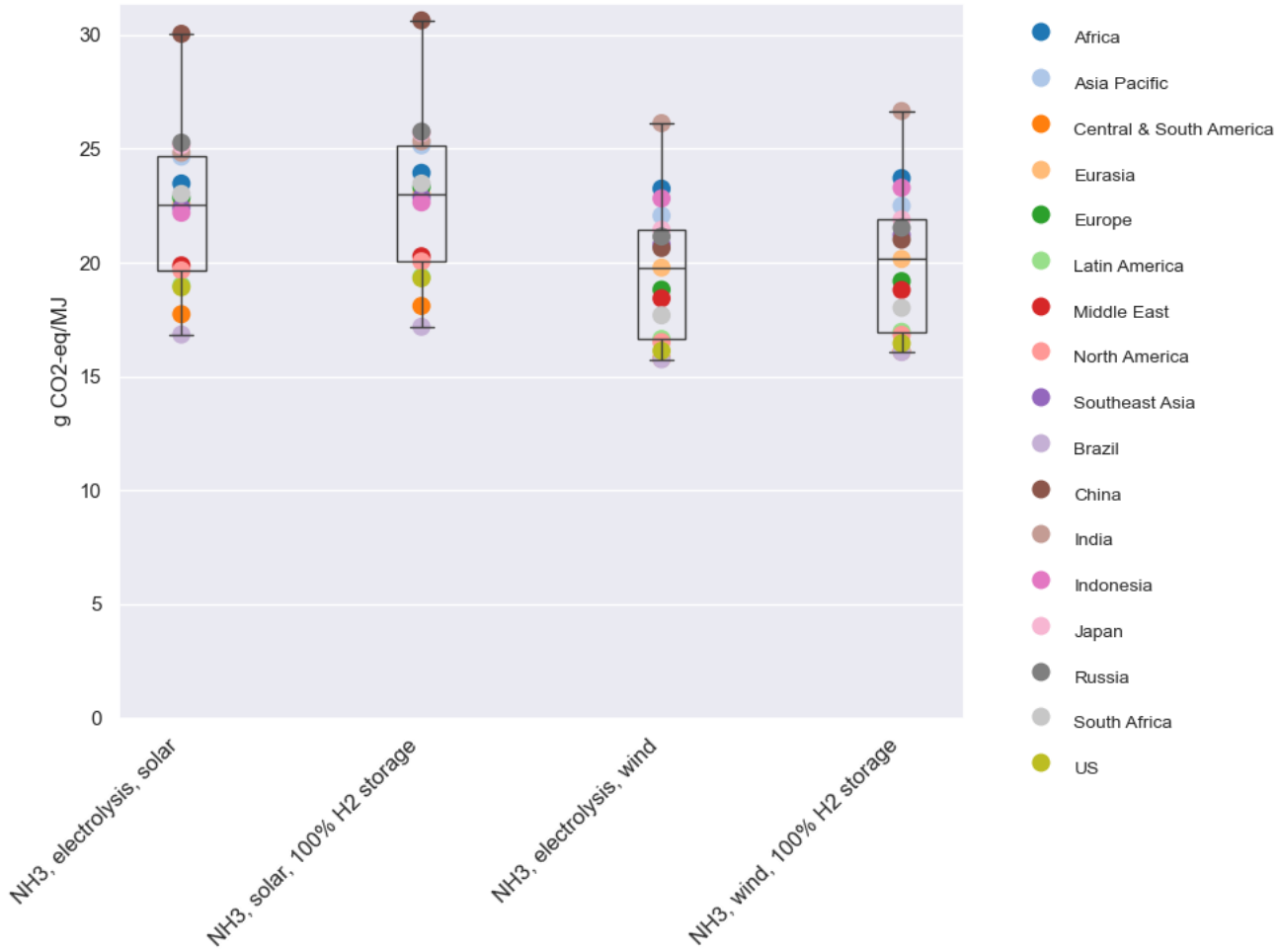

Figure 8.11: Change in **consequential** GWP100 results for ammonia (9.6% e/e VLSFO) with H_2 from electrolysis (both solar- and wind-based) with 25% and 100% H_2 storage.

8.12.2 Electricity input to electrolysis

According to the LCI data provided by an industrial expert, the electricity input to electrolysis can be up to 60 kWh/kg H_2. Thus, the upper value is applied for the sensitivity analysis in order to assess the importance of this parameter.

As seen in **Table 8.2** and **Table 8.3**, this parameter changes the results for ammonia with solar-based electrolysis with more than 10% for nature occupation due to the increased input of wood for the manufacture of plastic and glass used to produce the solar panels. For GWP100, the relative percentage change is 4% and 3% for ammonia with solar- and wind-based electrolysis, respectively. The change in GWP100 results is illustrated on **Figure 8.12**. Nevertheless, compared to other parameters, which are tested in this chapter, the input of electricity to electrolysis is of low importance for the LCIA results.

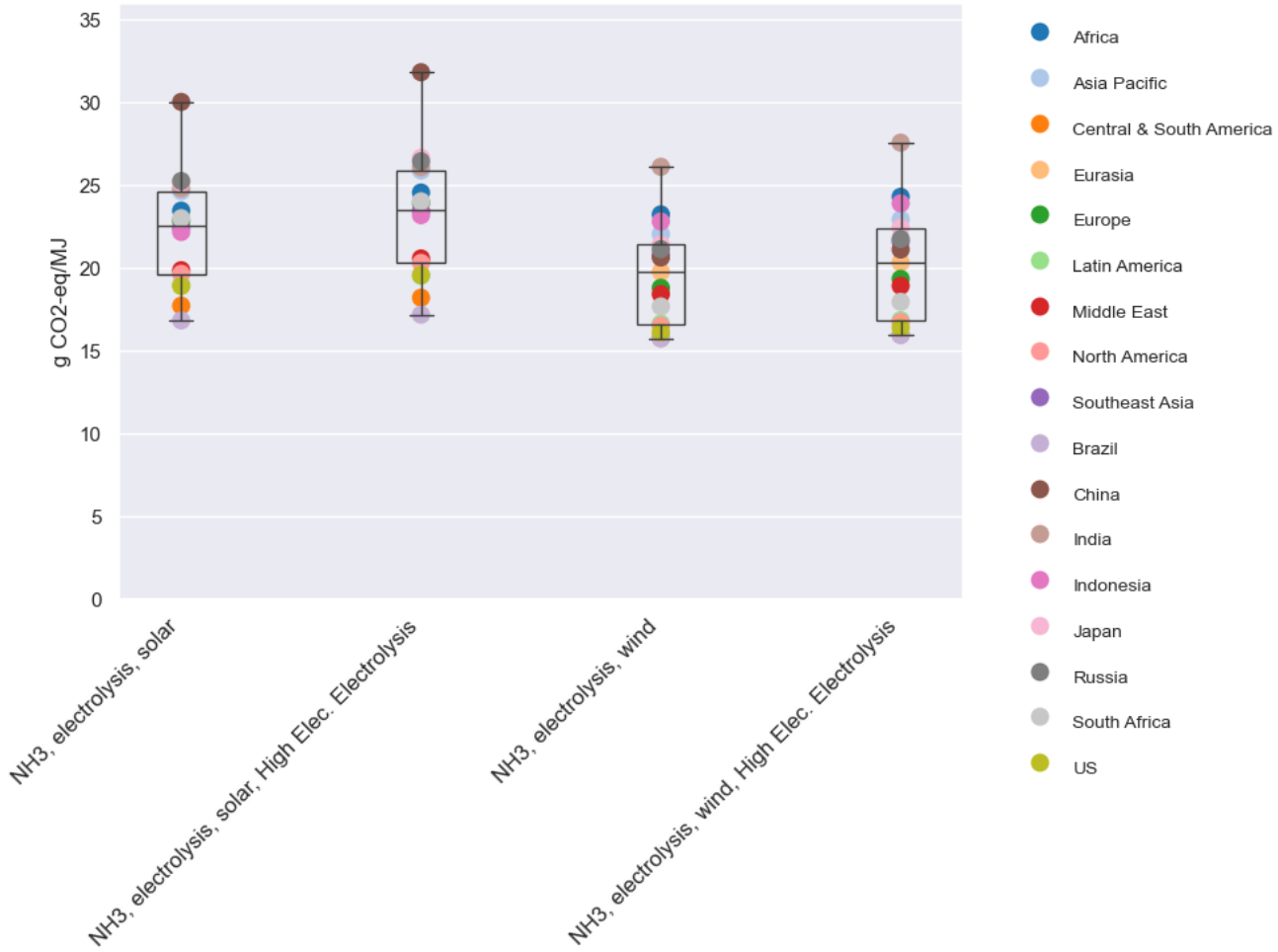

Figure 8.12: Change in **consequential** GWP100 results for ammonia (9.6% e/e VLSFO) with H_2 from electrolysis (both solar- and wind-based) with an input of 60 kWh/kg H_2 to the electrolysis process.

8.12.3 Carbon intensity of renewable electricity

The carbon intensity of electricity from solar and wind varies depending on the region with 5-24 and 3-20 g CO_2-eq/kWh, respectively. Nevertheless, when looking at the carbon intensity of electricity from solar and wind in the 48 countries, which the regions consist of, the impact varies with 17-110 and 7-91 g CO_2-eq/kWh for solar and wind, respectively. Some countries have a higher carbon footprint per kWh than others, e.g., because of a low average wind speed, low wind power efficiency, or a low average of sun hours (see details on the modelling of solar and wind electricity in **section 4.1.1.2** and **4.1.1.3**). Therefore, the sensitivity analysis includes a high and low value (100 and 5 g CO_2-eq/kWh) for the carbon intensity of the renewable electricity in order to assess this parameter's influence on the GWP100 results.

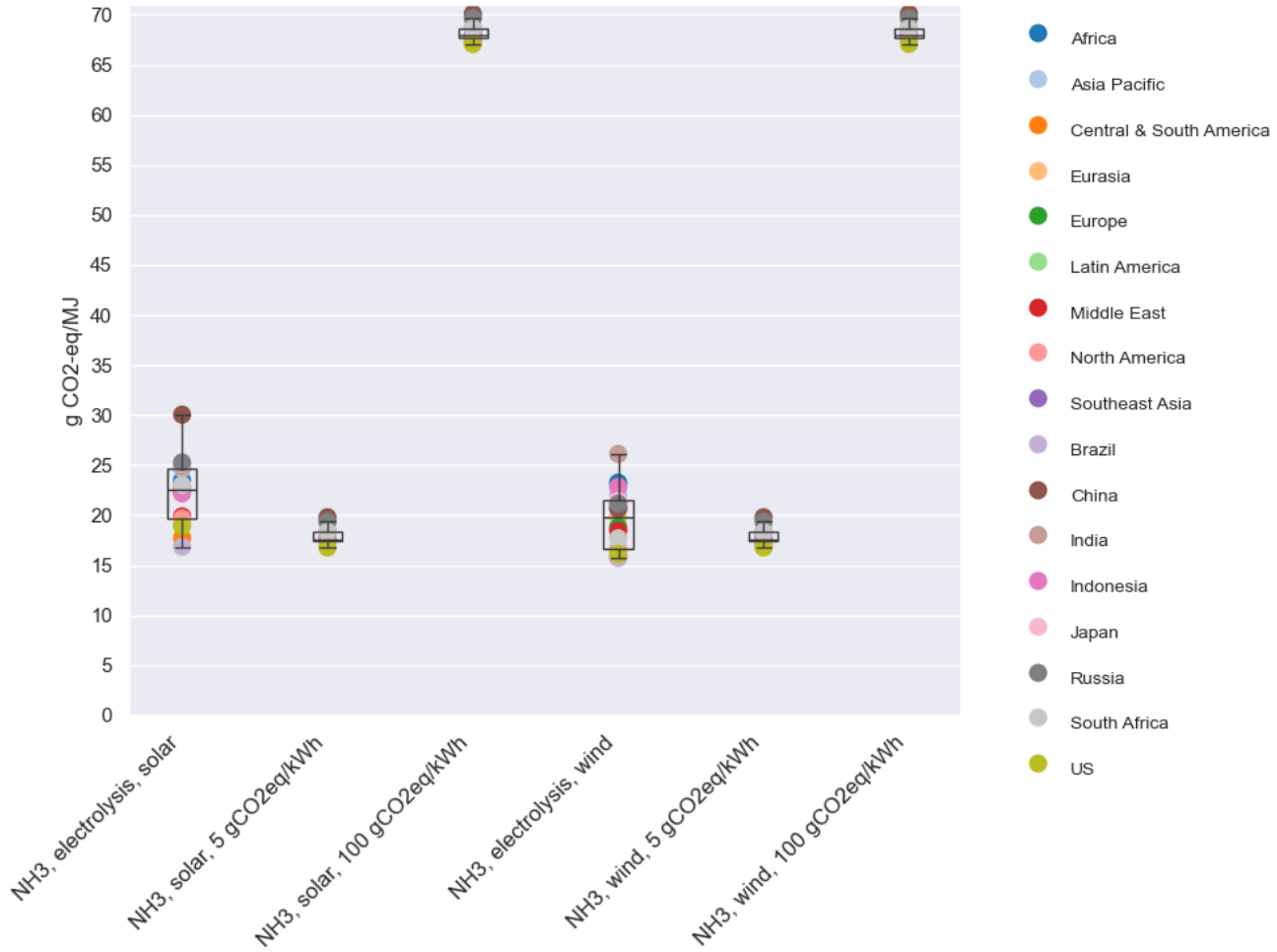

Figure 8.13: Change in **consequential** GWP100 results for ammonia (9.6% e/e VLSFO) with H_2 from electrolysis (both solar- and wind-based) where the carbon intensity of renewable electricity is varied.

Figure 8.13 clearly shows that a carbon intensity of 100 g CO_2-eq/kWh increases the GWP100 results for electrolysis-based ammonia to approximately 65-70 g CO_2-eq/MJ. The figure also shows that the geographical differences are reduced when the carbon intensity of the renewable electricity is set to the same value across the 17 regions, since the result range are minimised. Moreover, it is also seen that some countries, e.g., the US, already have renewable electricity with a carbon intensity close to 5 g CO_2-eq/kWh, since the results for the US on **Figure 8.13** do not change notably, when the carbon intensity of renewable electricity is set to 5 g CO_2-eq/kWh. The opposite is the case for ammonia with wind-based electrolysis in China, since the GWP100 result is reduced from around 30 g CO_2-eq/MJ to 20 g CO_2-eq/MJ with 5 g CO_2-eq/kWh for wind electricity.

Based on **Figure 8.13**, the carbon intensity of wind and solar electricity is an important parameter for electrolysis-based ammonia since the carbon intensity of wind and solar electricity can vary significantly between individual countries.

8.13 Ammonia with hydrogen from autothermal reforming

For ammonia with hydrogen from ATR, 11 parameters related to the grid electricity mix and the H_2 production technology are tested in the sensitivity analysis.

8.13.1 Grid electricity mix

8.13.1.1 Choice of marginal electricity mix

The applied marginal electricity mix for the default scenario is based on data from IEA for the time-series 2017-2021. Yet, since grid electricity is one of the important inputs for ammonia produced with H_2 from ATR with CCS, a sensitivity analysis is performed in order to assess, how sensitive the results are to the choice of data source, time-series, and time-series intervals for determining the marginal electricity mix. Therefore, five additional marginal electricity mixes have been created using the same methodology as described in **section 4.1.1.1** based on:

A. IEA data for 2019-2021
B. IEA data for 2015-2021
C. The Network for Greening the Financial System (NGFS) predicted data for 2020-2025
D. NGFS predicted data for 2015-2020
E. IEA data for 2015-2020

For the A and B marginal electricity mixes, time-series intervals of three and seven years are applied instead of the five-year time-series interval used for the marginal electricity mix in the default scenario. This is done, since the longer the time-series interval, the bigger the influence of the historical data and trends, while the shorter the time-series interval, the more prone the marginal electricity mix is to atypical data.

For the C and D marginal electricity mixes, forecasted data from NGFS is applied, which is based on countries' commitments before 2023 documented through United Nations Framework Convention on Climate Change (NGFS, 2024). Note that the forecasted data are based on all pledged policies, even if not implemented (NGFS, 2021) and that the NGFS data are only available for every fifth year, thus, limiting the time-series to 2015-2020, 2020-2025, 2025-2030 etc.

These forecasted scenarios are included, since the LCA study is intended to be used for decision support in the choice of and in investments in alternative fuel systems for shipping from current (2024) and the next 5-10 years. Therefore, it is important to assess how the demand for electricity is expected to change in the near future. Nevertheless, since NGFS data also include non-implemented policies, marginal electricity mix E is created in order to compare predictions with reported electricity production.

Appendix 9 (external appendix) presents the marginal mix for the default scenario and marginal mix A-E for each of the 48 countries in EXIOBASE.

As seen from **Table 8.4**, the different marginal electricity mixes change the global mean results with less than 5%, with the NGFS prediction for 2020-2025 reducing the global mean GWP100 result with 3%. **Figure 8.14** depicts the GWP100 changes.

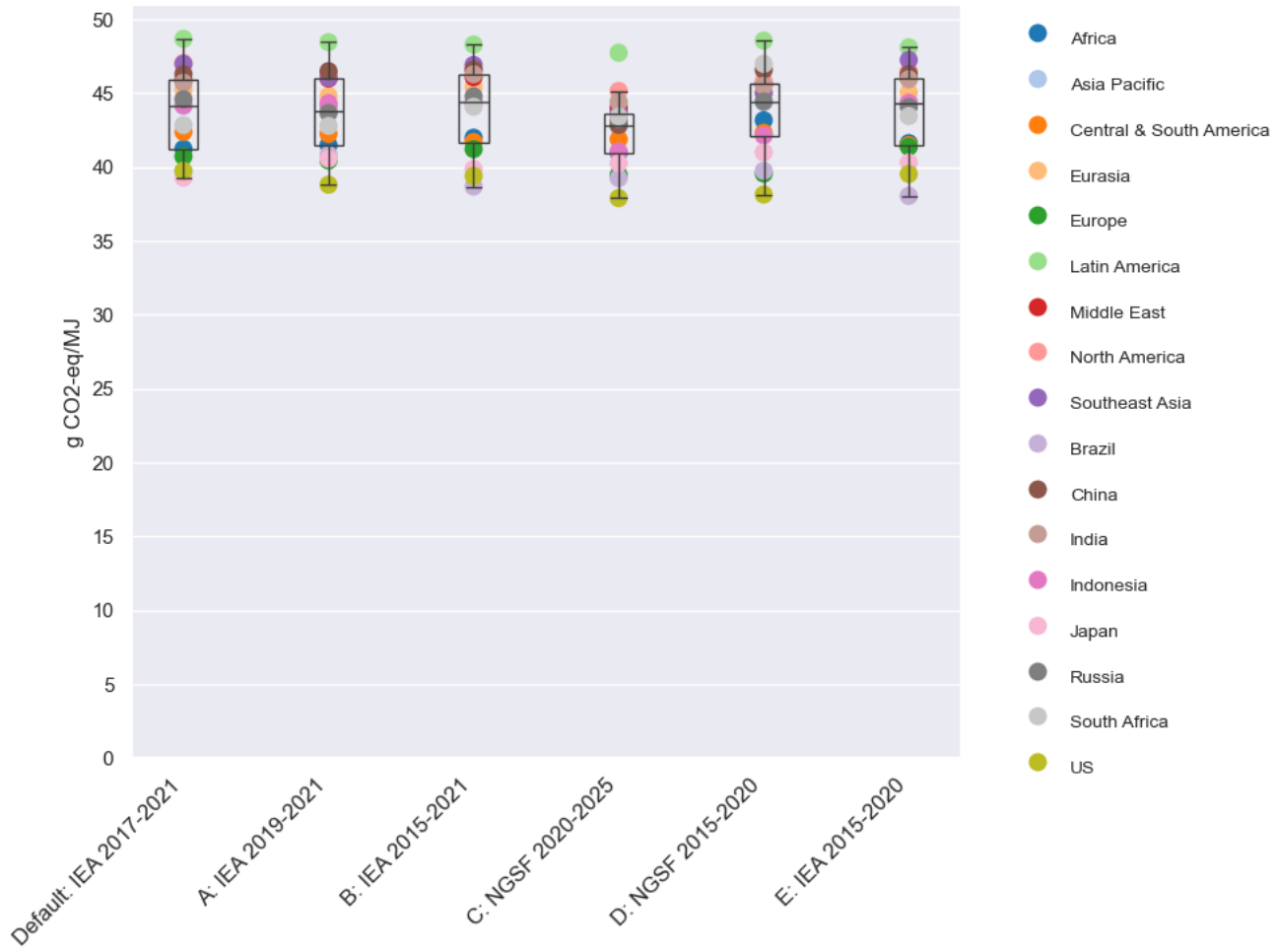

Figure 8.14: Change in **consequential** GWP100 results for ammonia (9.6% e/e VLSFO) with H2 from ATR with different data sources, time-series, and time-series internals for the marginal electricity mix.

When comparing the results on **Figure 8.14**, there is no large difference in the result ranges. Thus, for the overall result range, the choice of marginal mix does not have a significant influence on the global mean results.

However, the choice of marginal mix may have an influence for the individual regions, e.g., natural gas-based ammonia in South Africa has a GWP100 impact of 43 g CO_2-eq/MJ in the default scenario, while it is increased to 47 g CO_2-eq/MJ with marginal mix D. Yet, in general, most of the GWP100 results for the 17 regions change with 1-2 g CO_2-eq/MJ when the marginal electricity mix is changed.

8.13.1.2 Carbon intensity of grid electricity mix

The carbon intensity of the marginal electricity mix varies from 21-811 g CO_2-eq/kWh in the default scenario for the 17 regions. Therefore, the carbon intensity is a highly important parameter for the GWP100 results for ammonia with H_2 from ATR with CCS. Thus, the GWP100 results are presented in **Figure 8.15** with a carbon intensity of 64.7 and 8 g CO_2-eq/kWh for the marginal electricity.

The 8 g CO_2-eq/kWh corresponds to electricity from wind power in Norway, while 64.7 g CO_2-eq/kWh corresponds to the maximum carbon intensity of grid electricity according to the supplementing delegated regulation 2023/1185 to RED II (Hydrogen Europe, 2023). A carbon intensity of 811 g CO_2-eq/kWh is not tested, since the natural gas-based ammonia already has a high GWP100 impact, thus, this sensitivity analysis tests,

how much the carbon footprint of ammonia with H_2 from ATR with CCS can be lowered with a lower carbon intensity of the grid electricity.

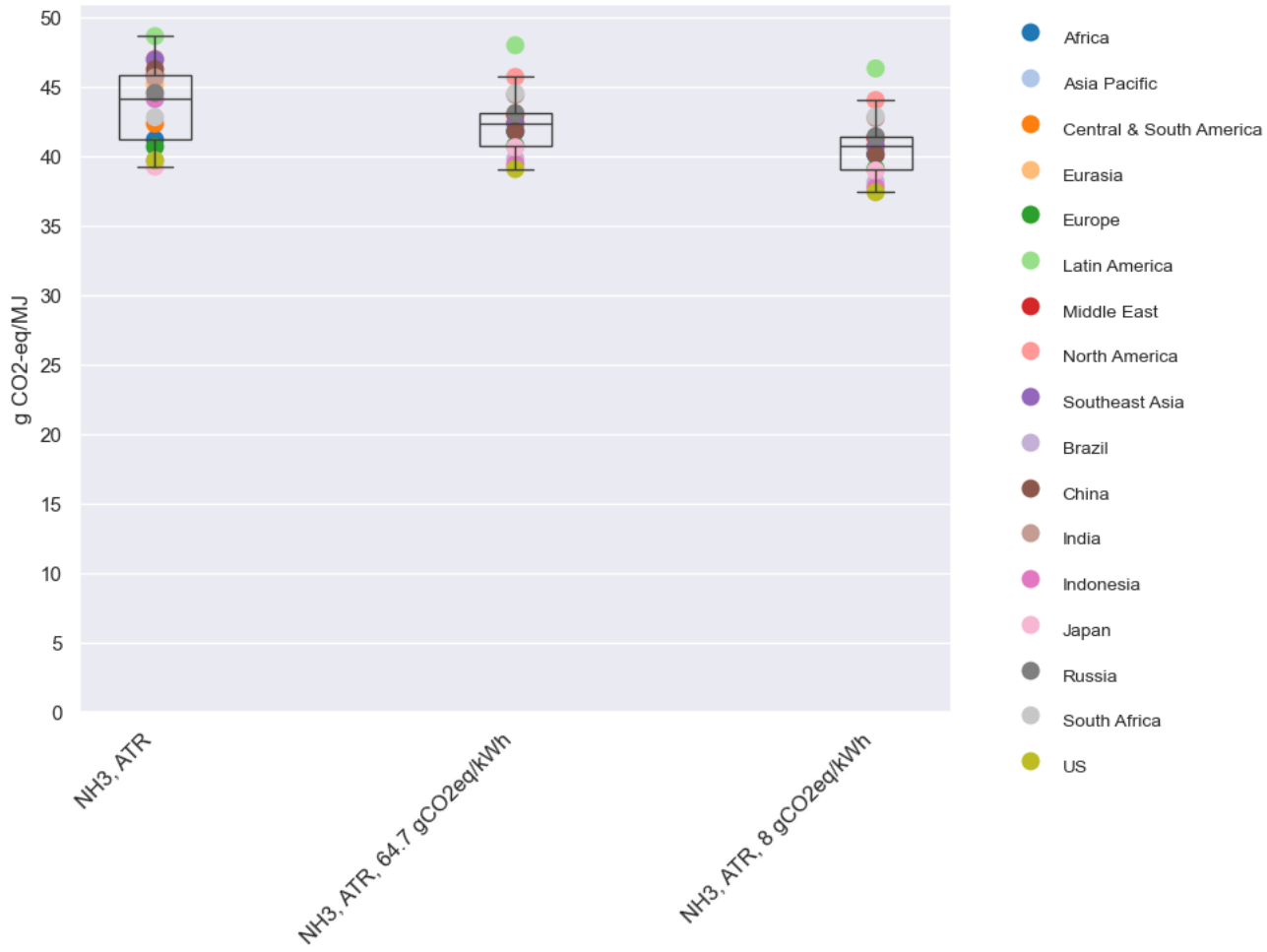

Figure 8.15: Change in **consequential** GWP100 results for ammonia (9.6% e/e VLSFO) with H_2 from ATR where the carbon intensity of grid electricity is varied.

Figure 8.15 shows that a carbon intensity of 64.7 g CO_2-eq/kWh for the grid electricity does not reduce the GWP100 result range notably. Yet, the GWP100 results for some regions – e.g., Japan and South Africa - are increased, the results for Europe, Brazil, and Central & South America do not change, while the results for the remaining regions are lowered.

Note that a carbon intensity of 8 g CO_2-eq/kWh for grid electricity reduces the GWP100 result range from 40-50 to 38-48 g CO_2-eq/MJ. This shows that the input of natural gas has a higher influence on the GWP100 results than the grid electricity.

8.13.2 Hydrogen production technology

8.13.2.1 Methane slip from natural gas extraction

The slip of methane from natural gas extraction is an important parameter for the impact from natural gas-based ammonia, especially because the methane slip rate can vary. According to Schneising et al. (2020), the bottom-up estimates of methane emissions are approximately 1%, while measurements from facilities range from 0.89-4%. Note that the findings by Schneising et al. (2020) are based on the US, and that methane slip

from natural gas extraction vary from country to country in EXIOBASE (see **section 4.2**). Nevertheless, since Schneising et al. (2020) finds that the methane emissions are estimated to approximately 1% but can be up to 4% according to measurements, a factor four is applied for all countries in EXIOBASE in order to assess this parameter's influence on the LCIA results.

The relative percentage change in **Table 8.4** shows that the increased slip of methane changes the results for GWP100 and respiratory organics with 40% and 9%, respectively. This is because methane emissions influence both impact categories since methane is both an important GHG while it also has indirect effects on human health. **Figure 8.16** illustrates the change in GWP100 results with the increased methane slip.

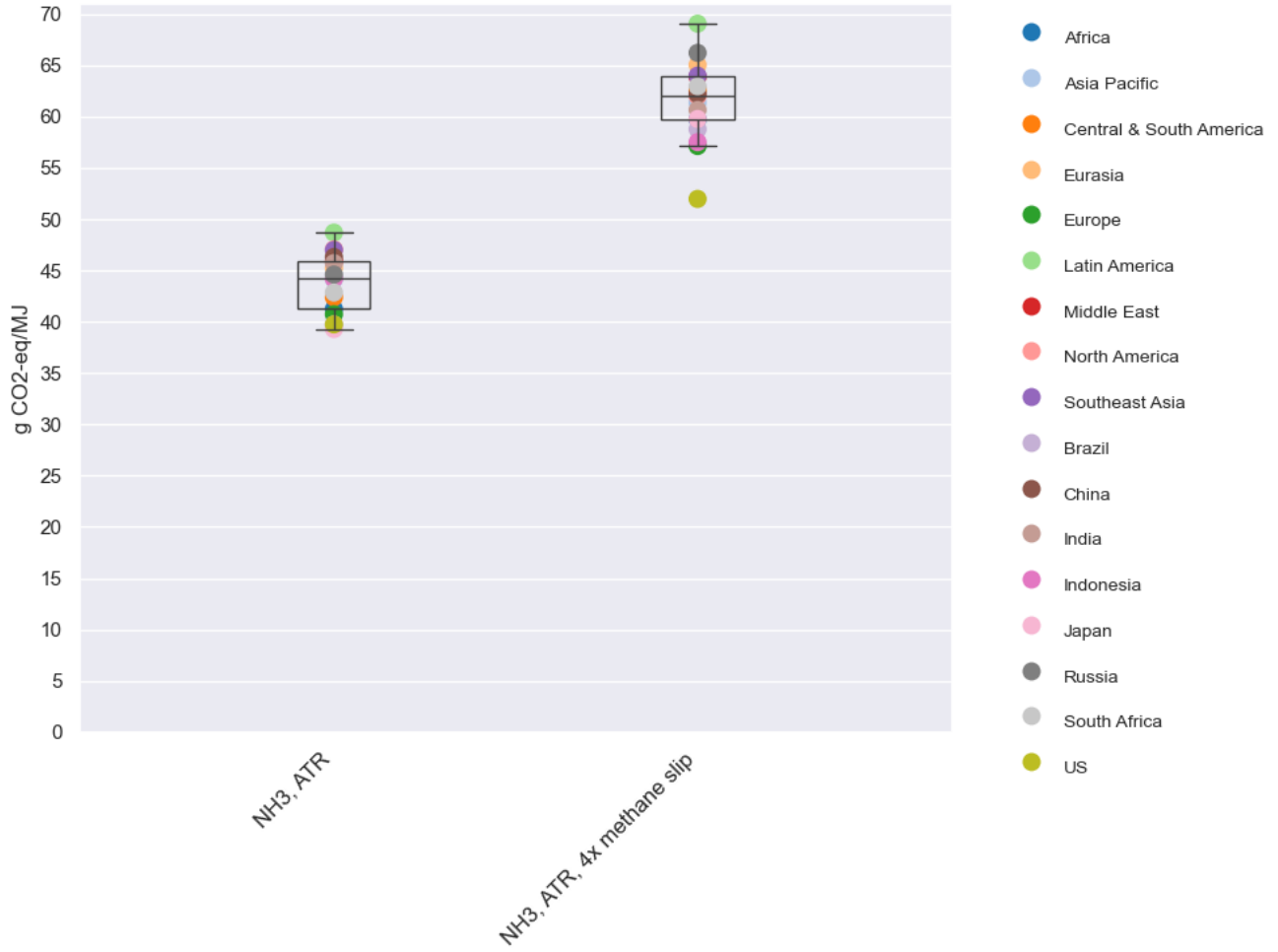

Figure 8.16: Change in **consequential** GWP100 results for ammonia (9.6% e/e VLSFO) with H_2 from ATR with increased methane slip from natural gas extraction.

Figure 8.16 illustrates the importance of limiting the slip of methane from natural gas extraction, since the GWP100 result range is increased from 40-50 g CO_2-eq/MJ to approximately 52-69 g CO_2-eq/MJ. Specifically, the slip of methane increases the GWP100 result with over 20 g CO_2-eq/MJ for natural gas-based ammonia in Russia and Japan, while the change in GWP100 result is only 12 g CO_2-eq/MJ for the US. To compare, the global mean change is 18 g CO_2-eq/MJ.

8.13.2.2 Methane slip in foreground system for natural gas-based ammonia

For ammonia based on H_2 from ATR with CCS, the default scenario includes a 0.3% slip of methane from the ATR process. This is based on the same assumption as for the other gases within the product system, since it is

one of the lower values presented in literature. Yet, the literature also suggests substantially higher leakage rates, up to 5% (Muñoz, 2023), thus, this upper value is applied for this sensitivity analysis. Note that when the slip from ATR is increased, it is done for both the ATR process for natural gas-based ammonia and for VLSFO. The impact of increased methane from ATR to VLSFO alone is tested in **section 8.14.3**.

The relative percentage change in **Table 8.4** shows that the increased slip of methane from ATR changes the results for GWP100, respiratory organics, and photochemical ozone, vegetation, with 107%, 25%, and 14%, respectively. Just as in **section 8.13.2.1**, this is because methane emissions influence all three impact categories since methane is both an important GHG while it also has indirect effects on human health. The change in GWP100 results for this sensitivity analysis is presented in **Figure 8.17**.

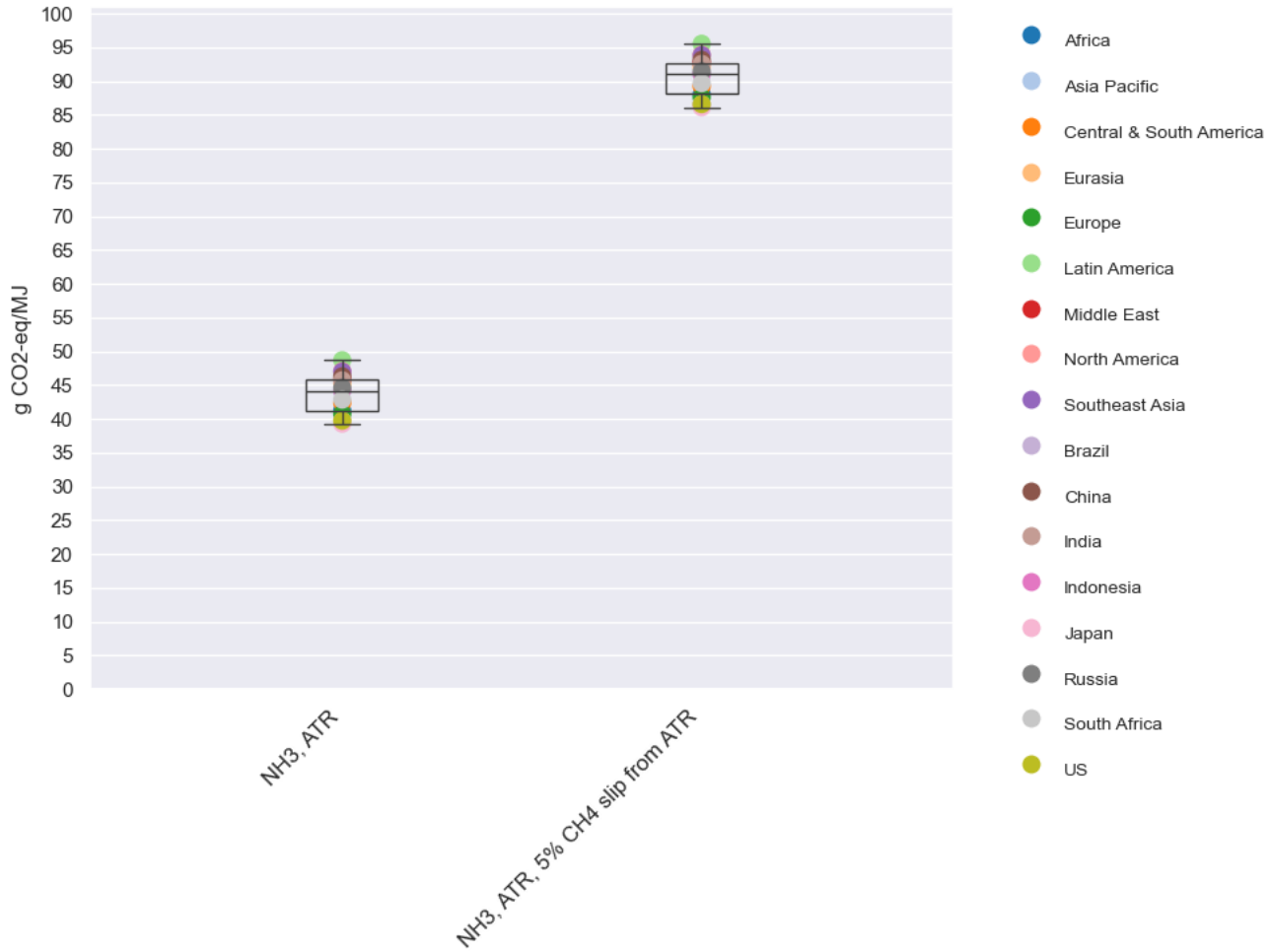

Figure 8.17: Change in **consequential** GWP100 results for ammonia (9.6% e/e VLSFO) with H_2 from ATR with increased methane slip from the ATR process for natural gas-based ammonia and from the ATR process used for production of the pilot fuel (VLSFO).

Figure 8.17 illustrates the importance of limiting the slip of methane from the ATR process, since the GWP100 result range for natural gas-based ammonia is increased from 40-50 g CO_2-eq/MJ to approximately 86-96 g CO_2-eq/MJ. Thus, the additional slip of methane from the ATR process increases the GWP100 results for all 17 regions with around 46 g CO_2-eq/MJ. The change is significant, because the input of 171 GJ/t H_2 has a slip of 0.01 t methane per t H_2 with the default slip (see **Table 5.4**), while this is increased to 0.17 t methane per t H_2 with a 5% slip.

8.13.2.3 Natural gas input to autothermal reforming

According to an industrial expert, the natural gas input to ATR can be up to 181 GJ/t H_2. Therefore, this upper value is applied for the sensitivity analysis. Yet, as shown in **Table 8.4**, applying the 181 GJ/t H_2 for the ATR process only results in relative percentage changes of 0.1-9%, with the largest percentage changes being 9% and 6% for nature occupation and GWP100, respectively (see the change in GWP100 results on **Figure 8.18**). Thus, applying the upper value for the natural gas input to ATR does not have a large effect on the LCIA results for natural gas-based ammonia.

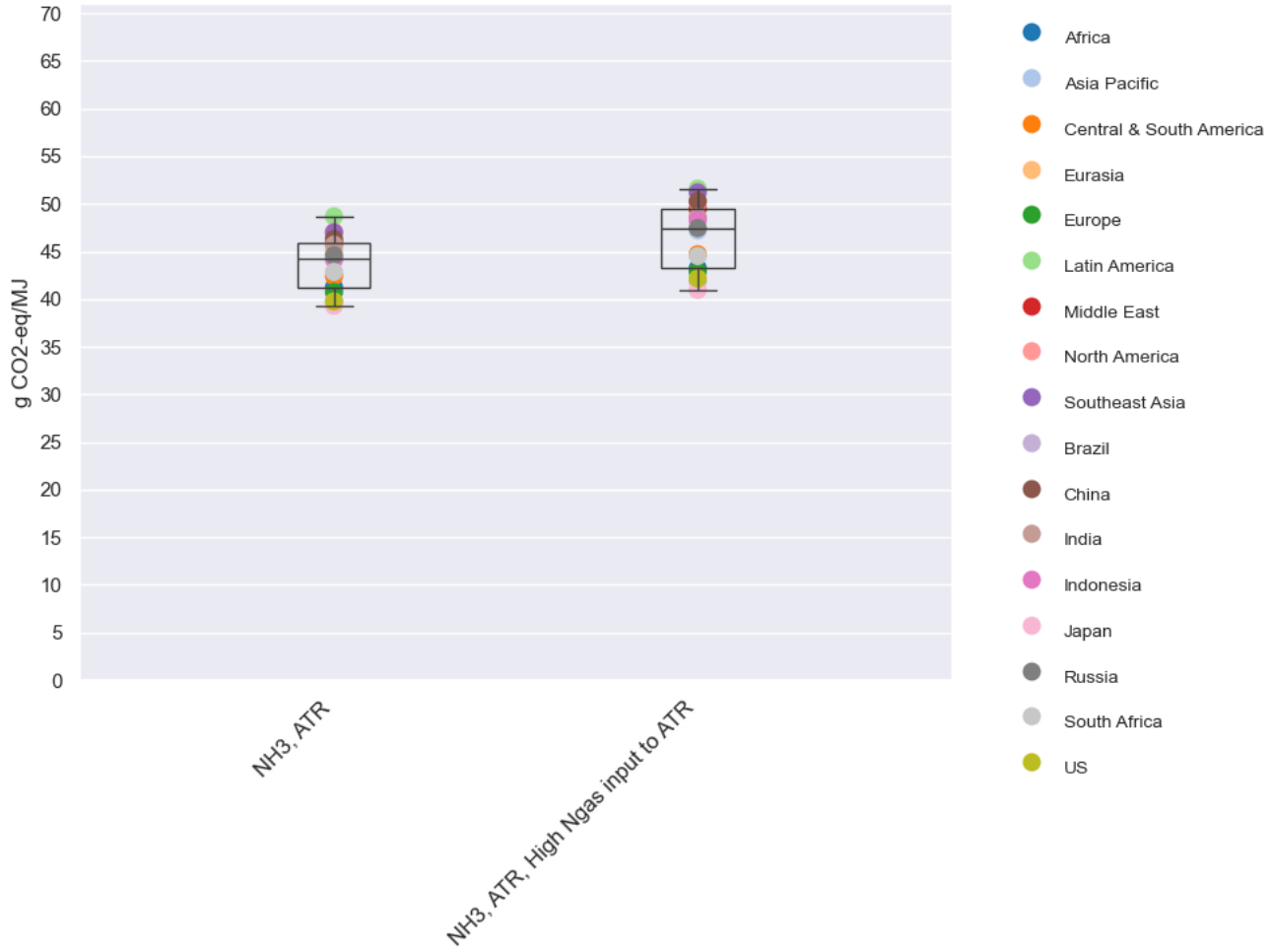

Figure 8.18: Change in **consequential** GWP100 results for ammonia (9.6% e/e VLSFO) with H_2 from ATR with an input of 181 GJ/H_2 to the ATR process.

8.13.2.4 Oxygen input to autothermal reforming

The ATR process requires O_2 which - according to an industrial expert - stems both from the steam produced from the water input to ATR along with the O_2 captured at the ASU. Nevertheless, in **section 5.1.1.2**, it was determined that the O_2 requirement from the ATR process could be supplied while N_2 is the determining product from the ASU. Yet, this contradicts an industrial expert's statement, stressing that the demand for O_2 from the ATR process results in excess N_2. Thus, this sensitivity analysis includes a scenario with O_2 as the determining product for the ASU.

Nevertheless, as seen from **Table 8.4**, changing the determining product of the ASU results in relative percentage changes of 0.02% or lower. Thus, since the changes in results are minor, a graphic visualisation is not presented for this sensitivity analysis.

8.13.2.5 Hydrogen production technology: steam methane reforming

ATR is applied as the H_2 production technology for the default scenario for natural gas-based ammonia since project partners argue that SMR cannot currently be considered a realistic option for producing ammonia for shipping. This is because it would be very difficult to produce ammonia with a low enough carbon footprint to meet decarbonization targets, e.g., from RED II.

Nevertheless, since SMR may also be applied, the sensitivity analysis assesses how choosing SMR as the H_2 production technology will impact the results. The LCI data from SMR in **Table 8.7** obtained from Spath & Mann (2001) is applied for this sensitivity analysis along with a capture rate of 60%, an energy requirement of 0.13 kWh/kg captured CO_2, and a yearly CO_2 slip from storage of 0.023%. The 60% capture rate is based on a statement from an industrial expert, which estimate that SMR typically has a capture rate of 60-70% which result in an additional energy requirement of 1.5%. Thus, the LCI data for CCS for SMR is based hereon.

Table 8.7: LCI summary for H_2 produced from steam methane reforming (SMR) for the **consequential** model.

Flow	Unit	H_2 production, SMR	Link to:
Output: reference flow			
Hydrogen (H_2)	t	1	Reference flow
Inputs:			
Natural gas (CH_4), as feedstock	GJ	144.2	See **section 4.2**
Natural gas (CH_4), as fuel	GJ	15.8	Natural gas incl. combustion emissions {region}, see **section 4.4**
Water (H_2O)	t	6.01	See **section 4.6**
Electricity	MWh	0.32	See **section 4.1**
Emissions			
Carbon dioxide (CO_2)	t	8.881	Emissions to air
Hydrogen (H_2) slip	t	0.003	
Methane (CH_4) slip	t	0.003	

The relative percentage change in **Table 8.4** shows that the differences between ATR and SMR H_2 production primarily changes the GWP100 and nature occupation. Note that the GWP100 results are increased with 94% when choosing SMR instead of ATR, because less CO_2 is captured. The change in GWP100 results is depicted on **Figure 8.19.**

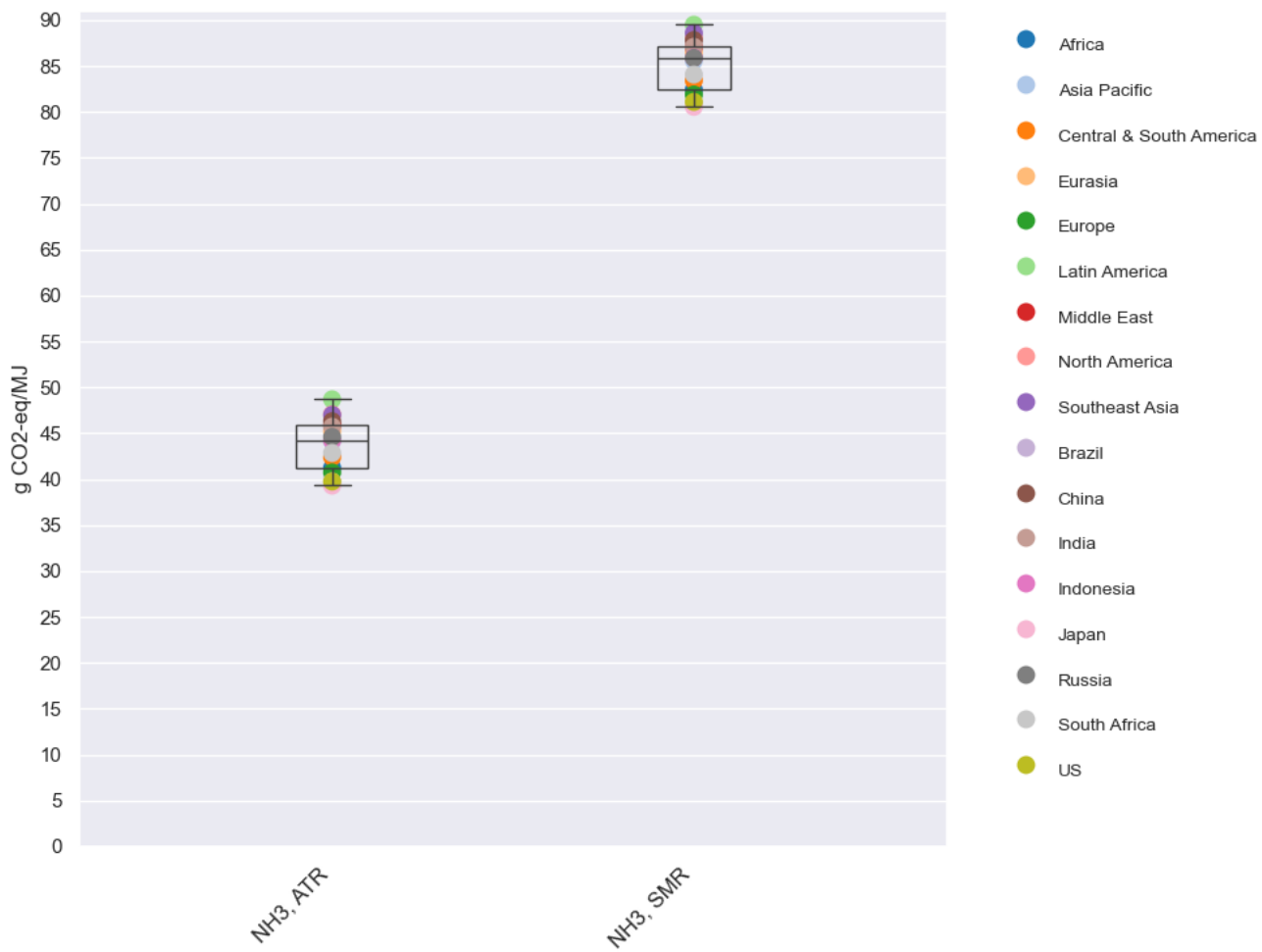

Figure 8.19: Comparison of **consequential** GWP100 results for natural gas-based ammonia (9.6% e/e VLSFO) with H_2 from ATR and SMR.

8.13.2.6 Carbon capture rate

For ammonia based on H_2 from ATR with CCS, the default scenario includes a carbon capture rate of 90%. Nevertheless, an industrial expert has stated that a capture rate of 95% is also possible, though it will require additional CAPEX and a larger energy input. On the other hand, Robertson & Mousavian (2022) has found that though carbon capture plants were designed to have a capture rate of 90%, in reality the average capture rate was only 50%. Therefore, the sensitivity analysis includes a capture rate of 95% and 50%. This impacts the GWP100 results, which are presented in **Figure 8.20**.

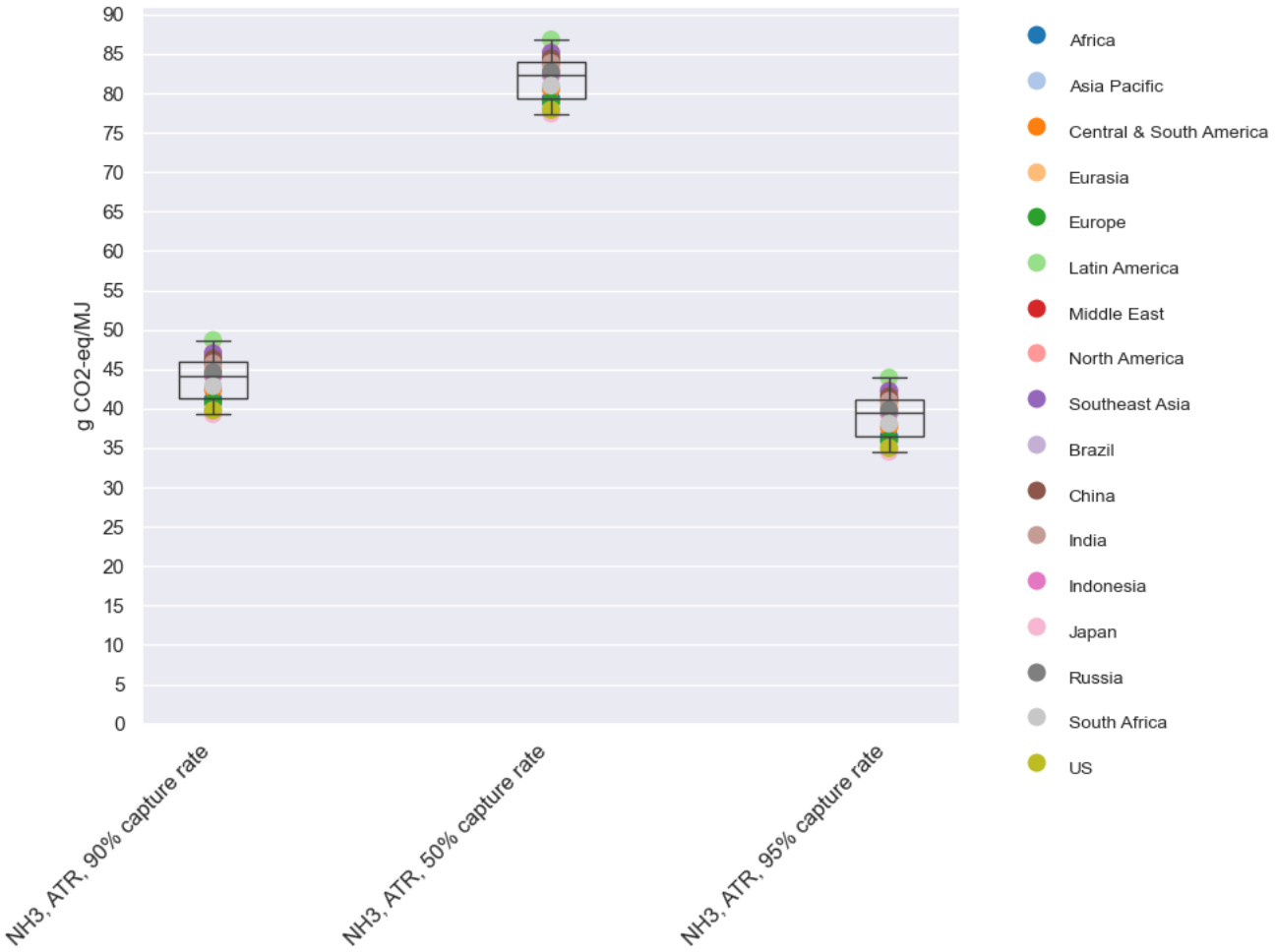

Figure 8.20: Change in **consequential** GWP100 results for ammonia (9.6% e/e VLSFO) with H_2 from ATR where the carbon capture rate is varied.

Table 8.4 shows that a carbon capture rate of 95% will lower the GWP100 results with 11%, while a capture rate of 50% increases the GWP100 results with 87%. Note that the energy input for the 95% capture rate is estimated based on a linear association, which may underestimate the energy requirement based on the project partner's statement above. Moreover, the additional need for CAPEX with a capture rate of 95% is not taken into account. Thus, the change in the GWP100 result for natural gas-based ammonia with 95% capture rate may be lower than 11%.

Moreover, **Figure 8.20** illustrates how a 50% carbon capture rate increases the results for natural gas-based ammonia from 40-50 g CO_2-eq/MJ to 77-87 g CO_2-eq/MJ, which is close to the default GWP100 result range for VLSFO of 99-122 g CO_2-eq/MJ. Thus, the carbon capture rate is one of the key parameters that influences the GWP100 results for natural gas-based ammonia.

8.13.2.7 Energy for carbon capture and storage

The energy requirement for CCS is important, as a high energy input may counteract the effect of capturing and storing CO_2. A sanity check of the energy data from a project partner was conducted in **section 5.1.1.2.1**, comparing it with data from Oni et al. (2022) and Kähler et al. (2022). This showed that the energy input could vary from 0.40 GJ/t CO_2 to 3.46 GJ/t CO_2 depending on the point source of the CO_2. Thus, the sensitivity analysis assesses how much the LCIA results for ammonia with H_2 from ATR with CCS change if the energy requirement for CCS is a factor 10 higher.

The relative percentage changes in **Table 8.4** show that the energy requirement for CCS primarily influences the GWP100 and nature occupation results, as they change with 48% and 40%, respectively. This is due to the additional input of natural gas and grid electricity to the CCS process. The change in GWP100 results is depicted on **Figure 8.21.**

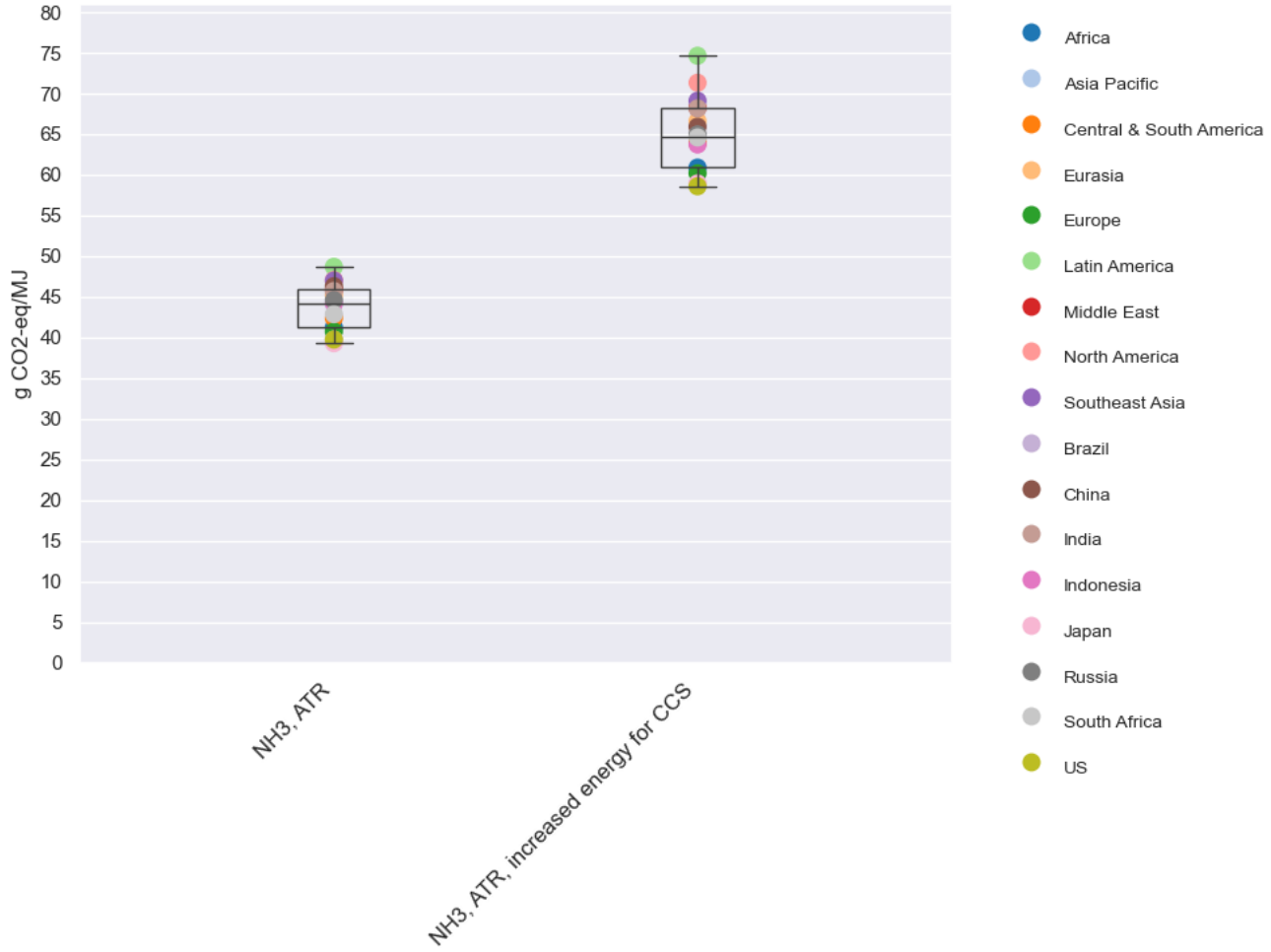

Figure 8.21: Change in **consequential** GWP100 results for ammonia (9.6% e/e VLSFO) with H_2 from ATR where the energy requirement for CCS is increased.

Figure 8.21 illustrates, how a higher energy requirement for CCS increases the geographical differences for ammonia with H_2 from ATR with CCS. This is caused by the difference in carbon intensities for natural gas and grid electricity between the 17 regions. The figure also shows that the higher energy requirement influences the results more for some regions than others. This is for example the case for Latin America, as the result for this region increases with 26 g CO_2-eq/MJ, while the change in result for the US is 19 g CO_2-eq/MJ.

Note that since 99% of the energy for the CCS process comes from natural gas (see **section 5.1.1.2.1**), it is the energy input to CCS along with the carbon intensity of the natural gas that are of high importance for the GWP100 results for natural gas-based ammonia.

8.13.2.8 Transport distance to carbon storage

The transport distance to carbon storage is 200 km based on Volkart et al. (2013). Nevertheless, as this distance is considered low by some project partners, this parameter is included in the sensitivity analysis. Thus, it is tested, how much the LCIA results change, if the transport distance to carbon storage is multiplied with a factor 10.

The relative percentage changes in **Table 8.4** show that the additional transport distance to carbon storage primarily influences the nature occupation results, as they change with 17%. The change in GWP100 result is 7%. The change in results is affected by the additional materials to a longer pipeline and by the additional grid electricity used for the pipeline transport. The change in GWP100 results is depicted on **Figure 8.22.**

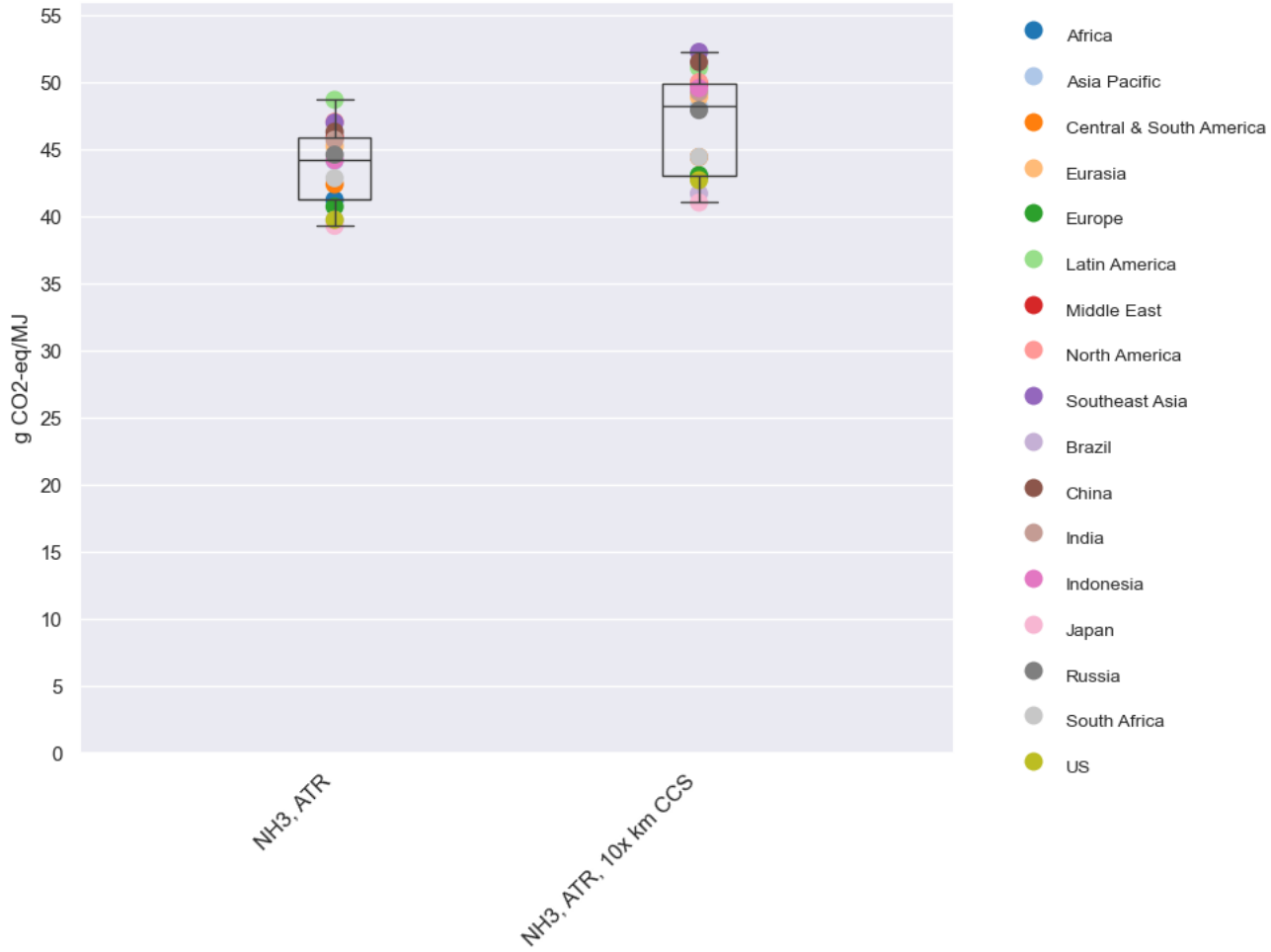

Figure 8.22 Change in **consequential** GWP100 results for ammonia (9.6% e/e VLSFO) with H_2 from ATR with 2,000 km by pipeline to carbon storage.

8.13.2.9 CO_2 leakage from storage

For ammonia based on H_2 from ATR, the default scenario includes a 0.023% slip from CO_2 storage per year based on an average of the slip rates of CO_2 from Suh et al. (2023) and Captura (2022). Nevertheless, for the other gases within the product system, a slip of 0.3% per year is applied since it is one of the lower values presented in literature. Yet, the literature also suggests substantially higher leakage rates, up to 5% (Muñoz, 2023). Therefore, a yearly slip of 0.3% and 5% is tested in the sensitivity analysis in order to assess the importance of the CO_2 slip parameter on the GWP100 results.

The relative percentage change in **Table 8.4** shows that the GWP100 results for ammonia with H_2 from ATR with CCS change with 28% and 166%, when the yearly slip of CO_2 is increased to 0.3% and 5%, respectively. The change in GWP100 results is presented on **Figure 8.23.**

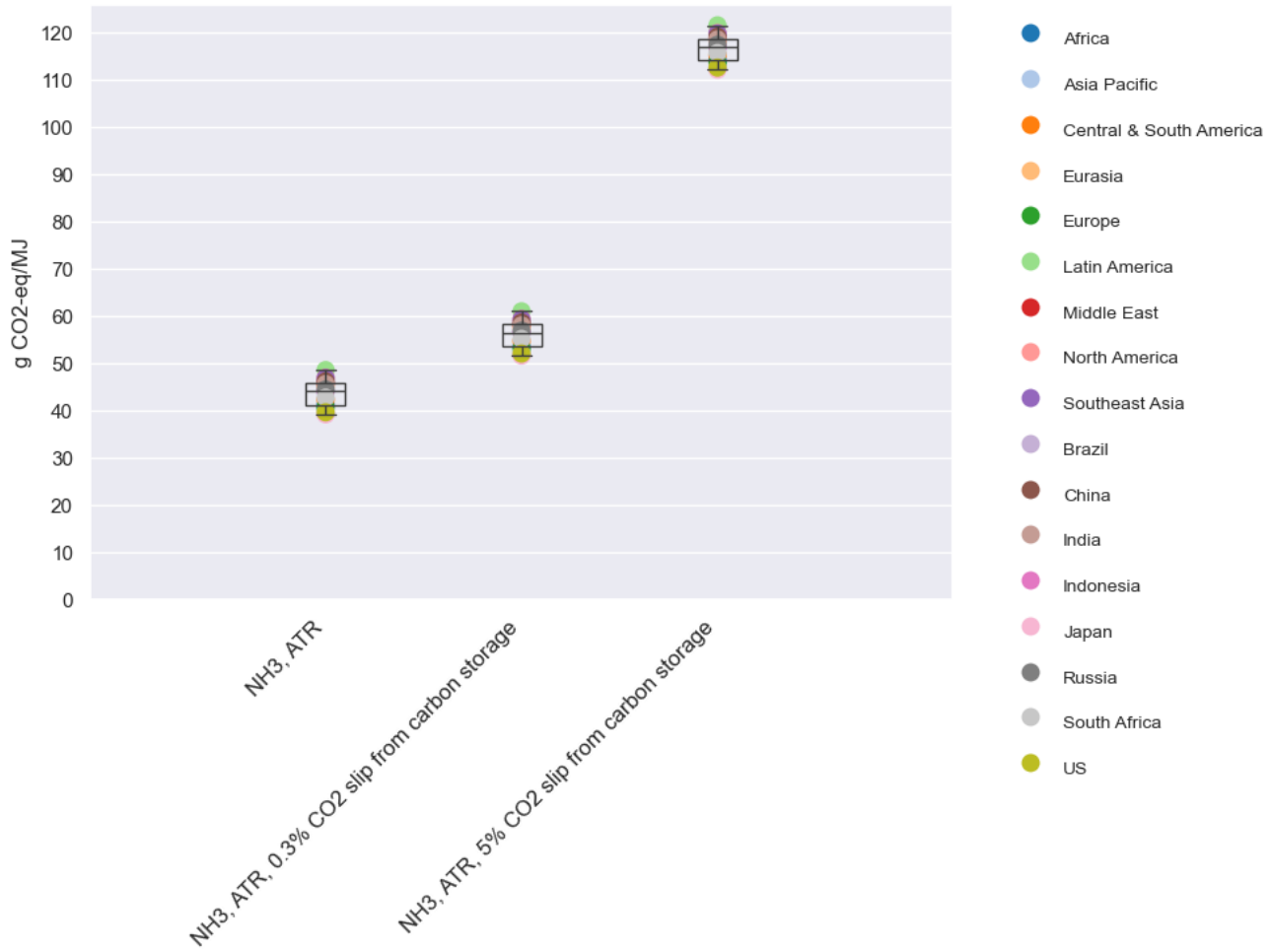

Figure 8.23: Change in **consequential** GWP100 results for ammonia (9.6% e/e VLSFO) with H_2 from ATR with a yearly CO_2 slip of 5% from carbon storage.

Figure 8.23 show that the result range for natural gas-based ammonia is increased from 40-50 g CO_2-eq/MJ to approximately 52-61 g CO_2-eq/MJ and 112-122 g CO_2-eq/MJ when the yearly slip of CO_2 is increased to 0.3% and 5%, respectively. Thus, a high slip of CO_2 from storage leads to a result range that is in the same magnitude as the default GWP100 result range for VLSFO of 99-122 g CO_2-eq/MJ. Thus, the slip of CO_2 from storage is of high importance and should – as other gas slips within the product system – be limited as much as possible.

8.14 Production of very low sulphur fuel oil

8.14.1 Carbon intensity of fuel oil as feedstock

The carbon intensity of the fuel oil used as feedstock for VLSFO is one of the most important factors for the GWP100 results for VLSFO. The carbon intensity of fuel oil ranges from 0.75 to 1.66 kg CO_2-eq/kg for the 17 regions in this LCA study, while the carbon intensity of fossil fuel is 0.71 kg CO_2-eq/kg according to RED II, when 77.29 g CO_2-eq/MJ stems from combustion and the lower heating value of VLSFO is 42.7 MJ/kg (Nielsen et al., 2018). Moreover, EC & COWI (2015) find that the carbon intensity of fuel oil can be as low as 0.43 kg CO_2-eq/kg. Therefore, the sensitivity analysis investigates how much the GWP100 results for VLSFO change, when the carbon intensity of fuel oil is lowered to 0.71 and 0.43 kg CO_2-eq/kg (see **Figure 8.24**).

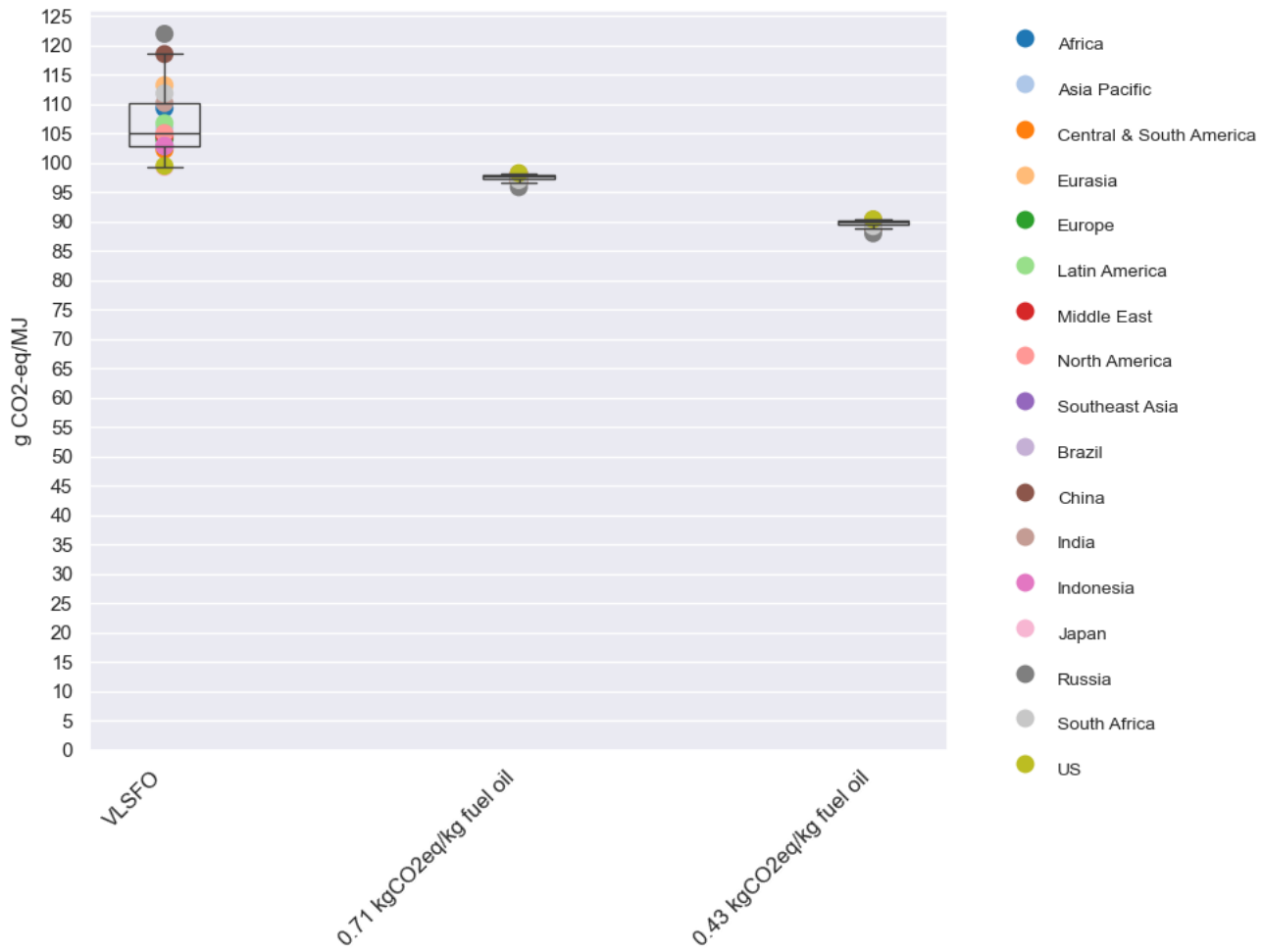

Figure 8.24: Change in **consequential** GWP100 results for VLSFO where the carbon intensity of fuel oil is varied.

Figure 8.24 illustrates the importance of the carbon intensity of the fuel oil for the GWP100 results of VLSFO. **Table 8.5** shows that the global mean GWP100 results are lowered with 9% and 16% with a carbon intensity of 0.71 ad 0.43 kg CO_2-eq/kg fuel oil, respectively. Note that the result for Russia changes the most, as the GWP100 results for this region has an impact of 122 g CO_2-eq/MJ in the default scenario, while it drops to 96 and 88 g CO_2-eq/MJ with a carbon intensity of 0.71 ad 0.43 kg CO_2-eq/kg fuel oil, respectively.

8.14.2 ATR hydrogen production with carbon capture

VLSFO is produced with H_2 from ATR without CCS. Nevertheless, the GWP100 results for VLSFO may be lowered if the CO_2 from the ATR process is captured. This is analysed with the LCI data from **Table 5.5.**

Based on **Table 8.5**, ATR with CCS does not change the LCIA results for any of the eight impact categories with more than 2%. This is because the H_2 production is not a significant contributor to the overall results compared to the fuel oil used as feedstock or the combustion emissions (see **section 6.3**). The largest relative percentage change is seen for GWP100, which is also visualised on **Figure 8.25.**

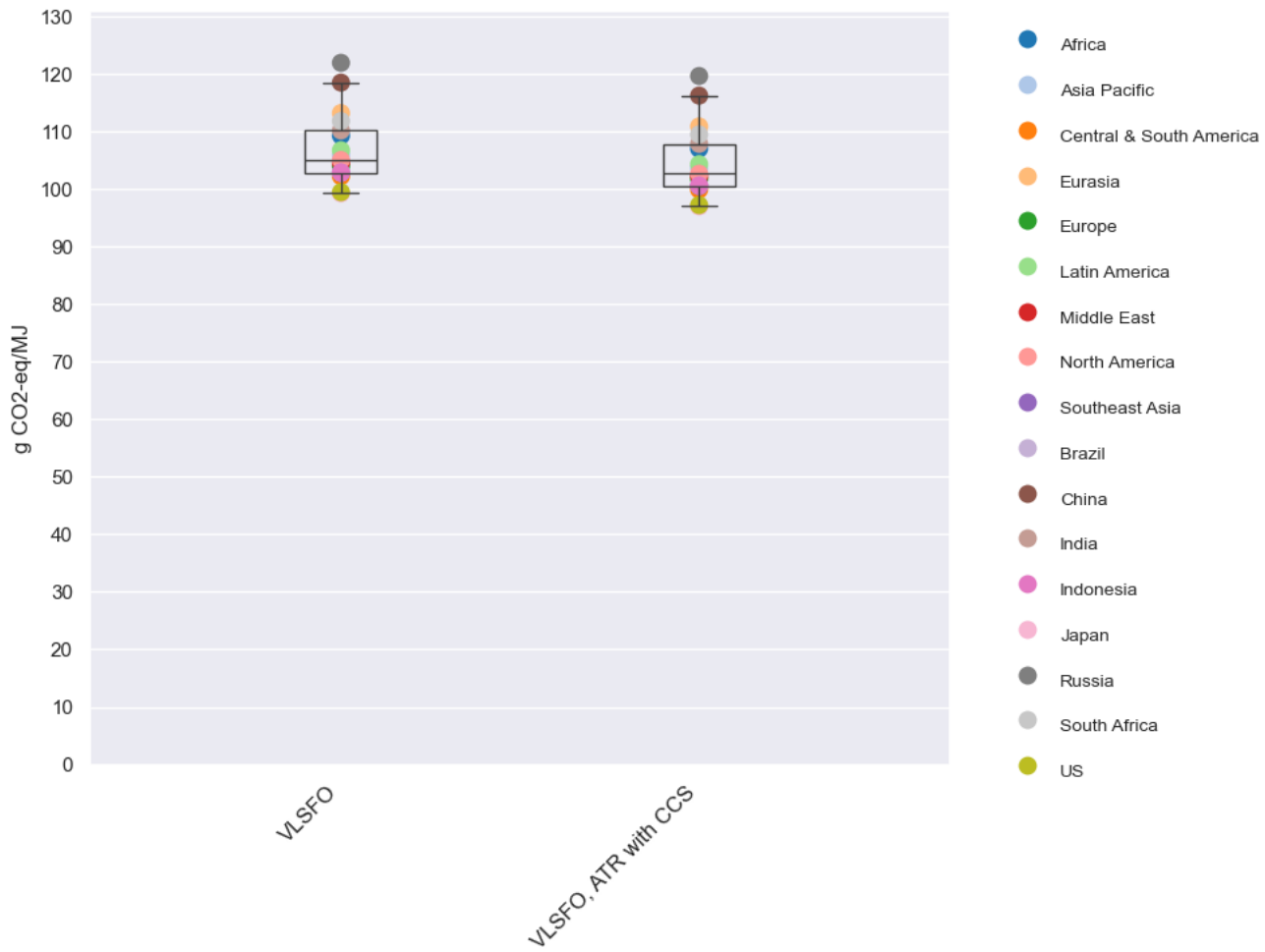

Figure 8.25: Change in **consequential** GWP100 results for VLSFO when the CO_2 from the ATR process is sent to CCS with a 60% capture rate.

8.14.3 Methane slip from autothermal reforming

For the ATR process, the default scenario includes a 0.3% slip of methane. This is based on the same assumption as for the other gases within the product system, since it is one of the lower values presented in literature. Yet, the literature also suggests substantially higher leakage rates, up to 5% (Muñoz, 2023). The change in GWP100 results for this sensitivity analysis is presented in **Figure 8.26.**

Based on **Table 8.5**, the increased slip of methane from ATR does not change the LCIA results for any of the eight impact categories with more than 1%. This is because the input of H_2 is 0.009 t per t VLSFO, thus, the production of H_2 from ATR and thereby the slip of methane from ATR is minor compared to the input of 1.14 t fuel oil per t VLSFO (see **Table 5.11**). Thus, the slip of methane does not have a significant influence on the results for VLSFO for the functional unit of 1 MJ, nevertheless, as methane is a strong GHG, it is important to limit leakage of the gas to the atmosphere.

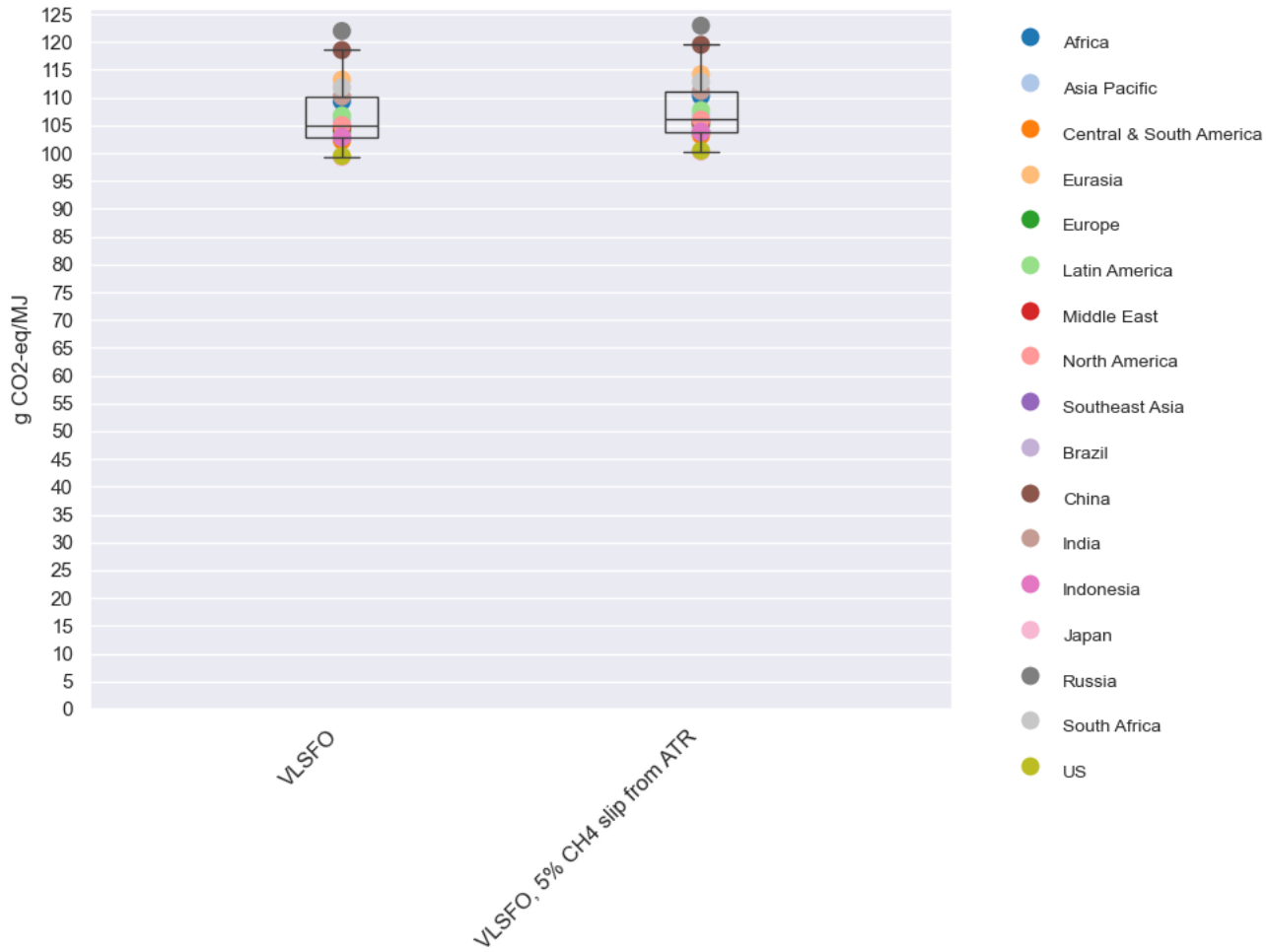

Figure 8.26: Change in **consequential** GWP100 results for VLSFO with increased methane slip from the ATR process.

9 Sensitivity analysis: attributional model

The sensitivity analysis for the attributional LCA model only includes three parameters: Desalination, the carbon intensity of the renewable electricity, and the grid electricity (see **Table 9.1**). This is because the attributional results are highly influenced by the carbon intensity of the electricity sources, which are modelled very differently than in the consequential model. Moreover, as the other parameters in **Table 8.1** will change the attributional results in a similar magnitude as the consequential results, the remaining parameters from **Table 8.1** are not displayed or discussed in this chapter.

Table 9.1: Overview of parameters in the sensitivity analysis for the **attributional model** and the default values used to calculate the LCIA results in **chapter 7**.

Parameter:	**Unit**	**Both ammonia pathways with 9.6% e/e VLSFO**	
		Default scenario	**Sensitivity**
Desalination (**section 9.1**)	-	0% desalination 100% ground/surface water	100% desalination 0% ground/surface water
Parameter:	**Unit**	**Ammonia with H_2 from electrolysis and 9.6% e/e VLSFO**	
		Default scenario	**Sensitivity**
Carbon intensity of renewable electricity (**section 9.2.2**)	g CO_2-eq / kWh	0	**High:** 100 **Low:** 5
Parameter:	**Unit**	**Ammonia with H_2 from ATR with CCS and 9.6% e/e VLSFO**	
		Default scenario	**Sensitivity**
Carbon intensity of electricity grid mix (**section 9.2.1**)	g CO_2-eq / kWh	145-1,346 (depending on region)	**Medium:** 64.7 (RFNBO limit) **Low:** 8

The relative percentage change for each sensitivity analysis is presented in **Table 9.2**, showing that the attributional results change with more than 10% when the carbon intensity of both renewable and grid electricity is changed. **Section 9.1** and **9.2** describe the analysis in more depth and present the changes visually.

Table 9.2: The relative percentage change for the global mean **attributional** GWP100 results based on the sensitivity parameters presented in **Table 9.1**. The orange colour code indicates if a change is ±10%.

Global warming (GWP100)	**Water technology**	**Carbon intensity of renewable electricity**		**Carbon intensity of grid electricity**	
Original value / parameter	Ground / surface water	0 g CO_2-eq/kWh renewable electricity		145-1,346 g CO_2-eq /kWh grid electricity (depending on region)	
Tested value / parameter	Desalination	5 g CO_2-eq/kWh renewable electricity	100 g CO_2-eq/kWh renewable electricity	64.7 g CO_2-eq/kWh grid electricity	8 g CO_2-eq/kWh grid electricity
Change in results					
Ammonia with H_2 from electrolysis (solar) and 9.6% e/e VLSFO	-1%	15%	291%		
Ammonia with H_2 from electrolysis (wind) and 9.6% e/e VLSFO	-1%	15%	291%		
Ammonia with H_2 from ATR with CCS and 9.6% e/e VLSFO	0.2%			-10%	-14%

Additionally, in **section 9.3**, a semi-quantitative analysis is presented for ammonia with 9.6% e/e bio-based pilot fuel, assuming a 65% reduction compared to the fossil fuel comparator in accordance with RED II.

9.1 Desalination

The LCA study applies surface/ground water as the default scenario. However, as the geographical scope of the study is global, some countries and regions will likely rely on desalination to some extent. Therefore, the attributional GWP100 results are calculated with desalinated water in the sensitivity analysis. Nevertheless, as the change is minor (less than 1%), the change in results is not visualised in this section.

When using desalinated water for ammonia with H_2 from electrolysis, the GWP100 results go down with 1% (see **Table 9.2**). This is because renewable electricity has a carbon footprint of zero in the attributional model, and use of desalinated water therefore has an impact of zero, since there are no other inputs besides the electricity. Thus, the input of ground/surface water has a higher impact since it is linked to activities from the ecoinvent, which has not been modified with a renewable electricity carbon footprint of zero and include other inputs as well.

Note that the GWP100 results for natural gas-based ammonia go up by 0.2% (see **Table 9.2**). This is because the grid electricity mix does have an impact in the attributional model. Nevertheless, a change of 0.2% for the global mean GWP100 result is insignificant.

9.2 Electricity

9.2.1 Carbon intensity of grid electricity mix

The carbon intensity of the average electricity mix varies from 40-374 g CO_2-eq/kWh in the default scenario. Therefore, the carbon intensity is an important parameter for the attributional GWP100 results for ammonia with H_2 from ATR with CCS. The sensitivity analysis investigates the change in GWP100 results by using the following carbon intensity values: 64.7 and 8 g CO_2-eq/kWh. The 8 g CO_2-eq/kWh is assumed to be representable for renewable electricity, when the rule regarding carbon footprint of zero for renewable electricity from RED II is disregarded, while 64.7 g CO_2-eq/kWh corresponds to the maximum carbon intensity of grid electricity according to the supplementing delegated regulation 2023/1185 (Hydrogen Europe, 2023). The change in the GWP100 results based on the different carbon intensities are shown in **Figure 9.1.**

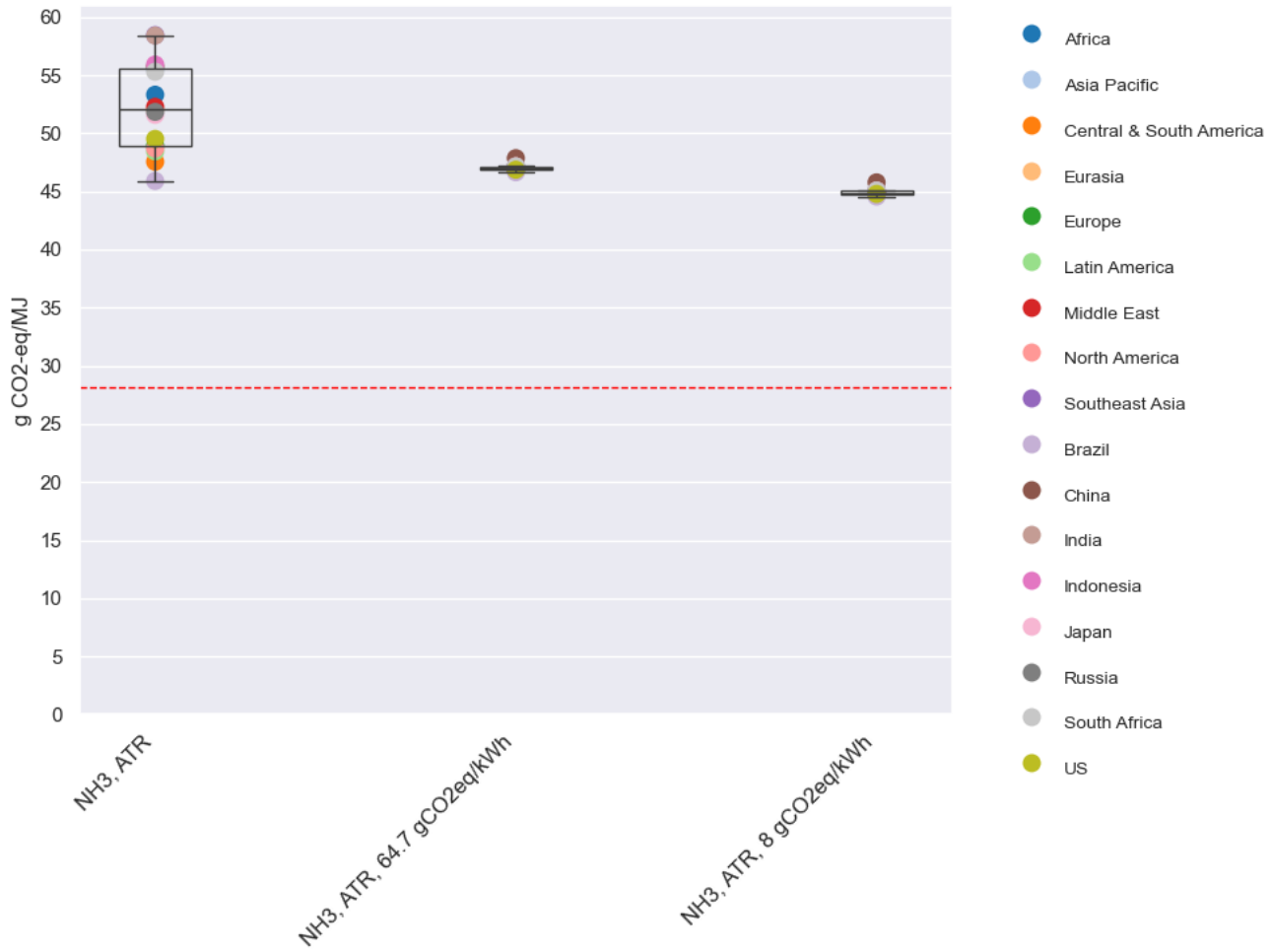

Figure 9.1: Change in **attributional** GWP100 results for ammonia (9.6% e/e VLSFO) with H_2 from ATR when the carbon intensity of grid electricity is varied. The dotted, red line indicates the RED II target of 28.2 g CO_2-eq/MJ.

Figure 9.1 shows that the main difference between the 17 regions is the carbon intensity of the grid electricity, since the results are the almost the same for all 17 regions, when the carbon intensity for each region is set to the same value.

When the carbon intensity is set to 64.7 and 8 g CO_2-eq/kWh, the GWP100 results change to approximately 47 and 46 g CO_2-eq/MJ, respectively. This is a change of -10% and -14% compared to the global mean default results, yet the sensitivity results are not far from the default results for Brazil and Central & South America, which are 46 and 48 g CO_2-eq/MJ, respectively. Note, there is not a large difference in GWP100 results when the carbon intensity of the grid electricity is lowered from 64.7 to 8 g CO_2-eq/kWh. This is because the main contributors to the GWP100 of ammonia with H_2 from ATR with CCS are natural gas extraction and the combustion emissions, thus, it is limited how much the carbon intensity of the grid electricity can lower the results.

9.2.2 Carbon intensity of renewable electricity

The carbon intensity of electricity from solar and wind is set to zero in the attributional model in accordance with the supplementing delegated regulation 2023/1185. Nevertheless, the production of wind turbines and solar panel is not without impact and the sensitivity analysis therefore includes a high and low value (100 and 5 g CO_2-eq/kWh) for the carbon intensity of the renewable energy in order to assess this parameter's influence

on the GWP100 results, when the rule regarding carbon footprint of zero for renewable electricity from RED II is disregarded (see **Figure 9.2**).

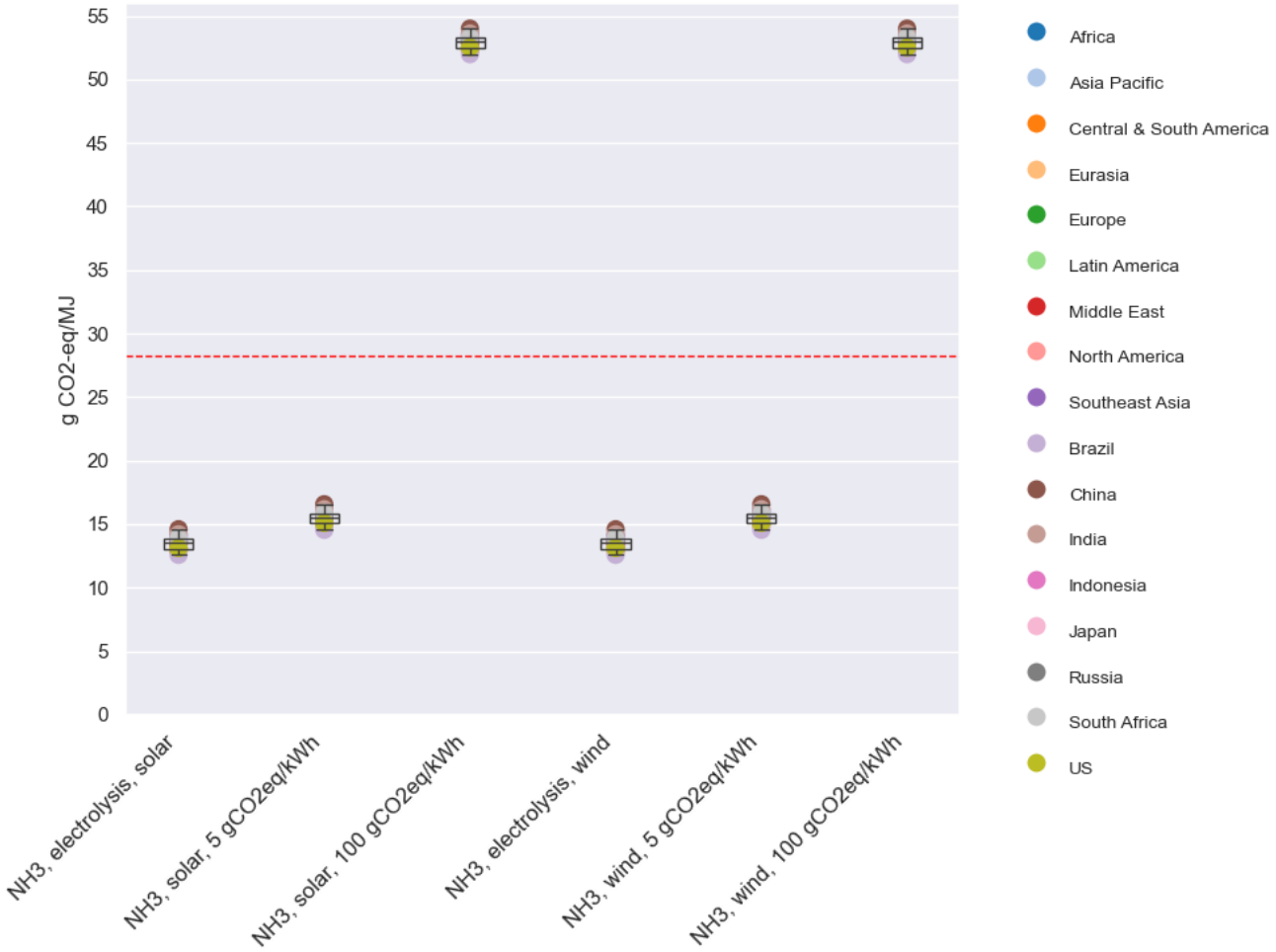

Figure 9.2: Change in **attributional** GWP100 results for ammonia (9.6% e/e VLSFO) with H_2 from electrolysis (both solar and wind-based) when the carbon intensity of renewable electricity is varied. In the default scenario, renewable electricity has a carbon footprint of zero. The dotted, red line indicates the RED II target of 28.2 g CO_2-eq/MJ.

As expected, **Figure 9.2** shows that the GWP100 results for ammonia with H_2 from electrolysis increase drastically, if the carbon intensity of renewable electricity is increased from zero to 100 g CO_2-eq/kWh. The results also increase when the carbon intensity of renewable electricity is increased from zero to 5 g CO_2-eq/kWh, nevertheless, it is worth noticing that with a carbon footprint of 5 g CO_2-eq/kWh for renewable electricity the results are still below the RED II target of 28.2 g CO_2-eq/kWh.

9.3 Bio-based pilot fuel

Through discussions with project partners, it has been argued that the pilot fuel for ammonia may consist of a bio-based alternative. Thus, this section presented a semi-quantitative analysis, estimating how the results for ammonia with 9.6% e/e pilot fuel will change if the pilot fuel was bio-based. As this LCA study does not include the modelling of bio-based fuels, a default value from RED II is applied, since RED II specifies that bio-based fuels must have a reduction of at least 65% compared to the WtW fossil fuel comparator of 94 g CO_2-eq/MJ. Therefore, it is assumed that the bio-based pilot fuel will have a carbon footprint of 32.9 g CO_2-eq/MJ from WtW.

The bio-based pilot fuel is assumed to emit the same amount of N_2O emissions from combustion as VLSFO. Yet, there is no impact from the CO_2 emissions from combustion of the bio-based pilot fuel, since biogenic CO_2 from combustion has a carbon footprint of zero according to the RED II guidelines (EP & EUCO, 2018). Therefore, the bio-based fuel is assumed to have a GWP100 impact of 1.52 g CO_2-eq/MJ from combustion. Thus, the majority of the impact of the bio-based fuel stems from its production.

Table 9.3 presents a contribution analysis for the semi-quantitative analysis for ammonia with a bio-based pilot fuel.

Table 9.3: Detailed GWP100 contribution analysis for ammonia with H_2 from electrolysis (based on either solar or wind) and ammonia with H_2 from ATR with CCS with **9.6% e/e bio-based pilot fuel** for the functional unit of 1 MJ for the **attributional model**. The contribution for the bio-based fuel is also presented per 1 MJ. Shades of red are used to highlight the highest values. Note that the results for the bio-based fuel is based on a 65% reduction compared to the WtW fossil fuel comparator of 94 g CO_2-eq/MJ from RED II.

Global mean	g CO_2-eq/MJ	Ammonia (9.6% e/e bio-based pilot fuel) with H_2 from electrolysis	Ammonia (9.6% e/e bio-based pilot fuel) with H_2 from electrolysis	Ammonia (9.6% e/e bio-based pilot fuel) with H_2 from ATR with CCS	Bio-based pilot fuel
Activity	**Input / Flow**	**Solar**	**Wind**		
N_2 production, for NH_3	Electricity, renewable	0	0		
	Electricity, grid			1.99	
H_2 production, electrolysis/ATR, for NH_3	Emissions to air, CO_2			0.02	
	Emissions to air, CH_4			2.98	
	Emissions to air, H_2	0.27	0.27	0.37	
	Water	0.09	0.09	0.11	
	Electricity, renewable				
	Electricity, grid			0.60	
	Natural gas, feedstock			16.00	
H_2 storage	Emissions to air, H_2	0.09	0.09		
	Electricity, renewable	0	0		
CCS, for ATR H_2 production for NH_3	Emissions to air, CO_2			11.61	
	Water			0.003	
	Amines			0.35	
	Electricity, grid, carbon capture			0.03	
	Natural gas, fuel			0.84	
	Electricity, grid, pipe transport			1.16	
NH_3 production	Emissions to air, NH_3				
	Electricity, renewable				
	Electricity, grid			3.92	
VLSFO production & distribution		3.09	3.09	3.09	32.14
Distribution and bunkering, NH_3	Emissions, NH_3				
	Sea transport	0.25	0.25	0.25	
	Fuel oil, cooling	1.63	1.63	1.63	
	Electricity, grid, bunkering	0.08	0.08	0.08	
	Electricity, grid, pipe transport	0.65	0.65	0.65	
Combustion	CO_2 emissions	0	0	0	0
	N_2O emissions	1.52	1.52	1.52	0.76
Total		**7.6**	**7.6**	**47.2**	**32.9**

When comparing the results in **Table 9.3** with attributional results for ammonia with VLSFO as pilot fuel from **Table 7.6**, the bio-based pilot fuel reduced the carbon footprint of electrolysis-based ammonia with 43%, as the results go from 13.5 to 7.6 g CO_2-eq/MJ. For natural gas-based ammonia, the result is reduced by 11%, as it goes from 53.1 to 47.2 g CO_2-eq/MJ. Note that contribution from the production and distribution of the bio-based pilot fuel is 32.14 g CO_2-eq/MJ biofuel, while the production and distribution of VLSFO only accounts for

16.71 g CO_2-eq/MJ VLSFO in **Table 7.6**. This also means that the production of the bio-based fuel is 3.09 g CO_2-eq/MJ ammonia with 9.6% e/e bio-based pilot fuel, whereas the production of VLSFO only accounts for 1.60 g CO_2-eq/MJ ammonia with 9.6% e/e VLSFO. Thus, the results in **Table 9.3** are highly influenced by the RED II guidelines specifying that biogenic CO_2 from combustion has a carbon footprint of zero.

10 Evaluation: Completeness, consistency, and sensitivity checks

According to ISO 14044, completeness, consistency, and sensitivity checks must be carried out in order to establish confidence in the results of the LCA study. These checks are described in the following sections.

10.1 Completeness check

The objective of the completeness check is to ensure that the data and information for each life cycle stage in the LCA is available, complete, and sufficient to make interpretations and conclusions.

The ammonia LCA study is cradle to grave (or well-to-wake), thus, it covers all life cycle stages of the shipping fuels, from feedstock provision and fuel production to the fuel use and combustion on board the vessel.

For the foreground data of this LCA study, the inventory data are judged to be complete, except for the following aspects:

- Service inputs related to the CAPEX activities (see **section 4.7**)
- Differentiated CAPEX activities for ammonia production since the CAPEX activity is the same for electrolysis-based and natural gas-based ammonia (see **section 4.7.1.2**)
- Differentiated CAPEX activities for distribution and bunkering since the CAPEX activity is the same for ammonia and VLSFO (see **section 4.7.1.3**)

Nevertheless, the lack of data on the points above is unlikely to have a substantial impact in the study results, since the CAPEX activities are not the main contributors to any of the eight impact categories presented in **chapter 6**. Yet, it is a limitation of the study that neither literature nor project partners can provide specific data for the CAPEX activities and their required service inputs.

For the background data for the consequential model, the LCI is considered to have a high level of completeness, since the EXIOBASE database operates with a cut-off criterion at 0%. A limitation of EXIOBASE is that it includes fewer number of emission flows compared to process-based databases, such as the ecoinvent database. This is potentially a drawback for certain indicators, most notably those related to toxicity. This is why results for six impact categories – aquatic and terrestrial ecotoxicity, ozone layer depletion, non-renewable energy, as well as carcinogen and non-carcinogen human toxicity – are not presented in this report, as described in **section 2.11**. This is a limitation of the study, especially since ammonia emissions have an effect on toxicity. Yet, on the other hand, results for toxicity are likely to be among the most uncertain in the study, which is a common feature in most LCA studies. Thus, even though EXIOBASE has a limited number of emissions flows compared to other databases, such as ecoinvent, it is deemed more important to have a cut-off criterion at 0% than to include the five before-mentioned impact categories.

10.2 Consistency check

The goal of the consistency check is to assess and verify the consistency of the applied assumptions, methods, and data in the LCA study, e.g., the consistency regarding data quality for the product chain and the applied methodology.

For the applied inventory, data for project partners and industrial experts have been prioritised, as this data have been deemed as current and of as high as possible given the technologies' maturity level. Moreover, the data has undergone sanity checks to ensure its validity. Nevertheless, it has only been possible to obtain data

on ammonia production from the project partners, while VLSFO production is based on a scientific paper from 2019. Nevertheless, as no other data have been found, this is deemed acceptable, especially since the scientific paper is quite recent.

For the combustion emissions, project partners have delivered data for both ammonia and VLSFO, except for the particle emissions from combustion of ammonia, which instead was estimated based on a literature source from 2021. Yet, it is important to highlight that the literature source does not specify the engine type, which the emission data applies for, and a project partner therefore stresses that the applied value can only be seen as an estimate, since particulate emissions can vary between engine designs. Nevertheless, since particle emissions were included in the LCI data for VLSFO, it was deemed necessary to also include particle emissions for ammonia to ensure a fair comparison of respiratory inorganic impacts from the two fuel types.

For the remaining data gaps, data from the ecoinvent database have been applied or assumptions have been made based on expert estimates. When no data were available, proxy data were applied, e.g., for the distribution and bunkering infrastructure for ammonia. Thus, there are some inconsistencies between the data applied for the individual product systems of ammonia and VLSFO, yet, as ammonia is considered a new shipping fuel, making data for its product system limited, the level of consistency is deemed acceptable.

For the consequential model, substitution has been applied instead of allocation, e.g., for the by-product of naphtha from the desulphurisation process (see **section 5.2**). Moreover, the foreground system for the consequential LCA models the processes, which are expected to produce ammonia and VSLFO when the demand for these shipping fuels increases. Also, the modelling of grid electricity described in **section 4.1.1.1** takes the marginal supply of electricity in each region into account. Thus, the fundamental principles for consequential LCA studies are applied throughout this report. Yet, it is important to highlight that when flows are linked to EXIOBASE activities, average suppliers to the national markets are used, including specified import shares from other countries (see details in **section 2.6**). Thus, for some inputs, e.g., the material inputs to the CAPEX activities, the marginal supply has not been determined.

For the attributional model, allocation has been applied in accordance with the RED II guidelines, along with other methodological rules, e.g., that renewable electricity has a carbon footprint of zero. Nevertheless, for the background data for the attributional model, there is a mismatch between the economic allocation in the ecoinvent database, the applied background database, and the energy allocation, which must be applied in the foreground system in accordance with the RED II guidelines. However, as allocation is only applied for one process within the product system (nitrogen production, see **section 5.1.2.1** and **5.1.2.2**), for which energy allocation was not possible, this is deemed to have a small influence on the results of the attributional model in this study.

10.3 Sensitivity check

The purpose of the sensitivity check is to assess the reliability of the LCA study's results, e.g., determining how the results are affected by uncertainties for the applied data and assumptions. An extensive sensitivity analysis is conducted in **chapter 8** and **9**. Several parameters are deemed of high importance for the conclusions and recommendations of this LCA study, e.g., the share of pilot fuel, N_2O emissions from ammonia combustion, as well as the carbon intensity of electricity and natural gas. Thus, the influence of these parameters is highlighted in both the executive summary as well as interpretation and conclusions to ensure that the reader and interpreter of this report understands the sensitivity of the results for the default scenarios.

11 Interpretation and conclusions

This chapter discusses the LCA study's limitations, assumptions, results, sensitivity analyses and finally draws conclusions. Throughout this chapter, the terms in the table below are used to refer to the four different fuel scenarios, three production pathways, and two fuel types:

4 fuel scenarios:	3 production pathways:	2 fuel types:
Ammonia with H_2 from solar-based electrolysis	Electrolysis-based ammonia	Ammonia with 9.6% e/e VLSFO
Ammonia with H_2 from wind-based electrolysis		
Ammonia with H_2 from ATR with CCS	Natural gas-based ammonia	
VLSFO	Desulphurisation	VLSFO

For ammonia to fulfil its function as a shipping fuel, ammonia needs to be ignited by a pilot fuel. It is assumed that VLSFO is the closest match to a pilot fuel in this LCA study. Thus, for the functional unit of 1 MJ shipping fuel, VLSFO accounts for 9.6% of the total fuel energy of 1 MJ ammonia. This is referred to as '*ammonia with 9.6% e/e VLSFO*' throughout the report.

The LCA study has a global geographical scope, but the results are presented for 17 regions, as groupings of countries and regions are needed for communicating results and for the results to be applicable by different actors. Grouping is done according to the groupings of the world regions from IEA as well as grouping definitions prescribed by A.P. Moller - Maersk. Moreover, a mean value is calculated based on the results for the 17 regions, in order to provide a simple overview and interpretation of the LCIA results.

11.1 Assumptions and limitations

Since both ammonia and VLSFO are relatively new fuels within the shipping industry, the LCA study is limited by the available data and knowledge about the two product systems. Moreover, assumptions have been made and proxy data have been applied when project partners or industrial experts have not been able to provide data or estimates and when information from the scientific literature has also been limited. Thus, this section will discuss the most important assumptions and the overall limitations for the LCA study.

The key limitations and assumptions for this LCA study are deemed to be:

- The assumed gas slips throughout the product system
- The assumed energy requirement and energy source for cooling of ammonia in the distribution phase
- The assumed transport distance for ammonia in the distribution phase
- The lack of specific data for CAPEX activities and their service inputs
- The assumed CAPEX needed for ammonia distribution
- Assuming that N_2O emissions from combustion of ammonia are similar to diesel oil

The assumed gas slips throughout the product systems are based on data from Bertagni et al. (2023) which relates to the slip of natural gas and ammonia. However, it is important to recognise that the slip of gases in reality will vary because of differences in, e.g., molecular mass, shape, and/or size. Yet, for this LCA study, it is assumed that the 0.3% is applicable for all gases – except for the slip of CO_2 from carbon storage – within the product system. Several project partners have argued that this assumption lacks nuances since the slip of methane may differ from the slip of H_2. Thus, to improve the validity of the results, it is recommended to determine the gas slips with higher accuracy.

Three of the key assumptions relate to the distribution phase for ammonia since the data availability for this life cycle stage is scarce. It is therefore prudent to determine the energy requirement and energy source for cooling of ammonia along with the transport distance of ammonia with more accuracy, since it can have a high influence on the LCIA results.

For the applied CAPEX activities, generic data is utilised since neither literature nor project partners was able to provide specific data. Moreover, the required service inputs for the CAPEX activities are not included due to lack of data. Thus, this is a limitation of the study. Nevertheless, the lack of specific CAPEX data and service input data are unlikely to have a substantial impact in the study results, since the CAPEX activities are not the main contributors to any of the eight impact categories presented in **chapter 6**.

Moreover, several project partners also argue that the CAPEX activity for distribution and bunkering of ammonia may underestimate the impact, since additional materials are needed to provide the thermal insulation for maintaining ammonia as a liquid until combustion onboard the vessel. Yet, based on the contribution from the other CAPEX activities within the ammonia product system, it is likely that additional materials for the ammonia CAPEX activity for distribution will have a minor influence on the results, especially since it is assumed that the additional materials will be used to distribute large amounts of ammonia in its lifespan.

Lastly, it is assumed that N_2O emissions from combustion of ammonia are similar to diesel oil. Yet, it is important to highlight that the data provided for combustion of ammonia on the vessel are based on assumptions and development targets for the engine, as the engine is still under development. On the other hand, since engine design and size influence the combustion emissions, the data for combustion of ammonia provided by project partners has been deemed the best available and most consistent data.
Additionally, Mærsk Mc-Kinney Møller Center (2023) expects N_2O emissions to be mostly around 0.06 g N_2O/kWh – corresponding to 0.0083 g N_2O/MJ – since higher values are not likely to be accepted from an ammonia ICE design. Thus, the difference between the development target for the ammonia engine (0.0056 g N_2O/MJ) and the Mærsk Mc-Kinney Møller Center's expected threshold for N_2O emissions (0.0083 g N_2O/MJ) is 0.0028 g N_2O/MJ. Moreover, the sensitivity analysis includes a test with other N_2O emission values from combustion of ammonia, thus, showing that the GWP100 results for the three ammonia fuel scenarios are increased with around 2 g CO_2-eq/MJ with 0.0083 g N_2O/MJ instead of 0.0056 g N_2O/MJ. Thus, if the design parameter of 0.0056 g N_2O/MJ is not met while the expectations by Mærsk Mc-Kinney Møller Center (2023) are complied with instead, a factor 1.5 increase in g N_2O/MJ will not have a large effect on the GWP100 results.

11.2 Results

This report presents a comparative, consequential LCA study of VLSFO and two production pathways for ammonia with 9.6% e/e VLSFO used as fuel in shipping, along with an attributional carbon footprint assessed in accordance with the RED II guidelines for RFNBOs. Note that the results presented in this section are based on the assumptions and LCI data presented in **chapter 5**, thus, **section 11.3** presents the findings of the sensitivity analysis, showcasing which parameters have the highest influence on the LCA study's results. Moreover, it is important to highlight that the consequential and attributional results should not be compared due to the methodological differences, and the attributional results should only be compared to other RED II-aligned studies.

The consequential LCA study aims to assess the environmental impacts of ammonia and VLSFO based on a change in demand for these shipping fuels. Thus, the current production methods for ammonia and VLSFO will not necessarily be reflected in this study, as a change in demand will be met by new capacity, e.g., H_2 for natural gas-based ammonia is assumed to be produced using ATR, while VLSFO is assumed to be produced through desulphurisation. These modelling choices are based on discussions with project partners and literature research. Moreover, the results of the LCA study are intended to be used for decision support in the choice of and investments in alternative fuel systems for shipping from current (2024) and the next 5-10 years, since choices or investment in fuel systems today have implications for the type of fuels used in shipping several years (decades) after the decision.

The attributional LCA study is performed to determine the carbon footprint of the before-mentioned fuels in accordance with RED II guidelines for RFNBOs. Moreover, the attributional approach is also used to assess whether the two ammonia pathways have a carbon footprint below the RED II reduction target of 70% for RFNBOs compared to the WtW fossil fuel comparator (94 g CO_2-eq/MJ). Following the RED II guidelines for RFNBOs means that the carbon intensity of renewable electricity is set to zero, that materials, equipment, and machinery necessary for fuel production and distribution are excluded, and that there no differentiation of timing of CO_2 emissions.

Note that the attributional results are calculated for WtW with both 9.6% e/e and 0% e/e VLSFO. This is done, because project partners argue that the share of pilot fuel will not be included when the results are used in relation to RFNBOs certifications.

11.2.1 Result for the consequential model

Based on the consequential model, ammonia with H_2 from wind-based electrolysis has the lowest mean value for GWP100, while VLSFO has the lowest results for acidification and both aquatic and terrestrial eutrophication. The three ammonia fuel scenarios have similar impacts on respiratory inorganics and their mean value is approximately 17% lower than the mean value for VLSFO. For nature occupation, photochemical ozone, vegetation, as well as respiratory organics, the result ranges overlap, thus, the difference between the four fuel scenarios depend on the regions being compared. The difference in results is largest for GWP100, since the mean value ammonia with H_2 from electrolysis has an impact that is five times lower than the mean value for VLSFO. **Table 11.1** gives an overview of the characterised results for the consequential model, presenting both the mean value and the result ranges for the 17 regions. The GWP100 results are presented with and without the GWP of H_2, since the GWP for H_2 is not included in IPCC (2021).

The contribution analysis for GWP100 for the consequential model showcases three main flows that contribute to the results for electrolysis-based ammonia: the CO_2 emissions from combustion of the pilot fuel share, the fuel oil used as feedstock for VLSFO, and the renewable electricity. For natural gas-based ammonia, there are three main flows that contribute to the GWP100 results: the natural gas used for ATR, the CO_2 emissions from the CCS process, and the CO_2 emissions from combustion of the pilot fuel share.

Table 11.1: Characterised results for ammonia (9.6% e/e VLSFO) with H_2 from electrolysis (based on either solar or wind), ammonia (9.6% e/e VLSFO) with H_2 from ATR with CCS, and VLSFO with the functional unit of 1 MJ for the **consequential model**. The table presents the mean result and the result range in parentheses.

Production pathway		**Haber-Bosch**			**Desulphurisation**
H_2 production		**Electrolysis**	**Electrolysis**	**ATR with CCS**	**ATR**
Electricity source		**Solar**	**Wind**	**Grid**	**Grid**
Fuel		**Ammonia with 9.6% e/e VLSFO**	**Ammonia with 9.6% e/e VLSFO**	**Ammonia with 9.6% e/e VLSFO**	**VLSFO**
Impact categories	**Unit**				
Global warming (GWP100)	g CO_2-eq/MJ	22.3 (16.8-30.1)	19.6 (15.8-26.1)	44.6 (40.1-49.5)	107.1 (99.3-122.0)
GWP100 without GWP of H_2	g CO_2-eq/MJ	21.8 (16.3-29.6)	19.2 (15.3-25.6)	44.2 (39.7-49.1)	107.1 (99.3-122.0)
Respiratory inorganics	mg $PM_{2.5}$-eq/MJ	323 (314-339)	321 (311-344)	318 (312-332)	387 (374-412)
Respiratory organics	pers*ppm*s/MJ	0.85 (0.83-0.89)	0.83 (0.81-0.84)	0.86 (0.85-0.87)	0.90 (0.87-0.94)
Nature occupation	PDF*m^2a/MJ	0.00033 (0.00010-0.00114)	0.00024 (0.00006-0.00084)	0.00020 (0.00001-0.00039)	0.00051 (0.00017-0.00086)
Acidification	cm^2 UES/MJ	242 (235-260)	241 (234-256)	239 (235-246)	195 (184-214)
Eutrophication, aquatic	mg NO_3-eq/MJ	225 (217-246)	222 (215-237)	221 (215-230)	163 (149-189)
Eutrophication, terrestrial	cm^2 UES/MJ	1,129 (1,123-1,138)	1,127 (1,123-1,132)	1,129 (1,123-1,134)	680 (671-696)
Photochemical ozone, vegetation	cm^2*ppm*hour s/MJ	33,439 (32,954-34,445)	32,920 (32,581-33,438)	33,810 (33,577-34,092)	34,643 (33,964-35,813)

11.2.2 Result for the attributional model

For the attributional model, only GWP100 results are presented, since the RED II guidelines focus on the carbon footprint of fuels. Moreover, the results for electrolysis-based ammonia are the same regardless of the use of solar and wind electricity, since the carbon footprint of renewable electricity is zero according to the RED II guidelines for RFNBOs. **Table 11.2** and **Table 11.3** give an overview of the GWP100 results for the attributional model for ammonia with both 9.6% and 0% e/e VLSFO, presenting both the mean value and the result ranges for the 17 regions. The GWP100 results are presented with and without the GWP of H_2, since the GWP for H_2 is not included in IPCC (2021).

For electrolysis-based ammonia with 9.6% e/e VLSFO, the GWP100 results are seven times lower than the fossil fuel comparator value of 94 g CO_2-eq/MJ, which is applied for VLSFO. The GWP100 result for ammonia with H_2 from ATR with CCS with 9.6% e/e VLSFO is 44% lower than the default value of the fossil fuel comparator. The result ranges are 12.6-14.6 g CO_2-eq/MJ and 46.7-59.2 g CO_2-eq/MJ for electrolysis-based and natural gas-based ammonia with 9.6% e/e VLSFO, respectively.

For electrolysis-based ammonia with 0% e/e VLSFO, the GWP100 results range from 4.0-6.4 g CO_2-eq/MJ and the mean value is 18 times lower than the fossil fuel comparator value of 94 g CO_2-eq/MJ. The GWP100 results for ammonia with H_2 from ATR with CCS with 0% e/e VLSFO range from 41.7-55.6 g CO_2-eq/MJ and the mean value is 48% lower than the default value of the fossil fuel comparator.

Thus, the attributional results for electrolysis-based ammonia with both 9.6% and 0% e/e VLSFO are below the 70% reduction target from RED II, as the results are lower than 28.2 g CO_2-eq/MJ.

The contribution analysis for the attributional carbon footprint shows that the CO_2 emissions from the share of pilot fuel is the largest contributor to the impact from electrolysis-based ammonia with 9.6% e/e VLSFO. Without the share of pilot fuel, the largest contributor to electrolysis-based ammonia is the fuel oil used for cooling during the distribution phase. For natural gas-based ammonia with both 9.6% and 0% e/e VLSFO, the two largest contributors are the natural gas input to ATR and CO_2 emissions from the CCS process. Note that the impact from CO_2 emissions from CCS is higher in the attributional model than in the consequential model, since the RED II guidelines do not include differentiation of timing of CO_2 emissions. Thus, the yearly slip of 0.023% CO_2 has the same GWP100 characterisation factor as if it was being emitted right after capture in the attributional model.

Table 11.2: GWP100 results for ammonia (9.6% e/e VLSFO) with H_2 from electrolysis (based on either solar or wind), ammonia (9.6% e/e VLSFO) with H_2 from ATR with CCS, and VLSFO with the functional unit of 1 MJ for the **attributional model**. The table presents the mean result and the result range in parentheses.

Production pathway		**Haber-Bosch**			**Desulphurisation**
H_2 production		**Electrolysis**	**Electrolysis**	**ATR with CCS**	**ATR**
Electricity source		**Solar**	**Wind**	**Grid**	**Grid**
Fuel		**Ammonia with 9.6% e/e VLSFO**	**Ammonia with 9.6% e/e VLSFO**	**Ammonia with 9.6% e/e VLSFO**	**VLSFO**
Impact categories	**Unit**				
Global warming (GWP100)	g CO_2-eq/MJ	13.5 (12.6-14.6)	13.5 (12.6-14.6)	53.1 (46.7-59.2)	94.0 (94-94)
GWP100 without GWP of H_2	g CO_2-eq/MJ	13.2 (12.3-14.3)	13.2 (12.3-14.3)	52.7 (46.3-58.8)	94.0 (94-94)

Table 11.3: GWP100 results for ammonia (0% e/e VLSFO) with H_2 from electrolysis (based on either solar or wind), ammonia (0% e/e VLSFO) with H_2 from ATR with CCS, and VLSFO with the functional unit of 1 MJ for the **attributional model**. The table presents the mean result and the result range in parentheses.

Production pathway		**Haber-Bosch**			**Desulphurisation**
H_2 production		**Electrolysis**	**Electrolysis**	**ATR with CCS**	**ATR**
Electricity source		**Solar**	**Wind**	**Grid**	**Grid**
Fuel		**Ammonia with 0% e/e VLSFO**	**Ammonia with 0% e/e VLSFO**	**Ammonia with 0% e/e VLSFO**	**VLSFO**
Impact categories	**Unit**				
Global warming (GWP100)	g CO_2-eq/MJ	5.1 (4.0-6.4)	5.1 (4.0-6.4)	48.8 (41.7-55.6)	94.0 (94-94)
GWP100 without GWP of H_2	g CO_2-eq/MJ	4.7 (3.6-6.0)	4.7 (3.6-6.0)	48.4 (41.3-55.2)	94.0 (94-94)

11.3 Sensitivity analysis

Since ammonia fuel is relatively new to the shipping industry, there are some uncertainties related to both the production of ammonia and the emissions from combustion. Therefore, an extensive sensitivity analysis has been conducted in order to determine the most important parameters which influence the environmental impacts of ammonia fuel.

There are three parameters that can have a high influence on the GWP100 results for both ammonia pathways in the consequential model:

1. The N_2O emissions from combustion of ammonia
2. The energy source and energy requirement for cooling of ammonia in the distribution phase
3. The H_2 slip in the product system

The relative percentage change and the mean value for the GWP100 results for the three above-mentioned parameters for the two ammonia pathways are shown in **Table 11.4** and **Table 11.5.**

The amount of N_2O emissions from combustion of ammonia is an important parameter, since N_2O has a characterisation factor of 273 kg CO_2-eq/kg. Two values were tested in the sensitivity analysis: 0.0083 g N_2O/MJ and 0.117 g N_2O/MJ. The first value is based on Mærsk Mc-Kinney Møller Center (2023), which expects N_2O emissions to be mostly around 0.06 g N_2O/kWh – corresponding to 0.0083 g N_2O/MJ – since higher values are not likely to be accepted from an ammonia ICE design, while the second value is based on data from Xu et al. (2023) for an experimental, dual ammonia engine for ammonia with approximately 24% e/e diesel as pilot fuel before selective catalytic reduction (SCR).

When applying the 0.0083 g N_2O/MJ in the sensitivity analysis, the GWP100 results for the three ammonia fuel scenarios are increased with around 1 g CO_2-eq/MJ. Thus, if the design parameter of 0.0056 g N_2O/MJ is not met while the expectations by Mærsk Mc-Kinney Møller Center (2023) are complied with instead, an increase of 0.0027 g N_2O/MJ will not have a large effect on the GWP100 results.

Nevertheless, when applying the 0.117 g N_2O/MJ, the GWP100 results increase with 137% and 155% for ammonia with solar- and wind-based electrolysis, respectively. For natural gas-based ammonia, the GWP100 result can increase with 69%. Yet, it is important to highlight that N_2O emissions will differ between engine designs according to the project partners, thus, the 0.117 g N_2O/MJ may not be applicable for the engine described in this LCA study. Yet, since the 0.117 g N_2O/MJ is before SCR, it is deemed the best estimate for an upper value for N_2O emissions from the ammonia engine. Note that the amount of N_2O emissions resulting in the same GWP100 from combustion of ammonia as for VLSFO corresponds to 0.253 g N_2O/MJ.

Moreover, if the energy requirement for cooling is 10 times larger than first assumed, the GWP100 results increase by 90% and 100%, corresponding to 42 and 39 g CO_2-eq/MJ for ammonia with solar- and wind-based electrolysis, respectively. For natural gas-based ammonia, the increase is 54%, corresponding to a mean GWP100 result of 67 g CO_2-eq/MJ. This shows that it is important to determine the energy source used to cool ammonia in the distribution phase, and to reduce the energy requirement, if the energy source has a high carbon footprint.

Lastly, it is important to limit the slip of H_2 within the product system, as it can increase the impact with 18-39% depending on the ammonia fuel scenario, when a GWP100 characterisation factor of 12.8 kg CO_2-eq/kg H_2 is applied.

11.3.1 Sensitivity of results for electrolysis-based ammonia: the consequential model

The sensitivity analysis shows that there are three parameters that can have a high influence on the GWP100 results for electrolysis-based ammonia in the consequential model:

1. The carbon intensity of the renewable electricity
2. The distribution distance for ammonia in the distribution phase
3. The share of pilot fuel

The relative percentage change and the mean value for the GWP100 results for the parameters, which can have a high influence on the GWP100 results for electrolysis-based ammonia, are shown in **Table 11.4**.

Table 11.4: Change in GWP100 results for the six most important parameters for electrolysis-based ammonia with 9.6% e/e VLSFO for the **consequential** model (see **section 11.3** and **11.3.1**).

Parameter	N_2O emissions from combustion		Energy for cooling during distribution		H2 slip	Carbon intensity of renewable electricity		Distribution distance	Share of pilot fuel	
Original value	0.0056 g N_2O/MJ from combustion		1.9%		0.3%	3-20 and 5-24 g CO_2-eq/kWh renewable electricity for wind and solar, respectively		707 km by ship 588 km by pipeline	9.6% e/e VLSFO	
Tested value	0.0083 g N_2O/MJ from combustion	0.117 g N_2O/MJ from combustion	0.11%	19%	5%	100 g CO_2-eq / kWh renewable electricity	5 g CO_2-eq / kWh renewable electricity	7,070 km by ship 5,880 km by pipeline	5% e/e VLSFO	15% e/e VLSFO
GWP100 change for the consequential model										
Ammonia with H_2 from electrolysis (solar) and 9.6% e/e VLSFO	3%	137%	-8%	90%	35%	206%	-20%	48%	-19%	23%
New mean result (g CO_2-eq/MJ)	23.0	52.7	20.5	42.3	30.0	68.2	17.9	33.0	18.0	27.3
Ammonia with H_2 from electrolysis (wind) and 9.6% e/e VLSFO	4%	155%	-9%	100%	39%	247%	-9%	55%	-23%	26%
New mean result (g CO_2-eq/MJ)	20.4	50.1	17.9	39.2	27.3	68.2	17.9	30.4	15.2	24.8

First, the GWP100 results for electrolysis-based ammonia are influenced by the carbon footprint of the renewable electricity. Two values are tested – 5 and 100 g CO_2-eq/kWh – since the carbon intensity of solar and wind electricity in the 48 countries, which the 17 regions consist of, can vary with 17-110 and 7-91 g CO_2-eq/kWh, respectively. The sensitivity analysis shows that a carbon intensity of 100 g CO_2-eq/kWh for renewable electricity increases the GWP100 mean value for electrolysis-based ammonia with over 200%, while a carbon intensity for renewable electricity of 5 g CO_2-eq/kWh decreases the GWP100 mean result with 9-20%. Thus, this sensitivity analysis highlights the importance of producing electrolysis-based ammonia in a country or region, which has renewable electricity with a low carbon intensity. This also means that the higher the carbon intensity of renewable electricity, the higher importance of the input of electricity to the N_2, H_2, and ammonia production.

The GWP100 results for electrolysis-based ammonia are also influenced by the distribution distance for the fuel. If the distribution distance for ammonia is 10 times longer than first assumed – which seems realistic based on transport distances applied in other studies – then the GWP100 results increase by 48% and 55%, corresponding to 33 and 30 g CO_2-eq/MJ for ammonia with solar- and wind-based electrolysis, respectively.

Lastly, the share of pilot fuel may also vary, since the ammonia engine described in this study is still under development. Therefore, the sensitivity analysis includes scenarios for ammonia with 5% and 15% e/e VLSFO. 5% e/e VLSFO for electrolysis-based ammonia will result in a decrease in the GWP100 results of 19% and 23%, corresponding to 18 and 15 g CO_2-eq/MJ for ammonia with solar- and wind-based electrolysis, respectively. If the share of VLSFO is instead 15% e/e, then the results increase with 23% and 26%, corresponding to 27 and 25 g CO_2-eq/MJ for ammonia with solar- and wind-based electrolysis, respectively. Thus, it is important to determine the exact share of pilot fuel in order to increase the accuracy of the results.

11.3.2 Sensitivity of results for natural gas-based ammonia: the consequential model

The sensitivity analysis shows that there are five parameters that can have high influence on the GWP100 results for natural gas-based ammonia in the consequential model:

1. Slip of CO_2 from carbon storage
2. The carbon capture rate
3. The energy input to CCS
4. The slip of methane from natural gas extraction
5. The slip of methane from the ATR process

The relative percentage change and the mean value for the GWP100 results for the above-mentioned parameters for natural gas-based ammonia are shown in **Table 11.5**.

Table 11.5: Change in GWP100 results for the eight most important parameters for natural gas-based ammonia with 9.6% e/e VLSFO for the **consequential** model (see **section 11.3** and **11.3.2**).

Parameter	N_2O emissions from combustion		Energy for cooling during distribution		H2 slip	Slip of CO_2 from storage		Carbon capture rate		Energy for CCS	Methane slip, natural gas extraction	Methane slip from ATR
Original value	0.0056 g N_2O / MJ from combustion		1.9%		0.3%	0.023%		90%		0.28 kWh/kg captured CO_2	Varies from country to country	0.3%
Tested value	0.0083 g N_2O/MJ from combustion	0.117 g N_2O/MJ from combustion	0.11%	19%	5%	0.3%	5%	50%	95%	2.8 kWh/kg captured CO_2	4x slip of methane from natural gas extraction	5%
GWP100 change for the consequential model												
Ammonia with H_2 from ATR with CCS and 9.6% e/e VLSFO	2%	69%	-5%	54%	18%	28%	166%	87%	-11%	48%	40%	107%
New mean result (g CO_2-eq/MJ)	44.6	74.2	41.6	67.4	51.9	56.2	1116.8	82.0	39.1	64.9	61.5	90.6

Slip of CO_2 from carbon storage is an important parameter for natural gas-based ammonia since CCS is used to reduce the carbon footprint of this ammonia pathway. Though 90% of the CO_2 is captured and intended to be stored for at least 100 years, part of the CO_2 is assumed to leak from storage throughout this time-period. A slip of 0.023% every year is assumed in the default scenario, yet, as slips of 0.3% and 5% are assumed for other gases within the product system, these values are also tested in the sensitivity analysis. This results in a change of 28% and 166% for the mean GWP100 value, respectively, corresponding to an impact of 62 and 91 g CO_2-eq/MJ, with the latter only being 16 g CO_2-eq/MJ lower than the mean GWP100 result for VLSFO.

The carbon capture rate can also influence the GWP100 results for natural gas-based ammonia, e.g., a capture rate of only 50% increases the mean GWP100 value with 87%, corresponding to an impact of 82 g CO_2-eq/MJ. Moreover, if the capture rate is increased to 95%, the GWP100 mean value is reduced by 11%.

Additionally, a sanity check of the energy input to CCS was conducted, showing that the energy input could vary from 0.40 GJ/t CO_2 to 3.46 GJ/t CO_2 depending on the point source of the CO_2. Thus, the sensitivity analysis tested how much the results for ammonia with H_2 from ATR with CCS would change if the energy requirement

for CCS is a factor 10 higher. As seen from **Table 11.5**, this results in an increase of 48% for the mean GWP100 value, corresponding to an impact of 65 g CO_2-eq/MJ for natural gas-based ammonia.

Lastly, the slip of methane from natural gas extraction and the ATR process also has a significant impact on the GWP100 results for natural gas-based ammonia. When the slip of methane from natural gas extraction is increased with a factor 4, the mean GWP100 result goes up with 40%, corresponding to an impact of 62 g CO_2-eq/MJ for natural gas-based ammonia. Moreover, if the slip of methane from the ATR process is increased from 0.3% to 5%, the impact increases by 107%, corresponding to an impact of 91 g CO_2-eq/MJ for natural gas-based ammonia. The change is significant, because the input of 171 GJ/t H_2 has a slip of 0.01 t methane per t H_2 with the default slip, while this is increased to 0.17 t methane per t H_2 with a 5% slip.

Thus, it is important to determine the carbon capture rate, the energy input to CCS, the yearly slip of CO_2, and the slip of methane in the product system with greater accuracy in order to increase the precision of the results for natural gas-based ammonia fuel. Moreover, this shows the importance of minimizing slip of methane and CO_2 in the product system for natural gas-based ammonia, while it is also important to have an energy efficient CCS process along with a high capture rate.

It is also important to highlight that the sensitivity analysis shows that applying SMR instead of ATR as the H_2 technology along with a carbon capture rate of 60% for natural gas-based ammonia will increase the GWP100 results with 94%, resulting in a mean GWP100 value of 85 g CO_2-eq/MJ for natural gas-based ammonia.

11.3.3 Sensitivity of results for electrolysis- and natural gas-based ammonia: attributional model

Several of the parameters which can have a large influence on the results from the consequential model also influence the results from attributional model, except for the carbon footprint of renewable electricity, since following the RED II guidelines for RFNBOs means that the carbon intensity of renewable electricity is set to zero. Moreover, the share of pilot fuel will not influence the results used for RFNBOs certifications, since project partners argue that the share of pilot fuel will not be included when the results are used in this regard.

Thus, for the following parameters, the attributional results are expected to change in a similar magnitude as the consequential results:

- The N_2O emissions from combustion of ammonia
- The H_2 slip in the product system
- Slip of CO_2 from carbon storage
- The carbon capture rate
- The energy input to CCS
- The slip of methane from natural gas extraction
- The slip of methane from the ATR process
- The energy source and energy requirement for cooling of ammonia in the distribution phase
- The distribution distance for ammonia in the distribution phase

Note that the slip of CO_2 from carbon storage will have an even higher influence on the attributional results, since the RED II guidelines do not include differentiation of timing of CO_2 emissions. Thus, the yearly slip of CO_2 from storage has the same GWP100 characterisation factor as if it was being emitted right after capture in the attributional model.

Additionally, the attributional results have been calculated with 9.6% e/e bio-based pilot fuel. This is done through a semi-quantitative analysis where a default value from RED II is applied, since RED II specifies that bio-based fuels must have a reduction of at least 65% compared to the WtW fossil fuel comparator of 94 g CO_2-eq/MJ. Therefore, it is assumed that the bio-based pilot fuel will have a carbon footprint of 32.9 g CO_2-eq/MJ from WtW.

The bio-based pilot fuel is assumed to emit the same amount of N_2O emissions from combustion as VLSFO. Yet, there is no impact from the CO_2 emissions from combustion of the bio-based pilot fuel, since biogenic CO_2 from combustion has a carbon footprint of zero according to the RED II guidelines. Therefore, the bio-based fuel is assumed to have a GWP100 impact of 0.76 g CO_2-eq/MJ from combustion. Moreover, it is assumed that the GWP100 impact from the distribution phase is the same as for VLSFO. Thus, the majority of the impact of the bio-based fuel stems from its production.

The semi-quantitative analysis shows that a RED II-compliant bio-based pilot fuel can reduce the attributional carbon footprint of electrolysis-based ammonia with 43%, as the mean result goes from 13.5 to 7.6 g CO_2-eq/MJ, when the RED II guidelines are used for the calculation. For natural gas-based ammonia, the mean result is reduced by 11%, as it goes from 53.1 to 47.2 g CO_2-eq/MJ.

11.4 Conclusions

The main conclusions for this LCA study are as follows:

- Generally, electrolysis-based ammonia has the lowest GWP100 impact, and – depending on the applied LCA methodology – the GWP100 mean result for this ammonia pathway is 5-18 times lower than the mean GWP100 result for VLSFO.

- Both electrolysis-based and natural gas-based ammonia have a lower impact on respiratory inorganics than VLSFO, with the mean value being approximately 17% lower than the mean value for VLSFO.

- VLSFO has the lowest results for acidification and both aquatic and terrestrial eutrophication.

- The attributional carbon footprint calculated in accordance with RED II guidelines for RFNBOs for electrolysis-based ammonia with both 9.6% and 0% e/e VLSFO are below the 70% reduction target from RED II, as the results are lower than 28.2 g CO_2-eq/MJ.

- A semi-quantitative analysis shows that a RED II-compliant bio-based pilot fuel can reduce the attributional carbon footprint of electrolysis-based ammonia with 9.6% e/e pilot fuel with 43%, as the mean result goes from 13.5 to 7.6 g CO_2-eq/MJ. For natural gas-based ammonia, the attributional mean result can be reduced by 11%, as it goes from 53.1 to 47.2 g CO_2-eq/MJ.

- The contribution analysis for the consequential model showcases three main flows that contribute to the GWP100 results for electrolysis-based ammonia: the CO_2 emissions from combustion of the pilot fuel share, the fuel oil used as feedstock for VLSFO, and the renewable electricity.

- For natural gas-based ammonia in the consequential model, there are three main flows that contribute to the GWP100 results: the natural gas used for ATR, the CO_2 emissions from the CCS process, and the CO_2 emissions from combustion of the pilot fuel share.

- The contribution analysis for the RED II-aligned results for ammonia with 9.6% e/e VLSFO shows that the CO_2 emissions from the share of pilot fuel is the largest contributor to the impact from electrolysis-based ammonia. Without the share of pilot fuel, the largest contributor to electrolysis-based ammonia is the fuel oil used for cooling during the distribution phase.

- For the RED II-aligned results for natural gas-based ammonia with both 9.6% and 0% e/e VLSFO, the two largest contributors are CO_2 emissions from the CCS process and the natural gas input to ATR. Note that the impact from CO_2 emissions from CCS is higher in the attributional model than in the consequential model, since the RED II guidelines do not include differentiation of timing of CO_2 emissions. Thus, the yearly slip of CO_2 has the same GWP100 characterisation factor as if it was being emitted right after capture in the attributional model.

- The GWP100 results for both ammonia pathways can be highly influenced by the following three parameters: The N_2O emissions from combustion of ammonia and the energy source, energy requirement for cooling of ammonia in the distribution phase and the slip of H_2 throughout the product system.

- The GWP100 results for electrolysis-based ammonia can be highly influenced by the following three parameters: The carbon intensity of the renewable electricity, the distribution distance for ammonia in the distribution phase, and the share of pilot fuel.

- The GWP100 results for natural gas-based ammonia can be highly influenced by the following five parameters: Slip of CO_2 from carbon storage, the carbon capture rate, the energy input to CCS, as well as the slip of methane from natural gas extraction and the ATR process.

It is recommended to improve the data availability and quality for the parameters that can have a high influence on the results for both ammonia pathways in order to increase the accuracy of the results for ammonia fuels.

12 References

Al-Breiki, M., & Bicer, Y. (2021). Comparative life cycle assessment of sustainable energy carriers including production, storage, overseas transport and utilization. Journal of Cleaner Production, 279, 123481. https://doi.org/10.1016/j.jclepro.2020.123481

Aleisa, E., & Al-Shayji, K. (2018). Ecological–economic modeling to optimize a desalination policy: Case study of an arid rentier state.
Alfa Laval, Haldor Topsøe, Siemens Gamesa, & Vestas. (2020). Ammonfuel—An industrial view of ammonia as a marine fuel. https://www.topsoe.com/hubfs/DOWNLOADS/DOWNLOADS%20-%20White%20papers/Ammonfuel%20Report%20Version%2009.9%20August%203_update.pdf (Accessed March 2025)

Aljaghoub, H., Alasad, S., Alashkar, A., AlMallahi, M., Hasan, R., Obaideen, K., & Alami, A. H. (2023). Comparative analysis of various oxygen production techniques using multi-criteria decision-making methods. International Journal of Thermofluids, 17, 100261. https://doi.org/10.1016/j.ijft.2022.100261

Andersson, J., & Grönkvist, S. (2019). Large-scale storage of hydrogen. International Journal of Hydrogen Energy, 44(23), 11901–11919. https://doi.org/10.1016/j.ijhydene.2019.03.063

Apodaca, L. E. (2022). 2018 Minerals Yearbook—Sulfur. U.S. Department of the Interior and U.S. Geological Survey. https://pubs.usgs.gov/myb/vol1/2018/myb1-2018-sulfur.pdf (Accessed March 2025)

Bertagni, M. B., Socolow, R. H., Martirez, J. M. P., Carter, E. A., Greig, C., Ju, Y., Lieuwen, T., Mueller, M. E., Sundaresan, S., Wang, R., Zondlo, M. A., & Porporato, A. (2023). Minimizing the impacts of the ammonia economy on the nitrogen cycle and climate. Proceedings of the National Academy of Sciences, 120(46), e2311728120. https://doi.org/10.1073/pnas.2311728120

Billing, E., & Fitzgibbon, T. (2019). What shipowners, refiners, and traders should know about IMO 2020. Www.Mckinsey.Com. http://ceros.mckinsey.com/the-next-normal-callout (Accessed March 2025)

Bonou, A., Laurent, A., & Olsen, S. I. (2016). Life cycle assessment of onshore and offshore wind energy-from theory to application. Applied Energy, 180, 327–337. https://doi.org/10.1016/j.apenergy.2016.07.058

Brandão, M., Levasseur, A., Kirschbaum, M. U. F., Weidema, B. P., Cowie, A. L., Jørgensen, S. V., Hauschild, M. Z., Pennington, D. W., & Chomkhamsri, K. (2013). Key issues and options in accounting for carbon sequestration and temporary storage in life cycle assessment and carbon footprinting. The International Journal of Life Cycle Assessment, 18(1), 230–240. https://doi.org/10.1007/s11367-012-0451-6

Captura. (2022). Carbon Dioxide Removal Purchase Application—Fall 2022. https://github.com/frontierclimate/carbon-removal-source-materials/blob/main/Project%20Applications/2022%20Fall/%5BCaptura%5D%20Frontier%20Carbon%20Removal%20Purchase%20Application.pdf (Accessed March 2025)

Chen, X., Matthews, H. S., & Griffin, W. M. (2021). Uncertainty caused by life cycle impact assessment methods: Case studies in process-based LCI databases. Resources, Conservation and Recycling, 172, 105678. https://doi.org/10.1016/j.resconrec.2021.105678 (Accessed March 2025)

consequential-lca.org. (2023). Consequential Life Cycle Assessment modelling – A collection of examples. https://consequential-lca.org/ (Accessed March 2025)

Damvad Analytics, 2.-0 LCA Consultants, Goritas, & BMT. (2016). Potentialer og barrierer for brugen af træ og bæredygtigt træ i byggeriet. https://lca-net.com/publications/danish/show/potentialer-og-barrierer-brugen-af-trae-og-baeredygtigt-trae-byggeriet/ (Accessed March 2025)

De Rosa, M., Knudsen, M. T., & Hermansen, J. E. (2016). A comparison of Land Use Change models: Challenges and future developments. Journal of Cleaner Production, 113, 183–193.

DECHEMA. (2022). Perspective Europe 2030—Technology options for CO2- emission reduction of hydrogen feedstock in ammonia production. DECHEMA Gesellschaft für Chemische Technik und Biotechnologie e.V. https://dechema.de/dechema_media/Downloads/Positionspapiere/Studie+Ammoniak.pdf (Accessed March 2025)

Deloitte. (2019). International Maritime Organization (IMO) 2020—Strategies in a Non-Compliant World. https://www2.deloitte.com/content/dam/Deloitte/us/Documents/finance/international-maritime-organization-pov-2020.pdf (Accessed March 2025)

Dong, T. (2022). Life cycle assessment of ammonia/hydrogen marine engines—CAHEMA - Concepts of ammonia/hydrogen engines for marine application. World Maritime University (WMU). https://www.nordicenergy.org/wordpress/wp-content/uploads/2022/05/LIFE-CYCLE-ASSESSMENT-CAHEMA.pdf (Accessed March 2025)

DTU, World Bank Group, ESMAP, & VORTEX. (2024). Global Wind Atlas. https://globalwindatlas.info (Accessed March 2025)

EC. (2023). COMMISSION DELEGATED REGULATION (EU) 2023/1185 of 10 February 2023 supplementing Directive (EU) 2018/2001 of the European Parliament and of the Council by establishing a minimum threshold for greenhouse gas emissions savings of recycled carbon fuels and by specifying a methodology for assessing greenhouse gas emissions savings from renewable liquid and gaseous transport fuels of non-biological origin and from recycled carbon fuels. European Commission (EC). https://eur-lex.europa.eu/legal-content/EN/TXT/PDF/?uri=CELEX:32023R1185 (Accessed March 2025)

EC, & COWI. (2015). Study on actual GHG data for diesel, petrol, kerosene and natural gas—Project executive summary. European Commission (EC).

ecoinvent. (2021). Ecoinvent database v3.8 [Dataset].

EcoQuery. (2024). Market group for natural gas, high pressure—Global—Natural gas, high pressure | ecoQuery. https://ecoquery.ecoinvent.org/3.8/cutoff/dataset/14395/documentation (Accessed March 2025)

Ember. (2024). Electricity Data Explorer | Open Source Global Electricity Data. Ember. https://ember-climate.org/data/data-tools/data-explorer/ (Accessed March 2025)

EP, & EUCO. (2018). DIRECTIVE (EU) 2018/2001 OF THE EUROPEAN PARLIAMENT AND OF THE COUNCIL of 11 December 2018 on the promotion of the use of energy from renewable sources. https://eur-lex.europa.eu/legal-content/EN/TXT/PDF/?uri=CELEX:32018L2001 (Accessed March 2025)

European Maritime Safety Agency. (2022). Potential of ammonia as fuel in shipping by ABS, CE-DELFT & ARCSILEA. https://www.emsa.europa.eu/newsroom/latest-news/download/7322/4833/23.html (Accessed March 2025)

Facchino, M., Popielak, P., Panowski, M., Wawrzyńczak, D., Majchrzak-Kucęba, I., & De Falco, M. (2022). The Environmental Impacts of Carbon Capture Utilization and Storage on the Electricity Sector: A Life Cycle Assessment Comparison between Italy and Poland. Energies, 15(18), Article 18. https://doi.org/10.3390/en15186809

FAOSTAT. (2024). Food and agriculture Organization of the United Nations. https://www.fao.org/faostat/en/#home (Accessed March 2025)

Friedl, M. A., Sulla-Menashe, D., Tan, B., Schneider, A., Ramankutty, N., Sibley, A., & Huang, X. (2010). MODIS Collection 5 global land cover: Algorithm refinements and characterization of new datasets. Remote Sensing of Environment, 114(1), 168–182.

Frischknecht, R., Stolz, P., Krebs, L., & de Wild-Scholten, M. (2020). Life Cycle Inventories and Life Cycle Assessments of Photovoltaic Systems 2020 Task. International Energy Agency Photovoltaic Power Systems Programme. 10.13140/RG.2.2.17977.19041

Goedkoop, M., & Spriensma, R. (2001). He Eco-Indicator'99—A Damage Oriented Method for Life Cycle Impact Assessment—Methodology Report. https://pre-sustainability.com/legacy/download/EI99_methodology_v3.pdf
Green Transition Denmark. (2021). Cleaner Shipping—Air pollution, climate, technical solutions and regulation. https://rgo.dk/wp-content/uploads/GTD_Cleaner_shipping_2021_Final.pdf (Accessed March 2025)

GTAI. (2021). Industry Overview: The Chemical Industry in Germany. Germany Trade & Invest. https://www.gtai.de/resource/blob/64542/9936fdacfc31ec29ebeff9224e2d1141/TheChemicalIndustryGermany.pdf (Accessed March 2025)

Haberl, H., Erb, K. H., Krausmann, F., Gaube, V., Bondeau, A., Plutzar, C., Gingrich, S., Lucht, W., & Fischer-Kowalski, M. (2007). Quantifying and mapping the human appropriation of net primary production in earth's terrestrial ecosystems. Proceedings of the National Academy of Sciences, 104(31), 12942–12947.

Hauschild, M., & Potting, J. (2005). Spatial differentiation in Life Cycle impact assessment- The EDIP2003 methodology. Environmental News, 80.

Hongfang, L., Ma, X., Huang, K., Fu, L., & Azimi, M. (2020). Carbon dioxide transport via pipelines: A systematic review. Journal of Cleaner Production, 266, 121994.

Hu, T., Zhou, H., Peng, H., & Jiang, H. (2018). Nitrogen Production by Efficiently Removing Oxygen From Air Using a Perovskite Hollow-Fiber Membrane With Porous Catalytic Layer. Frontiers in Chemistry, 6. https://doi.org/10.3389/fchem.2018.00329

Hydrogen Europe. (2023). Impact assessment of the RED II Delegated Acts on RFNBO and GHG accounting—Hydrogen Europe Analysis. https://hydrogeneurope.eu/wp-content/uploads/2023/07/Impact-Assessment-on-the-RED-II-DAs.pdf (Accessed March 2025)

IEA. (2019). Oil 2019 – Analysis and forecast to 2024. International Energy Agency. https://iea.blob.core.windows.net/assets/8fe25538-7e77-4d58-8705-ddc80fd9f693/V3_OIL2019_Final_Web.pdf (Accessed March 2025)

IEA. (2021, October 6). The Role of Low-Carbon Fuels in the Clean Energy Transitions of the Power Sector – Analysis. IEA. https://www.iea.org/reports/the-role-of-low-carbon-fuels-in-the-clean-energy-transitions-of-the-power-sector (Accessed March 2025)

IEA. (2023a). World Energy Outlook 2023. https://www.iea.org/reports/world-energy-outlook-2023 (Accessed March 2025)

IEA. (2023b). World Energy Statistics and Balances—Data product. IEA. https://www.iea.org/data-and-statistics/data-product/world-energy-statistics-and-balances (Accessed March 2025)

IEA. (2024). Renewables 2023 – Analysis and forecast to 2028. IEA. https://www.iea.org/reports/renewables-2023 (Accessed March 2025)

IMO. (2019). IMO 2020 – cutting sulphur oxide emissions. International Maritime Organization (IMO). https://www.imo.org/en/MediaCentre/HotTopics/Pages/Sulphur-2020.aspx (Accessed March 2025)

IMO. (2021). Industry News: IMO Publishes Review of 2020 Marine Fuels Quality. https://www.nepia.com/industry-news/imo-publishes-review-of-2020-marine-fuels-quality/ (Accessed March 2025)

IPCC. (2014). Climate Change 2014: Synthesis Report. Contribution of Working Groups I, II and III to the Fifth Assessment Report of the Intergovernmental Panel on Climate Change [Core Writing Team, R.K. Pachauri and L.A. Meyer (eds.)].

IPCC. (2019a). 2019 Refinement to the 2006 IPCC Guidelines for National Greenhouse Gas Inventories: Agriculture, Forestry and Other Land Use. 4. https://www.ipcc-nggip.iges.or.jp/public/2019rf/vol4.html (Accessed March 2025)

IPCC. (2019b). Chapter 11: N2O Emissions from managed soils, and CO2 emissions from lime and urea application. https://www.ipcc-nggip.iges.or.jp/public/2019rf/pdf/4_Volume4/19R_V4_Ch11_Soils_N2O_CO2.pdf (Accessed March 2025)

IPCC. (2021). Climate Change 2021: The Physical Science Basis. Contribution of Working Group I to the Sixth Assessment Report of the Intergovernmental Panel on Climate Change. doii:10.1017/9781009157896.

ISO. (2006a). ISO 14040 Environmental management – Life cycle assessment – Principles and framework. International Standard Organization.

ISO. (2006b). ISO 14044 Environmental management – Life cycle assessment – Requirements and guidelines. International Standard. International Standard Organization.

Joint Research Centre. (2022). JRC Photovoltaic Geographical Information System (PVGIS)—European Commission. https://re.jrc.ec.europa.eu/pvg_tools/en/ (Accessed March 2025)

Jolliet, O., Margni, M., Charles, R., Humbert, S., Payet, J., Rebitzer, G., & Rosenbaum, R. (2003). IMPACT 2002+: A new life cycle impact assessment methodology. The International Journal of Life Cycle Assessment, 8(6), 324.

Kähler, F., Carus, M., vom Berg, C., & Stratmann, M. (2022). CO2 Reduction Potential of the Chemical Industry Through CCU. https://renewable-carbon-initiative.com/wp-content/uploads/2022/05/22-05-03-CO2_Reduction_Potential_of_the_Chemical_Industry_Through_CCU.pdf (Accessed March 2025)

Kim, J., Park, J., Qi, M., Lee, I., & Moon, I. (2021). Process Integration of an Autothermal Reforming Hydrogen Production System with Cryogenic Air Separation and Carbon Dioxide Capture Using Liquefied Natural Gas Cold Energy. Industrial & Engineering Chemistry Research, 60(19), 7257–7274. https://doi.org/10.1021/acs.iecr.0c06265

Krishnan, S., Corona, B., Kramer, G. J., Junginger, M., & Koning, V. (2024). Prospective LCA of alkaline and PEM electrolyser systems. International Journal of Hydrogen Energy, 55, 26–41. https://doi.org/10.1016/j.ijhydene.2023.10.192

Lee, K., Liu, X., Vyawahare, P., Sun, P., Elgowainy, A., & Wang, M. (2022). Techno-economic performances and life cycle greenhouse gas emissions of various ammonia production pathways including conventional, carbon-capturing, nuclear-powered, and renewable production. Green Chemistry, 24(12), 4830–4844. https://doi.org/10.1039/D2GC00843B

Liu, X., Elgowainy, A., & Wang, M. (2020). Life cycle energy use and greenhouse gas emissions of ammonia production from renewable resources and industrial by-products. Green Chemistry, 22(17), 5751–5761. https://doi.org/10.1039/D0GC02301A

Ludwig, H. (2022). Reverse Osmosis Seawater Desalination Volume 1: Planning, Process Design and Engineering – A Manual for Study and Practice.

Maersk. (2024). Our fleet – equipment specifications DRY CONTAINERS. https://www.maersk.com/~/media_sc9/maersk/local-information/files/africa/south-africa/important-information/container-type-and-sizes/dry-equipment-specifications-updated.pdf (Accessed March 2025)

Mærsk Mc-Kinney Møller Center. (2023). Managing Emissions from Ammonia-Fueled Vessels—An overview of regulatory drivers,emission types, sources, scenarios, reduction technologies, and solutions. https://cms.zerocarbonshipping.com/media/uploads/documents/Ammonia-emissions-reduction-position-paper_v4.pdf (Accessed March 2025)

Merciai, S., & Schmidt, J. (2017a). Land Use Change and Electricity Models in a Multi-regional Hybrid Input Output Framework. In 25th IIOA Conference in Atlantic City. https://lca-net.com/publications/show/land-use-change-and-electricity-models-in-a-multi-regional-hybrid-input-output-framework/ (Accessed March 2025)

Muñoz, I. (2023). Literature review on climate effects and leakage rates in a hydrogen economy.

Muñoz, I., Schmidt, J., de Saxcé, M., Daalgaard, R., & Merciai, S. (2015). Inventory of country specific electricity in LCA - consequential scenarios. 2.-0 LCA consultants. http://lca-net.com/clubs/energy/ (Accessed March 2025)

Muñoz, I., & Weidema, B. P. (2023). Example—Marginal electricity in Denmark. Consequential LCA. https://consequential-lca.org/clca/marginal-suppliers/the-special-case-of-electricity/example-marginal-electricity-in-denmark/ (Accessed March 2025)

Myhre, G., Shindell, D., Bréon, F.-M., Collins, W., Fuglestvedt, J., Huang, J., Koch, D., Lamarque, J.-F., Lee, D., Mendoza, B., Nakajima, T., Robock, A., Stephens, G., Takemura, T., & Zhan, H. (2013). Anthropogenic and Natural Radiative Forcing. In T. F. Stocker, D. Qin, G.-K. Plattner, M. Tignor, S. K. Allen, J. Boschung, A. Nauels, Y. Xia, V. Bex, & P. M. Midgle (Eds.), Climate Change 2013: The Physical Science Basis. Contribution of Working Group I to the Fifth Assessment Report of the Intergovernmental Panel on Climate Change. Cambridge University Press.

NGFS. (2021). NGFS Climate Scenarios for central banks and supervisors. https://www.ngfs.net/sites/default/files/media/2021/08/27/ngfs_climate_scenarios_phase2_june2021.pdf (Accessed March 2025)

NGFS. (2024). NGFS Scenarios Portal. NGFS Scenarios Portal. https://www.ngfs.net/ngfs-scenarios-portal/faq (Accessed March 2025)

Nielsen, O.-K., Plejdrup, M. S., Winther, M., Nielsen, M., Gyldenkærne, S., Mikkelsen, M. H., Albrektsen, R., Thomsen, M., Hjelgaard, K., Fauser, P., Bruun, H. G., Johannsen, V. K., Nord-Larsen, T., Vesterdal, L., Stupak, I., Scott-Bentsen, N., Rasmussen, E., Petersen, S. B., Olsen, T. M., & Hansen, M. G. (2016). Denmark's National Inventory Report 2016. https://dce2.au.dk/pub/SR189.pdf (Accessed March 2025)

Nielsen, O.-K., Plejdrup, M. S., Winther, M., Nielsen, M., Gyldenkærne, S., Mikkelsen, M. H., Albrektsen, R., Thomsen, M., Hjelgaard, K., Fauser, P., Bruun, H. G., Johannsen, V. K., Nord-Larsen, T., Vesterdal, L., Stupak, I., Scott-Bentsen, N., Rasmussen, E., Petersen, S. B., Olsen, T. M., & Hansen, M. G. (2018). Denmark's National Inventory Report 2018. https://dce2.au.dk/pub/SR272.pdf (Accessed March 2025)

Olindo, R., & Vogtländer, J. G. (2019). The Role of Hydrogen in the Ecological Benefits of Ultra Low Sulphur Diesel Production and Use: An LCA Benchmark. Sustainability, 11(7), Article 7. https://doi.org/10.3390/su11072184

Oni, A. O., Anaya, K., Giwa, T., Di Lullo, G., & Kumar, A. (2022). Comparative assessment of blue hydrogen from steam methane reforming, autothermal reforming, and natural gas decomposition technologies for natural gas-producing regions. Energy Conversion and Management, 254, 115245. https://doi.org/10.1016/j.enconman.2022.115245

Palmgren, F., Glasius, M., Wåhlin, P., Ketzel, M., Berkowicz, R., Jensen, S. S., Winther, M., Illerup, J. B., Andersen, M. S., Hertel, O., Vinzents, P. S., Møller, P., Sørensen, M., Knudsen, L. E., Schibye, B., Andersen, Z. J., Hermansen, M., Scheike, T., Stage, M., … Clausen, P. A. (2005). Luftforurening med partikler i Danmark (Air Pollution with particles in Denmark) (Nr. 1021). Miljøministeriet.

Philipps, D. S., Warmuth, W., & GmbH, P. P. (2023). Photovoltaics Report. Fraunhofer Institute for Solar Energy Systems and PSE Projects GmbH.

https://www.ise.fraunhofer.de/content/dam/ise/de/documents/publications/studies/Photovoltaics-Report.pdf (Accessed March 2025)

PV resources. (2015). Photovoltaic Economics—LCoE. https://www.pvresources.com/en/economics/lcoe.php

Robertson, B., & Mousavian, M. (2022). The Carbon Capture Crux—Lessons Learned. Institute for Energy Economics and Financial Analysis (IEEFA). https://ieefa.org/sites/default/files/2022-09/The%20Carbon%20Capture%20Crux.pdf (Accessed March 2025)

Schmidt, J., & Brandão, M. (2013). LCA screening of biofuels - iLUC, biomass manipulation and soil carbon. https://lca-net.com/files/biomasse_bilag1_lcascreening.pdf (Accessed March 2025)

Schmidt, J., & Daalgaard, R. (2012). National and farm level carbon footprint of milk - Methodology and results for Danish and Swedish milk 2005 at farm gate. Arla Foods. https://lca-net.com/files/Arla-Methodology_report_20120724.pdf (Accessed March 2025)

Schmidt, J., & De Rosa, M. (2018a). Enhancing Land Use Change modelling with IO data. https://lca-net.com/files/SETAC_Rome_Schmidt_DeRosa_Extended-abstract_20180515.pdf (Accessed March 2025)

Schmidt, J., & De Rosa, M. (2020). Certified palm oil reduces greenhouse gas emissions compared to non-certified. Journal of Cleaner Production, 277, 124045.

Schmidt, J., & de Saxcé, M. (2016). Arla Foods Environmental Profit and Loss Accounting 2014 (Environmental Project No. 1860). https://lca-net.com/files/978-87-93435-75-9.pdf (Accessed March 2025)

Schmidt, J., Weidema, B., & Brandão, M. (2015). A framework for modelling indirect land use changes in Life Cycle Assessment. Journal of Cleaner Production, 99, 230–238. https://doi.org/10.1016/j.jclepro.2015.03.013

Schneising, O., Buchwitz, M., Reuter, M., Vanselow, S., Bovensmann, H., & Burrows, J. P. (2020). Remote sensing of methane leakage from natural gas and petroleum systems revisited. Atmospheric Chemistry & Physics, 20, 9169–9182. https://doi.org/10.5194/acp-20-9169-2020

Shu, D. Y., Deutz, S., Winter, B. A., Baumgärtner, N., Leenders, L., & Bardow, A. (2023). The role of carbon capture and storage to achieve net-zero energy systems: Trade-offs between economics and the environment. Renewable and Sustainable Energy Reviews, 178, 113246. https://doi.org/10.1016/j.rser.2023.113246

Sonnemann, G., & Vigon, B. (2011). Global Guidance Principles for Life Cycle Assessment Databases.

Spath, P., & Mann, M. (2001). Life Cycle Assessment of Hydrogen Production via Natural Gas Steam Reforming. National Renewable Energy Laboratory. https://www.nrel.gov/docs/fy01osti/27637.pdf (Accessed March 2025)

Sphera Solutions. (2024). 1st Life Cycle GHG Emission Study on the Use of Ammonia as Marine Fuel. https://www.ama-andros.gr/wp-content/uploads/2024/06/SGMF-Ammonia-as-Marine-Fuel.pdf (Accessed March 2025)

Stadler, K., Wood, R., Bulavskaya, T., Södersten, C. J., Simas, M., Schmidt, S., Usubiaga, A., Acosta-Fernández, J., Kuenen, J., Bruckner, M., Giljum, S., Lutter, S., Merciai, S., Schmidt, J. H., Theurl, M. C., Plutzar, C., Kastner, T., Eisenmenger, N., Erb, K. H., … Tukker, A. (2018). EXIOBASE 3: Developing a Time Series of Detailed

Environmentally Extended Multi-Regional Input-Output Tables. Journal of Industrial Ecology, 22(3), 502–515. https://doi.org/10.1111/jiec.12715

Steffen, B., Beuse, M., Tautorat, P., & Schmidt, T. S. (2020). Experience Curves for Operations and Maintenance Costs of Renewable Energy Technologies. Joule, 4(2), 359–375. https://doi.org/10.1016/j.joule.2019.11.012

Strojny, M., Gładysz, P., Hanak, D. P., & Nowak, W. (2023). Comparative analysis of CO2 capture technologies using amine absorption and calcium looping integrated with natural gas combined cycle power plant. Energy, 284, 128599. https://doi.org/10.1016/j.energy.2023.128599

Su-ungkavatin, P., Tiruta-Barna, L., & Hamelin, L. (2023). Biofuels, electrofuels, electric or hydrogen?: A review of current and emerging sustainable aviation systems. Progress in Energy and Combustion Science, 96, 101073. https://doi.org/10.1016/j.pecs.2023.101073

United Nations. (2022). UN Comtrade. https://comtradeplus.un.org/ (Accessed March 2025)

U.S. Department of Energy. (2015). Wind Vision: A New Era for Wind Power in the United States. https://www.energy.gov/sites/prod/files/WindVision_Report_final.pdf (Accessed March 2025)

USGS. (2019). How Much Water is There on Earth? | U.S. Geological Survey. https://www.usgs.gov/special-topics/water-science-school/science/how-much-water-there-earth (Accessed March 2025)

Volkart, K., Bauer, C., & Boulet, C. (2013). Life cycle assessment of carbon capture and storage in power generation and industry in Europe. International Journal of Greenhouse Gas Control, 16, 91–106. https://doi.org/10.1016/j.ijggc.2013.03.003

Weidema, B. (2003). Market information in life cycle assessment. https://lca-net.com/publications/show/market-information-life-cycle-assessment/ (Accessed March 2025)

Weidema, B. (2009). Using the budget constraint to monetarise impact assessment results. Ecological Economics, 68(6), 1591–1598.

Weidema, B. (2014). Has ISO 14040/44 Failed Its Role as a Standard for Life Cycle Assessment? Journal of Industrial Ecology, 18(3), 324–326.

Weidema, B. (2018). In Search of a Consistent Solution to Allocation of Joint Production. Journal of Industrial Ecology, 22(2), 252–262.

Weidema, B., Ekvall, T., & Heijungs, R. (2009). Guidelines for applications of deepened and broadened LCA (Deliverable D18 of Work Package 5 of the CALCAS Project.).

Weidema, B. P., Ekvall, T., & Heijungs, R. (2009). Guidelines for application of deepened and broadened LCA. Deliverable D18 of work package 5 of the CALCAS project.

Weidema, B., Pizzol, M., Schmidt, J., & Thoma, G. (2018). Attributional or consequential Life Cycle Assessment: A matter of social responsibility. Journal of Cleaner Production, 174, 305–314.

Weidema, B., & Schmidt, J. (2010). Avoiding Allocation in Life Cycle Assessment Revisited. Journal of Industrial Ecology, 14(2), 192–195.

Weidema, B., Wesnæs, M., Hermansen, J., Kristensen, T., & Halberg, N. (2008). Environmental improvement potentials of meat and dairy products. https://data.europa.eu/doi/10.2791/38863 (Accessed March 2025)

Worthington, M. J. H., Kucera, R. L., & Chalker, J. M. (2017). Green chemistry and polymers made from sulfur. Green Chemistry, 19(12), 2748–2761. https://doi.org/10.1039/C7GC00014F

Wulf, C., & Zapp, P. (2018). Assessment of system variations for hydrogen transport by liquid organic hydrogen carriers. International Journal of Hydrogen Energy, 43(26), 11884–11895.

Xu, L., Xu, S., Bai, X.-S., Repo, J. A., Hautala, S., & Hyvönen, J. (2023). Performance and emission characteristics of an ammonia/diesel dual-fuel marine engine. Renewable and Sustainable Energy Reviews, 185, 113631. https://doi.org/10.1016/j.rser.2023.113631 (Accessed March 2025)

Appendix 1: Country codes in EXIOBASE

Appendix table 1: List of country codes used in EXIOBASE.

Country	Acronym for EXIOBASE country/region	Included countries (when relevant)
Austria	AT	
Australia	AU	
Belgium	BE	
Bulgaria	BG	
Brazil	BR	
Canada	CA	
Switzerland	CH	
China	CN	
Cyprus	CY	
Czech Republic	CZ	
Germany	DE	
Denmark	DK	
Estonia	EE	
Spain	ES	
Finland	FI	
France	FR	
United Kingdom	GB	
Greece	GR	
Hungary	HU	
Indonesia	ID	
Ireland	IE	
India	IN	
Italy	IT	
Japan	JP	
South Korea	KR	
Lithuania	LT	
Luxembourg	LU	
Latvia	LV	
Malta	MT	
Mexico	MX	
Netherlands	NL	
Norway	NO	
Poland	PL	
Portugal	PT	
Romania	RO	
Russia	RU	
Sweden	SE	
Slovenia	SI	
Slovakia	SK	
Turkey	TR	
Taiwan	TW	
United States	US	
South Africa	ZA	
Rest-of-World Asia	WA	Afghanistan, American Samoa, Azerbaijan, Bangladesh, Bhutan, British Indian Ocean territory, Brunei, Cambodia, Caspian Sea, Christmas Island, Clipperton Island, Cocos Islands, Cook Islands, East Timor, Fiji, French Polynesia, French Southern Territories, Guam, Heard Island and McDonald Islands, Hong Kong, Kazakhstan, Kiribati, Kyrgyzstan, Laos, Macao, Malaysia, Maldives, Marshall Islands, Mauritius, Micronesia, Mongolia, Myanmar, Nauru, Nepal, New Caledonia, New Zealand, Niue, Norfolk Island, North Korea, Northern Mariana Islands, Pakistan, Palau, Papua New Guinea, Philippines, Pitcairn Islands, Reunion, Samoa, Seychelles, Singapore, Solomon Islands, Spratly Islands, Sri Lanka, Tajikistan, Thailand, Tokelau, Tonga, Turkmenistan, Tuvalu, United

		States Minor Outlying Islands, Uzbekistan, Vanuatu, Vietnam, Wallis and Futuna
Rest-of-World Europe	WE	Albania, Andorra, Belarus, Bosnia and Herzegovina, Croatia, Faroe Islands, Gibraltar, Guernsey, Iceland, Isla of Man, Jersey, Kosovo, Liechtenstein, Macedonia, Moldova, Monaco, Montenegro, San Marino, Serbia, Svalbard and Jan Mayen, Ukraine, Vatican City, Aaland
Rest-of-World Africa	WF	Algeria, Angola, Benin, Botswana, Burkina Faso, Burundi, Cameroon, Cape Verde, Central African Republic, Chad, Comoros, Ivory Coast, Democratic Republic of the Congo, Djibouti, Equatorial Guinea, Eritrea, Ethiopia, Gabon, Gambia, Ghana, Guinea, Guinea-Bissau, Kenya, Lesotho, Liberia, Libya, Madagascar, Malawi, Mali, Mauritania, Mayotte, Morocco, Mozambique, Namibia, Niger, Nigeria, Republic of Congo, Rwanda, Saint Helena, Sao Tome and Principe, Senegal, Sierra Leone, Somalia, South Sudan, Sudan, Swaziland, Tanzania, Togo, Tunisia, Uganda, Western Sahara, Zambia, Zimbabwe
Rest-of-World Latin America	WL	Anguilla, Antigua And Barbuda, Aruba, Bahamas, Barbados, Belize, Bermuda, Bolivia, Bonaire Sain Eustatius and Saba, Bouvet Island, BVIs, Cayman Islands, Chile, Colombia, Costa Rica, Cuba, Curacao, Dominica, Dominican Republic, Ecuador, El Salvador, Falkland Islands, French Guiana, Grenada, Guadeloupe, Guatemala, Guyana, Haiti, Honduras, Jamaica, Martinique, Montserrat, Nicaragua, Panama, Paraguay, Peru, Puerto Rico, Saint Barthelemy, Saint Martin, Saint Kitts and Nevis, Saint Lucia, Saint Pierre And Miquelon, Sint Maarten, South Georgia And The South Sandwich Islands, Suriname, Trinidad and Tobago, Turks and Caicos Islands, Uruguay, Venezuela, Virgin Islands US
Rest-of-World Middle East	WM	Armenia, Bahrain, Egypt, Georgia, Iran, Iraq, Israel, Jordan, Kuwait, Lebanon, Oman, Palestine, Qatar, Saudi Arabia, Syria, UAE, Yemen

Appendix 2: Explanation of units in the Stepwise LCIA method

This appendix briefly explains the impact categories included in the applied LCIA method: Stepwise 2006 (version 1.8). The original version is described in Weidema et al. (2008). Updates regarding nature occupation are described in Schmidt & de Saxcé (2016). Moreover, version 1.8 has been updated with characterisation factors for 100 year global warming potential (GWP100) from IPCC (2021). If no literature reference is given in the table, this means that the information is obtained from Weidema et al. (2008).

Appendix table 2: Explanation of the impact categories in the LCIA method Stepwise 2006.

Impact category	Unit	Original source		Explanation
		EDIP 2003	Impact 2002+	
Global warming	kg CO_2-eq.	x		The unit is GWP100 (kg CO_2 equivalents) based on the sixth IPCC Assessment report (IPCC, 2021).
Nature occupation	PDF*m^2*year		x	The unit 'm^2-equivalents arable land', represents the impact from the occupation of one m^2 of arable land during one year. Impact 2002+ (Jolliet et al., 2003) has obtained the method for LCIA from EcoIndicator (Goedkoop & Spriensma, 2001) where the impact is assessed on the basis of the duration of the occupation of the area (m2*years) multiplied by a severity score, representing the potentially disappeared fraction (PDF) of species in that area during the specified time. In order to include the impacts from transformation, the Stepwise method introduces an additional severity of 0.88 to represent the secondary impacts from this transformation (deforestation), calculated as the nature occupation during the later relaxation from deforestation.
Acidification	m^2 UES	x		The unit expresses the area of the ecosystem within the full deposition area (in Europe) which is brought to exceed the critical load of acidification as a consequence of the emission (area of unprotected ecosystem = m^2 UES). The impact indicator is based on modelling of deposition in Europe. (Hauschild & Potting, 2005) p 47.
Eutrophication, aquatic	kg NO_3-eq.	x		The aquatic eutrophication potentials of a nutrient emission express the maximum exposure of aquatic systems that it can cause. The aquatic eutrophication potentials are expressed as N- or P-equivalents. (Hauschild & Potting, 2005) p 73-74.
Eutrophication, terrestrial	m^2 UES	x		Same as for acidification.
Photochemical ozone, vegetation	m^2*ppm*h	x		The impact is expressed as the accumulated exposure (duration times exceed threshold) above the threshold of 40 ppb times the area that is exposed as a consequence of the emission. The threshold of 40 ppb is chosen as an exposure level below which no or only small effects occur. The unit for vegetation exposure is m^2*ppm*hours. (Hauschild & Potting, 2005) p 93.
Respiratory inorganics	kg $PM_{2.5}$-eq.		x	The impact on human health related to respiratory inorganics is expressed as equivalents of particles ($PM_{2.5}$).
Respiratory organics	pers*ppm*h	x		The category covers the impact on human health from photochemical ozone formation. The impact is expressed as the accumulated exposure above the threshold of 60 ppb times the number of persons which are exposed as a consequence of the emission. No threshold for chronic exposure of humans to ozone has been established. Instead, the threshold of 60 ppb is chosen as the long-term environmental objective for the EU ozone strategy proposed by the World Health Organisation, WHO. The unit for human exposure is pers*ppm*hours. (Hauschild & Potting, 2005) p 93.
Human toxicity, carcinogens	kg C_2H_3Cl-eq.		x	The impact on human health related to carcinogens is expressed as equivalents of chloroethylene (C_2H_3Cl). The Impact2002+ method determines the damage on human health in terms of DALY (disability adjusted life years). Since there is no real mid-point for human toxicity, the Impact2002+ method has chosen C_2H_3Cl-eq. as a reference substance. (Jolliet et al., 2003)
Human toxicity, non-carc.	Kg C_2H_3Cl-eq.		x	Same as for human toxicity, carcinogens

Ecotoxicity, aquatic	kg TEG-eq. w		**x**	The impact on ecosystems related to ecotoxicity is expressed as equivalents of chloroethylene triethylene glycol (TEG) into water. The Impact2002+ method determines the damage on ecosystems in terms of PAF (potentially affected fraction). Since there is no real mid-point for ecotoxicity, the Impact2002+ method has chosen TEG-eq. into water as a reference. (Jolliet et al., 2003)
Ecotoxicity, terrestrial	kg TEG-eq. s		**x**	Same as for ecotoxicity, aquatic
Ozone layer depletion	kg CFC_{11}-eq.		**x**	The unit is equivalents of CFC11 which is an important contributor to ozone layer depletion.
Non-renewable energy	MJ primary		**x**	Total use of primary non-renewable energy resources measured in MJ.

Appendix 3: Changes made in background database

This section lists the changes made in the background database, EXIOBASE:

_57 Petroleum Refinery {country} (product market, hybrid units, purchaser price)

The activity '*_57 Petroleum Refinery*' is used to model the fuel oil used as feedstock for desulphurisation. Yet, two countries - Bulgaria (BG) and Belgium (BE) – are not used to model Europe region, since BG and BE provide unrealistic results. Thus, for fuel oil feedstock, the Europe region only consists of 30 countries instead of 32.

124 Sea and coastal water transport {country} (product market, hybrid units, purchaser price)

The activity '*124 Sea and coastal water transport*' is used to model the distribution of ammonia and VLSFO. Yet, due to unrealistic results, Brazil (BR) and Hungary (HU) are not used. Thus, BR is removed from three regions - Brazil, Central & South America, and Latin America – and replaced by Rest of America (RoW America). HU is also removed, thus, the Europe region for sea transport only consists of 31 countries instead of 32.

Coal incl. combustion emissions {country}, Diesel incl. combustion emissions {country} and Fuel oil incl. combustion emissions {country}

The activities for coal, diesel and fuel oil including combustion emissions are used to model the fuel mix used to produce steam for the desulphurisation process. Yet, two countries - Bulgaria (BG) and Belgium (BE) – are not used to model Europe region, since BG and BE provide unrealistic results. Thus, the Europe region for coal, diesel and fuel oil including combustion emissions only consists of 30 countries instead of 32.

Natural gas incl. and excl. combustion emissions {country}

The activities for natural gas –including and excluding combustion emissions – are used to model natural gas as fuel and as feedstock, respectively. Yet, for two countries – Cyprus (CY) and Malta (MT) – there is no impact from natural gas extraction in EXIOBASE. Thus, these countries are excluded from the Europe region. Moreover, natural gas extraction in Croatia (HR) has an unrealistic impact on respiratory inorganics, and this country is therefore also excluded from the Europe region.

Appendix 4: Conversion factor from MJ to TEUkm

The conversion factor for the functional unit from MJ to TEUkm is based on a ship with a cargo capacity of 15,000 TEU, an average load capacity of 85% and a fuel tank size of 16,000 m^3 provided by A.P. Moller - Maersk. Additionally, one 20 ft standard steel container measures 2.4 m, 2.6 m, and 6.1 m and one TEU therefore has a volume of 39.0 m^3 (Maersk, 2024). Furthermore, a gross weight of 30.48 t is also applied based on Maersk (2024). **Appendix table 4** provides an overview of all parameters used to calculate the conversion factor.

The energy density is calculated for both VLSFO and liquid ammonia using the lower heating value (LHV) for both fuels:

$$Energy\ density, VLSFO = 41.2 \frac{GJ}{t\ VLSFO} * 0.936 \frac{t\ VLSFO}{m^3} = 38.6 \frac{GJ}{m^3}$$

$$Energy\ density, liquid\ NH_3 = 17.2 \frac{GJ}{t\ NH_3} * 0.698 \frac{t\ NH_3}{m^3} = 12.0 \frac{GJ}{m^3}$$

As the energy density of liquid ammonia is 3.22 times lower than VLSFO, 51,541 m^3 of fuel storage is needed to provide the same of amount of energy as 16,000 m^3 VLSFO. Nevertheless, in order for ammonia to function as a fuel, a percentage of VLSFO is still needed. Thus, the following table shows how the cargo capacity is reduced due to additional fuel storage:

Parameter	Unit	100% ammonia	Ammonia with a share of VLSFO			VLSFO
Share of liquid ammonia	%	100%	95%	90.4%	85%	0%
Share of pilot fuel	%	0%	5%	9.6%	15%	100%
Fuel storage, VLSFO	m^3	0	800	1,536	2,400	16,000
Fuel storage, liquid NH_3	m^3	51,541	48,964	46,593	43,810	0
Additional fuel storage needed for NH_3	m^3	35,541	33,764	32,129	30,210	0
Cargo capacity reduced due to additional fuel storage	TEU	912	867	825	775	0
Load capacity	%	84.0%	84.1%	84.1%	84.2%	85.0%
Remaining cargo capacity with load capacity	TEU	14,088	14,133	14,175	14,225	15,000

It is assumed that a typical cargo ship consumes 0.1 t VLFSO/km, which corresponds to 4.12 GJ/km. Thus, with an 85% load capacity and thereby a cargo amount of 15,000 TEU, 0.275 MJ VLFSO is used per TEUkm. Yet, for the default ammonia scenario, the cargo amount is reduced to 14,175 TEU. This means that 0.291 MJ ammonia with 9.6% e/e VLSFO is used per TEUkm, corresponding to 5.8% more energy per TEUkm than VLSFO.

Appendix table 4: Parameters used to calculate the conversion factor for the functional unit.

Parameter	Unit	Value	Source
Ship cargo capacity	TEU	15,000	Project partner
Average load capacity	%	85	Project partner
Ship fuel tank size	m3	16,000	Project partner
Measurements of 20 ft standard steel container	m	2.4*2.6*6.1	Maersk (2024)
Gross weight of 20 ft standard steel container	t	30.48	Maersk (2024)
LHV, VLSFO	GJ/t	41.2	Project partner
LHV, liquid ammonia	GJ/t	17.2	Project partner
Density, VLSFO	t/m^3	0.936	IMO (2021)
Density, liquid ammonia	t/m^3	0.696	European Maritime Safety Agency (2022)
Average fuel consumption per km	t VLSFO/km	0.01	Assumed

Appendix 5: Share of wind turbine and PV plant per kWh electricity from wind and solar in consequential model

Share of 3.2 MW wind turbine per kWh electricity from wind and wind power efficiency

The calculated annual production for a 3.2 MW wind turbine in each country, efficiency per country based on data from Ember (2024), and the calculated amount of wind turbine per kWh produced is listed in the table below.

Country name, EXIOBASE	Country code, EXIOBASE	Annual production [kWh]	Wind power efficiency	Turbine share per kWh
Austria	AT	6,972,389	23%	7.17E-09
Australia	AU	7,988,671	29%	6.26E-09
Belgium	BE	7,573,951	28%	6.60E-09
Bulgaria	BG	3,882,488	23%	1.29E-08
Brazil	BR	7,239,024	39%	6.91E-09
Canada	CA	9,871,867	28%	5.06E-09
Switzerland	CH	5,365,071	19%	9.32E-09
China	CN_TW	8,695,120	23%	5.75E-09
Cyprus	CY	2,452,459	25%	2.04E-08
Czech Republic	CZ	4,101,986	20%	1.22E-08
Germany	DE	6,637,819	21%	7.53E-09
Denmark	DK	11,264,006	26%	4.44E-09
Estonia	EE	8,128,444	27%	6.15E-09
Spain	ES	6,290,664	25%	7.95E-09
Finland	FI	7,327,928	30%	6.82E-09
France	FR	6,685,805	22%	7.48E-09
United Kingdom	GB	16,225,866	29%	3.08E-09
Greece	GR	8,388,120	26%	5.96E-09
Croatia	HR	6,848,725	24%	7.30E-09
Hungary	HU	3,850,749	24%	1.30E-08
Indonesia	ID	2,100,845	33%	2.38E-08
Ireland	IE	14,248,344	26%	3.51E-09
India	IN	2,965,157	19%	1.69E-08
Italy	IT	4,147,796	21%	1.21E-08
Japan	JP	5,585,850	22%	8.95E-09
Korea	KR	4,496,419	21%	1.11E-08
Lithuania	LT	6,060,304	23%	8.25E-09
Luxembourg	LU	5,608,007	25%	8.92E-09
Latvia	LV	4,912,553	20%	1.02E-08
Malta	MT	4,619,383	25%	1.08E-08
Mexico	MX	6,460,106	34%	7.74E-09
Netherlands	NL	9,735,614	26%	5.14E-09
Norway	NO	13,220,135	27%	3.78E-09
Poland	PL	6,664,645	27%	7.50E-09
Portugal	PT	6,592,862	28%	7.58E-09
Romania	RO	4,247,356	25%	1.18E-08
Russia	RU	4,916,514	15%	1.02E-08
Sweden	SE	8,338,368	26%	6.00E-09
Slovenia	SI	5,111,724	25%	9.78E-09
Slovakia	SK	4,619,383	25%	1.08E-08
Turkey	TR	6,994,950	33%	7.15E-09
United States	US	12,568,632	32%	3.98E-09
RoW Asia and Pacific	WA	5,125,106	27%	9.76E-09
RoW Europe	WE	7,800,584	25%	6.41E-09
RoW Africa	WF	3,201,850	22%	1.56E-08
RoW America	WL	9,101,257	25%	5.49E-09
RoW Middle East	WM	5,472,132	25%	9.14E-09
South Africa	ZA	8,267,400	33%	6.05E-09

Share of PV plant per kWh electricity from solar

The amount of PV plant per kWh produced is calculated based on the annual production for a 570 kWp crystalline silicone plant with optimised slope and azimuth for each country based on the GIS tool from Joint Research Centre (2022) and a PV plant lifespan of 30 years. The annual production and amount of PV plant per kWh produced is listed in the table below.

Country name, EXIOBASE	Country code, EXIOBASE	Annual production [kWh]	PV plant share per kWh
Austria	AT	585,550	5.693E-08
Australia	AU	949,040	3.512E-08
Belgium	BE	607,446	5.487E-08
Bulgaria	BG	771,080	4.323E-08
Brazil	BR	901,815	3.696E-08
Canada	CA	599,030	5.565E-08
Switzerland	CH	755,287	4.413E-08
China	CN_TW	570,023	5.848E-08
Cyprus	CY	855,688	3.896E-08
Czech Republic	CZ	604,922	5.51E-08
Germany	DE	564,252	5.908E-08
Denmark	DK	585,815	5.69E-08
Estonia	EE	523,517	6.367E-08
Spain	ES	901,815	3.696E-08
Finland	FI	493,904	6.749E-08
France	FR	685,536	4.862E-08
United Kingdom	GB	581,444	5.733E-08
Greece	GR	804,072	4.146E-08
Croatia	HR	709,164	4.7E-08
Hungary	HU	732,088	4.553E-08
Indonesia	ID	728,999	4.572E-08
Ireland	IE	549,535	6.066E-08
India	IN	922,354	3.614E-08
Italy	IT	767,082	4.345E-08
Japan	JP	722,906	4.611E-08
Korea	KR	760,350	4.384E-08
Lithuania	LT	578,796	5.759E-08
Luxembourg	LU	599,480	5.56E-08
Latvia	LV	552,117	6.037E-08
Malta	MT	945,969	3.524E-08
Mexico	MX	940,938	3.543E-08
Netherlands	NL	584,971	5.698E-08
Norway	NO	470,670	7.082E-08
Poland	PL	612,680	5.441E-08
Portugal	PT	881,177	3.783E-08
Romania	RO	680,119	4.901E-08
Russia	RU	593,878	5.613E-08
Sweden	SE	512,053	6.51E-08
Slovenia	SI	657,839	5.067E-08
Slovakia	SK	650,724	5.123E-08
Turkey	TR	852,079	3.912E-08
United States	US	925,060	3.603E-08
RoW Asia and Pacific	WA	744,603	4.477E-08
RoW Europe	WE	741,499	4.495E-08
RoW Africa	WF	742,033	4.492E-08
RoW America	WL	886,925	3.758E-08
RoW Middle East	WM	1,026,116	3.248E-08
South Africa	ZA	915,901	3.639E-08

Appendix 6: Country-specific fuel mixes in consequential LCA

	LCI
Materials/fuels	
Biomass incl. combustion emissions*	_18 Forestry, logging and related service activities {region}
Coal incl. combustion emissions*	_20 Mining of coal and lignite; extraction of peat {region}
Diesel incl. combustion emissions*	_57 Petroleum Refinery {region}
Fuel oil incl. combustion emissions*	_57 Petroleum Refinery {region}
Natural gas incl. combustion emissions*	_22 Extraction of natural gas and services related to natural gas extraction, excluding surveying {region}

* See combustion emissions in **section 4.4**

	AT	AU	BE	BG	BR	CA	CH	CN_TW	CY
Materials/fuels									
Biomass incl. combustion emissions	28.44%	15.07%	9.48%	14.60%	49.57%	14.38%	16.14%	0.01%	3.82%
Coal incl. combustion emissions	5.59%	13.05%	11.14%	10.60%	11.88%	4.45%	6.59%	71.60%	0.00%
Diesel incl. combustion emissions	9.41%	26.65%	6.30%	9.23%	9.05%	21.16%	18.49%	4.65%	21.91%
Fuel oil incl. combustion emissions	3.94%	5.38%	19.42%	9.81%	14.50%	11.31%	1.53%	5.80%	74.27%
Natural gas incl. combustion emissions	52.61%	39.85%	53.65%	55.77%	15.00%	48.71%	57.25%	17.95%	0.00%

	CZ	DE	DK	EE	ES	FI	FR	GB	GR
Materials/fuels									
Biomass incl. combustion emissions	14.99%	7.88%	12.34%	4.26%	11.10%	58.66%	9.07%	8.37%	8.09%
Coal incl. combustion emissions	16.77%	13.36%	6.32%	4.92%	1.89%	6.77%	10.93%	10.88%	9.10%
Diesel incl. combustion emissions	9.63%	2.37%	27.51%	45.24%	20.87%	12.09%	19.02%	12.72%	9.58%
Fuel oil incl. combustion emissions	1.85%	5.32%	14.42%	11.51%	13.82%	12.03%	8.54%	16.15%	47.39%
Natural gas incl. combustion emissions	56.76%	71.06%	39.42%	34.07%	52.32%	10.45%	52.45%	51.88%	25.84%

	HR	HU	ID	IE	IN	IT	JP	KR	LT
Materials/fuels									
Biomass incl. combustion emissions	2.13%	5.53%	17.80%	8.33%	19.10%	2.81%	4.61%	3.11%	18.25%
Coal incl. combustion emissions	6.99%	3.93%	27.23%	6.54%	44.87%	4.98%	20.25%	32.00%	15.47%
Diesel incl. combustion emissions	29.08%	18.65%	16.79%	16.43%	8.43%	16.10%	12.95%	7.36%	10.21%
Fuel oil incl. combustion emissions	20.35%	17.07%	10.03%	22.65%	15.95%	16.01%	27.97%	11.88%	3.51%
Natural gas incl. combustion emissions	41.45%	54.81%	28.15%	46.06%	11.65%	60.10%	34.22%	45.64%	52.57%

	LU	LV	MT	MX	NL	NO	PL	PT	RO
Materials/fuels									
Biomass incl. combustion emissions	6.91%	53.73%	0.11%	3.56%	2.23%	10.73%	16.56%	33.68%	7.08%
Coal incl. combustion emissions	13.23%	2.80%	0.00%	5.77%	2.21%	26.76%	31.30%	0.44%	10.09%
Diesel incl. combustion emissions	7.80%	21.84%	69.21%	19.24%	6.44%	25.38%	16.51%	13.84%	13.80%
Fuel oil incl. combustion emissions	0.33%	3.12%	30.69%	20.65%	26.18%	21.09%	3.74%	15.00%	14.14%
Natural gas incl. combustion emissions	71.73%	18.50%	0.00%	50.79%	62.95%	16.05%	31.89%	37.05%	54.89%

	RU	SE	SI	SK	TR	US	WA	WE	WF
Materials/fuels									
Biomass incl. combustion emissions	0.12%	70.05%	10.65%	17.85%	0.00%	14.55%	19.38%	2.50%	42.11%
Coal incl. combustion emissions	21.79%	8.13%	5.27%	13.39%	34.20%	7.12%	32.98%	28.65%	5.06%
Diesel incl. combustion emissions	7.51%	5.30%	16.42%	3.59%	15.74%	10.88%	15.29%	19.03%	18.19%
Fuel oil incl. combustion emissions	15.66%	8.86%	7.28%	6.68%	1.65%	5.57%	9.21%	4.44%	13.98%
Natural gas incl. combustion emissions	54.91%	7.66%	60.39%	58.50%	48.41%	61.87%	23.14%	45.37%	20.66%

	WL	WM	ZA
Materials/fuels			
Biomass incl. combustion emissions	18.22%	0.00%	9.63%
Coal incl. combustion emissions	8.96%	1.78%	50.68%
Diesel incl. combustion emissions	20.84%	10.86%	14.97%
Fuel oil incl. combustion emissions	24.01%	18.18%	5.08%
Natural gas incl. combustion emissions	27.97%	69.18%	19.65%

Appendix 7: CAPEX for German chemical industry

	Unit	_63 Chemicals nec {DE} (linked)	114 Construction (45) {DE} (linked)
Reference flow			
Materials and machinery for chemical production	t	17,843,941	
Materials Construction activities	t		561,422,890
Inputs:			
_18 Forestry, logging and related service activities (02) {DE}	t	32,844	16,942
_20 Mining of coal and lignite; extraction of peat (10) {DE}	t	399,250	
_22 Extraction of natural gas and services related to natural gas extraction, excluding surveying {DE}	t	815,567	
_32 Quarrying of stone {DE}	t	8,786	201,147,976
_33 Quarrying of sand and clay {DE}	t	50,367	313,756,580
_34 Mining of chemical and fertilizer minerals, production of salt, other mining and quarrying n.e.c. {DE}	t	12,007,276	
_39 Processing vegetable oils and fats {DE}	t	2,815,216	
_42 Sugar refining {DE}	t	651	
_46 Manufacture of tobacco products (16) {DE}	t	0.00000006	0.00000001
_47 Manufacture of textiles (17) {DE}	t	755	7,369
_48 Manufacture of wearing apparel; dressing and dyeing of fur (18) {DE}	t	0.07	1.31
_49 Tanning and dressing of leather; manufacture of luggage, handbags, saddlery, harness and footwear (19)	t	0.00001	0.00086
_50 Manufacture of wood and of products of wood and cork, except furniture; manufacture of articles of straw and plaiting materials (20) {DE}	t	15,066	4,003,611
_52 Pulp {DE}	t	16,098	46,358
_54 Paper {DE}	t	62,912	123,647
_55 Publishing, printing and reproduction of recorded media (22) {DE}	t	2,350	4,500
_63 Chemicals nec {DE}	t	433,916	119,509
_64 Manufacture of rubber and plastic products (25) {DE}	t	189,625	2,920,000
_65 Manufacture of glass and glass products {DE}	t	624,744	1,935,409
_67 Manufacture of ceramic goods {DE}	t	762	517,207
_68 Manufacture of bricks, tiles and construction products, in baked clay {DE}	t	326	7,185,207
_69 Manufacture of cement, lime and plaster {DE}	t	2,338	18,955,917
_71 Manufacture of other non-metallic mineral products n.e.c. {DE}	t	77,175	4,448,877
_72 Manufacture of basic iron and steel and of ferro-alloys and first products thereof {DE}	t	75,865	1,516,308
_76 Aluminium production {DE}	t	11,151	16,557
_78 Lead, zinc and tin production {DE}	t	12,134	97,213
_80 Copper production {DE}	t	5,584	35,985
_82 Other non-ferrous metal production {DE}	t	2,346	17,460
_84 Casting of metals {DE}	t	2,512	209,064
_85 Manufacture of fabricated metal products, except machinery and equipment (28) {DE}	t	107,563	4,341,194
_86 Manufacture of machinery and equipment n.e.c. (29) {DE}	t	22,093	
_87 Manufacture of office machinery and computers (30) {DE}	t	2,300	
_88 Manufacture of electrical machinery and apparatus n.e.c. (31) {DE}	t	25,914	
_89 Manufacture of radio, television and communication equipment and apparatus (32) {DE}	t	1,319	
_90 Manufacture of medical, precision and optical instruments, watches and clocks (33) {DE}	t	17,881	
_93 Manufacture of furniture; manufacturing n.e.c. (36) {DE}	t	1,255	19,531

Appendix 8: Consequential modelling of land use changes

Land use change refers to the process by which human activities transform the natural landscape, altering how land is used for various purposes. This can include deforestation, afforestation, urbanization, and rewilding, among other processes. Land use change has significantly affected the Earth's land surface, and it is important to include in LCA modelling (Schmidt et al., 2015).

According to IPCC (2019a), 11% of global GHG emissions (GWP100) are caused by CO_2 emissions from land use changes. We use a model for indirect land use changes (iLUC) proposed by Schmidt et al. (2015). This model has been used for a large number of LCA studies and carbon footprints[1] and the model is rated as the best among a comparison of six major LUC models by De Rosa et al. (2016). The ranking considers completeness, impact assessment relevance, scientific robustness, and transparency. The current study uses version 4.3 of the iLUC model, which is integrated in the multi-regional hybrid input-output model EXIOBASE v3 (Merciai & Schmidt, 2017b; Schmidt & De Rosa, 2018b). The applied iLUC model has been and is currently being developed through an initiative lead by 2.-0 LCA consultants: The 2.-0 iLUC club (http://lca-net.com/clubs/iluc/). The initiative is supported by more than 25 partners including large multinational companies, national research centres, NGOs, and universities. The partners are located in 11 different countries in Europe, Asia, North America, and Australia.

The iLUC model has several key characteristics that make it superior to many of the other models:

- It is applicable to all crops (also forest land, range land, built land etc.) in all regions in the world.
- It avoids arbitrary allocation/amortization of transformation impacts.
- It is based on modelling assumptions that follow cause-effect relationships consistent with the way any other links between LCA-processes are modelled.

1 ha*year average global arable land is associated with 1.307 t CO_2-eq. (calculated with the EXIOBASE v3.3.16 implementation of the iLUC model and GWP100 from IPCC (2021)).

According to Schmidt et al. (2015), the cause of land transformation is a change in the demand for land. The mechanism linking land use change to changes in demand for land is illustrated in **Figure A8.1**. The figure uses the example of adding a demand for land for rapeseed in Denmark of 1 ha*year. It appears from the figure that the land use effects can be divided into direct and indirect land use changes. This is further explained in the following.

[1] See list of examples of application areas at: https://lca-net.com/projects/show/indirect-land-use-change-model-iluc/

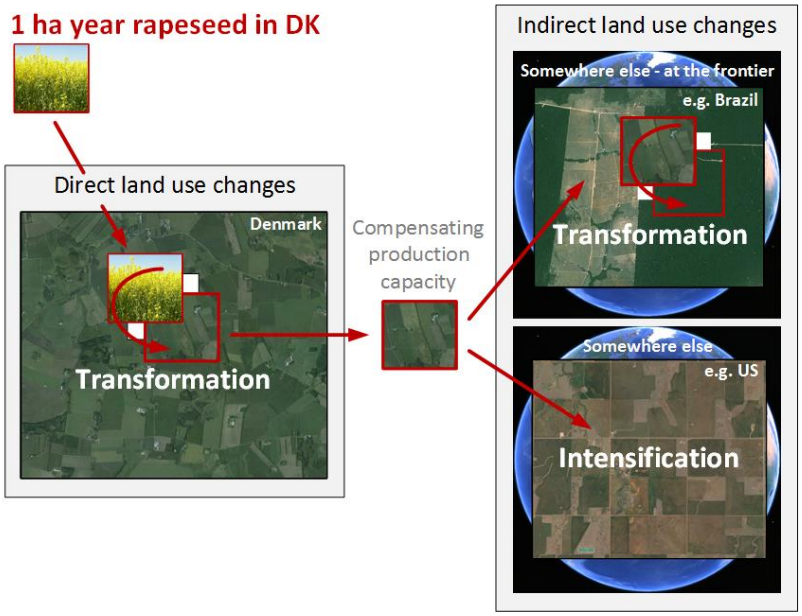

Figure A8.1: Illustration of the effects of adding a demand for land in Denmark of one hectare*year. The effects include indirect transformation of land and intensification to compensate for the production capacity in Denmark that is now no longer available due to being occupied by the new demand.

12.1.1 Direct land use changes (dLUC)

In the example in **Figure A8.1**, the direct land use change is the effect of changing from a reference situation to rapeseed. The reference situation is the current marginal use of the affected land, which will be arable land in most cases (Schmidt et al., 2015).

Obviously, any arable cropping will affect arable land, but also many other human activities are located on arable land, so that when demanding land for buildings, infrastructure, sites for resource extraction, etc., arable land is often affected. An example is the use of land for a residential house in an urban area. This change in demand for land will put equivalent pressure on the boundaries of the urban area that will likely expand into the surrounding arable land.

Most often, the impacts of direct land use changes are small, because the carbon stock and biodiversity hosted on the land are similar for the specific use and for the reference. When the crops under study are associated with a carbon stock that is equal to the reference in that country, then the direct land use changes are not associated with any change in carbon stock. However, if the crops under study store more carbon than the reference, then the crops under study contribute to an increase of stored carbon in crops in that country. This is the case of oil palm (which is affected in the current study), which stores more carbon than reference, which will be the average of arable land in Indonesia and Malaysia, excluding oil palm because that is the crop that expands.

12.1.2 Indirect land use changes (iLUC)

As illustrated in **Figure A8.1**, the indirect consequence of the direct land use change is the occupation of production capacity somewhere else to compensate for the production capacity now occupied by the additional demand. According to Schmidt et al. (2015), this compensation is partly expansion of arable land at the agricultural frontier, and partly intensification of land already in use. The use of land by the crop under study is what is considered as dLUC, while the supply of new land caused by the need for compensating the production capacity of the land required by the new demand is considered as iLUC. The link between the supply-side and the use-side of land is further elaborated in the next section.

12.1.3 Supply and use of land linked via the global market for land

The iLUC model described in Schmidt et al. (2015) assumes there is a global market for land. To be more precise, the market is not mainly concerned with the area of land but rather its production capacity. Hence, all countries that expand their arable land supplies land into this market as well as all countries that intensify their existing productive land supply arable land into the global market for arable land. This supply-side to the global market for land is illustrated in **Figure A8.2**.

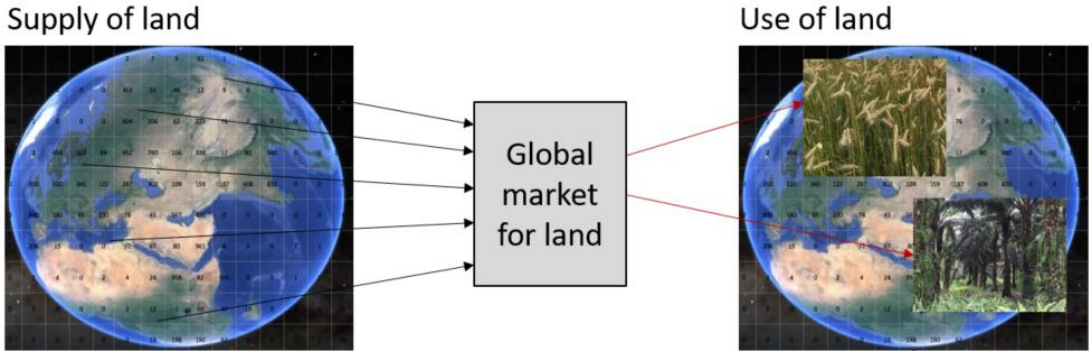

Figure A8.2: Illustration of the global supply and demand of land (Schmidt & De Rosa, 2020).

The supply-side of land is modelled using the EXIOBASE model, and the approach and data are described in Schmidt & De Rosa (2020) and Merciai & Schmidt (2017b).

The supply of land in the applied iLUC model is modelled by using data in the multi-regional hybrid input-output model EXIOBASE (Merciai & Schmidt, 2017b). The integration of the iLUC model in EXIOBASE is described in Merciai & Schmidt (2017b) and Schmidt & De Rosa (2018b). The land market modules of the model contain data on time-series of land use data and agricultural production data for all countries. The EXIOBASE data allow identifying the land supplied by each country, by expansion of the cultivated area as well as by intensifying existing agricultural land and linking the production trends with the land use trends. In EXIOBASE, the complete global economy is divided in 47 countries and regions, and each of them is divided in 164 industrial sectors. The agricultural and land use module in EXIOBASE make use of FAOSTAT (2024), which provide time series on area and production per crop. To have comparative yields, all crops are converted to dry matter. These data allow modelling the global supply of land (**Figure A8.2**) to the global market for land, distinguishing between land expansion (land transformation) and land intensifications (increased production per unit of land). Analogously, the demand side is modelled for every country using land for crop cultivation, pasture, forestry, and other purposes.

12.1.4 Adjustment for differences in potential productivity

To calculate how much land that needs to be compensated from occupying 1 ha*year in a specific country/region, its productivity must be adjusted for. Schmidt et al. (2015) use the potential net primary production (NPP_0) for this adjustment. Hence, the adjustment factor is calculated as the actual NPP_0 divided by the global average NPP_0 for arable land. When this adjustment is done, the unit is changed from ha*year to ha*year-equivalents, where 1 ha*year-equivalent refer to land with average global potential productivity.

The potential productivity of arable land in different countries is based on high resolution maps that allow to determine how much iLUC is induced by using land in different regions. For example, 1 ha arable land in Indonesia gives a potential productivity that is 1.9 times greater than in EU28, hence the induced iLUC emissions from 1 ha in Indonesia is 1.9 times higher than in EU28. The data used to determine national average potential productivity

of arable land relative to global average arable land is a detailed overlay analysis in GIS, with the following data sources:

- 10 x 10 km grid of potential net primary production (NPP_0) (Haberl et al., 2007)
- 0.05 x 0.05 km grid of land cover data (Friedl et al., 2010)
- National borders

12.1.5 Different land markets

Schmidt et al. (2015) operate with different markets for land: 1) Arable land, 2) Intensive forest land, 3) Extensive forest land, and 4) Grassland. This delimits land types with different potential uses. The potential uses represent the reference for each land type, e.g. grassland in the dry Brazilian Cerrado, which is to a large extent used for cattle grazing, cannot be used for forestry or arable cropping because it is too dry for these purposes. Therefore, a change in the use of these grasslands will not have any indirect effects on the markets for forest land or arable land. Similarly, forest land in some countries may not be fit for arable cropping because the land is too cold, rocky, or hilly for that purpose. Therefore, the use of this land will only affect the market for forest land. Sometimes land is used for less productive purposes (economically) than the land's potential use, e.g. when potential arable land in Indonesia and Malaysia is used for extensive forestry. In this case, using this land will still affect the market for arable land. (Schmidt & de Saxcé, 2016)

The markets for land are defined in **Table A8.1**.

Table A8.1: Different markets for land (Schmidt et al., 2015). GWP100 impact calculated with the EXIOBASE v3.3.16 implementation of the iLUC model and GWP100 from IPCC (2021).

Markets for land	Kg CO_2-eq / ha*year-eq	Description
Market for arable land (fit for arable and other)	1307	Fit for arable cropping (both annual and perennial crops), for intensive or extensive forestry, and pasture.
Market for forest land (fit for intensive/extensive forestry and grazing)	429	Fit for forestry and pasture but unfit for arable cropping e.g. because the soil is too rocky or because the climate is too cold. Forest land may also be used for other uses, e.g. livestock grazing.
Market for grassland (fit for grazing)	67	Too dry or cold for forestry and arable cropping. Grassland is most often used for grazing.

12.1.6 Temporal aspects: Avoiding amortization of land transformation

A challenge when modelling land use changes is that transformation of land (in unit ha), e.g. from forest to oil palm, is not proportional with FFB production (which is proportional with land occupation in unit ha*year). A common approach to overcome this is to amortize (allocate) impacts related to land transformation over a normatively defined period of time, e.g., 20 years. This approach is used in several LCA and carbon footprint guidelines, e.g., the PEF guideline, the GHG protocol, PAS2050 and the PalmGHG.

However, this approach does not reflect a cause-effect relationship, the amortization period is arbitrarily defined, and by allocating historical land use change impacts to current oil palm cultivation it implies a causality that goes backwards in time (current demand for crops causes deforestation 20 years ago), which is obviously not possible in reality.

The applied iLUC model overcomes this problem by modelling land transformation as accelerated denaturalisation (Schmidt et al., 2015). This approach models the observed and current relationships only: that deforestation is taking place as long as the demand for land grows and as long as deforestation is not stopped. To grow the functional unit under study in an LCA, the indirect effect could be an additional demand for 1

ha*year. When this demand is added to the background demand causing the current deforestation, the effect is that in year 0, an additional hectare of deforestation is taking place, while after one year when the functional unit is produced, the cleared land can be handed over to the next crops, which can then be grown without deforestation. The handing over of the land after 1 year thus avoids 1 ha deforestation. The net effect of the additional demand for 1 ha*year is thus a preponement of 1 ha deforestation by 1 year, i.e., the deforestation that would have taken place in year 1 is now taking place in year 0 because of the demand for the functional unit under study. When moving deforestation and associated CO_2 emissions in time, the impact on global warming can be calculated by using the time-dependent global warming potential. Further, the impact on nature occupation (biodiversity) can be modelled as occupation in units of PDF*ha*year. This is because moving land transformation in time is the same as occupation.